# Sex differences in endothelial function in the porcine coronary artery

Pui San Wong, MPharm (Hons) MRPharmS

*School of Life Sciences*

*University of Nottingham Medical School*

Thesis submitted to the University  of Nottingham

for the degree of Doctor of Philosophy

July 2015

# Abstract

The prevalence of cardiovascular disease is lower in premenopausal women compared to age-matched males and postmenopausal females. Differences in risk may be due to sex differences in endothelial function. Therefore, this thesis examined the effects of gender on endothelium-dependent vasorelaxation in porcine isolated coronary arteries (PCAs). Distal PCAs were studied under myographic conditions and pre-contracted with U46619. Concentration-response curves to bradykinin, an endothelium-dependent vasorelaxant, were constructed in the presence of various inhibitors. Inhibition of NO and prostanoid synthesis (EDH-type response) produced greater inhibition in males compared to females. Eliminating $H_2O_2$ using PEG-catalase significantly reduced the bradykinin-induced vasorelaxation in the absence, but not in the presence of L-NAME and indomethacin in females, and had no effect in males. Inhibition of gap junctions with carbenoxolone and 18α-GA inhibited the EDH-type response in females but not in males. Inhibition of $SK_{Ca}$ channels reduced the EDH-type response in PCAs from both sexes but inhibition of $IK_{Ca}$ had an effect only in females but not males. Western blot did not detect any differences in the expression of Cx40, 43 or $IK_{Ca}$ between sexes.

   $H_2O_2$ caused concentration-dependent vasorelaxations which were significantly inhibited by PEG-catalase, TEA, 60 mM $K^+$ and 500 nM ouabain. Inhibition of NOS, cyclo-oxygenase, gap junctions, $SK_{Ca}$, $IK_{Ca}$, $BK_{Ca}$, $K_{ir}$, $K_V$, $K_{ATP}$, cGMP, $Na^+$-$Ca^{2+}$ exchanger or removal of endothelium had no effect on the $H_2O_2$-induced vasorelaxation. 1 mM $H_2O_2$ inhibited both KCl-induced

vasorelaxation and rubidium-uptake consistent with inhibition of the $Na^+/K^+$-pump activity.

The effects of the antioxidant Tiron® under different gassing conditions (95% $O_2$/5% $CO_2$ or 95% air/5% $CO_2$) were investigated. The bradykinin-induced vasorelaxations in PCAs were unaffected by different levels of oxygenation. Tiron® increased the potency of bradykinin only when gassed with 95% $O_2$/5% $CO_2$ and the enhancement in vasorelaxation was prevented by catalase. Similarly, Tiron® enhanced the EDH-type response when gassed with 95% $O_2$/5% $CO_2$ in PCAs from both sexes. Biochemical analysis using Amplex Red demonstrated that $H_2O_2$ was generated in Krebs'-Henseleit solution when gassed with 95% $O_2$/5% $CO_2$, but not with 95% air/5% $CO_2$.

Inhibition of Nox had no effect in PCAs from females but DPI, a non-selective Nox inhibitor reduced the potency of the bradykinin-induced vasorelaxation in males. In the EDH-type responses, inhibition of Nox had no effect in females, but in males, ML-171 (a selective Nox inhibitor) and DPI enhances while VAS2870 (a selective Nox inhibitor) reduces the bradykinin-induced vasorelaxation. ML-171 had no effect on the forskolin-induced vasorelaxation but decreased the potency of U46619-induced tone in both sexes in the absence or presence of endothelium. Nox activity was reduced by DPI and ML-171, but not VAS2870 in PCAs from both sexes. Sex differences in the functional study of Nox could be attributed to the differential expression of Nox proteins where expression of Nox1 and Nox2 were greater in males but Nox4 was greater in females. This may underlie the greater oxidative stress observed in males.

Bradykinin-induced EDH-type responses in PCAs from both sexes were essentially abolished by 2-APB (TRPC&TRPM antagonist). SKF96365 (TRPC antagonist) inhibited the bradykinin-induced vasorelaxation in males, and EDH-type response in both sexes. Pyr3 (TRPC3 antagonist) inhibited both the NO and EDH components of the bradykinin-induced vasorelaxation in males, but not females. RN1734 (TRPV4 antagonist) reduced the potency of the NO component of the bradykinin-induced vasorelaxation in females only, but inhibited the EDH-type response in both sexes. 2-APB, SKF96365 and RN1734 all reduced the $H_2O_2$-induced vasorelaxation, whereas Pyr3 had no effect. No differences in expression level of TRPC3 and TRPV4 between sexes were detected using Western blot.

In conclusion, present study demonstrated clear sex differences in endothelial function in PCAs where $H_2O_2$, MEGJs, $IK_{Ca}$ and TRPV4 channels play a role in the bradykinin-induced vasorelaxation only in female pigs while Nox-generated reactive oxygen species and TRPC3 channels play a role in the bradykinin-induced vasorelaxation only in male pigs. Therefore, gender-specific drug treatment for cardiovascular disease may be a novel therapeutic strategy.

# Publications

**Papers**

1. **Wong PS**, Roberts RE, Randall MD (2014). Sex differences in endothelial function in porcine coronary arteries: a role for $H_2O_2$ and gap junctions? *Br J Pharmacol* **171**(11)**:** 2751-2766.

2. **Wong PS**, Garle MJ, Alexander SP, Randall MD, Roberts RE (2014). A role for the sodium pump in $H_2O_2$-induced vasorelaxation in porcine isolated coronary arteries. *Pharmacol Res* **90C:** 25-35.

3. **Wong PS**, Roberts RE, Randall MD (2015). Hyperoxic gassing with Tiron enhances bradykinin-induced endothelium-dependent and EDH-type relaxation through generation of hydrogen peroxide. *Pharmacol Res* **91:** 29-35.

4. **Wong PS**, Roberts RE, Randall MD (2015). Sex differences in the role of Transient Receptor Potential (TRP) channels in endothelium-dependent vasorelaxation in porcine isolated coronary arteries. *Eur J Pharmacol* **750C:** 108-117.

5. **Wong PS**, Randall MD, Roberts RE (2015). Sex differences in the role of NADPH oxidases in endothelium-dependent vasorelaxation in porcine isolated coronary arteries. *Vascul Pharmacol* doi:10.1016/j.vph.2015.04.001.

**Abstracts for conferences**

1. **Wong PS**, Roberts RE, Randall MD (2012). A Role For The Sodium Pump In Hydrogen Peroxide-Induced Relaxation In The Porcine Isolated Coronary Artery. *BPS Winter Meeting 2012* Queen Elizabeth II Conference Centre London. www.pA2online.org, 072P.

2. **Wong PS**, Randall MD, Roberts RE (2012). Sex Difference In Endothelial Function Of The Porcine Isolated Coronary Artery. *BPS Winter Meeting 2012* Queen Elizabeth II Conference Centre London. www.pA2online.org, 073P.

3. **Wong PS**, Roberts RE, Randall MD (2013). Gender differences in endothelial function. Abstracts of the 2nd Joint Meeting of the British and American Microcirculation Societies 62nd Meeting of the British Microcirculation Society. Microcirculation, 20: 42–109. PC121 DOI: 10.1111/micc.12018.

4. **Wong PS**, Roberts RE, Randall MD (2013). Effects of Tiron on Porcine Isolated Coronary Artery under different gassing conditions. *YLS2013 Cardiovascular Medicine: Bridging Basic and Clinical Researchers.* Barts and the London Charterhouse Square Campus.

5. **Wong PS**, Roberts RE, Randall MD (2013). The role of Transient Receptor Potential (TRP) channels in EDH-mediated vasorelaxation in Porcine Isolated Coronary Artery. *Pharmacology 2013* Queen Elizabeth II Conference Centre London. www.pA2online.org, 044P.

6. **Wong PS**, Randall MD, Roberts RE (2013). A comparison of protection against oxidative stress and endothelial function in female and male porcine coronary arteries. *Pharmacology 2013* Queen Elizabeth II Conference Centre London. www.pA2online.org, 045P.

7.  **Wong P.**, Roberts R., Randall M. (2014). A comparison of oxidative stress and endothelial function in female and male porcine coronary arteries. Special Issue: Abstracts of the 17th World Congress of Basic & Clinical Pharmacology, 13-18 July 2014, Cape Town, South Africa. Cardiovascular Pharmacology. Basic & Clinical Pharmacology & Toxicology, 115 (Suppl. 1), 13, DOI: 10.1111/bcpt.12259_1

8.  **Wong P.**, Randall M., Roberts R. (2014). The role of Transient Receptor Potential (TRP) channels in $H_2O_2$-induced vasorelaxation in the Porcine Isolated Coronary Artery (PCA). Special Issue: Abstracts of the 17th World Congress of Basic & Clinical Pharmacology, 13-18 July 2014, Cape Town, South Africa. Cardiovascular Pharmacology. Basic & Clinical Pharmacology & Toxicology, 115 (Suppl. 1), 160, DOI: 10.1111/bcpt.12259_1

# Acknowledgements

First and foremost, I would like thank both my supervisors Professor Michael Randall and Dr Richard Roberts for their excellent supervision and their continuous support and guidance over the years. Next, I would like to thank the School of Life Sciences, University of Nottingham for funding this PhD and I would like to acknowledge the great services provided by the local abattoir, G Woods & Sons, Clipstone, Nottinghamshire for their cooperation in providing me with pig tissues of specified sex despite their tight schedule.

I would also like to thank Dr Steve Alexander, Dr Michael Garle, Dr Sue Chan, Dr Amanda Wheal, Liaque Latif and Kelvin Wong for their time, excellent technical assistance and their valuable comments on this work. Not to forget the good friends and colleagues in E34, Dr Mouhamed Alsaqati, Dr Jemma Donovan, Dave Hunt, Esther Mokori, Hamza Denfria, Hamidah Abu Bakar, Alaa Habib, Fawaz Alassaf, Zainab Abbas and Jagdish Kaur for their company and help around the laboratory.

Selain itu, saya ingin mengucapkan terima kasih kepada rakan-rakan seperjuangan saya dari Malaysia yang juga berkerja di tingkat 'E-floor, QMC', iaitu Azlina Abdul Razak, Valerie Shang, Suvik Assaw dan Mohd Harizal Senik atas persahabatan dan sokongan yang berterusan. Next, I would like to thank my housemate also my ex-classmate, Szu Shen Wong (Susan) for looking out for me and putting up with me for the past 3 years.

Last but not least, I would like to thank my family for their continuous support, encouragement and advice throughout my studies.

# Table of Contents

*Chapter 2*

**Vascular responses in porcine isolated coronary arteries and Sex Differences in endothelial function: a role for $H_2O_2$, gap junctions and $IK_{Ca}$ channels**................................................................**41**

## *Chapter 3*

## A role for the sodium pump in $H_2O_2$-induced vasorelaxation in porcine isolated coronary arteries ........................................ 103

## *Chapter 4*

*Chapter 5*

**Sex differences in the role of NADPH oxidases in endothelium-dependent vasorelaxation in porcine isolated coronary arteries**

## *Chapter 6*

# Abbreviations

| | |
|---|---|
| **ACA** | 2-[3-(4-pentylphenyl)prop-2-enoylamino]benzoic acid |
| **BK$_{Ca}$** | Large-conductance calcium-activated K$^+$ channel |
| **Calcimycin (A23187)** | Calcium ionophore |
| **CNP** | C-type natriuretic peptide |
| **CPA** | Cyclopiazonic acid |
| **CVD** | Cardiovascular disease |
| **Cx** | Connexin |
| **DCB** | 2,4-dichlorobenzamil |
| **DCEBIO** | 5,6-dichloro-1-ethyl-1,3-dihydro-2H-benzimidazole-2-one |
| **DPI** | Diphenyliodonium chloride |
| **EDH** | Endothelium-derived hyperpolarization |
| **EDRF** | Endothelium-derived relaxing factor |
| **EETs** | Epoxyeicosatrienoic acids |
| **HCAs** | Human coronary arterioles |
| **h** | Hour |
| **H$_2$O$_2$** | Hydrogen peroxide |
| **IEL** | Internal elastic lamina |
| **IK$_{Ca}$** | Intermediate-conductance calcium-activated K$^+$ channel |
| **IP$_3$R** | 1,4,5-triphosphate receptor |
| **K$_{ATP}$** | ATP-sensitive K$^+$ channel |
| **K$_{ir}$** | Inwardly rectifying potassium channels |
| **K$_v$** | Voltage-gated K$^+$ channel |
| **KB-R7943** | 2-[4-[(4-nitrophenyl)methoxy]phenyl]ethyl ester |
| **L-NAME** | N$^G$-nitro-L-arginine methyl ester |
| **MEGJs** | Myoendothelial gap junctions |
| **min** | Minutes |
| **ML-171** | 2-acetylphenothiazine |
| **Na$^+$/K$^+$-ATPase** | Sodium-potassium adenosine triphosphatase |
| **NCX** | Sodium-calcium exchanger |
| **NO** | Nitric oxide |

| | |
|---|---|
| **Nox** | NADPH oxidase |
| **NS309** | 6,7-Dichloro-1$H$-indole-2,3-dione 3-oxime |
| **ODQ** | 1H-[1,2,4]Oxadiazolo[4,3-a]quinoxalin-1-one |
| **PCAs** | Porcine coronary arteries |
| **PEG-catalase** | Polyethylene glycol-catalase |
| **PGI$_2$** | Prostacyclin |
| **PKG1α** | Protein kinase G1α |
| **Pyr3** | Ethyl-1-(4-(2,3,3-trichloroprop-2-enoylamino)phenyl]-5-(trifluoromethyl)pyrazole-4-carboxylate |
| **RN1734** | 2,4-dichloro-N-propan-2-yl-N-[2-(propan-2-ylamino)ethyl]benzene sulfonamide |
| **ROS** | Reactive oxygen species |
| **sGC** | Soluble guanylyl cyclase |
| **SHR** | Spontaneously hypertensive rat |
| **SK$_{Ca}$** | Small-conductance calcium-activated $K^+$ channel |
| **SKF96365** | 1-[2-(4-methoxyphenyl)-2-[3-(4-methoxyphenyl)propoxy]ethyl] imidazole |
| **SNP** | Sodium nitroprusside |
| **SOD** | Superoxide dismutase |
| **TEA** | Tetraethylammonium |
| **TRP** | Transient receptor potential |
| **TRPC** | Transient receptor potential canonical channel |
| **TRPM** | Transient receptor potential melastatin channel |
| **TRPV** | Transient receptor potential vanilloid channel |
| **U46619** | 9,11-dideoxy-9α,11α -epoxymethanoprostaglandin $F_{2α}$ |
| **VSMC** | Vascular smooth muscle cell |
| **WKY** | Wistar-Kyoto rat |
| **ZDF** | Zucker diabetic fatty rat |
| **ZL** | Zucker lean rat |
| **1-EBIO** | 1-ethyl-2-benzimidazolinone |
| **2-APB** | 2-diphenylboranyloxyethanamine |
| **4-AP** | 4-aminopyridine |
| **18α-GA** | 18α-glycyrrhetinic acid |

# *Chapter 1*

---

**General Introduction**

## 1.1 Introduction

Regulation of the vascular tone plays an important role in maintaining blood pressure and flow. Increases in blood pressure can lead to cardiovascular diseases (CVDs) such as atherosclerosis, ischaemic heart disease, heart failure, renal damage and stroke. According to the British Heart Foundation, CVD is the UK's biggest killer and accounts for more than 50,000 premature deaths annually (Scarborough *et al.*, 2010). According to the European cardiovascular disease statistics, CVD causes more than 4 million deaths in Europe and more than 1.9 million deaths in the European Union each year (Nichols *et al.*, 2012). It is estimated that the overall CVD cost the European Union economy nearly €196 billion a year (Nichols *et al.*, 2012).

In the coronary circulation, regulation of vascular tone is controlled by endothelium-derived mediators such as endothelium-derived relaxing factors (EDRF), nitric oxide (NO) (Furchgott & Zawadzki, 1980; Palmer *et al.*, 1987), prostacyclin ($PGI_2$) (Dusting *et al.*, 1977; Moncada *et al.*, 1976) and endothelium-derived hyperpolarization-type (EDH) response (Feletou & Vanhoutte, 2013; Taylor & Weston, 1988). These endothelium-derived mediators are produced following increase in intracellular calcium upon stimulation by agonists such as bradykinin, acetylcholine (ACh) or shear stress (Griffith, 2004; Inagami *et al.*, 1995). The release of NO and $PGI_2$ will then activate guanylyl cyclase and adenylyl cyclase respectively causing an increase in the cGMP and cAMP levels in the vascular smooth muscle followed by cell hyperpolarization and relaxation (Inagami *et al.*, 1995) (Figure 1.2). Conversely, in pathological conditions such as diabetes, hypertension and aging, similar endothelium-dependent agonist including ACh, bradykinin or

shear stress stimulate the release of endothelium-derived contracting factors (EDCFs) causing vasoconstriction (Versari *et al.*, 2009). Examples of EDCFs include endothelin, angiotensin II and cyclooxygenase-derived products thromboxane $A_2$ and prostaglandin $H_2$ (Versari *et al.*, 2009).

In the normal healthy vasculature, endothelial cells play an important role in maintaining vascular homeostasis (Figure 1.1). The significant role of endothelial function in regulation of vascular tone was first reported in 1980 by Furchgott and Zawadzki. Using rabbit isolated thoracic aorta , Furchgott and Zawadzki demonstrated that acetylcholine-induced vasorelaxation was endothelium-dependent and removal of the endothelial cells either mechanically or by collagenase essentially abolished the vasorelaxation (Furchgott & Zawadzki, 1980). A small contraction was uncovered at higher concentration of acetylcholine in the endothelium-denuded aorta (Furchgott & Zawadzki, 1980).



Endothelial cells
Internal elastic lamina
Vascular smooth muscles cells
Fibrous tissue
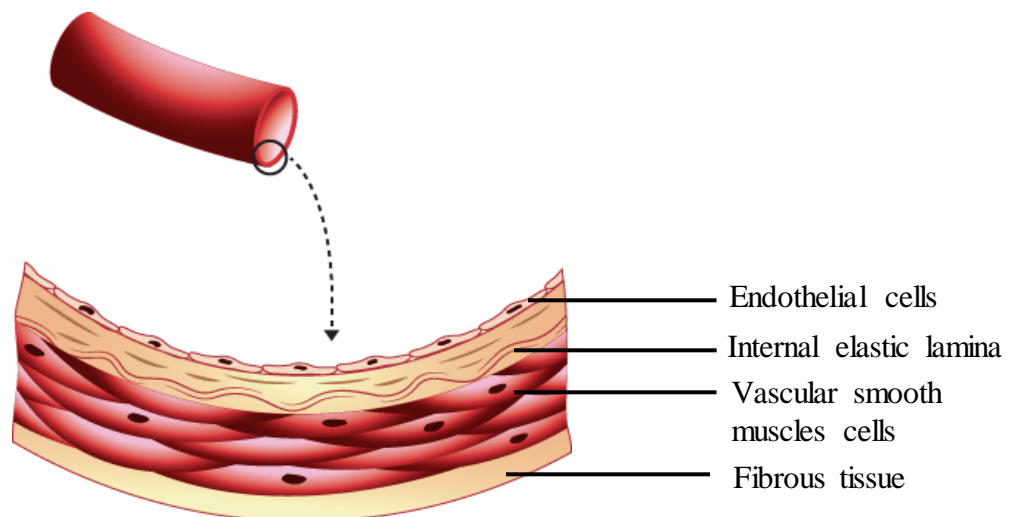
**Figure 1.1** Structure and composition of blood vessel. The innermost layer is made up of endothelial cells, followed by the internal elastic lamina and vascular smooth muscle cells. Figure adapted from Silverthorn & Johnson (2010).

At the time of discovery, it was hypothesized that the endothelium-derived substance(s) induced by ACh acted directly on the vascular smooth muscle to produce vasorelaxation (Furchgott & Zawadzki, 1980). This endothelium-derived relaxing factor (EDRF) was later identified as nitric oxide (NO) (Palmer *et al.*, 1987). Prostacyclin, a derivative of arachidonic acid was first reported to inhibit platelet aggregation (Moncada *et al.*, 1976). It was later confirmed by the same research group that the endogenous prostacyclin causes vasorelaxation in bovine coronary artery (Dusting *et al.*, 1977).

A third endothelium-derived mediator termed endothelium-derived hyperpolarizing factor (EDHF) was reported in the 1980s (Bolton *et al.*, 1984; Taylor & Weston, 1988). In mesenteric arteries from guinea-pig, Bolton *et al.* (1984) demonstrated that carbachol produced a concentration-dependent hyperpolarization and proposed that the hyperpolarization is caused by a factor released from the endothelium. A later study defined EDHF responses as the remaining proportion of endothelium-dependent vasorelaxation which is independent of NO or prostacyclin (Taylor & Weston, 1988). Taylor & Weston (1988) described a clear difference between EDHF and EDRF where EDHF causes vascular smooth muscle relaxation through hyperpolarization of the cells with no changes in the cGMP or cAMP levels. Since the introduction of the term EDHF nearly three decades ago, many entities have then been proposed to be an EDHF (Campbell *et al.*, 1996; Edwards *et al.*, 1998; Edwards *et al.*, 2010; Griffith, 2004; Shimokawa, 2010). However, it has now been agreed that the term 'EDHF' should no longer be used and the endothelium-derived mediators which cause endothelium-dependent

hyperpolarization (EDH) should be indicated by their proper names such CNP, EETs, $H_2O_2$, $H_2S$ and CO (Feletou & Vanhoutte, 2013).

## 1.2 The release and mechanism of action of Endothelium-Derived Hyperpolarization (EDH)-type responses

A present view on the release of endothelium-derived hyperpolarization mediators within the endothelial cells and the responses of the vascular smooth muscle cells is summarised in Figure 1.2. Many endothelium-derived mediators have been proposed to be responsible for EDH-type responses over the past decade, yet none has appeared to be a 'universal EDH' (Griffith, 2004). In 2010, the EDH-mediated responses were classified into two categories (Edwards *et al.*, 2010): The first category is the 'classical' EDH pathway in which an increase in intracellular $Ca^{2+}$ concentration hyperpolarizes the endothelial cells leading to activation of the small ($SK_{Ca}$) and intermediate ($IK_{Ca}$) conductance $Ca^{2+}$-activated potassium channels on endothelial cells (Busse *et al.*, 2002; Edwards *et al.*, 2010; Gluais *et al.*, 2005a). Activation of these potassium channels in turn hyperpolarizes the vascular smooth muscle either through the transfer of electrical signalling via myoendothelial gap junctions (MEGJs) (Chadha *et al.*, 2011; Chaytor *et al.*, 2003; Chaytor *et al.*, 1998; de Wit & Griffith, 2010; Edwards *et al.*, 2000; Harris *et al.*, 2000; Kenny *et al.*, 2002b; Kerr *et al.*, 2012; Sandow *et al.*, 2002) or through efflux of $K^+$ ions from endothelial $SK_{Ca}$ and $IK_{Ca}$ channels acting on barium-sensitive inwardly rectifying potassium channels ($K_{ir}$) and the ouabain-sensitive $Na^+/K^+$ ATPase pump respectively (Edwards *et al.*, 1998; Edwards *et al.*, 2010).

The second EDH-type pathway involves direct hyperpolarization of the vascular smooth muscle by endothelium-derived mediators including arachidonic acid derivatives (epoxyeicosatrienoic acids, EETs) (Campbell *et al.*, 1996), C-type natriuretic peptide (CNP) (Chauhan *et al.*, 2003; Wei *et al.*, 1994), hydrogen peroxide ($H_2O_2$) (Matoba *et al.*, 2000; Shimokawa, 2010) and $K^+$ ions (Edwards *et al.*, 1998; Feletou & Vanhoutte, 2013). In most studies, the EDH-type response is defined as the remaining proportion of endothelium-dependent vasorelaxation which are resistance to NO synthase and COX inhibition using pharmacological inhibitors L-NAME and indomethacin respectively (Beny & Schaad, 2000; Edwards *et al.*, 2010; McCulloch *et al.*, 1997; Quignard *et al.*, 1999; Senadheera *et al.*, 2012).

Emerging evidence has now shown that transient receptor potential (TRP) channels, expressed on both the endothelial cells and vascular smooth muscle cells play a role in regulation of vascular tone (Earley & Brayden, 2010; Sukumaran *et al.*, 2013). More specifically, TRPV4 channels from the vanilloid TRP subfamily and TRPC3 from the canonical TRP subfamily have been reported to play a role in NO- and EDH-mediated vasorelaxation (Bagher *et al.*, 2012; Bubolz *et al.*, 2012; Earley *et al.*, 2009; Huang *et al.*, 2011; Luksha *et al.*, 2009; Senadheera *et al.*, 2012; Zheng *et al.*, 2013b). TRP channels are $Ca^{2+}$-permeable cation channels which can be activated by shear stress, oxidative stress, light, temperature or chemical stimuli (Balzer *et al.*, 1999; Bari *et al.*, 2009; Earley & Brayden, 2010; Yao & Garland, 2005). To date, 28 mammalian TRP isoforms have been identified and they have been divided into six subfamilies based on their protein sequence homology and

DNA: ankyrin TRPA, canonical TRPC, melastatin TRPM, mucoliptin TRPML, polycystin TRPP, vanilloid TRPV (Earley & Brayden, 2010).
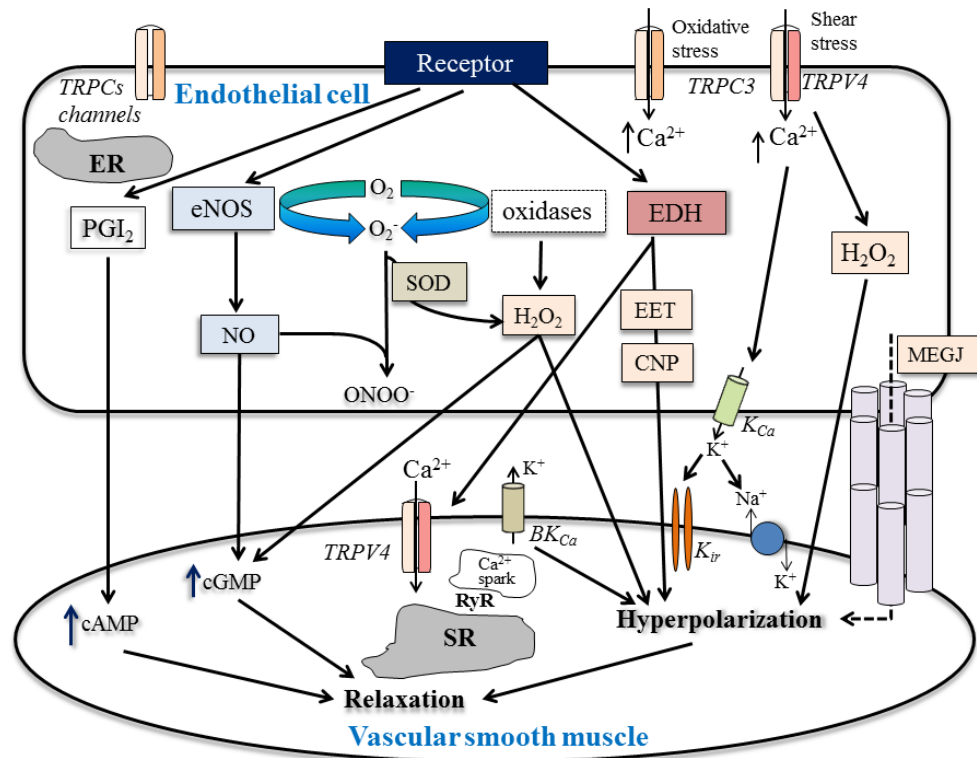


**Figure 1.2** The release and mechanisms of action of endothelium-derived vasorelaxant in regulation of vascular tone. Schematic diagram demonstrates potential pathways in nitric oxide (NO), prostacyclin (PGI$_2$) and endothelium-derived hyperpolarization (EDH)-mediated vasorelaxation involving transient receptor potential (TRP) channels, myoendothelial gap junction (MEGJ), calcium-activated potassium (K$_{Ca}$) channels, inwardly rectifying potassium (K$_{ir}$) channels and sodium-potassium adenosine triphosphatase (3Na$^+$/2K$^+$ ATPase). Endothelium-derived K$^+$ ions, epoxyeicosatrienoic acids (EET), C-type natriuretic peptide (CNP) and hydrogen peroxide (H$_2$O$_2$) are some of the candidates that have been proposed to be factors for EDH-type mediated relaxation. Figure adapted from Shimokawa (2010) and Earley & Brayden (2010).

## 1.3 Factors for the EDH-type mediated responses

### 1.3.1 C-type natriuretic peptide (CNP)

C-type natriuretic peptide (CNP), a 22-amino-acid peptide is a vasodilator which has been reported to be expressed in human cultured aortic endothelial cells and is present in human plasma (Stingo *et al.*, 1992). In patients with congestive heart failure, the urinary excretion of CNP has been reported to be three times higher than in healthy subjects with no differences detected in the plasma CNP levels between the two groups (Mattingly *et al.*, 1994).

In porcine coronary arteries (PCAs), rat mesenteric arteries, human penile resistance arteries and human omental fat resistance arteries, CNP caused a concentration-dependent vasorelaxation which was attenuated by high potassium (Barton *et al.*, 1998; Chauhan *et al.*, 2003; Kun *et al.*, 2008; Moyes *et al.*, 2014; Wei *et al.*, 1994). In previous studies using PCAs conducted by two different research groups, similar maximum relaxation to exogenously applied CNP have been reported (Barton *et al.*, 1998; Wei *et al.*, 1994). However, further studies using electrophysiological techniques led them to generate contradicting conclusions (Barton *et al.*, 1998; Wei *et al.*, 1994). Wei *et al.,* (1994) was the first group to propose that CNP could be a factor for EDH-type responses on the basis that CNP hyperpolarizes porcine coronary smooth muscle cells, which was inhibited by the $K^+$ channel inhibitor TEA, and that the CNP-induced vasorelaxation was charybdotoxin (calcium-activated $K^+$ channel inhibitor)-sensitive. However, in a later study in intact PCAs, due to the relatively smaller hyperpolarization and relaxation induced by CNP compared to bradykinin, Barton *et al.* (1998) concluded that CNP is unlikely to be a factor for EDH-type responses.

In the Langendorff-perfused rat heart, CNP produced a concentration-dependent decrease in perfusion pressure (Hobbs *et al.*, 2004) which was sensitive to inhibition of NO synthase and blockade of $K_{ATP}$ and $BK_{Ca}$ channels (Brunner & Wolkart, 2001). Measurement of cGMP levels in the coronary effluent demonstrated that CNP produces a concentration-dependent increase in cGMP levels (Brunner & Wolkart, 2001). However, in the same study using rat isolated aorta, inhibition of NO synthase had no effect on the CNP-induced vasorelaxation, demonstrating that the mechanism of CNP-induced vasorelaxation differs between vascular bed (Brunner & Wolkart, 2001).

In rat isolated mesenteric arteries, inhibition of the $K_{ir}$ and $Na^+/K^+$-pump essentially abolished the ACh-, CNP- and cANF[4-23] (a selective NPR-C agonist)-induced EDH-type vasorelaxation (Chauhan *et al.*, 2003). This lead to their conclusion that CNP-induced vasorelaxation involved activation of the NPR-C receptor (Chauhan *et al.*, 2003). Later studies using the selective NPR-C receptor antagonist, M372049 further confirmed that this receptor is involved in the CNP-induced vasorelaxation pathway (Hobbs *et al.*, 2004; Villar *et al.*, 2007). In the absence of NO and $PGI_2$, HS-142-1, a selective NPR-A/B antagonist had no effect on the ACh- or CNP-induced vasorelaxation suggesting that NPR-A/B receptors are not involved in the CNP-induced vasorelaxation (Chauhan *et al.*, 2003). CNP bioassay using effluent collected from rat isolated superior mesenteric arterial bed after perfusion with ACh (in the presence of L-NAME and indomethacin) demonstrated that, the EDH-type response involved the release of CNP (Chauhan *et al.*, 2003). This was dependent on the endothelium and

myoendothelial gap junction communication (Chauhan *et al.*, 2003; Hobbs *et al.*, 2004).

In endothelial cell CNP knock-out (ecCNP KO) mice or NPR-C receptor knock-out (NPR-C KO) mice, sex differences in the ACh-induced vasorelaxation in the absence or presence of L-NAME and indomethacin have been reported (Moyes *et al.*, 2014). Moyes *et al.* (2014) reported a decrease in potency for ACh in the EDH-type response only in mesenteric arteries from female ecCNP KO and NPR-C KO mice but not males. Similarly, in the absence of L-NAME and indomethacin, there is a decrease in potency for ACh-induced vasorelaxation only in mesenteric arteries from female but not male ecCNP KO mice (Moyes *et al.*, 2014). Their pharmacological response study corresponds with their *in vivo* study, where they have reported that in ecCNP KO mice with impaired endothelial function, there is a significant increase in mean arterial pressure in female but not male mice compared with their respective WT littermates (Moyes *et al.*, 2014).

In contrast to the studies described above, researchers from other laboratories using rat mesenteric arteries and guinea pig carotid arteries reported that CNP in unlikely to be a factor for EDH-type response on the basis that exogenously applied CNP only produce modest relaxation without hyperpolarization and the ACh-induced EDH-type response was insensitive to M372049, a selective NPR-C receptor antagonist (Dora *et al.*, 2008; for a review see Garland & Dora, 2008; Leuranguer *et al.*, 2008b).

In human forearm resistance arteries, CNP has been reported to be a factor for EDH-type response as the CNP-induced concentration-dependent vasodilatation was abolished in the presence of a relatively low concentration

of TEA (0.5 mM)  (Honing *et al.*, 2001), a concentration used to inhibit $K_{Ca}$ channels. In human penile isolated resistance arteries, CNP produced an endothelium-independent hyperpolarization and concentration-dependent vasorelaxation which was sensitive to the blockade of the $Na^+/K^+$-pump, $K_{ir}$, $SK_{Ca}$, $IK_{Ca}$ and $BK_{Ca}$ (Kun *et al.*, 2008). Further studies using $cANF^{4-23}$ as a selective NPR-C agonist resulted in concentration-dependent vasorelaxation, suggesting the presence of NPR-C receptors in these arteries (Kun *et al.*, 2008). In human resistance arteries from omental fat, the CNP-induced vasorelaxation in the presence of L-NAME and indomethacin were significantly attenuated in the presence of M372049, a selective NPR-C receptor antagonist  (Moyes *et al.*, 2014).

After more than two decades of studies on CNP, due to the conflicting results presented by different research groups using various species of study and different vascular bed, a direct comparison or a definitive role for CNP as a factor for EDH-type response is still not possible and remains to be determined in future studies (Luksha *et al.*, 2009; Sandow & Tare, 2007).

## 1.3.2 Epoxyeicosatrienoic acids (EETs)

Apart from prostacyclin, other metabolites of arachidonic acid (AA) produced by endothelial cells include epoxyeicosatrienoic acids (EETs) which are derived from the cytochrome P450-dependent pathways (Edwards *et al.*, 2010; Rosolowsky & Campbell, 1993). These EETs consist of four different regioisomers including 5,6-EET; 8,9-EET; 11,12-EET and 14,15-EET and have been proposed to be factors for EHD-type responses (Figure 1.3) (Campbell *et al.*, 1996; Weston *et al.*, 2005). An early study on bovine coronary arteries demonstrated that AA caused endothelium-dependent vasorelaxation (Rosolowsky & Campbell, 1993). Further work by the same group found that the relaxations to AA and EET were attenuated by the presence of high potassium, TEA and charybdotoxin leading to their conclusion that EET is a factor for EDH-type response (Campbell *et al.*, 1996).
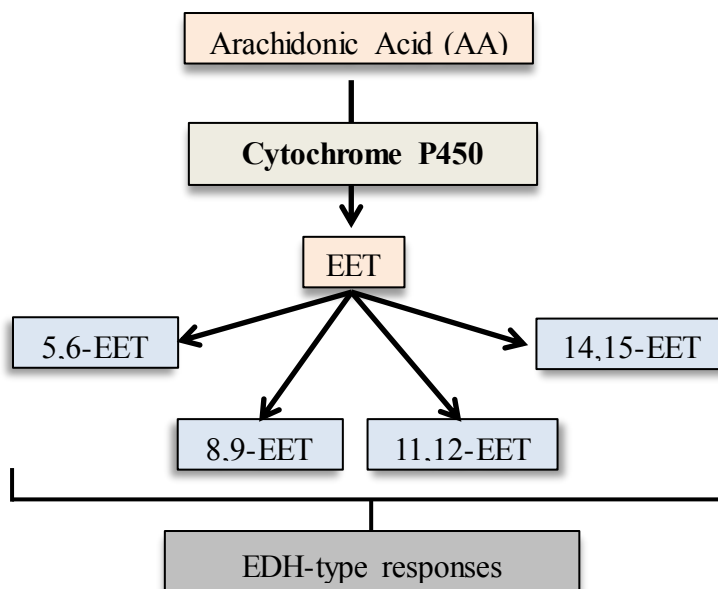


**Figure 1.3** Different cytochrome P450 metabolites of arachidonic acid including 5,6-EET; 8,9-EET; 11,12-EET and 14,15-EET that have been proposed to be a factor for EDH-mediated response. EET, epoxyeicosatrienoic acids.

Other studies have reported that 11,12-EET hyperpolarizes bovine, porcine and guinea-pig coronary smooth muscle cells (Campbell *et al.*, 1996; Eckman *et al.*, 1998; Edwards *et al.*, 2000). In guinea-pig coronary arteries, the hyperpolarization and potency of the AA- and 11,12-EET-induced vasorelaxations were significantly reduced in the presence of iberiotoxin, indicating that the $BK_{Ca}$ channels play a role in the EET-induced EDH-type response (Eckman *et al.*, 1998). In porcine coronary smooth muscle cells, hyperpolarization to 11,12-EET was essentially abolished in the presence of iberiotoxin (Edwards *et al.*, 2000). Using selective EET antagonists, Weston *et al,* (2005) reported that in PCAs, bradykinin-induced EET release involved both the 'classical' EDH-type response (activation of endothelial $SK_{Ca}$ and $IK_{Ca}$) and activation of the iberiotoxin-sensitive $BK_{Ca}$ channels.

In mouse isolated mesenteric arteries, the effects of 11,12-EET-induced vasorelaxation and hyperpolarization were both endothelium-dependent and – independent (Earley *et al.*, 2009). These vasorelaxant and hyperpolarization responses were significantly reduced when either both $SK_{Ca}$ and $IK_{Ca}$ channels were blocked together or when $BK_{Ca}$ was blocked (Earley *et al.*, 2009). When all three $K_{Ca}$ channels were blocked, the 11,12-EET-induced hyperpolarization was completely abolished, whereas the vasorelaxation was nearly abolished (Earley *et al.*, 2009). In human isolated coronary arterioles (HCAs), the presence of both $SK_{Ca}$ and $IK_{Ca}$ inhibitors significant reduced the AA-induced vasorelaxation (Zheng *et al.*, 2013b). The AA-induced vasorelaxation was essentially abolished in the presence of high potassium, indicating that in HCAs, the AA-induced vasorelaxation involved the EDH-type response (Miura & Gutterman, 1998; Zheng *et al.*, 2013b).

**1.3.3 Hydrogen Peroxide ($H_2O_2$)**

Hydrogen peroxide ($H_2O_2$) is one of the many reactive oxygen species (ROS) generated within the endothelium following stimulation by agonists such as acetylcholine and bradykinin or stimuli such as shear stress (Matoba *et al.*, 2003; Matoba *et al.*, 2000; Miura *et al.*, 2003). Other ROS generated within the endothelium include nitric oxide (NO), peroxynitrite ($ONOO^-$), superoxide anions ($O_2^-$) and hydroxyl radicals ($OH^-$) (Brandes & Mugge, 1997; Edwards *et al.*, 2010; Gryglewski *et al.*, 1986; Shimokawa, 2010). The precursor of $H_2O_2$, superoxide anions, can be generated within the endothelium from sources such as eNOS, NADPH oxidases (Nox), xanthine oxidase, cyclooxygenases, lipoxygenases, CYP450 epoxygenases and mitochondria (Edwards *et al.*, 2010; Shimokawa & Morikawa, 2005). Through uncoupling of eNOS, superoxide anions can be generated as by-product from the catalysis of L-arginine to NO (Figure 1.2) (Matoba *et al.*, 2000). The generated superoxide anions can then form $H_2O_2$ either by spontaneous dismutation or catalysed by superoxide dismutase (SOD) (Faraci & Didion, 2004). Alternatively, superoxide can also react with endothelial NO to form $ONOO^-$ (Figure 1.2) (Gryglewski *et al.*, 1986). Therefore, the second major function of SOD is to prolong the half-life of NO protecting NO and NO-mediated signalling in the blood vessels (Faraci & Didion, 2004; MacKenzie *et al.*, 1999; Shimokawa, 2010).

In tissues, another significant source of intracellular ROS is the NADPH oxidase enzymes where superoxide anions are formed through reduction of $O_2$ using NADPH or NADH as an electron donor (Chen *et al.*, 2012; Paravicini & Touyz, 2008). To date, seven different Nox isoforms have

been identified including Nox1-5, Duox1 and Duox2 (Paravicini & Touyz, 2008), but within the vasculature, only Nox1, Nox2, Nox4 and Nox5 isoforms have been reported to be involved in many cardiovascular diseases such as hypertension, atherosclerosis, stroke, diabetes and ischaemia-reperfusion damage (Kleinschnitz *et al.*, 2010; Paravicini & Touyz, 2008; Streeter *et al.*, 2013; Wingler *et al.*, 2011).

In rat aortic smooth muscle cells, it has been shown that Nox1 produces primarily superoxide, while Nox4 produces mainly $H_2O_2$ (Dikalov *et al.*, 2008). In transgenic mice overexpressed with endothelial Nox4, a significantly higher amount of $H_2O_2$ has been detected in the aortic homogenates compared to the control (Ray *et al.*, 2011). The blood pressures in the Nox4 overexpressed mice were significantly lower compared to the WT before and after chronic treatment of angiotensin II (1.1 mg/kg/day) (Ray *et al.*, 2011). In experiments using isolated aortae, the ACh-induced vasorelaxation was enhanced in the Nox4 overexpressed transgenic mice compared to the WT littermate mice and the enhancement was abolished by catalase, indicating that the enhancement is attributed to $H_2O_2$ (Ray *et al.*, 2011). Hence, these authors concluded that the increase in endothelial Nox4 activity may provide beneficial effects to the vascular tone as opposed to the functional effects of Nox1 and Nox2 (Ray *et al.*, 2011).

In a different study, a higher level of Nox4 proteins has been detected in ischaemic brain samples taken from stroke patients and mice (Kleinschnitz *et al.*, 2010). In this study, Kleinschnitz *et. al.* (2010) reported that pharmacological inhibition with the NADPH oxidase inhibitor, VAS2870, but not apocynin, given *in vivo* 2 h and 12 h post-stroke mimicked the

neuroprotective effects observed in Nox4 knock-out mice where the ROS formation and brain infarct volume were reduced with significant improvement in neurological function (Kleinschnitz *et al.*, 2010). Given the fact that whilst endothelial Nox4 overexpressed mice provide beneficial effects on the vascular tone (Ray *et al.*, 2011), the same Nox isoform, Nox4, seems to be the major source of oxidative stress after acute stroke, having a detrimental effect in the brain (Kleinschnitz *et al.*, 2010). Therefore, the role of Nox4 generated $H_2O_2$ within the vasculature may provide contradictory effects depending on the experimental conditions and vascular beds (Kleinschnitz *et al.*, 2010; Streeter *et al.*, 2013).

$H_2O_2$ was first reported to hyperpolarize smooth muscle cells and produce concentration-dependent vasorelaxation in PCAs in 1991 (Beny & von der Weid, 1991). However, due to the lack of effect to bradykinin and substance P-induced endothelium-dependent hyperpolarization in the presence of catalase, Bény and van der Weid concluded that the EDH-type response induced by bradykinin or substance P and $H_2O_2$ may be of two different entities (Beny & von der Weid, 1991). A later study in rabbit iliac arteries similarly reported that catalase had no effect on the ACh- and A23187-induced hyperpolarization, but significantly inhibited the vasorelaxation to both compounds, leading the authors to conclude that, endogenous $H_2O_2$ is not a hyperpolarizing factor, but is a relaxing factor (Chaytor *et al.*, 2003). Further studies in various vascular beds, including porcine and human coronary arterioles, human and murine mesenteric arteries and murine aortae, $H_2O_2$ has been reported to act as a vasodilator (Beny & von der Weid, 1991; Liu *et al.*,

2011; Matoba *et al.*, 2002; Matoba *et al.*, 2003; Miura *et al.*, 2003; Ohashi *et al.*, 2012).

Early studies in bovine isolated pulmonary arteries and PCAs reported that $H_2O_2$–induced endothelium-independent vasorelaxation through activation of soluble guanylyl cyclase producing cGMP (Burke & Wolin, 1987; Hayabuchi *et al.*, 1998). However, a study from a different group failed to demonstrate the involvement of cGMP in the $H_2O_2$-induced response in PCAs (Barlow & White, 1998). Instead they have reported that $H_2O_2$-induced hyperpolarization and relaxation through potassium channels and large conductance calcium-activated $K^+$ channels ($BK_{Ca}$) (Barlow & White, 1998). Other studies in human coronary arterioles and PCAs similarly reported that $BK_{Ca}$ channels play a role in the $H_2O_2$-induced vasorelaxation (Hayabuchi *et al.*, 1998; Liu *et al.*, 2011; Miura *et al.*, 2003). However, this observation was not universal as studies from other laboratories reported that inhibition of $BK_{Ca}$ channels had no effect on the $H_2O_2$-induced vasorelaxation in mouse mesenteric arteries (Ellis *et al.*, 2003; Matoba *et al.*, 2000). Nonetheless, studies in a variety of different vessels including PCAs, murine mesenteric arteries and aortae, human mesenteric arteries and coronary arterioles and canine coronary arteries all came to the same conclusion that $K^+$ channels play a role in the $H_2O_2$-induced response as the $H_2O_2$-induced vasorelaxation was sensitive to high potassium and/or tetrabutylammonium (Ellis *et al.*, 2003; Matoba *et al.*, 2002; Matoba *et al.*, 2003; Matoba *et al.*, 2000; Miura *et al.*, 2003; Ohashi *et al.*, 2012; Rogers *et al.*, 2006; Thengchaisri & Kuo, 2003). In small mesenteric arteries from mice, Matoba *et al*. (2000) reported that the ACh–induced EDH-type response was sensitive to catalase and the formation

of endothelial $H_2O_2$ was detected using confocal microscope with dichlorodihydrofluorescein diacetate (DCF) dye. Therefore, they concluded that $H_2O_2$ is a factor for EDH-type response in murine small mesenteric arteries (Matoba *et al.*, 2000). Similarly in porcine coronary microvessels, Matoba and colleagues have provided further evidence that $H_2O_2$ acts as a factor for EDH-type response by demonstrating that bradykinin-induced EDH-type vasorelaxation is sensitive to catalase and the production of endothelial $H_2O_2$ was detected using electron spin resonance method (Matoba *et al.*, 2003). They have also reported that exogenous $H_2O_2$ hyperpolarizes and relaxes vascular smooth muscle through $K^+$ channels (Matoba *et al.*, 2003). In human coronary arterioles, endogenous $H_2O_2$ induced by shear stress have been reported to be a factor for EDH-type response (Miura *et al.*, 2003).

Conversely, a study from another laboratory using small mesenteric arteries isolated from WT or type II diabetic mice failed to demonstrate that $H_2O_2$ plays a role in the ACh-induced EDH-type vasorelaxation (Ellis *et al.*, 2003). In the same arteries, although the $H_2O_2$-induced vasorelaxation was abolished by high potassium (60 mM), inhibition of the $Na^+/K^+$-ATPase, $K_{ir}$, $K_v$ or the $K_{Ca}$ channels had no effects on the $H_2O_2$-induced vasorelaxation (Ellis *et al.*, 2003). This is in contrast with other studies where, in human coronary arterioles, the $H_2O_2$-induced vasorelaxation was sensitive to apamin ($SK_{Ca}$ channel inhibitor) and charybdotoxin (Miura *et al.*, 2003), while in rat and canine coronary arteries, the $H_2O_2$-induced vasorelaxation was sensitive to 4-aminopyridine ($K_v$ channel blocker) (Rogers *et al.*, 2006). Hence, it is possible that the response to $H_2O_2$ may vary between species, vascular beds and experimental conditions (Edwards *et al.*, 2010; Thakali *et al.*, 2006).

**1.3.4 Potassium ($K^+$) ions, Calcium-activated Potassium ($K_{Ca}$) Channels and Transient Receptor Potential (TRP) Channels**

As described above, in the 'classical' EDH pathway, activation of the endothelial $SK_{Ca}$ and $IK_{Ca}$ channels causes efflux of $K^+$ ions into the extracellular space (Figure 1.4) (Edwards *et al.*, 1998; Edwards & Weston, 2004; Weston *et al.*, 2005). In rat hepatic arteries, the concentration of $K^+$ detected in the myoendothelial space was raised to ~6 mM in ACh (10 μM)-induced hyperpolarization (Edwards *et al.*, 1998). In these vessels, the increase in $K^+$ concentration in the myoendothelial space is abolished in the presence of apamin plus charybdotoxin, inhibitors of the $SK_{Ca}$, $IK_{Ca}$ and $BK_{Ca}$ channels (Edwards *et al.*, 1998). In endothelial cells from PCA, hyperpolarization induced by bradykinin (in the presence of L-NAME and indomethacin) was significantly inhibited by TRAM-39 and apamin, inhibitors of the $IK_{Ca}$ and $SK_{Ca}$ channels respectively (Weston *et al.*, 2005). This residual hyperpolarization was completely abolished in the additional presence of iberiotoxin, an inhibitor of the $BK_{Ca}$ channel, indicating that all three channels are involved in the EDH-type response (Weston *et al.*, 2005).

In human coronary arterioles, flow-induced vasodilatation and hyperpolarization were abolished in the presence charybdotoxin suggesting that $K_{Ca}$ channels play a role in the shear stress-induced endothelium-dependent vasorelaxation (Miura *et al.*, 2001).
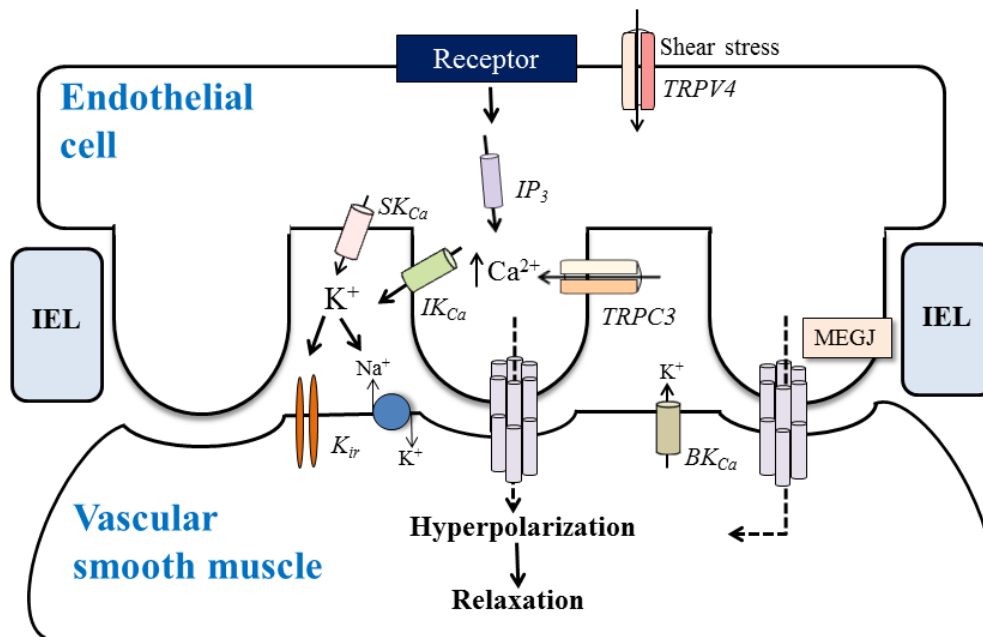
**Figure 1.4** Hypothesized schematic diagram of the EDH-type mediated vasorelaxation signalling at the myoendothelial contact sites involving endothelial cell projections through internal elastic lamina (IEL). Senadheera *et al.* (2012) reported that in rat mesenteric artery, TRPC3 channels, intermediate-conductance calcium-activated potassium channels (IK$_{Ca}$), gap junction connexins and 1,4,5-triphosphate receptor (IP$_3$R) occur in close proximity within the endothelial cell projections. Ca$^{2+}$ influx from TRPC3 channels or Ca$^{2+}$ release from IP$_3$-sensitive stores activates endothelial SK$_{Ca}$ and IK$_{Ca}$ channels, followed by K$^+$ efflux and activation of K$_{ir}$ and Na$^+$/K$^+$ ATPases on the vascular smooth muscle. TRPV4 channels have also been shown to play a role in endothelium-dependent vasorelaxation. Figure adapted from Edwards *et al.* (2010) and Senadheera *et al.* (2012).

The efflux of K$^+$ ions from the endothelium will, in turn, activate the Na$^+$/K$^+$-ATPase pump and K$_{ir}$ channels on the vascular smooth muscle leading to hyperpolarization and relaxation of the smooth muscle (Edwards *et al.*, 1998). In rat hepatic and mesenteric arteries, Edwards *et al.* (1998) reported that extracellular K$^+$ mimics the effect of EDH-type response, hyperpolarizing and relaxing vascular smooth muscle. These EDH-type responses were

abolished by the presence of ouabain ($Na^+/K^+$-ATPase inhibitor) and barium ($K_{ir}$ channel blocker) leading to their conclusion that $K^+$ is likely to be factor for EDH-type response via activation of the $Na^+/K^+$-ATPase and $K_{ir}$ channels (Edwards *et al.*, 1998). This conclusion was further supported by studies conducted on other vascular beds including human thyroid arteries, rat middle cerebral arteries and PCAs (Beny & Schaad, 2000; McNeish *et al.*, 2005; Torondel *et al.*, 2004). However, studies from other laboratories using rat hepatic arteries, human subcutaneous arteries, PCAs, guinea-pig carotid and coronary arteries reported that $K^+$ is unlikely to be a factor for EDH-type responses and that ouabain and/or barium had no effect on the ACh- or bradykinin-induced hyperpolarization (Coleman *et al.*, 2001; Quignard *et al.*, 1999). This leads to the proposal that in vessels where activation of the $Na^+/K^+$-ATPase and $K_{ir}$ channels were not involved, electronic signalling were transferred from the endothelial cells to the smooth muscle cells via gap junctions (Figure 1.4) (Chaytor *et al.*, 2003; Edwards *et al.*, 2000; for a review see Griffith, 2004; Harris *et al.*, 2000). Further details about the involvement of gap junctions in EDH-mediated responses will be discussed later (Section 1.3.5).

As mentioned briefly in Section 1.2, studies have now provided evidence that TRP channels play a role in regulation of vascular tone (Earley & Brayden, 2010; Sukumaran *et al.*, 2013). In murine isolated mesenteric arteries, the vasorelaxation and hyperpolarization of the EDH-type response induced by ACh were significantly reduced (~75%) in TRPV4 knockout mice compared to the WT mice (Earley et al., 2009). Furthermore, this group of researchers demonstrated that the 11,12-EET-induced vasorelaxation and

hyperpolarization were completely abolished in TRPV4 KO mice compared to the control (Earley *et al.*, 2009). In human isolated coronary arterioles (HCAs), AA-induced vasorelaxation was significantly reduced in the presence of RN1734, a selective TRPV4 antagonist (Zheng *et al.*, 2013b). Whereas, in TRPV4 overexpressed HCAECs, all four of the different AA metabolites; 5,6-EET; 8,9-EET; 11,12-EET and 14,15-EET were less potent than AA in activation of TRPV4 channels (Zheng *et al.*, 2013b).

In rat mesenteric artery endothelial cells, physical and functional interaction between TRPV4 and $SK_{Ca}$ channels have been reported (Ma *et al.*, 2013). Using inhibitors of the TRPV4 and $SK_{Ca}$ channels, RN1734 and apamin respectively, Ma *et al.* (2013) demonstrated that the membrane potential and relaxation to ACh in rat isolated mesenteric arteries were significantly attenuated. Both inhibitors have been shown to reduce the local blood flow in *ex vivo* mesenteric arterial bed induced by 4α-PDD (activator of TRPV4 channels) and ACh (Ma *et al.*, 2013). This group of researchers also reported that the $BK_{Ca}$ channels expressed in the vascular smooth muscle cells isolated from rat aortae are physically associated with TRPC1 channels where influx of $Ca^{2+}$ through TRPC1 activates $BK_{Ca}$ which then leads to membrane hyperpolarization (Kwan *et al.*, 2009).

A different study has reported that TRPC3 channels are involved in endothelial NO release in PCAs (Huang *et al.*, 2011). In rat mesenteric arteries, blocking $SK_{Ca}$, $IK_{Ca}$ or TRPC3 channel individually using pharmacological inhibitors significantly reduced the ACh-induced, EDH-type vasorelaxation (Senadheera *et al.*, 2012). The residual relaxation was completely abolished in the presence of either a combination of $SK_{Ca}$ and TRPC3 channel antagonists

or a combination of $IK_{Ca}$ and TRPC3 channel antagonists (Senadheera *et al.*, 2012). Immunohistochemical studies have demonstrated that ~73% of these TRPC3 channels are expressed in the internal elastic lamina (IEL) hole sites with about three-fold higher frequency than the expression of myoendothelial gap junctions (MEGJs) (Figure 1.4) (Senadheera *et al.*, 2012). Therefore, the authors concluded that in rat mesenteric artery, $Ca^{2+}$ influx through TRPC3 channels facilitates EDH-type response through activation of endothelial $SK_{Ca}$ and $IK_{Ca}$ channels.

A different study conducted by the same research group comparing isolated third order uterine radial arteries from pregnant rats with age-matched non-pregnant rats reported that the EDH-type activity is enhanced in vessels from pregnant rats (Senadheera *et al.*, 2013). These authors suggested that the increase in EDH-type activity in vessels from pregnant rats could be related to the increase in expression and activity of TRPV4 channels (Senadheera *et al.*, 2013). However, a reduction in the incidence of MEGJs in pregnant rats was also reported (Senadheera *et al.*, 2013). As opposed to rat cremaster arterioles where TRPV4 channels and $IK_{Ca}$ channels have been reported to cluster within the endothelial cell projection microdomain (Bagher *et al.*, 2012), TRPV4 channels in radial arteries from both pregnant or non-pregnant rats were not expressed near the IEL (Senadheera *et al.*, 2013). Therefore, the roles of TRP or $K_{Ca}$ channels may vary between species and vascular bed under study.

**1.3.5 Myoendothelial Gap Junctions (MEGJs)**

As previously mentioned (Section 1.2), increases in intracellular calcium in the endothelium activate endothelial $SK_{Ca}$ and $IK_{Ca}$ channels which in turn hyperpolarize VSMCs either through release of $K^+$ ions from these channel leading to activation of VSMCs $K_{ir}$ channel and ouabain-sensitive $Na^+/K^+$ ATPase pump (Edwards *et al.*, 1998; Edwards *et al.*, 2010) or through electrical signalling via myoendothelial gap junctions (de Wit & Griffith, 2010; Edwards *et al.*, 2010). Gap junctions have been reported to facilitate communication between endothelial cells, between VSMCs and between endothelial cells and VSMCs (Edwards *et al.*, 2010).

Gap junctions are made up of two docking hemichannels or connexons which allow passage of small molecules or second messenger of less than 1 kDa to diffuse through (de Wit & Griffith, 2010; van Kempen & Jongsma, 1999). Each connexon is composed of six connexins (Cx), transmembrane proteins. Within the vasculature, expression of Cx37, Cx40, Cx43 and Cx45 subunits has been detected in the endothelial and/or VSMCs (Chaytor *et al.*, 2003; Hill *et al.*, 2002; Kerr *et al.*, 2012; Lang *et al.*, 2007; Luksha *et al.*, 2009; van Kempen & Jongsma, 1999). However, the expression and distribution of different connexin proteins varies between vascular bed and species of studied (Hill *et al.*, 2002; Luksha *et al.*, 2009; van Kempen & Jongsma, 1999). Hill *et al.* (2002) reported that the number of MEGJs increased with decreasing vessel size in rat mesenteric arteries, while Sandow *et al.* (2002) detected MEGJs in rat mesenteric arteries but not femoral arteries.

In functional studies, non-selective gap junction inhibitors, 18α-glycyrrhetinic acid, carbenoxolone and palmitoleic acid have been reported to

inhibit the endothelium-dependent, EDH-type vasorelaxation in rat isolated mesenteric arterial bed, human myometrial arteries, omental arteries and veins isolated from pregnant women, suggesting that gap junctional communications play a role in the EDH-type response (Hammond *et al.*, 2011; Harris *et al.*, 2000; Kenny *et al.*, 2002b). Similarly, in PCAs, Gap 27, a connexin mimetic peptide, significantly reduced the substance P- and bradykinin-induced hyperpolarization demonstrating the involvement of gap junctional communication in the EDH-type response (Edwards *et al.*, 2000).

A different study using different Cx-mimetic peptide [37,43]Gap27, [40]Gap27 and [43]Gap26 to disrupt intercellular communication by targeting Cx37, Cx40 and Cx43 of the MEGJs in rabbit isolated iliac arteries demonstrated these peptides had no effect on the A23187-induced EDH-type vasorelaxation when used alone (Chaytor *et al.*, 2003). However, in the presence of all three peptides in combination, the potency of A23187-induced EDH-type response was significantly reduced confirming that more than one Cx subtype are involved in the gap junctional communications (Chaytor *et al.*, 2003; Luksha *et al.*, 2009). Furthermore, the presence of all three peptides in combination abolished the ACh- and A23187-induced hyperpolarization (Chaytor *et al.*, 2003). Similarly, the presence of all three peptides essentially abolished the bradykinin-induced EDH-type vasorelaxation in resistance arteries isolated from subcutaneous fat of healthy pregnant women (Lang *et al.*, 2007). In addition, immunohistochemistry confirmed the expression of Cx37, Cx40 and Cx43 proteins in resistance arteries isolated from subcutaneous fat of healthy pregnant women (Lang *et al.*, 2007), omental arteries and veins isolated from healthy pregnant women (Hammond *et al.*, 2011) and in iliac

arteries isolated from rabbit (Chaytor *et al.*, 2003). Interestingly, in the presence of all three Cx-mimetic peptides, the additional presence of catalase abolished the A23187-induced vasorelaxation in resistance arteries isolated from subcutaneous fat of healthy pregnant women (Lang *et al.*, 2007). In a different study, the presence of carbenoxolone and catalase produced a greater inhibition compared to when used alone in bradykinin-induced EDH-type response in omental arteries and veins isolated from healthy pregnant women (Hammond *et al.*, 2011). These authors proposed that gap junctional communication and endogenous $H_2O_2$ compensate each other in the EDH-type response (Hammond *et al.*, 2011).

As mentioned in Section 1.3.4, MEGJs have been reported to cluster in the endothelial cell projection within the internal elastic lamina space (IEL) (Figure 1.4) (Kerr *et al.*, 2012; Sandow *et al.*, 2002). In rat mesenteric arteries, studies have demonstrated that endothelial $IK_{Ca}$ channels and $Na^+/K^+$-ATPase are highly expressed in the endothelial cell projections and are co-localised with MEGJs specifically Cx37 and Cx40 proteins (Dora *et al.*, 2008; Sandow *et al.*, 2006). Similarly, endothelial $IK_{Ca}$ channels and Cx37 proteins were detected within the IEL which corresponds with the functional study where presence of carbenoxolone and TRAM-34 essentially abolished the bradykinin-induced EDH-type response in human mesenteric arteries (Chadha *et al.*, 2011). See Section 1.3.4 for discussion on interactions between MEGJs and TRP channels.

## 1.4 Physiological relevance of EDH-type responses

In the vasculature, endothelial cells play an important role in maintaining vascular homeostasis, exerting both vasodilatation and vasoconstrictor effects on the VSMCs to control blood pressure (Durand & Gutterman, 2013). The EDH-type responses have been reported to play a role under physiological conditions, either in health or in disease (acting as a 'back-up' system for NO, see Section 1.6) (Durand & Gutterman, 2013; McCulloch *et al.*, 1997; Yang *et al.*, 2007). In humans, the contribution of different types of endothelium-derived vasodilators varies with age and under certain physiological conditions such as pregnancy (Al-Shaer *et al.*, 2006; Durand & Gutterman, 2013; Miura *et al.*, 2001; Yang *et al.*, 2007).

A preliminary study of flow-induced vasodilatation in human isolated coronary microvessels from different age groups demonstrated that in vessels isolated from children (age 0-18) vasodilatation was mainly mediated by prostaglandins, and the contribution of prostaglandin reduces with age as the role of NO increases (Zinkevich *et al.*, 2010). However, in disease, human coronary arterioles isolated from adults with coronary artery disease showed a reduction in the flow-induced vasodilatation with an increase in EDH-type responses to compensate the loss of NO (Miura *et al.*, 2001). A later study conducted by the same research group reported that endothelium-dependent $H_2O_2$ plays a role in the flow-induced vasodilatation in human coronary arterioles from patients with heart disease (Miura *et al.*, 2003).

In vascular responses measuring forearm blood flow of healthy human subjects, ACh-induced vasodilatation was significantly lower in elderly subjects compared to young subjects and the reduction in vasodilatation was

attributed to the loss of NO (Al-Shaer *et al.*, 2006). In addition to that, a reduction in the human forearm blood flow to an endothelium-independent vasodilator, sodium nitroprusside was reported in healthy elderly subject compared to the young subjects suggesting that vascular dysfunction occurred with the aging process (Al-Shaer *et al.*, 2006).

The other physiological condition which alters the contribution of endothelium-dependent vasorelaxation is during pregnancy (Yang *et al.*, 2007). A previous study demonstrated an enhancement in the bradykinin-induced vasorelaxation in resistance arteries from normotensive pregnant women compared to non-pregnant women (Knock & Poston, 1996). In the presence of NO synthase inhibitor, no differences between both groups were detected in the bradykinin-induced vasorelaxation suggesting a greater role for NO in resistance arteries from pregnant women (Knock & Poston, 1996). In isolated resistance arteries from women with pre-eclampsia, the bradykinin-induced vasorelaxation was significantly reduced compared to women with normotensive pregnancy (Knock & Poston, 1996). The presence of NO synthase inhibitor further reduced the bradykinin-induced vasorelaxation in arteries from women with pre-eclampsia, with a greater reduction in the endothelium-dependent vasorelaxation compared to arteries from normotensive pregnancy (Knock & Poston, 1996). A different study in human isolated myometrial arteries from women with normotensive pregnancy demonstrated that gap junctional communications play a role in the EDH-type response (Kenny *et al.*, 2002b) with a greater EDH-type responses compared to non-pregnant women and in pre-eclampsia (Kenny *et al.*, 2002a).

## 1.5 Sex differences in the EDH-type responses

Studies have reported that the cardiovascular risk in premenopausal women is significantly lower compared to age-matched men or postmenopausal women and sex differences in vascular function have been suggested for the differences in risk (Lerner & Kannel, 1986; McCulloch & Randall, 1998; Villar *et al.*, 2008). Previous studies in rat isolated mesenteric arteries and in mesenteric arterial bed have demonstrated a greater EDH-type response in females compared to males (McCulloch & Randall, 1998; White *et al.*, 2000). This was further confirmed by a study using eNOS and COX-1 double knockout mice, where the mean arterial pressure in females was unaffected whereas in males there was a significant increase in the blood pressure compared to the WT control (Scotland *et al.*, 2005). Similarly, in pressurised rat isolated mesenteric arteries, a greater ACh-induced EDH-type response was observed in females compared to males and the enhancement in EDH-type response in females was attributed to the apamin-sensitive $SK_{Ca}$ channels (White *et al.*, 2000).

Sex differences in the EDH-type response in the vasculature have been implicated with the sex hormone, oestrogen which has been shown to exert a cardioprotective effect (Gilligan *et al.*, 1994; Tagawa *et al.*, 1997; Villar *et al.*, 2008). A previous study in PCAs reported that 18-22 h incubation with 17β-estradiol significantly enhanced endothelium-dependent, A23187-induced vasorelaxation in female and castrated male pigs (Bell *et al.*, 1995). Similarly in rat mesenteric arteries, A23187-induced EDH-type vasorelaxation and hyperpolarization were essentially abolished in ovariectomised female rats and the responses were restored in 17β-estradiol treated rats (Liu *et al.*, 2002).

Further studies using the gap junction inhibitor 18α-GA have demonstrated that the impairment in the EDH-type responses in ovariectomised rats were associated with the loss of gap junction communication with a significant reduction in expression of connexin 43 proteins (Liu *et al.*, 2002). In forearm blood flow responses of postmenopausal women, acute treatment with 17β-estradiol enhanced the endothelium-dependent, ACh-induced vasodilatation (Gilligan *et al.*, 1994; Tagawa *et al.*, 1997).

In PCAs from female pigs, incubation with 17β-estradiol for 24 h significantly reduced superoxide anion production measured using lucigenin-enhanced chemiluminescence technique (Cox *et al.*, 2005). Therefore, another possibility which may contribute to sex differences in the vascular function is the oxidative stress level in the vasculature. In rat isolated aortae with intact endothelium, a higher superoxide level was detected in blood vessels from males compared to females (Brandes & Mugge, 1997; Kerr *et al.*, 1999). This conclusion was further supported by a study conducted on human subjects where a greater oxidative stress has been reported in healthy young men compared to premenopausal women (Ide *et al.*, 2002).

Studies in diabetic or hypertensive animals similarly reported sex differences in endothelial function (Han *et al.*, 2014; Loria *et al.*, 2014). For instance, in mesenteric arteries and thoracic aortae from streptozotocin (STZ)-induced diabetic rats, both males and females demonstrated impairment in the endothelium-dependent vasorelaxation compared to their age-matched controls (Han *et al.*, 2014; Zhang *et al.*, 2012b). However, after 8 weeks of STZ treatment, the impairment of the endothelium-dependent vasorelaxation in the mesenteric arteries were greater in females compared to males and this was

attributed to the shift in the relative contribution of EDH-type responses to NO-mediated responses in both sexes (Zhang *et al.*, 2012b).

In spontaneously hypertensive rats (SHRs), the ACh-induced vasorelaxation was significantly reduced in aortae from male animals compared to the WKY control whereas in females, no differences in the endothelium-dependent vasorelaxation were detected between the SHRs compared to the WKY control (Loria *et al.*, 2014). However, differences in the functional response between SHRs and WKY in males cannot be explained by the expression and activity of the NOS proteins as a higher expression level of NOS3 proteins has been detected in aortae from the SHRs and no differences in the NOS activity was detected (Loria *et al.*, 2014). These authors suggested that the reduction in the endothelium-dependent vasorelaxation in aortae from male SHRs could be related to the increased production of ROS which reduces the bioavailability of NO (Loria *et al.*, 2014). On the other hand, in small mesenteric arteries, an increased in ACh-induced NO production was reported in SHRs from both sexes compared to the WKY control (Loria *et al.*, 2014).

## 1.6 EDH-type responses and cardiovascular diseases

In cardiovascular diseases, endothelial dysfunction has been reported, where the release of NO is compromised (Angulo *et al.*, 2003; Feletou & Vanhoutte, 2009; Gilligan *et al.*, 1994). In many studies, EDH-type response has been proposed to be enhanced in diseases acting as a 'back up' system to compensate for the loss of NO in the endothelium (Feletou & Vanhoutte, 2009; Katz & Krum, 2001; McCulloch *et al.*, 1997; Miura *et al.*, 2001). However, in some studies, a reduction in both the NO and EDH-type vasorelaxations were reported in disease state including diabetes in man (Angulo *et al.*, 2003), rat (Brondum *et al.*, 2010; Fukao *et al.*, 1997; Leo *et al.*, 2011; Ma *et al.*, 2013; Schach *et al.*, 2014) and murine models (Fitzgerald *et al.*, 2007; Makino *et al.*, 2008), but this observation could possibly be species, vascular bed or vessel size specific (Angulo *et al.*, 2003; Fitzgerald *et al.*, 2007; Fitzgerald *et al.*, 2005). Therefore, future work involving tissue and disease specific pharmacological intervention to improve either the NO or the EDH-type mediated response is required.

### 1.6.1 Atherosclerosis

As mentioned in Section 1.3.3, NADPH oxidase-derived ROS have been linked to development of atherosclerosis forming lesion in the intima layer of the blood vessels (Lassegue & Clempus, 2003). To study the role of Nox2 in development of atherosclerosis, plaque formation along the aortae of Nox2/ApoE double KO were compared with age-matched ApoE KO mice (Judkins *et al.*, 2010). In this study, the area of atherosclerotic lesion formed in the aortae of the Nox2/ApoE double KO mice were ~50% less than the lesion formed in age-matched ApoE KO mice indicating that Nox2 protein contributes to formation of atherosclerotic lesion (Judkins *et al.*, 2010). The superoxide production in the aortae of the Nox2/ApoE double KO mice was also significantly reduced with an increase in NO bioavailability when compared with the ApoE KO mice (Judkins *et al.*, 2010).

As CNP has been reported to be a factor for EDH-type mediated response (Chauhan *et al.*, 2003; Hobbs *et al.*, 2004; Honing *et al.*, 2001; Kun *et al.*, 2008; Wei *et al.*, 1994), ecCNP KO mice have been developed to further characterise the effects of endothelial CNP in maintaining vascular homeostasis (Moyes et al., 2014). To study the effects of CNP on development of atherosclerosis, the entire aorta of ecCNP KO/ApoE KO mice were compared to CNP WT/ApoE KO mice (Moyes *et al.*, 2014). The development of atherosclerotic plaque, particularly at the aortic arch and abdominal aortae, was accelerated in ecCNP/ApoE double KO mice from both sexes compared to the WT (Moyes *et al.*, 2014). The development of atherosclerotic plaques subsequently caused formation of aortic arch or abdominal aortic aneurysms observed in about 50% of the male double KO mice (Moyes *et al.*, 2014).

**1.6.2 Diabetes**

A high prevalence of erectile dysfunction has been reported in diabetic patients and this was attributed to endothelial dysfunction associated with diabetes (Angulo *et al.*, 2003). In diabetic patients, impaired endothelial function leads to a reduction in endothelium-dependent vasorelaxation in the human corpus cavernosum and in penile resistance arteries (Angulo *et al.*, 2003). Consistent with a previous study where Shimokawa *et al.* (1996) have reported that the EDH-type responses increase with decreasing vessel size (Shimokawa *et al.*, 1996), Angulo *et al.* (2003) reported that the ACh-induced vasorelaxation in human corpus cavernosum is mainly mediated by NO whereas in penile resistance arteries, both the NO- and EDH-type responses play a role in the ACh-induced vasorelaxation. In diabetic patients, a reduction in the ACh-induced NO-mediated vasorelaxation has been reported in human corpus cavernosum, whereas in the resistance arteries, reduction in both NO and EDH-type mediated vasorelaxations have been observed (Angulo *et al.*, 2003).

Similarly, in rat model of Type I diabetes (streptozotocin-induced) or Type II Zucker diabetic fatty (ZDF) rats, the ACh-induced EDH-type vasorelaxation and hyperpolarization in small mesenteric arteries were significantly reduced (Brondum *et al.*, 2010; Fukao *et al.*, 1997). A later study reported that the basal release of NO and ACh-induced NO-mediated response were also impaired in mesenteric arteries from streptozotocin-induced diabetic rat (Leo *et al.*, 2011). These authors suggested that the impairment of the NO-mediated vasorelaxation in the diabetic rat could be associated with the up-regulation of Nox2 protein expression where an increased production of superoxide has been detected in the diabetic arteries (Leo *et al.*, 2011). Despite

reporting an impairment in the $SK_{Ca}$ and $IK_{Ca}$-channel mediated EDH-type responses in the mesenteric arteries from diabetic rats, an increased in the $SK_{Ca}$ and $IK_{Ca}$ proteins expression were observed (Leo *et al.*, 2011). These authors suggested that the impairment in the EDH-type response could be related to other downstream microdomain signalling such as MEGJ communications (Leo *et al.*, 2011). In contrast, a study from a different laboratory using primary cultured mesenteric artery endothelial cells reported that the impairment in the EDH-type response in streptozotocin-induced diabetic rats is a result of reduction in the expression level of $SK_{Ca}$ and TRPV4 proteins (Ma *et al.*, 2013). Here, the discrepancy between the expression level of $SK_{Ca}$ reported by Leo *et al.* (2011) and Ma *et al.* (2013) could be due to differences in experimental condition where cultured cells were used in the experiment conducted by Ma *et al.* (2013).

In thoracic aortae isolated from streptozotocin-induced diabetic rats, a significant reduction in ACh-induced vasorelaxation has been reported where the EDH-type vasorelaxation was completely abolished in both the diabetic and control group (Csanyi *et al.*, 2007). These authors concluded that there was no up-regulation of the EDH-type responses in the diabetic rat group. However, as mentioned above, the lack of EDH-type response in both the control group and the diabetic rat group could be due to the size of vessel used where the EDH-type response plays a greater role in smaller vessels, hence no EDH-type responses were observed in larger vessels (Shimokawa *et al.*, 1996). Therefore, the discrepancies in findings between studies from different research groups could be due to differences in experimental conditions, species studied, type of vessels used, or age of animal used (Fitzgerald *et al.*, 2007).

In coronary arteries isolated from streptozotocin-induced diabetic mice, significant reductions in ACh-induced vasorelaxation and EDH-type mediated response were reported (Makino *et al.*, 2008). These authors reported that the reduction in ACh-induced vasorelaxation can be associated with the decrease in expression of Cx37 and Cx40 in the coronary arteries from diabetic mice where the gap junction communication was also reported to be attenuated using Lucifer-Yellow assay (Makino *et al.*, 2008). In mesenteric arteries from non-diabetic mice, the ACh-induced vasorelaxation was mainly mediated by EDH-type response (Fitzgerald *et al.*, 2007). After 7 days of exposure to streptozotocin (representing early stages of diabetes mice), Fitzgerald *et al.* (2007) reported that the NO activity is up-regulated to compensate the loss of EDH-type responses in the mesenteric arteries to maintain the vascular function. Similarly, a reduction in the functional and expression of Cx40 protein and Cx40 mRNA level were reported in mesenteric arteries from type II diabetic ZDF rats (25-week-old) (Young *et al.*, 2008). Furthermore, a reduction in Cx37 but not Cx43 protein and mRNA level was reported in the homogenates from the diabetic samples (Young *et al.*, 2008).

Interestingly, similar to Type 1 diabetic rats where an increase in $IK_{Ca}$ proteins have been reported (Leo *et al.*, 2011), a different study using mesenteric arteries from 18-week-old ZDF rats similarly demonstrated an increase in $IK_{Ca}$ mRNA and protein expression levels (Schach *et al.*, 2014). Indeed, a previous study reported that NS309 (1 μM), a selective $SK_{Ca}$ and $IK_{Ca}$ channel activator can restore the ACh-induced endothelium-dependent and EDH-type mediated vasorelaxation in mesenteric arteries from ZDF rats (Brondum *et al.*, 2010). These authors reported no differences in protein

expression of $SK_{Ca}$ channels between ZDF and ZL rats and suggested that the endothelial dysfunction in ZDF rats is due to changes in the vascular function rather than changes in the protein expression level (Brondum *et al.*, 2010).

### 1.6.3 Hypertension

Early studies have shown that inhibition of NOS increases blood pressure in mice and further knockout of the eNOS gene in mice abolished the ACh-induced vasorelaxation in the aortae (Huang *et al.*, 1995). The mean arterial pressure in eNOS KO mice was also significantly higher than the WT mice (Huang *et al.*, 1995; Shesely *et al.*, 1996). Other study using $SK_{Ca}/IK_{Ca}$-deficient mice reported that the mean arterial pressure was significantly higher than the WT mice indicating that the $SK_{Ca}/IK_{Ca}$ channels, which is involved in the 'classical' EDH pathway play a role in regulation of blood pressure and vascular tone (Brahler *et al.*, 2009).

In monocytes from SHRs, an upregulation of TRPC3 channel expression level with significant increase in calcium influx compared to normotensive Wistar-Kyoto rats (WKY) has been previously reported (Liu *et al.*, 2005). Similarly, in VSMCs and aortic tissues from SHRs, there was an increase in TRPC3, but not TRPC6, expression level when compared to the WKY (Liu *et al.*, 2009). The increase in TRPC3 expression level in the VSMCs from SHRs was reported to be associated with the increased in angiotensin II-induced calcium influx and with a significantly greater angiotensin II-induced contraction compared to the normotensive WKY (Liu *et al.*, 2009). Long term *in vivo* treatment in these SHRs for 4 weeks with telmisartan, an angiotensin II $AT_1$ receptor antagonist, but not amlodipine, a

calcium channel blocker significantly reduces the TRPC3 expression level (Liu *et al.*, 2009). Results from these animal studies were in agreement with studies using isolated vascular endothelium of preglomerular arteries from patients with malignant hypertension, where a higher level of TRPC3 protein expression has been reported (Thilo *et al.*, 2009). Therefore, TRPC3 channels could be of potential target for future drug treatment of hypertension.

In human studies, a significantly higher amount of plasma $H_2O_2$ production was reported in subjects with essential hypertension compared to normotensive subjects (Lacy *et al.*, 2000). This observation may be related to the NADPH oxidase pathway where a different study using human resistance arteries (<300 μM in diameter) isolated from subcutaneous fat reported that the angiotensin II-induced ROS generation was significantly greater in VSMCs isolated from hypertensive patients compared to normotensive subjects and this ROS formation was sensitive to DPI, an inhibitor of the NADPH oxidases (Touyz & Schiffrin, 2001). Therefore, apart from the NO-mediated pathway, the EDH-type responses or the NADPH oxidase pathway may be potential targets for treatment of hypertension.

## 1.7 Aims

Although previous studies have demonstrated clear sex differences in endothelial function, most current cardiovascular studies are conducted on either male only animals or animals from both sexes. This could be one of the possible explanations for contradictory findings between studies. Therefore, the principal aim of the present study was to elucidate whether the effects of sex in PCAs from male and female pigs contribute to any differences on endothelium-dependent vasorelaxation.

In the present study, bradykinin, an endothelium-dependent vasorelaxant was mainly used in isometric tension studies in the presence of various inhibitors. In some studies, Western immunoblotting was used to compare protein expression levels in PCAs from male and female pigs. The aims of the present study include the following;

✂ In preliminary studies, the effects of various endothelium-dependent agents including substance P, carbachol and bradykinin on PCAs were investigated. Next, sex differences in the EDH-type response were investigated using L-NAME and indomethacin to inhibit the synthesis of nitric oxide and prostacyclin. The study was then extended to investigate if endogenous $H_2O_2$, gap junction communications, $SK_{Ca}$ and/or $IK_{Ca}$ channels play a role in endothelium-dependent and EDH-type responses in PCAs from male and female pigs.

✂ As $H_2O_2$ has been detected in various pathological states and has been reported to be a factor for EDH-type response, present study examined the mechanism of action of exogenous $H_2O_2$ on PCAs using various potassium channel inhibitors.

❧ Hyperoxic gassing conditions have been regularly used in isometric tension studies. High amount of superoxide generated in the buffer may influence pharmacological responses. Here, the effects of the antioxidant, Tiron® on endothelium-dependent vasorelaxation were examined under different gassing conditions (95% $O_2$/5% $CO_2$ or 95% air/5% $CO_2$) in PCAs from male and female pigs.

❧ One of the sources for generation of endogenous $H_2O_2$ is through the NADPH oxidase (Nox) system. Previous studies have reported greater oxidative stress in males compared to females. Therefore, sex differences in the role of Nox-generated ROS in the endothelium-dependent and EDH-type responses were investigated.

❧ Given that TRP channels have been reported to play a role in endothelium-dependent vasorelaxation, sex differences in the role of TRP channels in endothelium-dependent, EDH-type responses and $H_2O_2$-induced vasorelaxation in PCAs from male and female pigs were examined in the present study using a range of selective and non-selective TRP channel antagonists.

# *Chapter 2*

**Vascular responses in porcine isolated coronary arteries and Sex Differences in endothelial function: a role for $H_2O_2$, gap junctions and $IK_{Ca}$ channels**

## 2.1 Introduction

Regulation of vascular tone is controlled by endothelium-derived relaxants including nitric oxide (NO) (Furchgott & Zawadzki, 1980; Palmer *et al.*, 1987), prostacyclin (PGI$_2$) (Moncada *et al.*, 1976) and endothelium-dependent hyperpolarization (EDH)-type mechanisms (Edwards *et al.*, 2010; Feletou & Vanhoutte, 2013; Taylor & Weston, 1988). As mentioned under Section 1.2 about the two different categories of EDH-type responses, this aim of this chapter was to examine the role of different factor(s) which have been proposed to be putative factor for EDH-type response released by bradykinin including $K^+$ ions which is mediated through the $SK_{Ca}$ and $IK_{Ca}$ channels, myoendothelial gap junction communications and hydrogen peroxide (H$_2$O$_2$) (Edwards *et al.*, 2010; Hayabuchi *et al.*, 1998; Shimokawa, 2010; Yada *et al.*, 2003). H$_2$O$_2$ has been reported to act as a factor responsible for EDH in porcine coronary arteries, human, murine and rat mesenteric arteries (Matoba *et al.*, 2002; Matoba *et al.*, 2003; Matoba *et al.*, 2000; Wheal *et al.*, 2012) (for a review see Shimokawa, 2010). However, the responses to H$_2$O$_2$ may vary between species, vascular beds and experimental conditions (Chaytor *et al.*, 2003; Gluais *et al.*, 2005b; Lucchesi *et al.*, 2005).

Cardiovascular risk in men and postmenopausal women is higher than premenopausal women and sex differences in endothelial function have been suggested (McCulloch & Randall, 1998; Villar *et al.*, 2008). To date, most studies on endothelial function have been conducted on either arteries from male animals only (Edwards *et al.*, 1998; Garry *et al.*, 2009; Harris *et al.*, 2000; Leung *et al.*, 2006; Matoba *et al.*, 2003) or from both sexes (Chadha *et al.*, 2011; Edwards *et al.*, 2000; Huang *et al.*, 2011; Quignard *et al.*, 1999;

Yang *et al.*, 2003). However, previous studies have demonstrated clear sex differences in vascular function of the EDH-mediated pathways (for review see Feletou & Vanhoutte, 2006; Villar *et al.*, 2008). EDH-type responses have been reported to be up-regulated to compensate for the loss of NO (McCulloch *et al.*, 1997; Wheal *et al.*, 2012; Yada *et al.*, 2003) and this compensation was greater in females compared to males (McCulloch & Randall, 1998; White *et al.*, 2000). Furthermore, in endothelial NO synthase and cyclo-oxygenase-1 (eNOS/COX-1) double knockout mice ('EDH mice'), the male mice were hypertensive while female mice were normotensive with greater endothelium-dependent vasorelaxation in female mice (Scotland *et al.*, 2005). However, in rat cerebral arteries, the EDH-type responses were greater in males compared to females (Sokoya *et al.*, 2007). In a previous study on mesenteric arteries from rats, the EDH-type responses in females were partly dependent on increased expression of Cx43, which was driven by oestrogen (Liu *et al.*, 2002).

The aim of this chapter was to investigate the roles and relative contributions of NO, PGI$_2$ and EDH-type responses in porcine isolated coronary arteries (PCAs). The study was then extended to investigate the effects of sex differences on endothelium-dependent vasorelaxation of PCAs, specifically the role of gap junction communications, endogenous H$_2$O$_2$ and calcium-activated potassium channels in bradykinin-induced vasorelaxation.

## 2.2 Materials and methods

### 2.2.1 Preparation of rings of distal PCAs

Hearts from male and female pigs (large white hybrid pigs, 4-6 months old, weighing ~ 50 kg) were collected from a local abattoir and transported to the laboratory in ice-cold modified Krebs'-Henseleit solution (118 mM NaCl, 4.8 mM KCl, 1.1 mM MgSO$_4$, 25 mM NaHCO$_3$, 1.2 mM KH$_2$PO$_4$, 11.6 mM D-glucose, 1.25 mM CaCl$_2$) previously gassed with 5% CO$_2$ and 95% O$_2$. The distal part of the coronary artery was then dissected and placed in 2% w/v Ficoll in Krebs'-Henseleit solution for overnight storage at 4°C. The 2% w/v Ficoll component was added to minimise osmotic swelling. The following day, tissues were finely dissected, cleaned of adherent connective and fatty tissues. PCAs were then cut into rings of about 2 mm in length and mounted in a multichannel wire myograph (Model 610M, DMT, Aarhus N, Denmark) (Figure 2.1) filled with 5 ml Krebs'-Henseleit solution gassed with 95% O$_2$/5% CO$_2$ and maintained at 37°C.



**Figure 2.1** A multichannel wire myograph.

Here, the distal part of the PCAs was used because it has previously been reported that the EDH response is greater with decreasing vessels size (Shimokawa *et al.*, 1996) and the number of myoendothelial gap junctions appears to be greater in the distal part of the rat mesenteric arteries compared to the proximal (Sandow & Hill, 2000). The mean vessel size of PCAs from female pigs (0.86 ± 0.02 mm) did not differ significantly from the mean vessel size of male pigs (0.89 ± 0.02 mm) (2-tailed, unpaired Student's *t*-test). Seasonal variations in pig responses were not factored into the present study design but each set of experiment has been carried out with an internal, contemporaneous control.

### 2.2.2 Wire myography

To determine the basal optimal tension, vessels mounted in the wire myograph were placed at baseline tensions from 9.81 mN to 68.67 mN and were left to equilibrate for approximately 30 min. Tension was measured and recorded using a PowerLab recording system (ADInstruments, Oxfordshire, UK). After 30 min of equilibration, contractile responses to 60 mM KCl were determined and were analysed.

Subsequent vessels were then set at a baseline tension of 24.5 mN which was the optimal tension for KCl contraction and left to equilibrate for approximately 30 min. The vessels were then challenged with the addition of 60 mM KCl twice and following this the vascular tone was then raised to about 50-80% of the second KCl contraction tone by the addition of the thromboxane $A_2$ mimetic, U46619 (1 nM - 90 nM). Once stable tone was achieved, concentration-response curves to carbachol (1 nM – 10 μM) and two different

endothelium-dependent vasorelaxants, substance P (0.01 nM – 3 nM) and bradykinin (0.01 nM – 1 μM), or the nitric oxide donor, sodium nitroprusside (10 nM – 30 μM) or NS309, (6,7-Dichloro-1$H$-indole-2,3-dione 3-oxime), a positive modulator of $SK_{Ca}$ and $IK_{Ca}$ channels (Brondum $et$ $al.$, 2010; Dalsgaard $et$ $al.$, 2009; Leuranguer $et$ $al.$, 2008a) (0.1 μM – 0.1 mM) were constructed. To examine the selectivity of NS309, some experiments were pre-contracted with 60 mM KCl with their respective controls raised to the same tone with U46619.

All inhibitors were incubated with the tissues for 1 h before pre-contraction with U46619 except for experiments with17β-estradiol (Bell $et$ $al.$, 1995; Cox $et$ $al.$, 2005; Teoh & Man, 2000) which were incubated for 2 h (1 nM) or 4 h (1 μM). Vasorelaxation to bradykinin was studied in the absence or presence of $N^G$-nitro-L-arginine methyl ester (L-NAME) (300 μM) which is a NO synthase inhibitor to determine the NO-mediated component (Randall & Griffith, 1991). Indomethacin (10 μM) was used to inhibit the synthesis of prostanoids. In some experiments polyethylene glycol (PEG)-catalase (300 $Uml^{-1}$) (Hedegaard $et$ $al.$, 2011) was added to eliminate intracellular hydrogen peroxide. To study the role of gap junctions, non-selective gap junction inhibitors carbenoxolone (100 μM) (Harris $et$ $al.$, 2002; Tang & Vanhoutte, 2008) and 18α-glycyrrhetinic acid (18α-GA) (100 μM) (Kenny $et$ $al.$, 2002b; Matoba $et$ $al.$, 2003) were used. Apamin (500 nM) and TRAM-34 (10 μM) (Gluais $et$ $al.$, 2005a), small ($SK_{Ca}$) and intermediate ($IK_{Ca}$) - calcium activated potassium channel inhibitors, respectively, were used to study the role of $K^+$ channels in the bradykinin-induced vasorelaxation.

The concentration of U46619 used was significantly higher in the presence of L-NAME, indomethacin with carbenoxolone in PCAs from males and females (P<0.01) and in the presence of 18α-GA in PCAs from males (P<0.05) (Table 2.1A). The concentration of U46619 used was also significantly higher in the presence of L-NAME, indomethacin with 18α-GA in females (P<0.01) or in the presence of 1 μM 17β-estradiol in males (P<0.05) (Table 2.1A). The concentration of U46619 used was the same under all other conditions (Table 2.1A and 2.2A). The level of tone achieved with U46619 was the same under all conditions in PCAs from males and females (Table 2.1B and 2.2B).

| A Concentration of U46619 (nM) | | | | L-NAME, indomethacin | |
| --- | --- | --- | --- | --- | --- |
| | | Control | Inhibitor | Control | Inhibitor |
| PEG-Catalase | Male | 11.0 ± 1.6 | 12.8 ± 4.1 | 15.6 ± 1.8 | 16.5 ± 3.0 |
| | Female | 15.6 ± 2.2 | 15.1 ± 1.8 | 28.6 ± 7.7 | 18.9 ± 3.3 |
| Carbenoxolone | Male | 11.1 ± 2.0 | 103 ± 34 | 15.0 ± 1.5 | 308 ± 116** |
| | Female | 14.0 ± 2.4 | 173 ± 69 | 26.6 ± 7.1 | 3386 ± 1752** |
| 18α-GA | Male | 18.5 ± 2.7 | 77.8 ± 26.2* | 20.8 ± 2.2 | 40.7 ± 5.3 |
| | Female | 17.7 ± 1.9 | 41.3 ± 11.6 | 23.0 ± 1.9 | 59.3 ± 8.7** |
| 1nM 17β-estradiol | Male | | | 14.7 ± 1.8 | 15.5 ± 3.8 |
| 1µM 17β-estradiol | | | | 7.83 ± 1.54 | 10.9 ± 1.2* |

**Table 2.1** Summary of (A) concentration of U46619 used (nM) in the presence or absence of 300 μM L-NAME and 10 μM indomethacin with or without 300 UmL$^{-1}$ PEG-catalase, 100 μM carbenoxolone, 100 μM 18α-GA, 1 nM or 1 μM 17β-estradiol in porcine coronary arteries from male and female pigs. Data are expressed as mean ± S.E.M. of 6-15 experiments. *P<0.05, **P<0.01; one-way ANOVA followed by Bonferroni's *post hoc* test or 2-tailed, paired Student's *t*-test.

| B  % KCl response | | Control | Inhibitor | L-NAME, indomethacin | |
|---|---|---|---|---|---|
| | | | | Control | Inhibitor |
| PEG-Catalase | Male | 68.8 ± 3.5 | 70.9 ± 2.1 | 66.1 ± 3.0 | 65.9 ± 3.0 |
| | Female | 68.8 ± 3.0 | 71.2 ± 3.9 | 67.4 ± 3.3 | 69.9 ± 2.7 |
| Carbenoxolone | Male | 71.4 ± 4.3 | 67.3 ± 3.4 | 69.7 ± 3.3 | 55.7 ± 4.6 |
| | Female | 68.7 ± 3.2 | 64.3 ± 2.6 | 67.4 ± 3.3 | 55.4 ± 7.4 |
| 18α-GA | Male | 65.8 ± 5.6 | 70 ± 6.2 | 63.67 ± 7.8 | 62.83 ± 5.0 |
| | Female | 58.7 ± 4.0 | 64.0 ± 4.1 | 60.8 ± 3.2 | 67.0 ± 5.3 |
| 1nM 17β-estradiol | Male | | | 53.2 ± 0.6 | 56.8 ± 2.2 |
| 1μM 17β-estradiol | | | | 58.0 ± 3.4 | 63.5 ± 5.9 |

**Table 2.1** Summary of (B) the levels of tone achieved with U46619 expressed in percentage to the second KCl-induced tone in the presence or absence of 300 μM L-NAME and 10 μM indomethacin with or without 300 UmL$^{-1}$ PEG-catalase, 100 μM carbenoxolone, 100 μM 18α-GA, 1 nM or 1 μM 17β-estradiol in porcine coronary arteries from male and female pigs. Data are expressed as mean ± S.E.M. of 6-15 experiments.

| A Concentration of U46619 (nM) | L-NAME, indomethacin | | | |
|---|---|---|---|---|
| | Control | TRAM-34 | Apamin | Apamin, TRAM-34 |
| Male | 12.1 ± 1.3 | 16.7 ± 4.5 | 11.6 ± 1.7 | 11.8 ± 1.7 |
| Female | 19.0 ± 3.3 | 12 ± 2.7 | 21.3 ± 6.6 | 18.7 ± 3.6 |

| B U46619-induced tone (% KCl response) | L-NAME, indomethacin | | | |
|---|---|---|---|---|
| | Control | TRAM-34 | Apamin | Apamin, TRAM-34 |
| Male | 72.0 ± 4.6 | 66.3 ± 5.2 | 75.9 ± 4.8 | 67.8 ± 4.4 |
| Female | 79.2 ± 5.4 | 67.0 ± 7.7 | 73.1 ± 7.5 | 66.3 ± 5.9 |

**Table 2.2** Summary of (A) concentration of U46619 used (nM) and (B) the levels of tone achieved with U46619 expressed in percentage to the second KCl-induced tone in the presence or absence of 300 μM L-NAME and 10 μM

indomethacin with or without 10 μM TRAM-34 and/or 500 nM apamin in porcine coronary arteries from male and female pigs.

### 2.2.3 Western Blotting

Western Blot studies were carried out to determine the relative expression levels of connexin 37, 40, 43 and $IK_{Ca}$ between PCAs from male and female pigs. PCAs from male and female pigs were finely dissected and cut into rings of about 1 cm in length. Vessels were then gassed with 5% $CO_2$ and 95% $O_2$ in Krebs'-Henseleit solution at 37°C for 1 h. The method described below is the result of substantial method development including different batches of antibodies and different lysis buffers. Results of these developments are included in the Appendix B. For detailed contents of the buffers and chemicals used for Western blot, please refer to Appendix A.

Segments (designated F1 - F5 for samples from females and M1 - M5 for samples from males) were homogenised on ice in lysis buffer (80 mM sodium β-glycerophosphate, 20 mM imidazole, 1 mM dithiothreitol, 1 mM sodium fluoride, pH7.6) containing protease inhibitor cocktail (Calbiochem, VWR International Ltd, Lutterworth, Leicestershire, UK). Protein concentrations of the supernatants were determined by Bradford method (Bradford, 1976) using bovine serum albumin (BSA) to generate the standard curve (2, 1, 0.5, 0.25, 0.125, 0 mg/mL). In duplicates, 10 μL of supernatants (diluted 1:5 or 1:10) followed by 40 μL of Bradford reagent (Bio-Rad, Hemel Hempstead, Hertfordshire, UK) were added into a 96-well plates. 150 μL of distilled water was then added into each well to make up a final total volume of 200 μL. The intensity of the absorbance value of 595 nm was then measured using a SpectraMAX 340 PC microplate reader (Molecular Devices,

Wokingham, Berkshire, UK). Protein concentrations of the samples were extrapolated from the BSA standard curve.

Samples (F1-F5 and M1-M5) were diluted 1:1 in 2x Laemmli sample buffer and heated at 95°C for 5 min. After centrifugation at 13,000x g for 1 min, 5 µg of protein were loaded on a 4-20% Mini-PROTEAN TGX precast gel (Bio-Rad, Hemel Hempstead, Hertfordshire, UK). Gel was run at 100 V for 5 min followed by 175 V for 45 min in 1X electrophoresis buffer (Appendix A) and was then transferred onto nitrocellulose membrane (GE Healthcare, Little Chalfont, Buckinghamshire, UK) using a Bio-Rad mini-transblot at 100 V for 1 h in transfer buffer (Appendix A). The nitrocellulose membrane was then blocked with 5% w/v non-fat milk (The Co-Operative instant dried skimmed milk, Manchester, UK) in tris-buffered saline containing 0.1% Tween 20 (TBS-T) for 1 h at room temperature with shaking before overnight incubation with mouse monoclonal anti-Cx-43 antibody (C8093 Sigma-Aldrich) (1:1000) and mouse monoclonal anti-myosin light chain (MLC) antibody (M4401 Sigma-Aldrich) (1:500) diluted in 5% w/v non-fat milk at 4°C with shaking. The immunoblot was then washed three times for 15 min each wash with TBS-T then incubated with secondary antibody IRDye 800CW Goat anti-mouse IgG (1:10,000) (LI-COR Biosciences, Cambridge, UK) diluted in 5% w/v non-fat milk for 1 h at 37°C. This was followed by another three times 15 min washing with TBS-T buffer. The immunoblot was then visualised using a LI-COR Odyssey Infrared Imaging Scanner and densities of the bands were determined using Odyssey (Application Software Version 3.0 LI-COR Biosciences, Cambridge, UK).

Due to the high concentration of proteins required for all other antibodies, samples (designated F6-F10 and M6-M10) were prepared in a slightly modified protocol. Samples (F6-F10 and M6-M10) were homogenised on ice in lysis buffer (20 mM Tris, 1 mM EGTA, 320 mM sucrose, 0.1% Triton X100, 1 mM sodium fluoride, 10 mM sodium β-glycerophosphate, pH7.6) containing protease inhibitor cocktail (Calbiochem) followed by centrifugation at 3,000x g for 5 min at 4°C (Hermle LaborTechnik Z216MK, Wehingen, Germany). Supernatant of the samples were then solubilised in 6x solubilisation buffer and diluted to 1 mg/ml of protein with 1x solubilisation buffer. Samples were then heated at 95°C for 5 min followed by centrifugation at 13,000x g for 1 min before loading to the precast gel.

The amounts of protein concentration loaded with the respective dilution of antibody used were as followed; for connexin 40, 10 μg of PCAs samples with 20 μg of pig kidney (PK) lysate used as positive control were incubated with rabbit polyclonal anti-connexin 40 - aminoterminal end antibody (ab38580 Abcam®, Cambridge, UK) (1:100) and mouse monoclonal anti-GAPDH antibody (G8795 Sigma-Aldrich) (1:40,000). For connexin 37, 15 μg of PCAs samples with 20 μg of pig (PK) and rat (RK) kidney lysate used as positive controls were incubated with rabbit polyclonal anti-GJA4 antibody (C15878 Assay Biotech, Stratech Scientific Limited, Suffolk, UK) (1:500) and mouse monoclonal anti-β-Actin antibody (A2228 Sigma-Aldrich) (1:40,000). For $IK_{Ca}$, 15 μg of PCAs samples with 10 μg of pig kidney lysate used as positive control were incubated with mouse polyclonal anti-KCNN4 antibody (H00003783-B01P Abnova, Taipei, Taiwan) (1:500) and mouse monoclonal anti-GAPDH antibody (G8795 Sigma-Aldrich) (1:40,000). For all

antibodies, the blocking and washing steps used were as described above and the same secondary antibody, IRDye® 800CW Goat anti-mouse IgG (1:10 000) (LI-COR Biosciences, Cambridge, UK) were used for anti-mouse antibody and IRDye® 680LT Goat anti-rabbit IgG (1:10 000) (LI-COR Biosciences, Cambridge, UK) for anti-rabbit antibody.


## 2.2.4 Polymerase chain reaction (PCR) amplification of the Sry gene for sex identification

### 2.2.4.1 DNA extraction from porcine tissue

Tissue samples were collected from respective pig hearts used for myograph and Western Blot study. In between each sample, the scissors and forceps were rinsed with 70% industrial methylated spirit (IMS) followed by plenty of Mili-Q water to minimised contamination between samples. DNA samples for the polymerase chain reaction amplification (PCR) was extracted from approximately 2 mm$^3$ of respective heart tissue using 200 μL of lysis buffer (50 mM KCl, 10 mM Tris-HCl pH8.3, 0.45% v/v Nonidet P40, 0.45% v/v Tween 20 - filtered through a 0.2 μm Sartorius Minisart® filter) and digested with 5 μL proteinase K (20 mg/ml). Samples were incubated at 37°C for 3 h until tissues were fully degraded. Samples were then heated to 95°C for 10 min in a heating block to inactivate proteinase K. Method was adapted from Bryja & Koneân (2003).

**2.2.4.2 PCR amplification of the pig tissues for sex identification**

Primers that amplify the 163-bp region of the *Sry* gene were adapted from Pomp *et. al.,* (1995) with the 5' upstream primer SRYB-5 (5'-TGAACGCTTTC AT TGTGTGGTC-3') and 3' downstream primer SRYB-3 (5'-AGGAGGCA CAGA GGCTACAGGC–3'). The 447/445-bp region of the *Zfy-Zfx* genes taken from Aasen & Medrano (1990) were used as positive control for successful PCR amplification (Bryja & Koneân, 2003; Henrique-Silva *et al.*, 2007; Pomp *et al.*, 1995) - 5' upstream primer (5'-ATAATCACATGG AGAGCCACAAGCT-3') and 3' downstream primer (5'-GCACTTCTTTGG TATCTGAGAAAGT-3'). For PCR analysis of a successful amplification in male samples, bands representing *Zfy-Zfx* (positive control) and *Sry* band should be visible while in female samples only the *Zfy-Zfx* (positive control) band should be detected. The *Zfy-Zfx* band should be fainter in males compared to females because of the competing *Sry* amplification system in males.

The amplifications were performed in the following conditions: 1 μL SRYB primers, 1 μL *Zfy-Zfx* primers, 200 μM dNTPs, 1 U Phusion DNA polymerase, and 5 μL of tissue lysate in a 50 μL reaction volume (method adapted from PCR guidelines from NEB Phusion® High-Fidelity DNA polymerase). All reaction was assembled on ice and the Phusion DNA polymerase was added last to prevent any primer degradation caused by exonuclease activity. The cycling conditions were 30 cycles of denaturation at 98 °C (1 min), annealing at 54°C (1 min) and extension at 72°C (1 min). The PCR amplifications were performed in SensoQuest Thermocycler (Geneflow Limited, Staffordshire, UK). Following PCR amplifications, 5 μL samples

were mixed with 5 μL of distilled H$_2$O and 2 μL 6x loading buffer and 10 μL of samples were loaded into a 1.5% ethidium bromide stained agarose gel.

## 2.2.4.3 Optimisation of the PCR conditions using purified or unpurified DNA samples, varying annealing temperature and concentration of magnesium chloride

To optimise the PCR protocol, a range of annealing temperatures (42°C, 45°C, 50°C, 54°C) and different concentrations of MgCl$_2$ were examined (1.5 mM, 2.0 mM, 2.5 mM). PCR amplification using purified and unpurified DNA samples were also compared. DNA samples were purified using DNeasy Tissue Kit (Qiagen, Manchester, UK) following protocol from the DNeasy Tissue Kit Handbook. Briefly, 180 μL tissue lysate was added with 200 μL AL buffer, votexed and incubated at 70°C for 10 min. 200 μL of ethanol was then added and sample was vortex and transferred to a spin column and centrifuged at 8000 rpm for 1 min (GenFuge 24D, Progen, Mexborough, UK). Flow through were discarded and 500 μL AW1 buffer was added and sample was centrifuged again at 8000 rpm for 1 min. Flow through was discarded and 500 μL of AW2 buffer were added and sample was centrifuged at 13 000 rpm for 3 min. The spin column was then transferred to a 1.5 mL Eppendorf and 200 μL AE buffer were added into the spin column and incubated at room temperature for 1 min. Purified DNA sample was finally eluted by centrifuging at 8000 rpm for 1 min and concentration of DNA was measured using NanoDrop 2000 spectrophotometer (Thermo Scientific, Fisher Scientific UK Ltd, Loughborough, UK).

## 2.2.4.4 The effects of running singleplex or duplex PCR amplification

The *Sry* gene was amplified in either singleplex or duplex PCR reaction using two sets of primers. In singleplex reaction, amplification of the two sets of primers was carried out in separate PCR tube whereas in a duplex PCR amplification, the 447/445-bp regions of the *Zfy-Zfx* genes were co-amplified with the SRYB primers.

## 2.2.5 Statistical analysis

Data are presented as mean percentage relaxation of U46619-induced tone with standard error of the mean (S.E.M.) and $n$ being the number of separate animals. The concentration-response curves were fitted to a sigmoidal curve with a variable slope using four-parameter logistic equation in GraphPad Prism (Version 6, GraphPad Software, La Jolla, California, USA). The maximum percentage relaxation ($R_{max}$) and the negative log of concentration required to produce half the maximal relaxation of the induced tone ($EC_{50}$) were calculated by fitting the data to the logistic equation:

$$R = \frac{R_{max} \bullet A^{nH}}{EC_{50}{}^{nH} + A^{nH}}$$

where R is the reduction in tone, $R_{max}$ is the maximum vasorelaxation of the established tone, A is the concentration of the vasorelaxant. $nH$ is the slope function and $EC_{50}$ is the concentration of the vasorelaxant required to produce half the maximal relaxation (McCulloch & Randall, 1998). Data were analysed using 2-tailed, paired or unpaired Student's *t*-test to compare differences between 2 groups (tissue segments from the same animal). In 3 or more groups, one-way ANOVA was used and significant differences between

groups were detected by Bonferroni's *post hoc* test. P-values of less than 0.05 were considered statistically significant.

### 2.2.6 Drugs and chemicals

All drugs were purchased from Sigma-Aldrich (Poole, Dorset, UK) except for apamin and NS309 from Tocris Bioscience (Bristol, UK). Stock solutions of carbachol, substance P, sodium nitroprusside, $N^G$-nitro-L-arginine methyl ester (L-NAME), PEG-catalase, carbenoxolone, and apamin were dissolved in distilled water. Stock solution of indomethacin was dissolved in absolute ethanol whereas TRAM-34, 18α-glycyrrhetinic acid and NS309 were dissolved in DMSO. 10 mM stock solution of bradykinin was made in water while 17β-estradiol and U46619 thromboxane $A_2$-mimetic were made in ethanol. All further dilutions of the stock solutions were made using distilled water except for NS309 which was further diluted with DMSO to 10 mM, 30% DMSO to 1 mM and distilled water to 0.1 mM. Primers for PCR amplifications were ordered from Eurofins Genomics (Ebersberg, Germany).

## 2.3 Results

### 2.3.1 Optimal tension in porcine distal coronary arteries (PCAs) for contractile responses

Segments of porcine distal coronary arteries mounted in a wire myograph were subjected to increasing amounts of tension. Tissue segments were then allowed to recover before the contractile responses to 60 mM KCl were measured. Initially an increase in the contractile response was observed with a mean maximum contraction of $22.0 \pm 5.0$ mN obtained at tension set at 19.6 mN. The response obtained with 60 mM KCl then decreased with increasing amounts of tension applied (Figure 2.2). Based on these observations, the average of 24.5 mN tension was used in subsequent experiments.
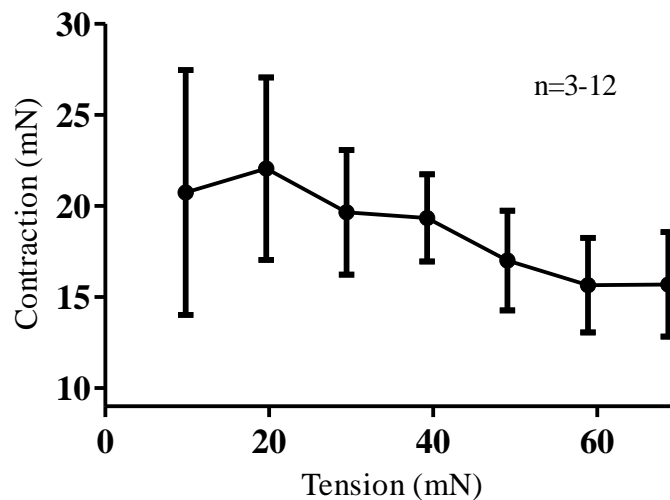


**Figure 2.2** The effects of increasing tension (mN) on the contractile response to 60 mM KCl in porcine distal coronary arteries from male and female pigs. Data points are expressed as a change in tension (mN) and are mean $\pm$ S.E.M. of 3-12 experiments.

**2.3.2 Vascular effects of carbachol, substance P, bradykinin and sodium nitroprusside in porcine distal coronary arteries (PCAs)**

Carbachol produced concentration-dependent contractions with a $pEC_{50}$ of $6.36 \pm 0.31$ and a maximum response ($R_{max}$) of $143 \pm 43\%$, $n=5$ (Figure 2.3). In contrast, substance P produced concentration-dependent vasorelaxations with an $R_{max}$ of $86.6 \pm 8.1\%$ ($pEC_{50} = 9.71 \pm 0.12$, $n=4$) (Figure 2.4A). Similarly bradykinin also produced relaxations described by $R_{max}$ of $99.9 \pm 5.4\%$ and $pEC_{50} = 8.57 \pm 0.14$ ($n=4$) (Figure 2.4B). Sodium nitroprusside (SNP) caused a concentration-dependent vasorelaxation with an $R_{max}$ of $107 \pm 13\%$ and $pEC_{50} = 6.46 \pm 0.21$ ($n=5$) (Figure 2.4C).
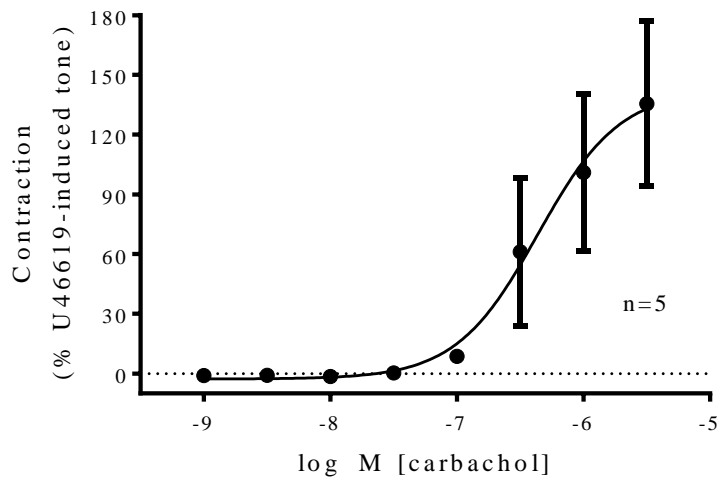


**Figure 2.3** Log concentration-response curve to carbachol in U46619 pre-contracted porcine coronary arteries from male and female pigs. Data are expressed as a percentage change from the U46619-induced tone and are mean $\pm$ S.E.M. of 5 experiments.
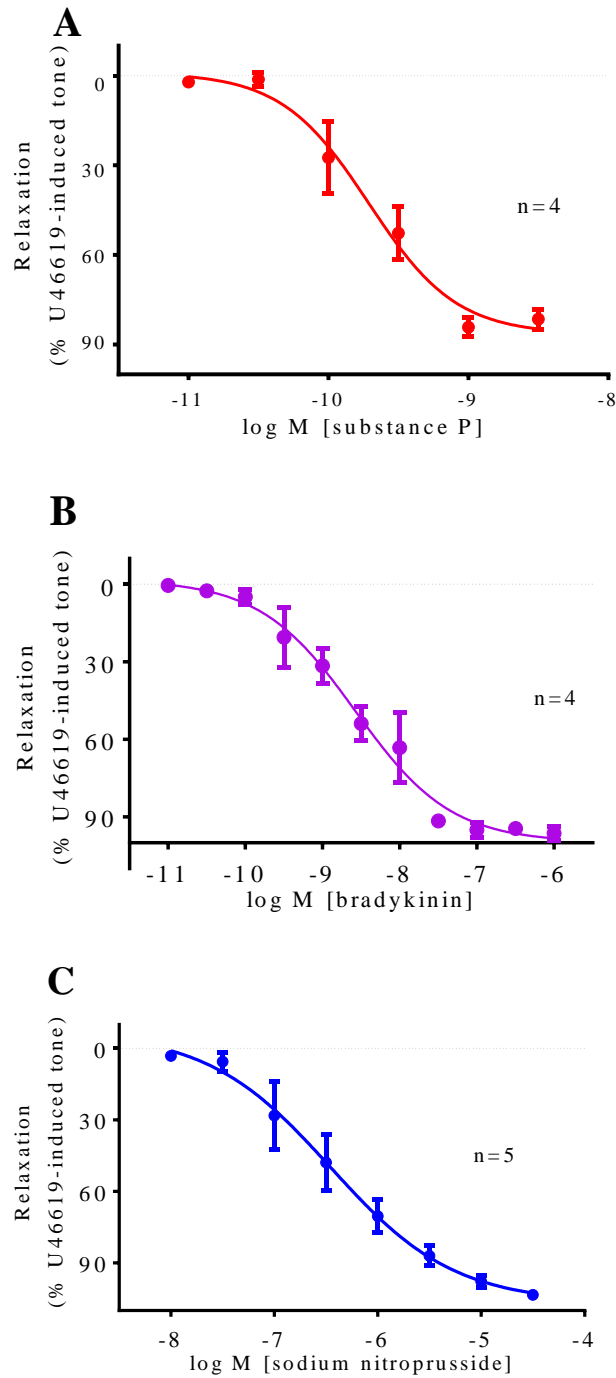
**Figure 2.4** Log concentration-response curves for the vasorelaxant effects of (A) substance P, (B) bradykinin and (C) sodium nitroprusside in U46619 pre-contracted porcine coronary arteries from male and female pigs. Data are expressed as a percentage change from the U46619-induced tone and are means ± S.E.M. of 4-5 experiments.

## 2.3.3 The effects of L-NAME and removal of the endothelium on bradykinin-induced vasorelaxation in PCAs from male and female pigs

In PCAs from pigs of either sex, bradykinin produced concentration-dependent vasorelaxations. Under control conditions the maximum bradykinin-induced vasorelaxation was $89.7 \pm 3.3\%$ with $pEC_{50} = 8.46 \pm 0.08$ ($n=12$). In the presence of 300 μM L-NAME (Figure 2.5) the responses to bradykinin were significantly inhibited such that the maximum relaxation was reduced to $53.4 \pm 4.7\%$ ($P<0.01$) ($pEC_{50} = 7.99 \pm 0.17$, $n=12$). The presence of 300 μM L-NAME also significantly shifted the curve 3-fold to the right ($P<0.05$). Removal of the endothelium abolished the bradykinin-induced vasorelaxation and a small contraction ($12.9 \pm 4.0\%$) was uncovered ($pEC_{50} = 7.67 \pm 0.70$, $n=4$) (Figure 2.5).
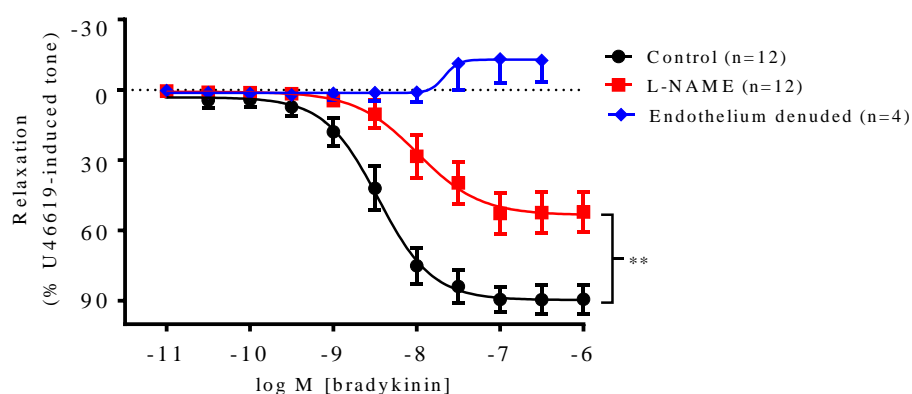


**Figure 2.5** Log concentration-response curves to bradykinin in the absence and presence of 300μM L-NAME or endothelium denuded tissue in U46619 pre-contracted porcine coronary arteries from male and female pigs. Data are expressed as a percentage change from U46619-induced tone and are mean ± S.E.M. of 4-12 experiments. \*\*P< 0.01; 2-tailed, paired Student's *t*-test.

## 2.3.4 The effects of L-NAME and/or cyclooxygenase inhibitor indomethacin on bradykinin-induced vasorelaxation in PCAs from male and female pigs

In PCAs from either sex, the presence of L-NAME alone significantly inhibited the maximum bradykinin-induced vasorelaxation from $89.7 \pm 3.3\%$ ($pEC_{50} = 8.46 \pm 0.08$, $n=12$) under control conditions to $53.4 \pm 4.7\%$ ($pEC_{50} = 7.99 \pm 0.17$, $n=12$) ($P<0.0001$) in the presence of L-NAME (Figure 2.6). The presence of indomethacin alone had no effect on the bradykinin-induced vasorelaxation producing an $R_{max}$ of $89.5 \pm 2.9\%$ ($pEC_{50} = 8.23 \pm 0.07$, $n=11$) and the additional presence of indomethacin to L-NAME had no further effects on the $R_{max}$ or $pEC_{50}$ of the bradykinin-induced vasorelaxation compared to L-NAME alone, producing an $R_{max}$ of $63.5 \pm 7.4\%$ ($pEC_{50} = 7.58 \pm 0.20$, $n=12$).
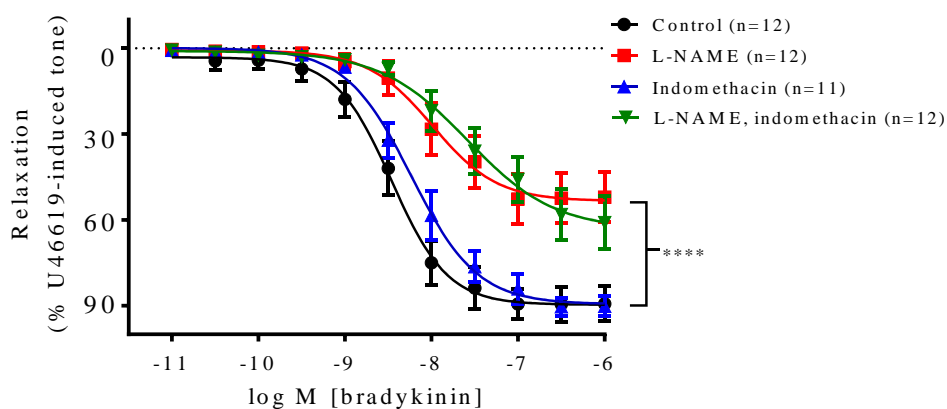


**Figure 2.6** Log concentration-response the vasorelaxant effects of bradykinin in the absence or presence of 300 μM L-NAME and/or 10 μM indomethacin in U46619 pre-contracted porcine coronary arteries from male and female pigs. Data are expressed as a percentage change from U46619-induced tone and are mean ± S.E.M. of 11-12 experiments. ****$P<0.0001$; one-way ANOVA followed by Bonferroni's *post hoc* test.

## 2.3.5 The effects of sex on EDH-type vasorelaxations

In PCAs from male and female pigs, bradykinin produced comparable, concentration-dependent vasorelaxant effects (Figure 2.7A) described by $R_{max}$ of 91.4 ± 3.4% and $pEC_{50}$ of 8.50 ± 0.08 ($n=8$ in females) and $R_{max}$ of 91.9 ± 3.4% and $pEC_{50}$ of 8.38 ± 0.08 ($n=12$ in males). In either sex, the presence of L-NAME and indomethacin significantly reduced the bradykinin-induced vasorelaxation compared to controls. The reduction in vasorelaxation was significantly ($P<0.05$) greater in males ($R_{max}$ = 45.0 ± 7.9%, $pEC_{50}$ = 7.33 ± 0.27, $n=11$) compared to females ($R_{max}$ = 66.8 ± 6.2%, $pEC_{50}$ = 7.65 ± 0.16, $n=8$). The bradykinin-induced vasorelaxation in arteries from both male and female pigs was shifted significantly to the right in the presence of L-NAME and indomethacin compared to their respective control responses ($P<0.05$). Original traces showing the tissue responses with increasing concentrations of bradykinin are shown in Figure 2.7B and C.
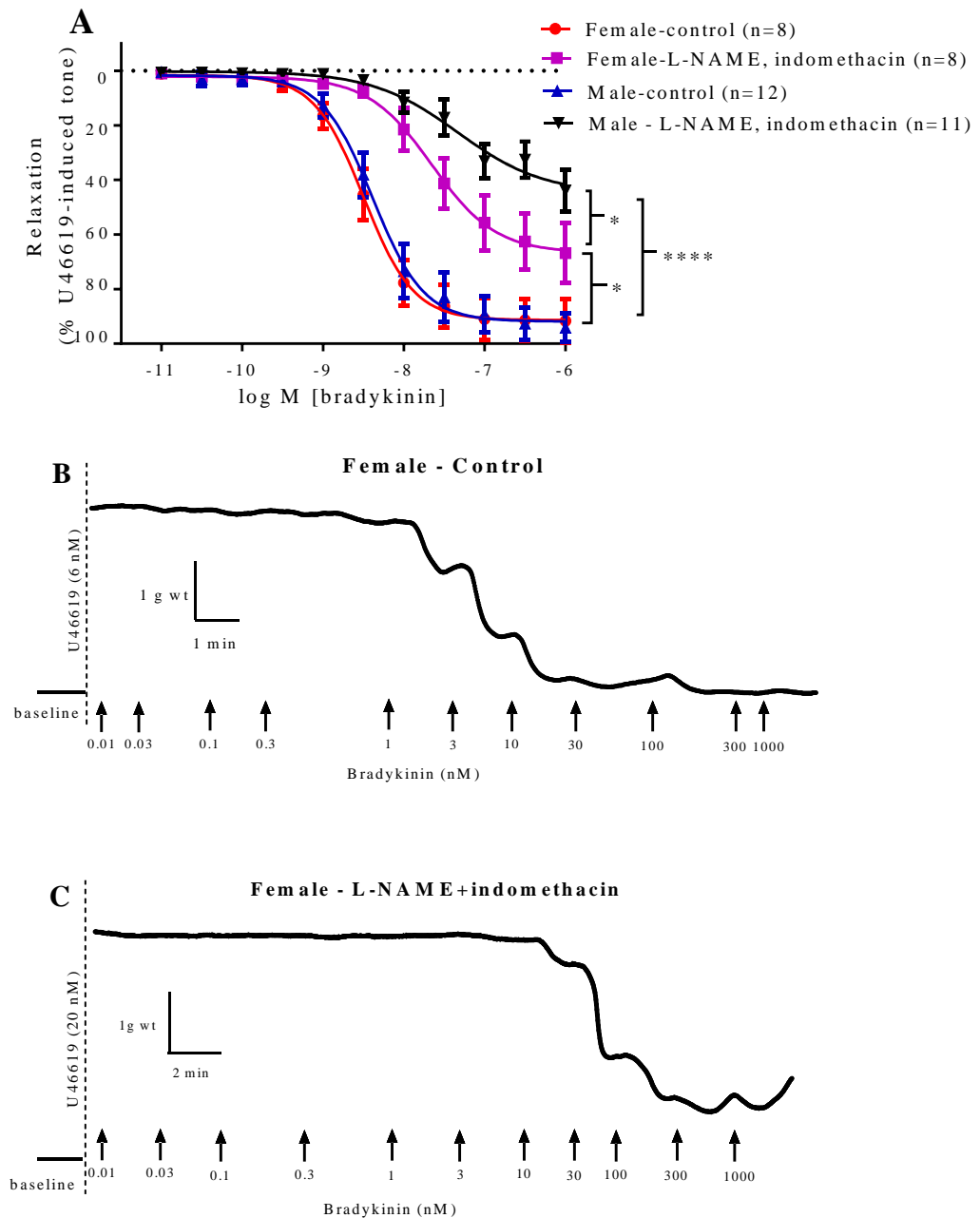
**Figure 2.7** (A) Log concentration-response curves for the vasorelaxant effects of bradykinin in the absence or presence of 300 μM L-NAME and 10 μM indomethacin in U46619 pre-contracted porcine coronary arteries from male and female pigs. Data are expressed as a percentage change from U46619-induced tone and are mean ± S.E.M. of 8-12 experiments. Original traces showing the responses to increasing concentration of bradykinin in the (A) absence or (B) presence of L-NAME and indomethacin *P<0.05, ****P<0.0001; one-way ANOVA followed by Bonferroni's *post hoc* test.

**2.3.6 The effects of 1 nM 17β-estradiol in the presence of L-NAME and indomethacin on bradykinin-induced vasorelaxation in PCAs from male pigs**

To examine if the enhanced EDH-mediated vasorelaxation to bradykinin observed in PCAs from female pigs was due to exposure to oestrogen, this study explored the acute effects of exposure to low concentration of 17β-estradiol (1 nM) in the presence of L-NAME and indomethacin on PCAs from male pigs. Here, the presence of 17β-estradiol had no effects on the bradykinin-induced vasorelaxation such that the $R_{max}$ under control condition was $71.2 \pm 9.4\%$ ($pEC_{50} = 7.79 \pm 0.29$, $n=6$) compared to a maximum relaxation of $68.5 \pm 6.7\%$ ($pEC_{50} = 7.66 \pm 0.20$, $n=6$) in the presence of 1 nM 17β-estradiol (Figure 2.8).
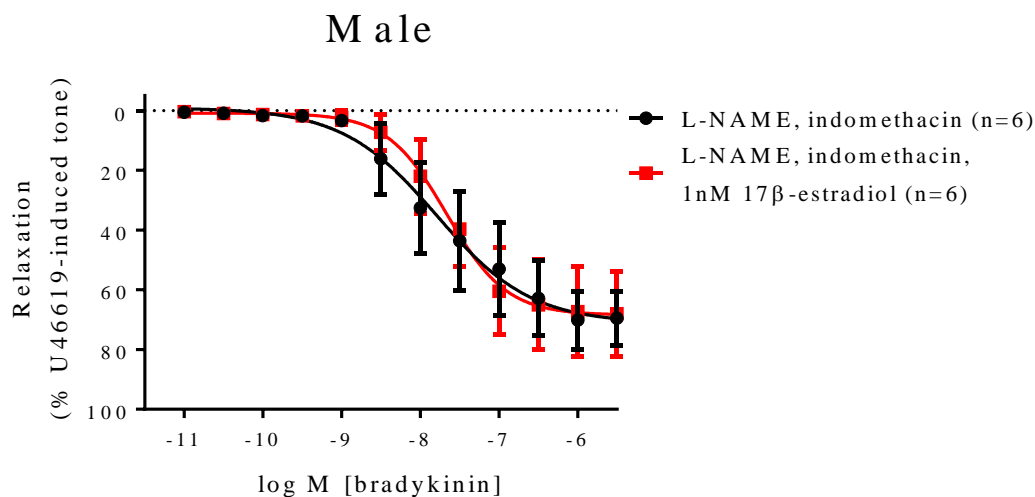


**Figure 2.8** Log concentration-response curves for the vasorelaxant effects of bradykinin in the presence of 300 μM L-NAME, 10 μM indomethacin and 1 nM 17β-estradiol (2 h incubation) in U46619 pre-contracted porcine coronary arteries from male pigs. Data are expressed as a percentage change from U46619-induced tone and are mean ± S.E.M. of 6 experiments.

**2.3.7 The effects of 1 μM 17β-estradiol in the presence of L-NAME and indomethacin on bradykinin-induced vasorelaxation in PCAs from male pigs**

As the exposure to 1 nM of 17β-estradiol had no effect on the bradykinin-induced vasorelaxation in the presence of L-NAME and indomethacin, a higher concentration of 17β-estradiol (1 μM) was used. As some of the individual concentration-response curve did not achieve a defined $R_{max}$, data were analysed at each individual concentration. At 10 nM and 30 μM of bradykinin, the presence of 1 μM 17β-estradiol significantly inhibited the vasorelaxation (*n*=6) (Figure 2.9).



**Figure 2.9** Log concentration-response curves for the vasorelaxant effects of bradykinin in the presence of 300 μM L-NAME, 10 μM indomethacin and 1 μM 17β-estradiol (4 h incubation) in U46619 pre-contracted porcine coronary arteries from male pigs. Data are expressed as a percentage change from U46619-induced tone and are mean ± S.E.M. of 6 experiments. *P<0.05; 2-tailed, paired Student's *t*-test.

**2.3.8 The effects of L-NAME, indomethacin and PEG-catalase on bradykinin-induced vasorelaxation in PCAs from male and female pigs**

In PCAs from females, treatment with 300 $UmL^{-1}$ PEG-catalase alone (Figure 2.10A) significantly reduced the vasorelaxation to bradykinin ($R_{max}$ = 70.8 ± 4.7%, $pEC_{50}$ = 8.23 ± 0.13, $n$=9) compared to an $R_{max}$ of 87.3 ± 2.6% ($pEC_{50}$ = 8.46 ± 0.06, $n$=15) under control conditions (P<0.05). However, in the presence of L-NAME and indomethacin ($R_{max}$ = 54.7 ± 5.8%, $pEC_{50}$ = 7.92 ± 0.2, $n$=9) no further inhibition was observed in the additional presence of 300 $UmL^{-1}$ PEG-catalase ($R_{max}$ = 52.1 ± 4.6%, $pEC_{50}$ = 7.63 ± 0.15, $n$=14).

Treatment of PCAs from males with 300 $UmL^{-1}$ PEG-catalase (Figure 2.10B) did not affect the vasorelaxation to bradykinin ($R_{max}$ = 82.7 ± 5.3%, $pEC_{50}$ = 8.05 ± 0.13, $n$=10) compared to control ($R_{max}$ = 86.1 ± 3.5%, $pEC_{50}$ = 8.34 ± 0.09, $n$=14). The presence of L-NAME and indomethacin in male PCAs significantly reduced the vasorelaxant responses to bradykinin ($R_{max}$ = 48.2 ± 9.3%, $pEC_{50}$ = 7.26 ± 0.30, $n$=10) but the additional presence of 300 $UmL^{-1}$ PEG-catalase did not cause further reduction in the bradykinin-induced vasorelaxation ($R_{max}$ = 47.2 ± 15.8%, $pEC_{50}$ = 7.07 ±0.50, $n$=11). A further experiment conducted in the presence of 600 $UmL^{-1}$ PEG-catalase had no effect on the $R_{max}$ or $EC_{50}$ of the bradykinin-induced vasorelaxation (Figure 2.10C), such that in the presence of 600 $UmL^{-1}$ PEG-catalase the $R_{max}$ = 95.3± 6.6% ($pEC_{50}$ = 7.63 ±0.11, $n$=4) and $R_{max}$ = 42.9± 12.5% ($pEC_{50}$ = 7.62 ±0.53, $n$=4) in the additional presence of L-NAME and indomethacin.

**Figure 2.10** Log concentration-response curves for the vasorelaxant effects of bradykinin in the absence or presence of 300 μM L-NAME, 10 μM indomethacin or 300 UmL$^{-1}$ PEG-catalase in U46619 pre-contracted porcine coronary arteries from (A) female and (B) male pigs or with (C) 600 UmL$^{-1}$ PEG-catalase in males. Data are expressed as a percentage change from U46619-induced tone and are mean ± S.E.M. of 4-15 experiments. *P<0.05; one-way ANOVA followed by Bonferroni's *post hoc* test.

**2.3.9 The effects of L-NAME, indomethacin and carbenoxolone on bradykinin-induced vasorelaxation in PCAs from male and female pigs.**

In PCAs from females, treatment with carbenoxolone alone did not affect vasorelaxation to bradykinin such that the maximum relaxation in controls was $87.1 \pm 2.8\%$ ($pEC_{50} = 8.48 \pm 0.07$, $n$=14) compared to a response of $81.6 \pm 5.9\%$ ($pEC_{50} = 8.38 \pm 0.17$, $n$=8) in the presence of carbenoxolone (Figure 2.11A). However, in the presence of L-NAME and indomethacin, addition of carbenoxolone further reduced the maximum relaxation to bradykinin from $54.7 \pm 5.8\%$ ($pEC_{50} = 7.92 \pm 0.20$, $n$=9) in the presence of L-NAME and indomethacin to a response of $31.1 \pm 4.1\%$ ($pEC_{50} = 7.62 \pm 0.23$, $n$=7) in the presence of carbenoxolone in combination with L-NAME and indomethacin ($P<0.01$).

In PCAs from males, the presence of carbenoxolone alone or in combination with L-NAME and indomethacin did not affect vasorelaxation to bradykinin (Figure 2.11B). The responses to bradykinin in the presence of carbenoxolone alone ($R_{max} = 81.5 \pm 5.7\%$, $pEC_{50} = 8.20 \pm 0.14$, $n$=6) were comparable with the responses to bradykinin under control conditions ($R_{max} = 87.7 \pm 5.3\%$, $pEC_{50} = 8.17 \pm 0.12$, $n$=9). Similarly, in the presence of L-NAME and indomethacin ($R_{max} = 51.7 \pm 10.3\%$, $pEC_{50} = 7.06 \pm 0.28$, $n$=7) the responses to bradykinin did not differ significantly in the additional presence of carbenoxolone ($R_{max} = 44.2 \pm 3.1\%$, $pEC_{50} = 7.54 \pm 0.11$, $n$=6).
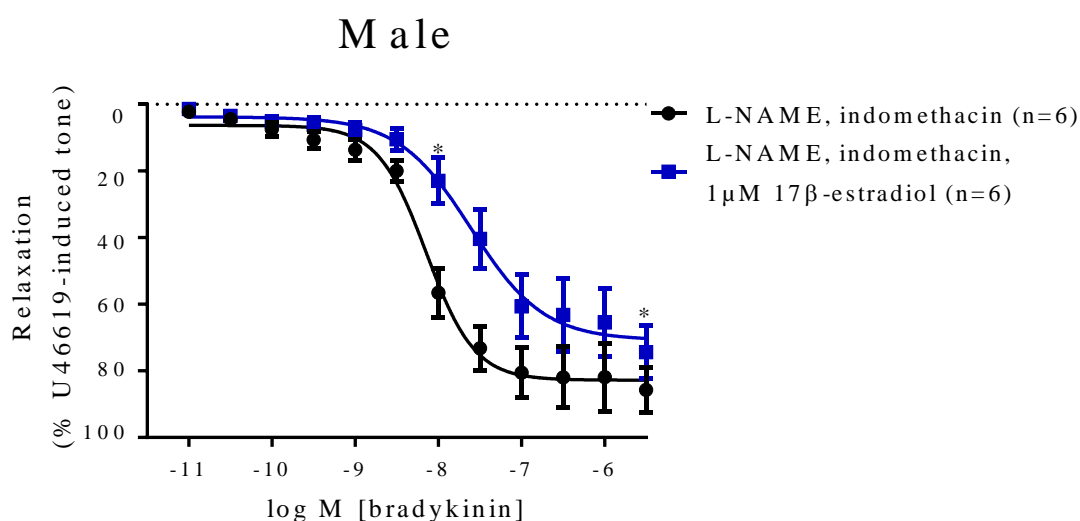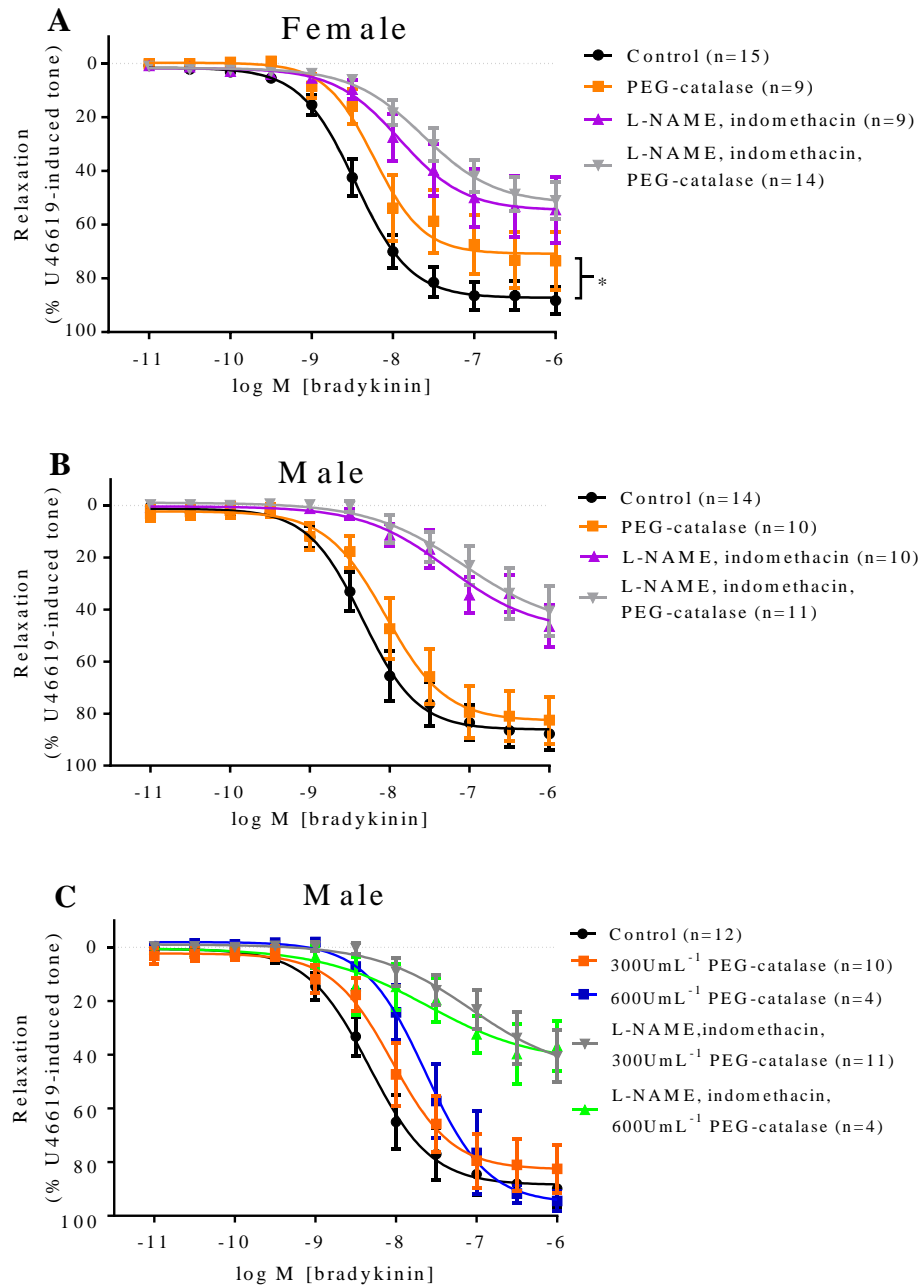
**Figure 2.11** Log concentration-response curves for the vasorelaxant effects of bradykinin in the absence or presence of 300 μM L-NAME, 10 μM indomethacin or 100 μM carbenoxolone in U46619 pre-contracted porcine coronary arteries from (A) female and (B) male pigs. Data are expressed as a percentage change from U46619-induced tone and are mean ± S.E.M. of 6-14 experiments. **P<0.01; one-way ANOVA followed by Bonferroni's *post hoc* test.

**2.3.10 The effects of L-NAME, indomethacin and 18α-glycyrrhetinic acid on bradykinin-induced vasorelaxation in PCAs from male and female pigs**

The presence of 18α-glycyrrhetinic acid ($R_{max}$ = 97.9 ± 2.0%, $pEC_{50}$ = 8.46 ± 0.04, $n$=6) in PCAs from female pigs did not affect the bradykinin-induced vasorelaxation compared to the control ($R_{max}$ = 99.3 ± 2.8%, $pEC_{50}$ = 8.61 ± 0.06, $n$=6) (Figure 2.12A). In the presence of L-NAME and indomethacin ($R_{max}$ = 88.2 ± 4.9%, $pEC_{50}$ = 7.95 ± 0.09, $n$=6), addition of 18α-glycyrrhetinic acid ($R_{max}$ = 88.4 ± 4.4%, $pEC_{50}$ = 7.60 ± 0.07, $n$=6) significantly shifted the curve to the right by 2.2-fold (P<0.05).

In PCAs from male pigs, the presence of 18α-glycyrrhetinic acid ($R_{max}$ = 96.0 ± 3.7%, $pEC_{50}$ = 8.69 ± 0.08, $n$=6) alone had no effect on the bradykinin-induced vasorelaxation compared to the control ($R_{max}$ = 101.9 ± 2.5%, $pEC_{50}$ = 8.80 ± 0.06, $n$=6) (Figure 2.12B). 18α-glycyrrhetinic acid in the presence of L-NAME and indomethacin ($R_{max}$ = 81.3 ± 6.2%, $pEC_{50}$ = 8.10 ± 0.14, $n$=6) had no effect on the bradykinin-induced vasorelaxation compared to L-NAME and indomethacin ($R_{max}$ = 82.7 ± 7.8%, $pEC_{50}$ = 8.04 ± 0.18, $n$=6).

**Figure 2.12** Log concentration-response curves for the vasorelaxant effects of bradykinin in the absence or presence of 300 μM L-NAME, 10 μM indomethacin or 100 μM 18α-glycyrrhetinic acid (18α-GA) in U46619 pre-contracted porcine coronary arteries from (A) female and (B) male pigs. Data are expressed as a percentage change from U46619-induced tone and are mean ± S.E.M. of 6 experiments. In female PCAs, presence of 18α-GA in L-NAME and indomethacin significantly shifted the bradykinin-induced vasorelaxation curve 2.2-fold to the right (P<0.05; one way ANOVA followed by Bonferroni's *post hoc* test).

**2.3.11 The effects of L-NAME, indomethacin, TRAM-34 and/or apamin on bradykinin-induced vasorelaxation in PCAs from male and female pigs**

In PCAs from females, treatment with TRAM-34 in the presence of L-NAME and indomethacin significantly inhibited the maximum relaxation to bradykinin from $R_{max}$ of 87.5 ± 2.7% ($pEC_{50}$ = 7.6 ± 0.05, $n$=5) to $R_{max}$ of 58.4 ± 7.9% ($pEC_{50}$ = 7.5 ± 0.2, $n$=5) (Figure 2.13A) (P<0.0001). Similarly, the maximum relaxation to bradykinin was significantly inhibited by apamin in the presence of L-NAME and indomethacin such that the $R_{max}$ was reduced to 72.2 ± 10.5% ($pEC_{50}$ = 7.6 ± 0.2, $n$=5) (P<0.01). The maximum relaxation to bradykinin was further inhibited with a combination of TRAM-34 and apamin in the presence of L-NAME and indomethacin ($R_{max}$ = 26.6 ± 3.7%, $pEC_{50}$ = 7.2 ± 0.2, $n$=6) (P<0.0001) (Figure 2.13A).

In PCAs from males, vasorelaxation produced at 1 μM of bradykinin was used for statistical analysis instead of $R_{max}$ because the maximum relaxation was not fully defined in some of the groups. Treatment with TRAM-34 in the presence of L-NAME and indomethacin (52.4 ± 9.5%, $n$=11) had no effect on the bradykinin-induced vasorelaxation at 1 μM bradykinin compared to L-NAME and indomethacin (63.3 ± 7.9%, $n$=11) (Figure 2.13B). In contrast, addition of apamin alone significantly inhibited the vasorelaxation produced at 1 μM bradykinin (39.8 ± 9.7%, $n$=11) (P<0.05) compared to L-NAME and indomethacin. Similarly, combination of TRAM-34 and apamin in the presence of L-NAME and indomethacin (27.0 ± 4.7%, $n$=11) significantly inhibited the vasorelaxation produced at 1 μM bradykinin compared to L-NAME and indomethacin (P<0.01) but vasorelaxation in these arteries did not

differ significantly with the apamin, L-NAME and indomethacin treated arteries.
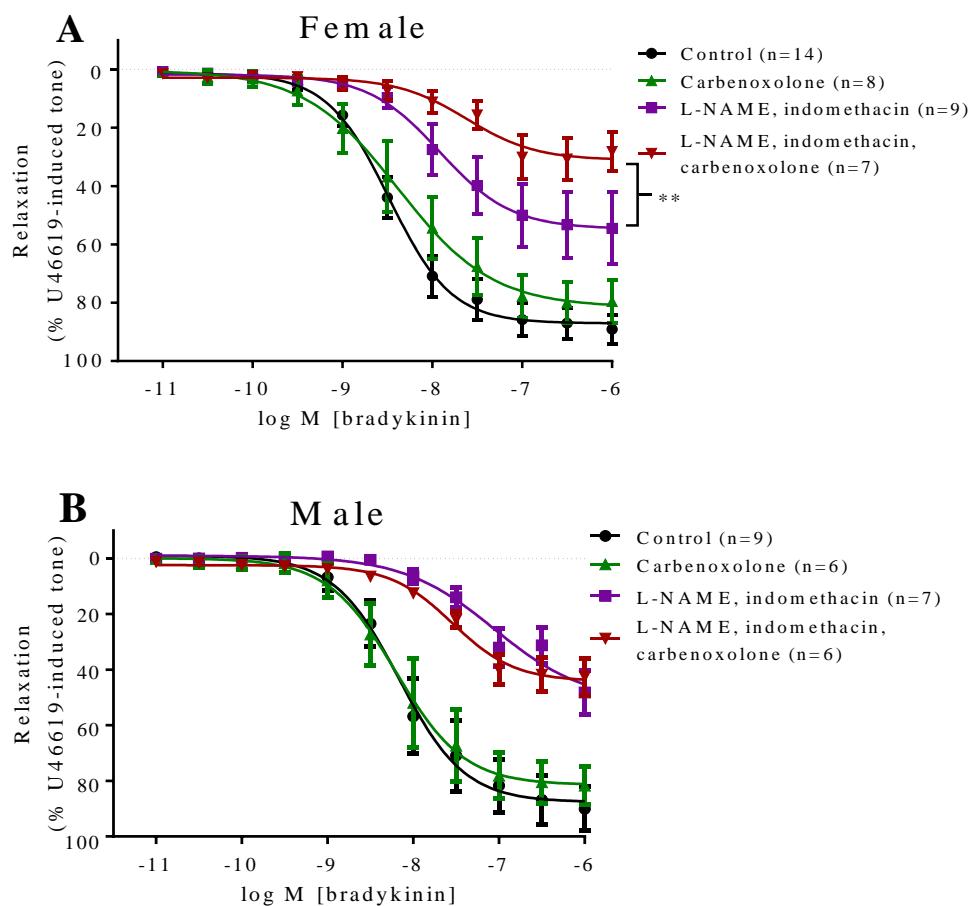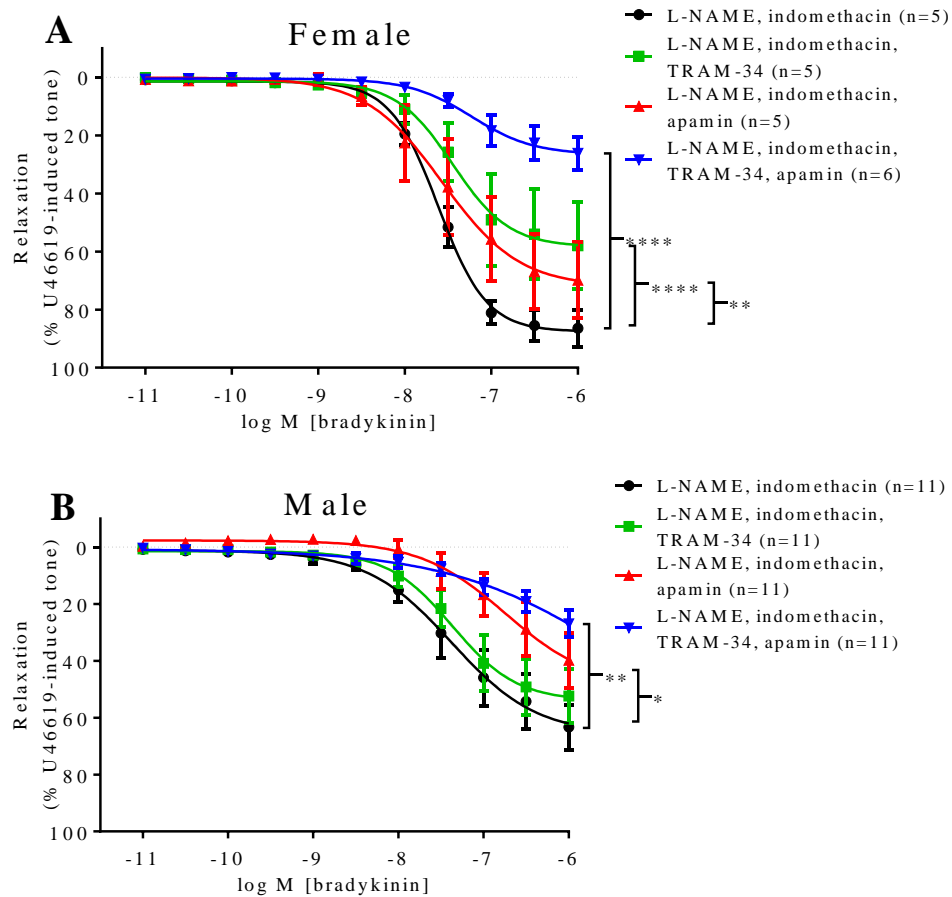


**Figure 2.13** Log concentration-response curves for the vasorelaxant effects of bradykinin in the presence of 300 μM L-NAME, 10 μM indomethacin, 500 nM apamin and/or 10 μM TRAM-34 in U46619 pre-contracted porcine coronary arteries from (A) female and (B) male pigs. Data are expressed as a percentage change from U46619-induced tone and are mean ± S.E.M. of 5-11 experiments. *P<0.05, **P<0.01, ****P<0.0001; one-way ANOVA followed by Bonferroni's *post hoc* test.

**2.3.12 The effects of L-NAME, indomethacin and apamin and/or TRAM-34 on NS309-induced vasorelaxation in PCAs from male and female pigs**

To further determine if there are sex differences in the functional role of the $IK_{Ca}$ channels in PCAs from male and female pigs, NS309, a selective $SK_{Ca}$ and $IK_{Ca}$ channels activator (Leuranguer *et al.*, 2008a) was used in the presence of apamin and/or TRAM-34. In PCAs from female pigs in the presence of L-NAME and indomethacin, NS309 produced an $R_{max}$ of $117 \pm 3\%$ ($pEC_{50} = 5.81 \pm 0.05$, *n*=6) and treatment with apamin had no effect on the NS309-induced vasorelaxation ($R_{max} = 114 \pm 3\%$, $pEC_{50} = 5.74 \pm 0.05$, *n*=6) (Figure 2.14A). Similarly, in PCAs from male pigs, in the presence of L-NAME and indomethacin, apamin no effect on the $R_{max}$ or $pEC_{50}$ values on NS309-induced vasorelaxation ($R_{max} = 116 \pm 3\%$, $pEC_{50} = 5.82 \pm 0.05$, without apamin; $R_{max} = 117 \pm 3\%$, $pEC_{50} = 5.73 \pm 0.05$; with apamin, *n*=6) (Figure 2.14B). In PCAs from male pigs, in the presence of L-NAME and indomethacin, the addition of TRAM-34 did not affect responses to NS309 such that $R_{max} = 113 \pm 4\%$ and $pEC_{50} = 5.84 \pm 0.06$ (*n*=6) in the absence and $R_{max} = 112 \pm 5\%$ and $pEC_{50} = 5.91 \pm 0.10$ (*n*=6) in the presence of TRAM-34 (Figure 2.14C).

Further experiments with PCAs from male pigs in the presence of L-NAME and indomethacin with both apamin and TRAM-34 had no effect on the NS309-induced vasorelaxation (Figure 2.14D) compared to the control. The $R_{max}$ was $119 \pm 5\%$ ($pEC_{50} = 5.83 \pm 0.90$, *n*=6) under control conditions and $R_{max}$ of $119 \pm 5\%$ ($pEC_{50} = 5.86 \pm 0.91$, *n*=6) in the presence of apamin and TRAM-34. On the other hand, in PCAs from female pigs, the presence of L-NAME, indomethacin and both apamin and TRAM-34 significantly

inhibited the NS309-induced vasorelaxation (Figure 2.14E) at 0.3 μM of NS309 (P<0.05) with no significant differences in $R_{max}$ between control ($R_{max}$ of 115 ± 6%, $pEC_{50}$ = 5.96 ± 0.12, $n$=10) and in the presence of apamin and TRAM-34 ($R_{max}$ of 115 ± 4%, $pEC_{50}$ = 5.72 ± 0.07, $n$=10).
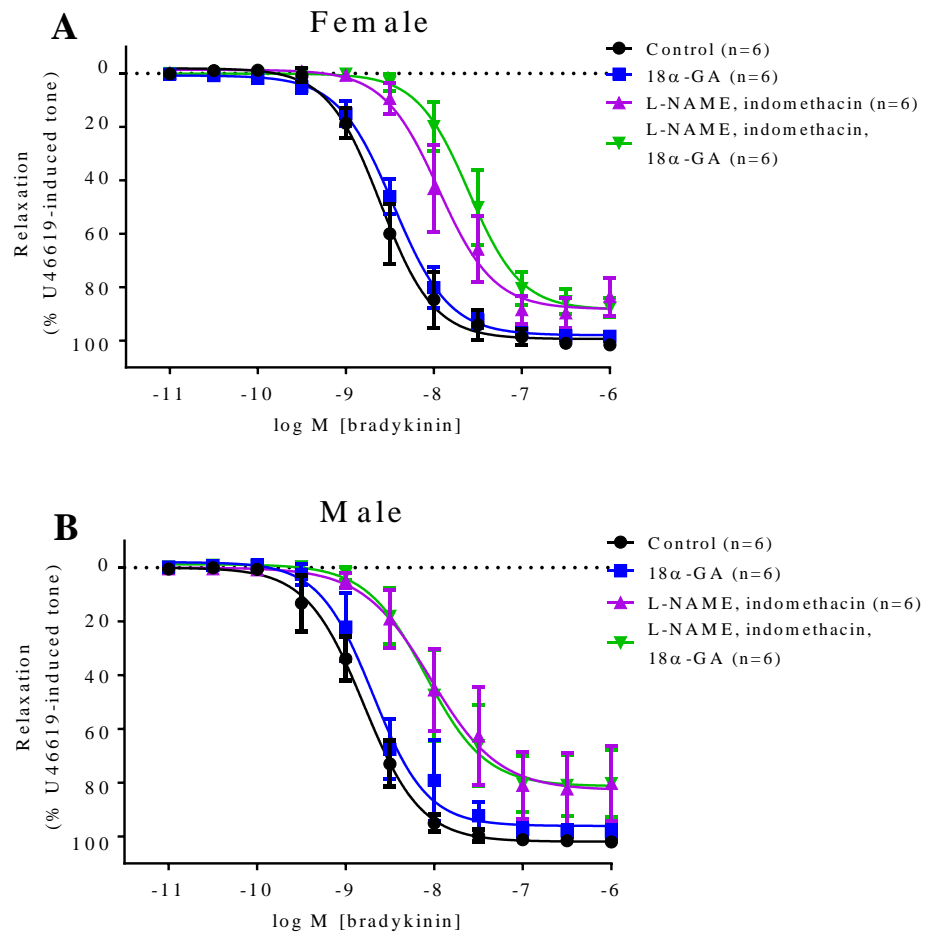


**Figure 2.14** Log concentration-response curves for the vasorelaxant effects of NS309 in the presence of 300 μM L-NAME, 10 μM indomethacin and 500 nM apamin in U46619 pre-contracted porcine coronary arteries from (A) female and (B) male pigs. Data are expressed as a percentage change from U46619-induced tone and are mean ± S.E.M. of 6 experiments.
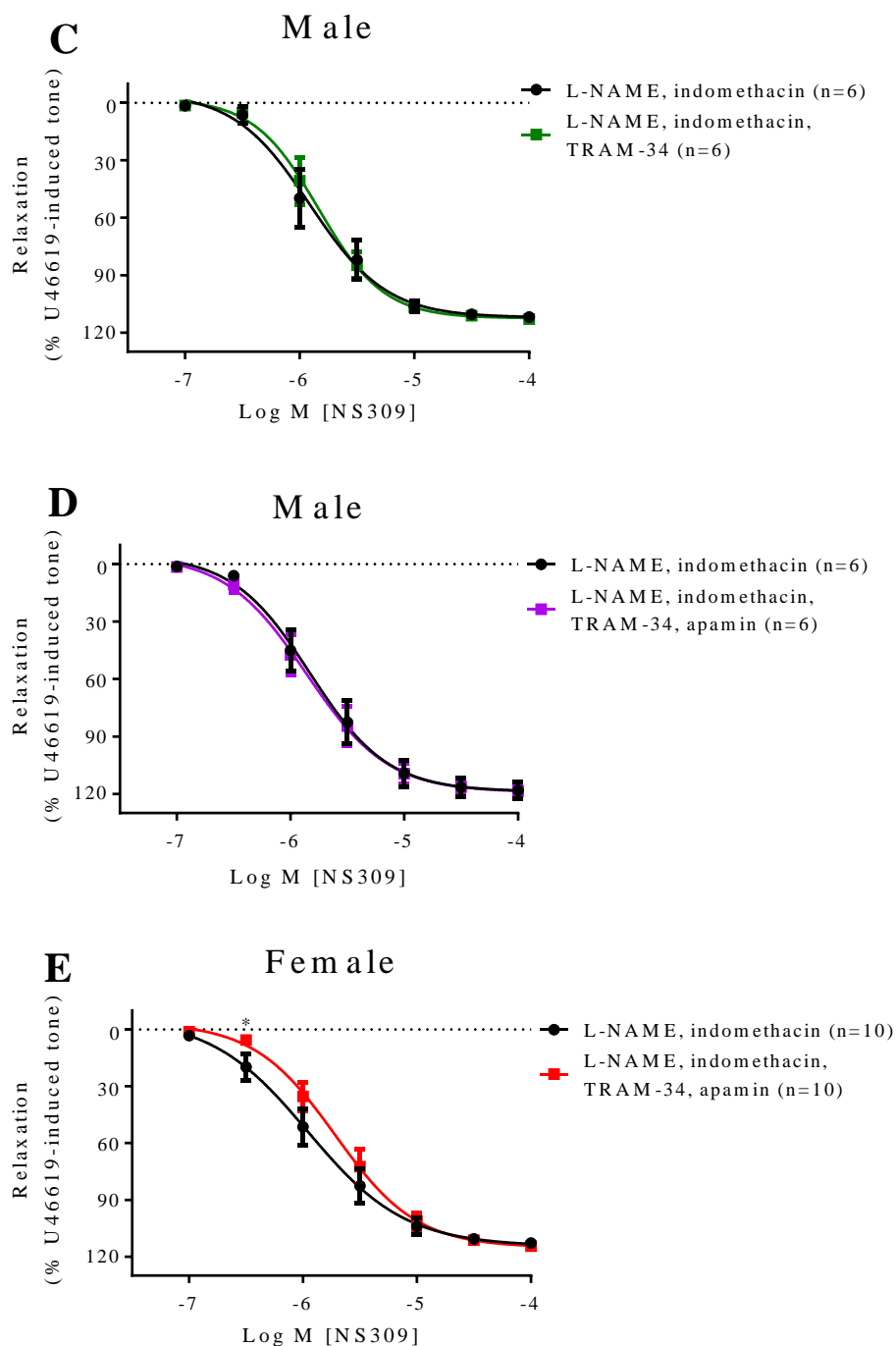
**Figure 2.14** Log concentration-response curves for the vasorelaxant effects of NS309 in the presence of 300 μM L-NAME, 10 μM indomethacin and 10 μM TRAM-34 in U46619 pre-contracted porcine coronary arteries from (C) male pigs or in the presence of both apamin and TRAM-34 in (D) male and (E) female pigs. Data are expressed as a percentage change from U46619-induced tone and are mean ± S.E.M. of 6-10 experiments. *P<0.05; 2-tailed, paired Student's *t*-test.

## 2.3.13 The effects of 60 mM KCl or U46619-induced tone on NS309-induced vasorelaxation in PCAs from female pigs

Additional experiments to examine the selectivity of NS309 were carried out by pre-contracting vessels with either 60 mM KCl or U46619 in the presence of L-NAME and indomethacin (Figure 2.15A). Vessels pre-contracted with either U46619 or KCl produced a similar maximum relaxation to NS309 such that the $R_{max}$ for U46619 pre-contracted vessels was $113 \pm 3\%$ compared to $R_{max}$ of $116 \pm 3\%$ in vessels pre-contracted with KCl. However, vessels pre-contracted with KCl significantly shifted the NS309-induced vasorelaxation curve 8.1-fold to the right (P<0.001) compared to vessels pre-contracted with U46619 (Figure 2.15A) ($pEC_{50} = 5.67 \pm 0.04$, pre-contracted with U46619; $pEC_{50} = 4.76 \pm 0.02$, pre-contracted with KCl, $n$=6). See Figure 2.15B for original trace showing responses to NS309.
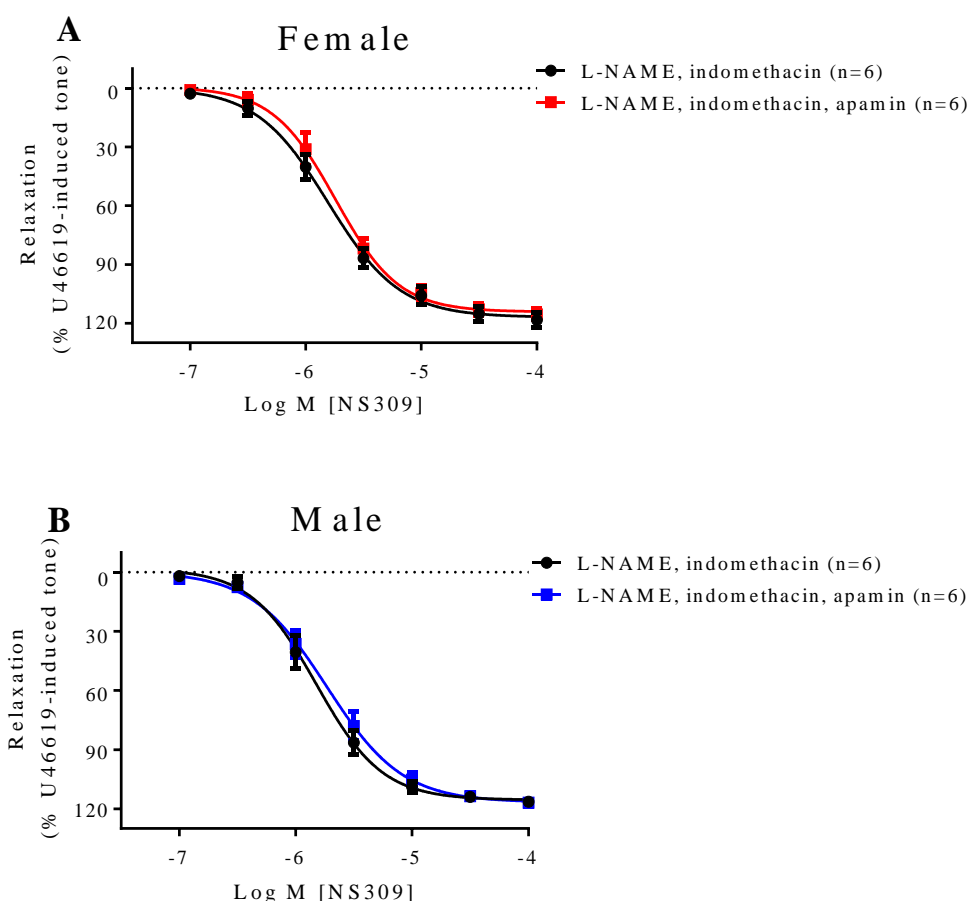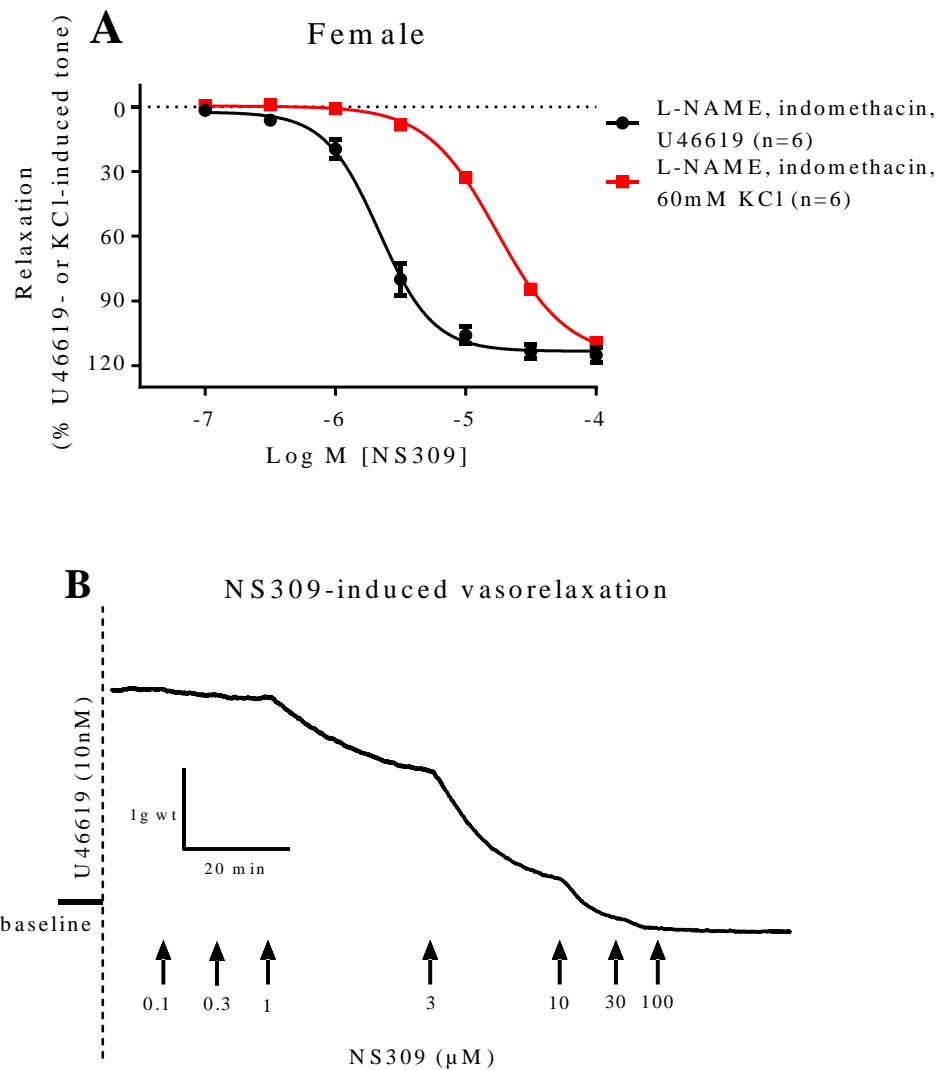
**Figure 2.15** (A) Log concentration-response curves for the vasorelaxant effects of NS309 in the presence of 300 μM L-NAME and 10 μM indomethacin pre-contracted with either U46619 or 60 mM KCl in porcine coronary arteries from female pigs. Presence of 60 mM KCl significantly shifted the NS309-induced vasorelaxation 8.1-fold to the right (P<0.001; 2-tailed, paired Student's *t*-test). Data are expressed as a percentage change from U46619- or KCl-induced tone and are mean ± S.E.M. of 6 experiments. (B) Original trace showing the responses to increasing concentration of NS309, a selective $SK_{Ca}$ and $IK_{Ca}$ channels activator.

## 2.4 Determination of expressions of Connexins 37, 40 and 43 and IK$_{Ca}$ in PCAs from male and female pigs via Western blotting

Western Blot analysis demonstrated the presence of connexin 43 (Figure 2.16A), connexin 40 (Figure 2.17A) and IK$_{Ca}$ (Figure 2.19A), but connexin 37 (Figure 2.18) proteins were not detected in PCAs from male and female pigs. Further quantitative analysis based on the ratio of the protein band intensities to their respective loading control showed no significant differences between PCAs from male and female pigs in connexin 43:MLC (Figure 2.16B), connexin 40:GAPDH (Figure 2.17B), and IK$_{Ca}$:GAPDH (Figure 2.19B). In Figure 2.17A and 2.18 the presence of the red lower band below 37 kDa is a non-specific band produced by the secondary antibody, IRDye$^{®}$ 680LT Goat anti-rabbit IgG (1:10 000) (LI-COR Biosciences, Cambridge, UK) (Figure 2.17C). For connexin 40 (Figure 2.17A), no bands were observed at 40 kDa in the absence of the primary antibody (Figure 2.17C).
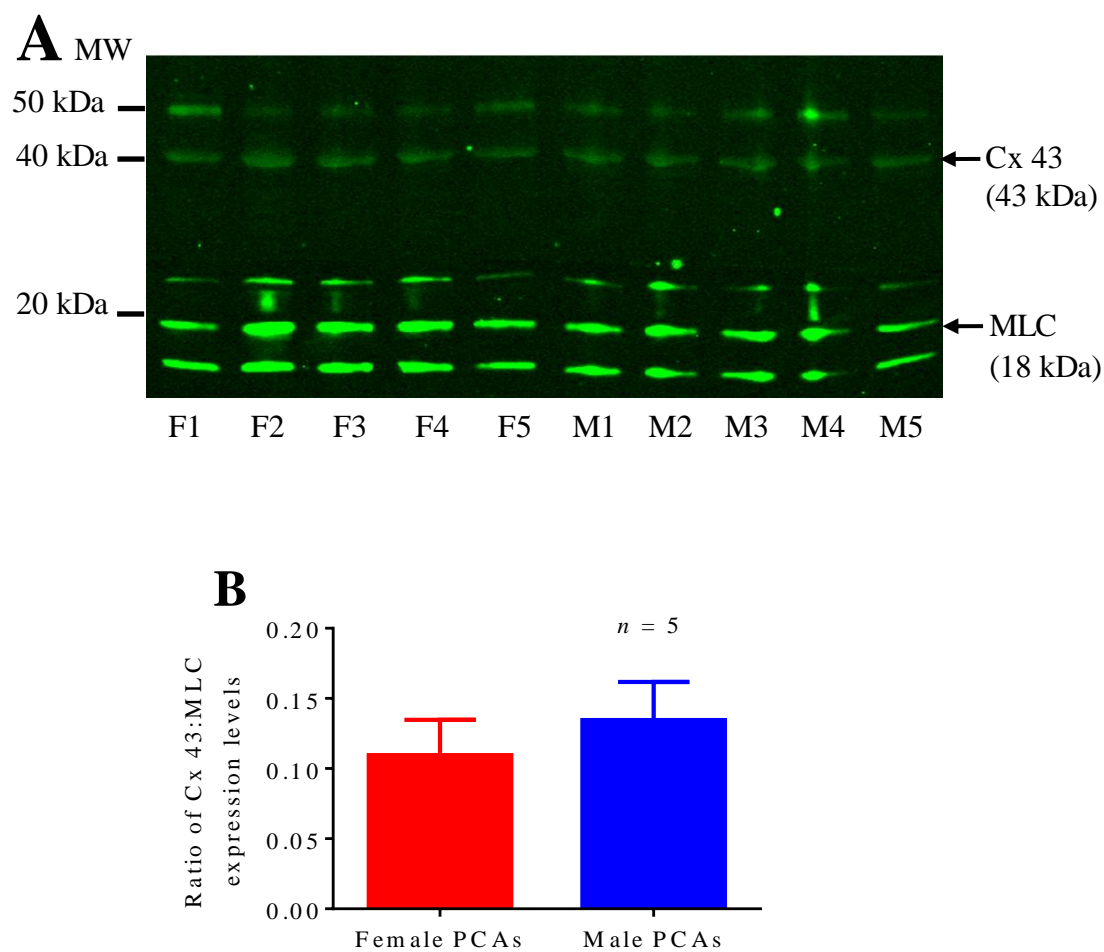
**Figure 2.16** (A) Connexin 43 (43 kDa) and MLC (18 kDa) expression levels in 5 μg of porcine coronary artery samples (PCAs) from female (F1-F5) and male (M1–M5) pigs. (B) Ratio of the expression levels of connexin 43 to MLC in male and female PCAs based on the intensities of their bands. Data are expressed in the ratio of Cx43 to MLC intensities bands and are mean ± S.E.M. of 5 PCAs.
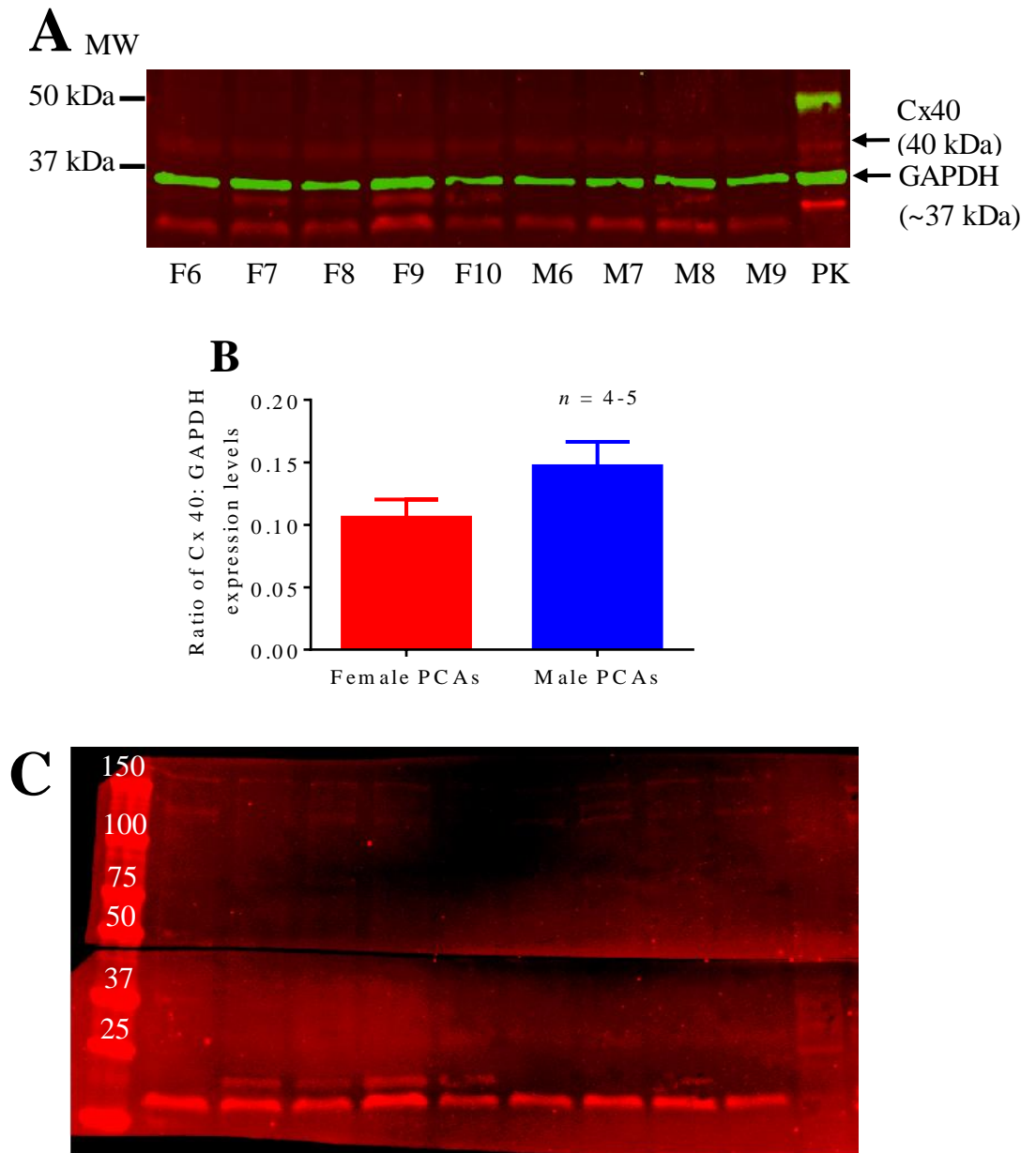
**Figure 2.17** (A) Connexin 40 (40 kDa) and GAPDH (~37 kDa) expression levels in 10 μg of porcine coronary artery samples (PCAs) from female (F6–F10) and male (M6–M9) pigs with 20 μg of pig kidney (PK) lysate as positive control. (B) Ratio of the expression levels of Cx40 to GAPDH in male and female PCAs based on the intensities of their bands. (C) Blot incubated with secondary antibody alone demonstrating that the lower band slightly above 25 kDa is a non-specific band produced by the secondary antibody, IRDye® 680LT Goat anti-rabbit IgG with no bands observed at 40 kDa in the absence of the primary antibody. Data are expressed in the ratio of Cx40 to GAPDH intensities bands and are mean ± S.E.M. of 4-5 PCAs.
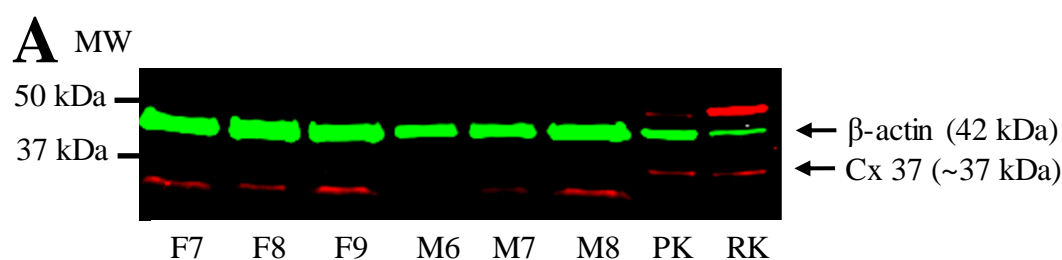
**Figure 2.18** Connexin 37 (~37 kDa) and β-actin (42 kDa) expression levels in 15 μg of porcine coronary artery samples from female (F7–F9) and male (M6–M8) pigs with 20 μg of pig (PK) and rat kidney (RK) lysate as positive controls.
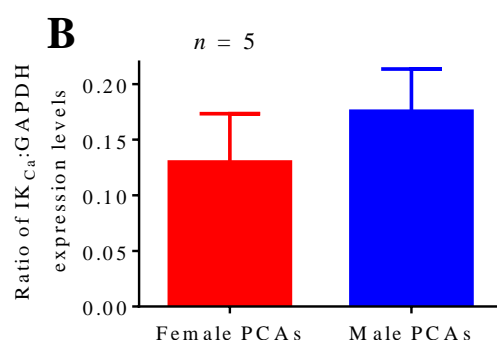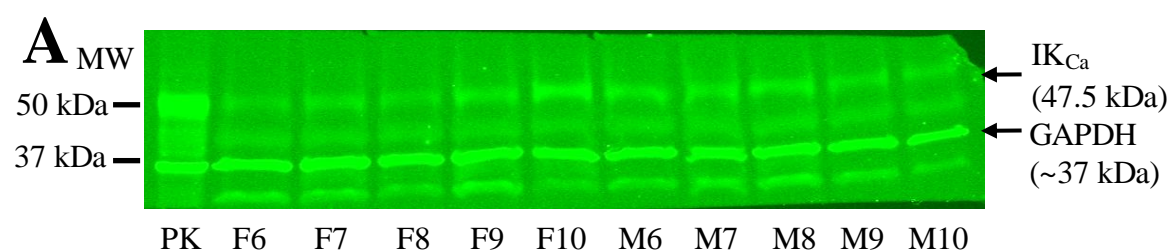


**Figure 2.19** (A) $IK_{Ca}$ (47.5 kDa) and GAPDH (~37 kDa) expression levels in 15 μg of porcine coronary artery samples (PCAs) from female (F6–F10) and male (M6–M10) pigs with 10 μg of pig kidney (PK) lysate as positive control. (B) Ratio of the expression levels of $IK_{Ca}$ to GAPDH in male and female PCAs based on the intensities of their bands. Data are expressed in the ratio of $IK_{Ca}$ to GAPDH intensities bands and are mean ± S.E.M. of 5 PCAs.

## 2.5 Polymerase chain reaction (PCR) amplification of the *Sry* gene for sex identification in pigs

### 2.5.1 The effects of DNA purification on PCR of the Sry gene

Preliminary work demonstrated that purified DNA samples (Figure 2.20B) produced a sharper *Zfy/Zfx* band (447 bp) compared to unpurified samples (Figure 2.20A) and that PCR amplification of the *Sry* band (163 bp) in DNA samples from pigs' heart with male and female samples from rat liver (MK and FK) as positive control was unsuccessful. Failure of the PCR amplification in rat liver could be due to species differences as the primers were based on porcine DNA sequence.
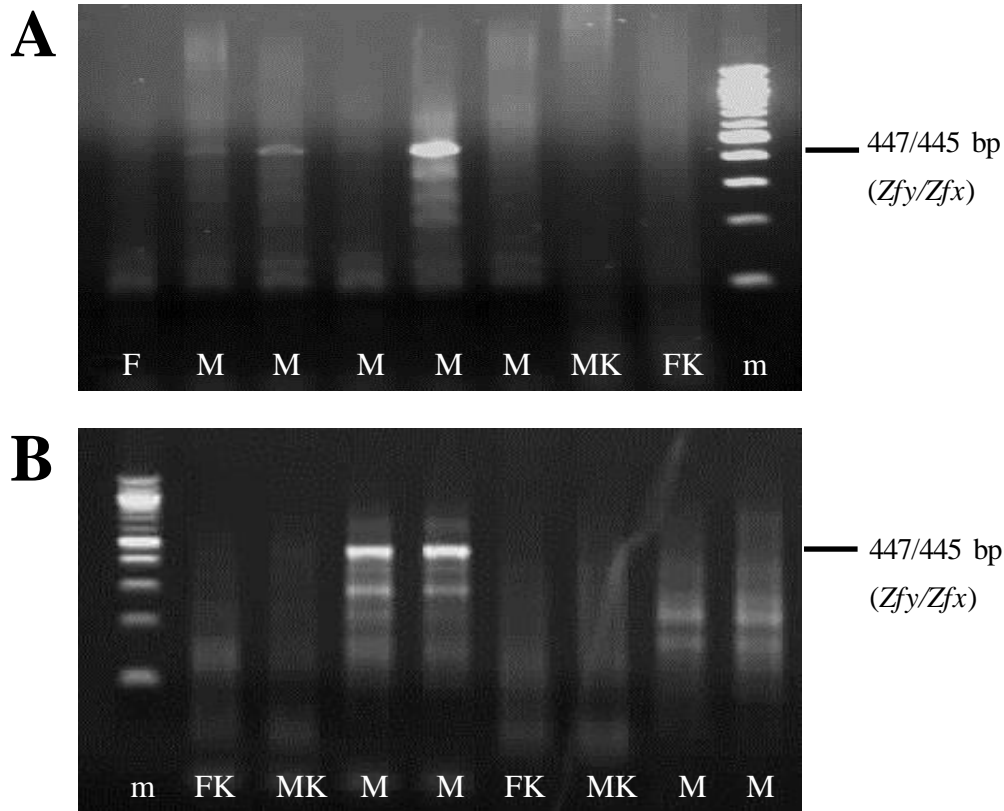
**Figure 2.20** PCR amplification of the *Sry* gene for sex identification in porcine heart tissue using (A) unpurified and (B) purified DNA samples. Upper band (445 bp) corresponds to the positive control *Zfy/Zfx* PCR product and (B) purified samples produced a sharp and strong band compared to (A) unpurified samples. However, amplification of the *Sry* band (163 bp) was unsuccessful under both conditions. Lane m = DNA ladder, MK = liver from male rat and FK = liver from female rat were used as positive controls for the *Sry* gene but no band was observed, this could possibly be due to species differences as the *Sry* primers for PCR amplification were based on porcine.

### 2.5.2 Optimisation of the PCR conditions varying the annealing temperature and magnesium chloride concentration

As the PCR amplification of the *Sry* gene was successful, a range of annealing temperatures and different concentrations of magnesium chloride were examined. Figure 2.21 demonstrates that the annealing temperature of 54°C appeared to be the optimised condition for PCR amplification, a temperature previously used by Brya & Koneân (2003) for sex identification.
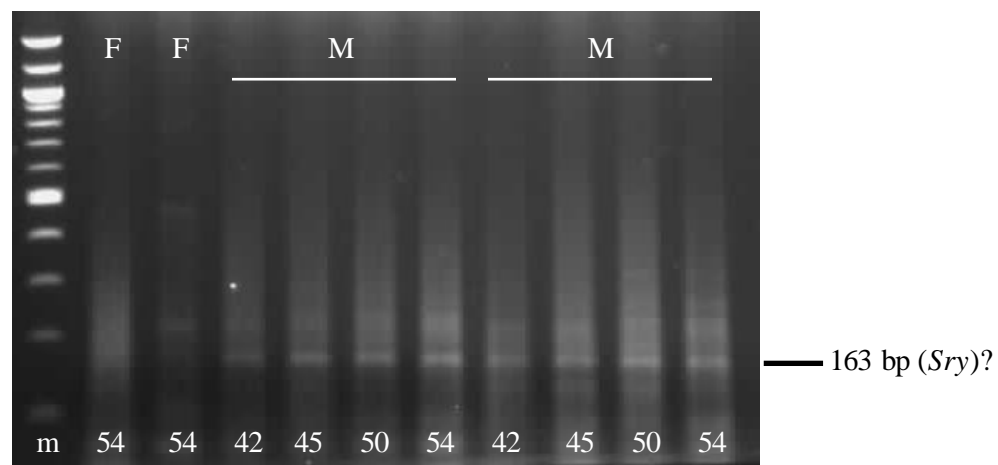


**Figure 2.21** Varying annealing temperatures for confirmation of the *Sry* PCR amplification in purified DNA samples from female (F) and male (M) pigs' heart tissues. Lane 1 (marker), lanes 2-3 (PCR amplification of female DNA in duplex was unsuccessful), lanes 4-11 (two different male DNA samples annealed under different temperature and 54°C appeared to produce the strongest band).

Next, different concentrations of magnesium chloride were examined in singleplex or duplex PCR reaction using purified DNA samples from male pigs. Figure 2.22 demonstrated no differences in the *Zfy-Zfx* band between 1.5 - 2.5 mM of magnesium chloride concentrations and that amplification of the *Sry* band was unsuccessful either in singleplex or duplex form. It was later discovered that the 3' downstream primer ordered was not converted and inverted, contributing to the failure in amplifying the *Sry* band. New primer was re-ordered for subsequent experiments.
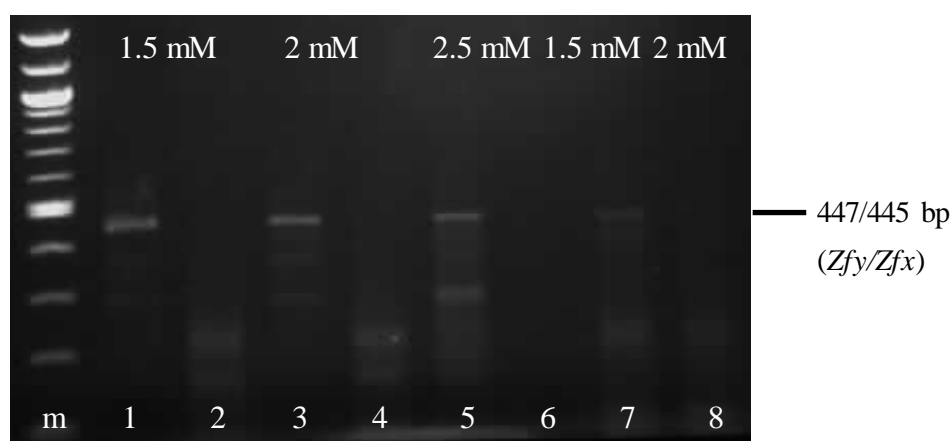


**Figure 2.22** Varying magnesium chloride concentrations for confirmation of the *Sry/Zfy-Zfx* PCR amplification in singleplex (1-6) or duplex (7-8) using purified DNA samples from male pigs' heart tissues. Lane 1 (marker), singleplex of *Zfy/Zfx* PCR amplification (1, 3, 5) and singleplex of *Sry* PCR amplification (2, 4, 6). Upper band (447 bp) corresponds to the positive control of the *Zfy/Zfx* PCR product but the lower faint band (~250 bp) do not correspond to the *Sry* PCR product. Amplification of the *Sry* gene was unsuccessful because the 3' downstream primer was not inverted and converted. New primer was ordered for subsequent experiments.

### 2.5.3 The effects of running singleplex or duplex PCR amplification

Using a new set of primers, PCR amplification of the *Sry/Zfy-Zfx* genes were carried out in singleplex or duplex using purified DNA samples from male and female pigs (Figure 2.23). Results demonstrated that running *Zfy-Zfx* in singleplex form a stronger band compared to duplex with no differences in the visibility of the *Sry* band. Figure 2.23 also demonstrates that the *Sry* band was stronger in males compared to females (last two lanes).
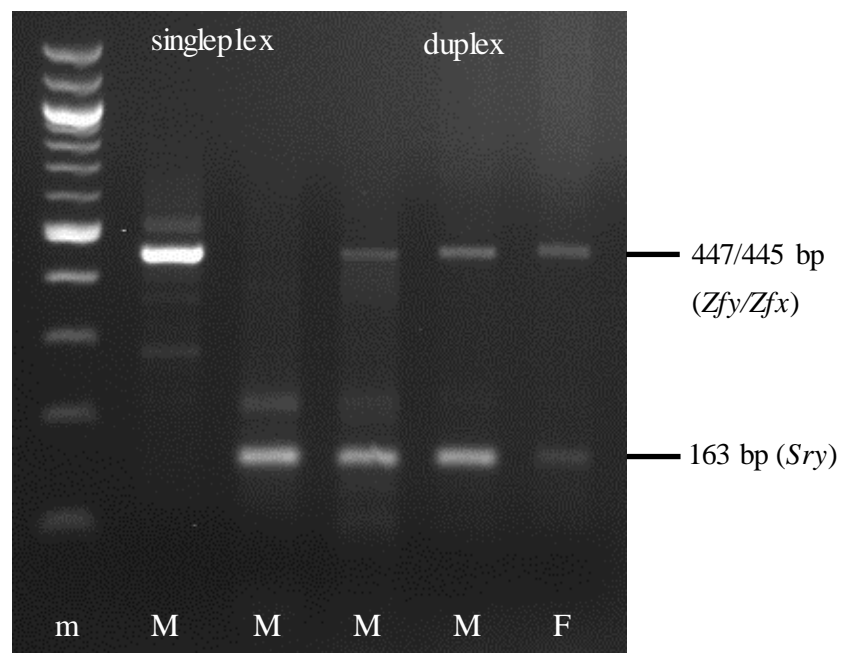


**Figure 2.23** Confirmation of *Sry/Zfy-Zfx* PCR amplification in singleplex or duplex using purified DNA samples from male (M) and female (F) pigs' heart tissues. Lane 1 (marker), lane 2-3 PCR amplification in singleplex and lane 4-6 PCR amplification in duplex. Upper band (447 bp) corresponds to the positive control of the *Zfy/Zfx* PCR product. Lane 4 and 5 were DNA samples from two different male pigs extracted on separate days. The 163 bp band visualised was stronger in males compared to females.

**2.5.4 PCR amplification of the Sry gene for sex identification in pig tissue samples collected from hearts used for myograph and Western Blot study**

Using purified DNA samples from male and female pigs' heart tissue which correspond to the PCAs used for Western Blotting and myography studies, PCR amplification of the *Sry* (Figure 2.24A) *and Zfy-Zfx* (Figure 2.24B) were conducted in singleplex. Figure 2.24A demonstrated that the *Sry* band was detected in all male DNA samples (*n*=7) and not in female DNA samples (*n*=6) collected on separate days.

Figure 2.25 demonstrated that the *Sry* band (163 bp) was detected in five out of six male DNA samples and not in the female samples (*n*=7). In the female DNA samples, seven out of the eight PCR amplification were successful, using the *Zfy-Zfx* band as positive control for successful PCR (Bryja & Koneân, 2003; Pomp *et al.*, 1995) and the *Sry* band was absence in the female samples.
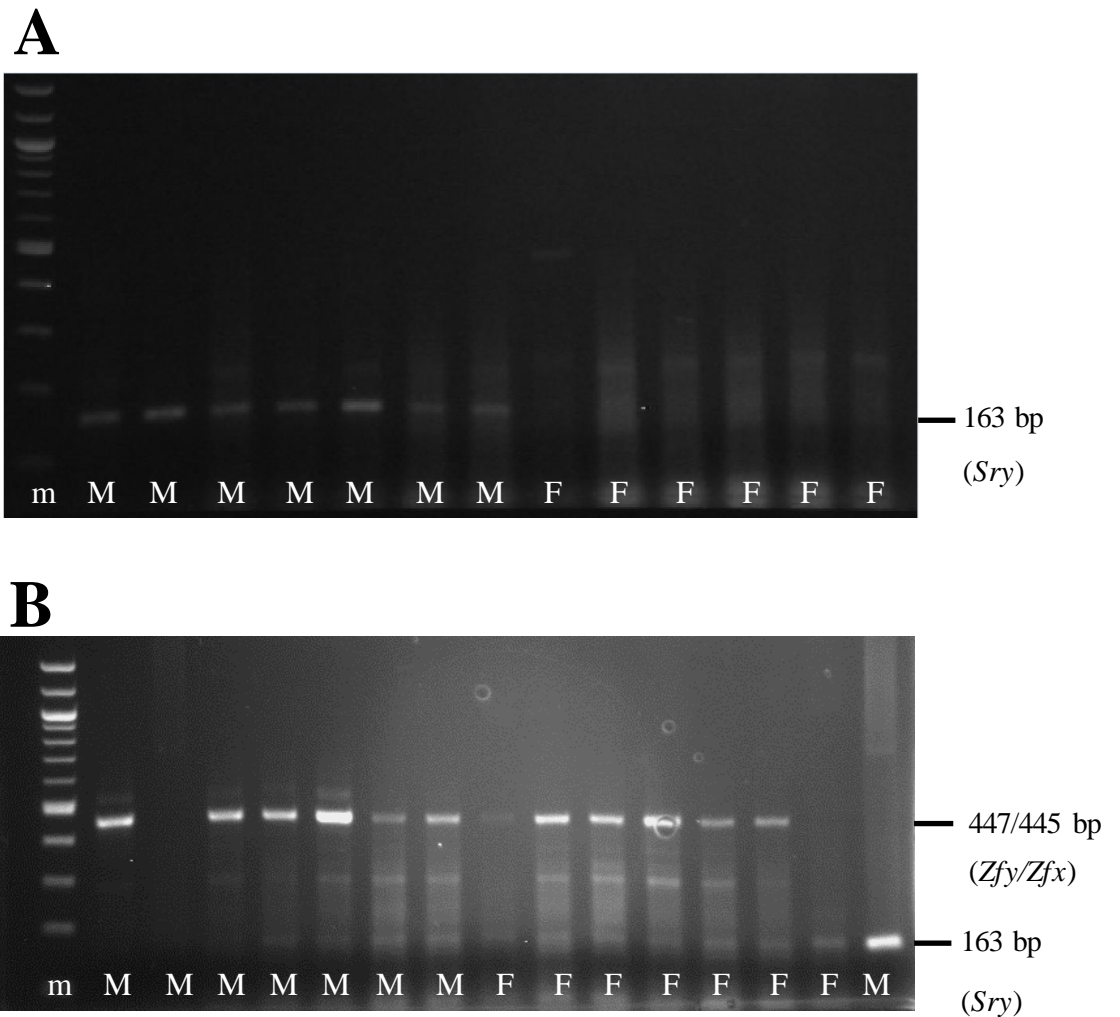
**Figure 2.24** Confirmation of (A) *Sry and* (B) *Zfy-Zfx* in singleplex PCR amplification using purified DNA samples from male and female pigs' heart tissue which correspond to the porcine coronary arteries used for Western blotting and myography studies. Lane m = marker, M = male and F = female. Upper band (447 bp) corresponds to the positive control of the *Zfy/Zfx* PCR product. Singleplex PCR amplification of the *Zfy/Zfx* in B was from the same samples as A except for the last two lanes in B where the *Sry* primers were added and here the 163 bp band detected was stronger in males compared to females.
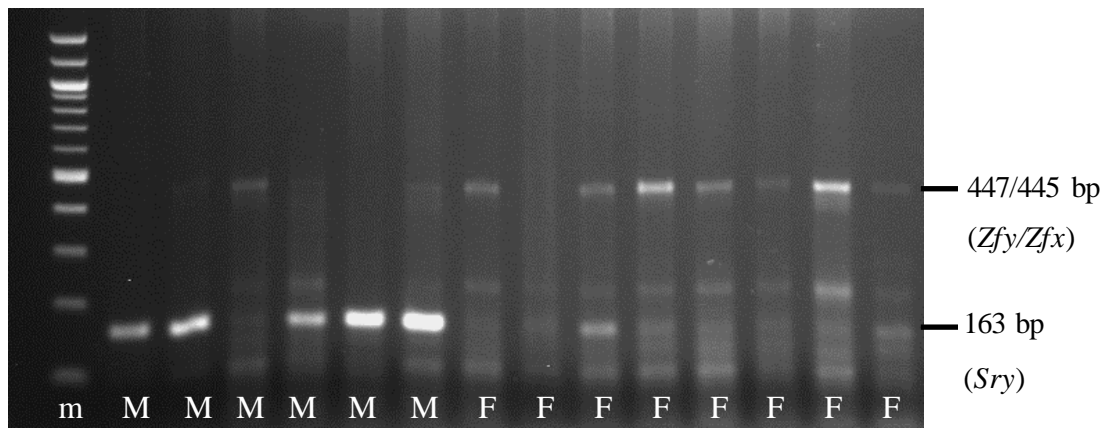
**Figure 2.25** Confirmation of *Sry/Zfy-Zfx* PCR amplification in duplex using unpurified DNA samples from male and female pigs' heart tissue which correspond to the porcine coronary arteries used in Western blotting and myography studies. Lane m = marker, M = male and F = female. Upper band (447 bp) corresponds to the positive control of the *Zfy/Zfx* PCR product and appears fainter in the males compared to females due to competing *Sry* amplification system in the males.

## 2.6 Discussion

In PCAs from either sex, bradykinin produced a concentration-dependent vasorelaxation with a maximum relaxation of almost 90% and this relaxation was abolished with the removal of endothelium. This indicates that the vasorelaxation to bradykinin in porcine isolated coronary arteries is endothelium-dependent and a similar observation had been previously reported by Nagao & Vanhoutte (1992). Treatment with indomethacin alone had no effect on the bradykinin-induced vasorelaxation, whereas treatment with L-NAME alone significantly reduced the maximum vasorelaxation to bradykinin in PCAs from either sex. This result demonstrated that the endothelium-derived nitric oxide plays a significant role in the endothelium-dependent relaxation to bradykinin. In the presence of L-NAME, a residual relaxation was observed in the present study and this relaxation was insensitive to the presence of indomethacin. The substantial proportion of bradykinin-induced vasorelaxation which is insensitive to NO synthase inhibition and cyclooxygenase inhibition is attributed to endothelium-derived hyperpolarization (EDH)-type response (Edwards *et al.*, 2010; McCulloch *et al.*, 1997; Taylor & Weston, 1988).

In the second part of the study, a significant sex difference in the EDH-mediated response induced by bradykinin was demonstrated. Specifically, the EDH responses were more prominent in females compared to males. Similar conclusions have been made in previous studies including isolated mesenteric arteries from rats (McCulloch & Randall, 1998; White *et al.*, 2000), mesenteric arteries from 'EDH mice' (eNOS/COX-1 double knockout mouse) as well as an *in vivo* study with 'EDH mice' (Scotland *et al.*, 2005). However, another

study in PCAs reported that the presence of L-NAME and indomethacin did not show any significant sex differences in the endothelium-dependent vasorelaxation to bradykinin (Barber & Miller, 1997). This difference could possibly be due to the size of the vessels used. In the present study, small distal PCAs, where EDH is believed to be more prominent in endothelium-dependent relaxations (Shimokawa *et al.*, 1996), were used. However, in the study conducted by Barber *et al.,* (1997), the size of the vessels used was not reported.

To examine if the enhanced EDH-type relaxation in PCAs from female pigs could be influenced *ex vivo* by oestrogen levels, the present study examined the effects of low concentrations (1 nM) and high concentrations (1 μM) 17β-estradiol on bradykinin-induced EDH-type relaxation in PCAs from male pigs. Treatment with 1 nM 17β-estradiol for 2 h in the presence of L-NAME and indomethacin had no effect on the bradykinin-induced vasorelaxation. A similar result has previously been reported, where acute exposure (20 min) of 1 nM 17β-estradiol or 24 h exposure to 1 nM – 100 nM 17β-estradiol in PCAs from either sex had no effect on the bradykinin-induced vasorelaxation (Cox *et al.*, 2005; Teoh & Man, 2000). However, in the present study, exposure to high concentrations of 17β-estradiol (1 μM) for 4 h significantly inhibited the bradykinin-induced EDH-type relaxation in PCAs from male pigs. This is in contrast to a previous study in isolated carotid arteries from male rabbits, where chronic treatment (8 weeks) of 17β-estradiol had no effect on the acetylcholine-induced EDH-type responses in control animals, but significantly enhanced the EDH-type responses in hypercholesterolaemic animals (Ghanam *et al.*, 2000). Here, the mechanism in

which 1 μM 17β-estradiol inhibited the EDH-mediated response remains unclear and is beyond the scope of the present study. The sex of the PCAs used in the present study was confirmed by PCR amplification of the *Sry* (sex-determining region Y) gene.

The present study also demonstrates that NO plays a greater role in PCAs from male pigs compared to female pigs. This could possibility be due to higher expression levels of eNOS in males compared to females as a previous study in rat thoracic aortae reported that the gene expression levels of eNOS mRNA is higher in male rats compared to female rats (Kerr *et al.*, 1999). However, expression levels of eNOS alone do not necessarily translate to activity and function of NO because NO availability decreases rapidly as it reacts with superoxide anion ($O_2^-$) forming peroxynitrite (Figure 2.26A) (Kerr *et al.*, 1999).

Another relevant endogenous mediator is $H_2O_2$, formed by spontaneous dismutation or catalysed by superoxide dismutase (SOD) (Figure 2.26B) (Shimokawa, 2010). $H_2O_2$ on its own has previously been reported to produce a concentration-dependent vasorelaxation in PCAs (Matoba *et al.*, 2003) and studies have reported that $H_2O_2$ is an EDH mediator (Edwards *et al.*, 2008; Hammond *et al.*, 2011; Matoba *et al.*, 2002; Matoba *et al.*, 2003; Matoba *et al.*, 2000; Shimokawa & Morikawa, 2005) or modulator (Wheal *et al.*, 2012). Therefore, the present study investigated the effects of sex differences in endothelium-derived $H_2O_2$. Here, the presence of PEG-catalase alone significantly reduced the vasorelaxation to bradykinin in PCAs from females, but not males. This result suggests that endogenous $H_2O_2$ plays a significant role in the responses induced by bradykinin in PCAs, but only in female pigs.

Conversely, in the presence of L-NAME and indomethacin, PEG-catalase did not affect the bradykinin-induced vasorelaxation in PCAs from both sexes, indicating that $H_2O_2$ does not play a significant role in the EDH-mediated pathway in distal PCAs. These findings differ from a previous study conducted on the male porcine coronary arteries where they have concluded that $H_2O_2$ is an EDH mediator (Matoba *et al.*, 2003). In their study, porcine coronary microvessels (250 - 300 μm in diameter) were used and endothelium-dependent vasorelaxations to bradykinin were insensitive to indomethacin and L-NAME, which also differs from the findings in the present study. These differences, or at least that in the absence of $NO/PGI_2$, could be due to the difference in vessel size used. In the present study, experiments were repeated with a higher concentration of PEG-catalase (600 Uml$^{-1}$) in PCAs from males, but no further inhibition of the bradykinin-induced vasorelaxation was observed. Thus, the possibility that insufficient PEG-catalase concentration was used can be excluded. Endothelium-derived $H_2O_2$ can be generated from superoxide anion ($O_2$ $^-$) as a by-product from the catalysis of L-arginine to NO by endothelial NO synthase (eNOS) (Figure 2.26A) (Heinzel *et al.*, 1992). Previous studies have reported that L-NAME caused a reduction in $O_2^-$ generation (Kerr *et al.*, 1999) and inhibition of $H_2O_2$ formation (Heinzel *et al.*, 1992). Therefore, it is possible that formation of endogenous $H_2O_2$ in distal PCAs used in the present study is dependent on the eNOS system where formation of $H_2O_2$ is inhibited in the presence of L-NAME. However, it should be noted that all present experiments were conducted in the presence of both L-NAME and indomethacin, therefore the involvement of the cyclo-oxygenase or prostanoid pathway in the effect of $H_2O_2$ cannot be ruled out.

On the other hand, in the NO-mediated response, a higher level of NO in PCAs from males could have reacted with superoxide forming peroxynitrite rather than $H_2O_2$, as it has been previously reported that the reaction of superoxide with NO is three to four times faster than with SOD (Wolin, 2009). This could be a possible explanation as to why $H_2O_2$ did not play a role in the NO-mediated pathway in males. As for the response observed in PCAs from female pigs where endothelium-derived $H_2O_2$ plays a role in the NO-mediated bradykinin-induced vasorelaxation, it is possible that a higher level of SOD is present in the endothelial cells in females leading to $H_2O_2$ formation. A previous study in mitochondria isolated from rat brain and liver showed higher expression and activities of manganese-SOD (Mn-SOD) and glutathione peroxidase in females compared to males, therefore providing a protective effect in females during oxidative stress (Borras *et al.*, 2003). However, further studies to determine the SOD levels and activity are required. Also, as superoxide anions in blood vessels can be generated from a few different pathways (Wolin, 2009) including NAPDH oxidase, it is possible that there are sex differences in the upstream reaction. Previous studies in age-matched rat aortae (Brandes & Mugge, 1997) and in young healthy human subjects (Ide *et al.*, 2002) concluded that males experience a greater oxidative stress compared to females and this is attributed to the increased production of $O_2^-$ and reduced activity/availability of $O_2^-$ scavengers.

Next, the role of gap junctional communication in male and female arteries was investigated as it has been reported that gap junctions play a role in the EDH-type response. Here, the effects of two different inhibitors (carbenoxolone and 18α-glycyrrhetinic acid) were examined either alone or in

combination with L-NAME and indomethacin against bradykinin-induced vasorelaxation. In PCAs from male and female pigs, the presence of carbenoxolone or 18α-glycyrrhetinic acid alone had no effect on vasorelaxation to bradykinin indicating that gap junctional communication does not play a significant role in the NO-mediated response. Conversely, in the EDH pathway, carbenoxolone significantly reduced the maximum relaxation to bradykinin in PCAs from female but not male pigs. The inhibitory effects of both carbenoxolone and 18α-glycyrrhetinic acid in the presence of L-NAME and indomethacin confirm that gap junction communication plays a significant role in the EDH responses induced by bradykinin in PCAs from female pigs, but not male pigs. The finding in PCAs from female pigs concur with previous studies on isolated myometrial arteries and subcutaneous resistance arteries from pregnant women (Kenny *et al.*, 2002b; Lang *et al.*, 2007) while the finding in PCAs from male pigs is in agreement with a previous study using 18α-glycyrrhetinic acid in PCAs from male pigs (Matoba *et al.*, 2003). Gap junctions have been reported to play a role in both NO-dependent and EDH-mediated endothelium-dependent vasorelaxation in mesenteric arteries and thoracic aortae from male rabbits (Chaytor *et al.*, 1998), human mesenteric arteries (Chadha *et al.*, 2011) and PCAs of unspecified sex (Edwards *et al.*, 2000). However, another study conducted on PCAs of unspecified sex using three different types of gap junction inhibitors (18α-glycyrrhetinic acid, 1-heptanol and Gap27) had no effect on the EDH response (Yang *et al.*, 2003). In the NO-dependent responses of the present study, the difference in findings could be due to the difference in the size and/or type of vascular tissue used or species differences

(Feletou & Vanhoutte, 2006). The inconsistency of findings for the role of gap junctions in all previous studies could possibly be due to the unspecified sex used (Chadha *et al.*, 2011; Yang *et al.*, 2003). As Cx43 has previously been implicated in EDH-mediated relaxations (Lang *et al.*, 2007), the present study investigated whether the differential expression of this protein could explain the difference in the sensitivity to gap junction inhibition. However, the Western Blot analysis for Cx43 protein in PCAs from male and female pigs did not detect any differences in the expression level of this gap junction protein, indicating that expression *per se* does not contribute to the sex differences observed. Further Western Blot analysis on other subtypes of connexin proteins that have been previously identified in blood vessels (Chaytor *et al.*, 2003; de Wit & Griffith, 2010; Lang *et al.*, 2007) showed no differences in the expression level of Cx40 proteins and Cx37 proteins were not detected in PCAs from male or female pigs. Therefore, the differences in EDH-mediated responses between PCAs from male and female pigs may be due to differences in gap junctional communication, rather than expression of gap junction proteins. For example, it could be that the calcium-activated potassium channels ($K_{ca}$) (Chadha *et al.*, 2011; Gluais *et al.*, 2005a), which are located near the myoendothelial gap junctions differentially influence gap junctional communication between the sexes.

Given the potential differences in $K_{Ca}$-channel activity between sexes, the effects of apamin, the small conductance calcium-activated potassium channel ($SK_{Ca}$) blocker, and TRAM-34, an inhibitor of intermediate conductance calcium-activated potassium ($IK_{Ca}$) channels on EDH-mediated responses (Chadha *et al.*, 2011; Edwards *et al.*, 2010; Gluais *et al.*, 2005a;

Yang *et al.*, 2003) were examined. The present study demonstrated that in the EDH-mediated response, $IK_{Ca}$ channels play a role only in PCAs from female pigs, while the $SK_{Ca}$ channels play a role in both sexes. This is in agreement with a previous study conducted on carotid arteries from male guinea-pigs where TRAM-34 alone had no effect on endothelium-dependent hyperpolarization, but apamin significantly inhibited acetylcholine-evoked hyperpolarization (Gluais *et al.*, 2005a). Furthermore, another study examining sex differences in EDH-mediated responses reported that apamin had the same effect on the maximum relaxation to acetylcholine in male and female rat mesenteric arteries (White *et al.*, 2000), which is comparable to the present study. Taken together, the present study demonstrates that gap junctional communication and $IK_{Ca}$ channels play a role in the EDH-mediated response in PCAs from female pigs, but not male pigs. Interestingly, previous studies using immunohistochemistry with specific antibodies have shown that $IK_{Ca}$ channels are found co-localised with myoendothelial connexin proteins with their functionality being related to the EDH-mediated activity (Chadha *et al.*, 2011; Sandow *et al.*, 2006). A previous study in male obese rats demonstrated an upregulation in $IK_{Ca}$ and MEGJ expression and activity to compensate for the loss of NO-mediated responses as observed in age-matched control male rats (Chadha *et al.*, 2010). However, Western Blot analysis in the present study for $IK_{Ca}$ expression level showed no differences between PCAs from male and female pigs.

In order to determine whether there is a difference in the function of $IK_{Ca}$ channels between males and females, NS309 was used as a potent and selective $SK_{Ca}$ and $IK_{Ca}$ channel activator (Leuranguer *et al.*, 2008a). NS309

produced a comparable concentration-dependent vasorelaxation in PCAs from male and female pigs. Blocking $SK_{Ca}$ channels specifically with apamin had no effect on the NS309-induced vasorelaxation in either male or female pigs. Further experiments blocking $IK_{Ca}$ channels specifically with TRAM-34 also had no effect on the NS309-induced vasorelaxation. This finding is in line with a previous study measuring the membrane potential of guinea pig carotid arteries where NS309 (10 μM)-induced hyperpolarization was not significantly affected by TRAM-34 or apamin alone in the presence of L-NAME and indomethacin. It is therefore possible that when either $SK_{Ca}$ or $IK_{Ca}$ channels are blocked separately there is a compensatory response involving the other $K_{Ca}$ channels activated by NS309. However, blocking both $SK_{Ca}$ and $IK_{Ca}$ channels together had little effect on the NS309-induced vasorelaxation, although there was slight inhibition at 0.3 μM in PCAs from female pigs. These data suggest that NS309 is not mediating relaxation through $SK_{Ca}$ or $IK_{Ca}$ channels in the PCAs and therefore cannot be used to determine if there is a difference in the activity of these channels between males and females. Additional experiments to investigate the selectivity of NS309 using high potassium demonstrated that at higher concentration of NS309 (>3 μM) other vasorelaxation pathway may be involved. This observation is in line with previous studies where loss of selectivity for $IK_{Ca}$ and $SK_{Ca}$ has been reported at higher concentrations of NS309 (Dalsgaard *et al.*, 2009; Kroigaard *et al.*, 2012). Furthermore, it has been reported that NS309 inhibits voltage-dependent calcium-channels (Morimura *et al.*, 2006). Therefore in the present study, use of NS309 as a selective activator of $SK_{Ca}$ and $IK_{Ca}$ is questionable and may not be suitable to draw any conclusion to support the bradykinin-

induced vasorelaxation findings. NS309 is a more potent and selective $SK_{Ca}$ and $IK_{Ca}$ activator compared to other activators such as 1-EBIO (Leuranguer *et al.*, 2008a) or DCEBIO (Morimura *et al.*, 2006).

In summary, the present study confirmed that bradykinin is an endothelium-dependent vasorelaxant, stimulating the release of NO- and EDH-type mediated responses in PCAs. The second part of the study demonstrates that both NO and EDH-type responses contribute significantly towards the endothelium-dependent vasorelaxation induced by bradykinin in male and female isolated distal PCAs. Clear sex differences in endothelial function have been demonstrated where the EDH-type responses play a greater role in PCAs from female compared to male pigs. In PCAs from female pigs, endogenous $H_2O_2$ plays a role in the bradykinin-induced vasorelaxation. Furthermore, gap junctional communication and the $IK_{Ca}$ channels appear to be more important in the EDH-mediated pathway in PCAs from female pigs and these could be compensation for the diminished response of NO-mediated pathway in PCAs from female pigs. The sex differences in endothelial function demonstrated in the present study may contribute to the cardiovascular protective effects observed in females (Figure 2.26B).
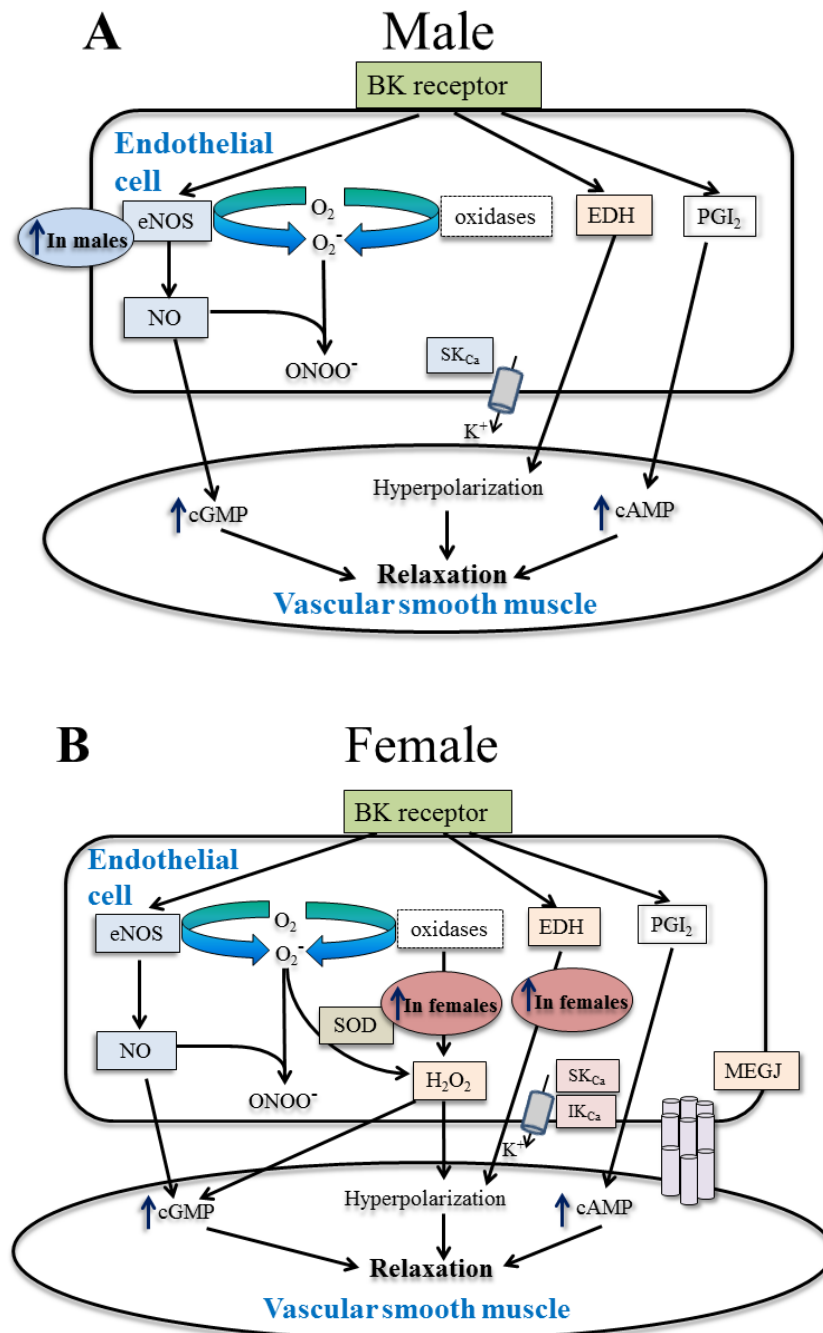
**Figure 2.26** Hypothesized mechanism of action of sex differences in endothelial function to bradykinin-induced vasorelaxation in porcine coronary arteries from (A) male and (B) female pigs. Present study demonstrated a clear sex differences in endothelial function where only in PCAs from female pigs have greater EDH-mediated responses specifically the gap junction communication whereas endogenous $H_2O_2$ play a role in the NO-mediated pathway in female pigs. Figure adapted from Shimokawa (2010).

# *Chapter 3*

---

**A role for the sodium pump in $H_2O_2$-induced vasorelaxation in porcine isolated coronary arteries**

## 3.1 Introduction

In Chapter 2, endogenous $H_2O_2$ has been reported to plays a role in the endothelium-dependent vasorelaxation in porcine distal coronary arteries (PCAs) from female but not male pigs. Other studies have reported that endothelium-derived $H_2O_2$ is a factor for EDH-type response in mouse, rat and human mesenteric arteries (Matoba *et al.*, 2002; Matoba *et al.*, 2000; Wheal *et al.*, 2012), human coronary arterioles (Miura *et al.*, 2003), porcine coronary microvessels (Matoba *et al.*, 2003) and in canine coronary arteries (Yada *et al.*, 2003).

Studies measuring membrane potential of vascular smooth muscle cells (VSMCs) from PCAs have also shown that exogenously applied $H_2O_2$ hyperpolarizes and relaxes the smooth muscle (Beny & von der Weid, 1991; Matoba *et al.*, 2003). Elevation of $H_2O_2$ has been reported in various pathological states including ischaemia and reperfusion of rat brain, where up to 100 μM of $H_2O_2$ was detected (Hyslop *et al.*, 1995). In human, plasma levels of the $H_2O_2$ detected in subjects with essential hypertension (3.36 ± 0.15 μM, *n*=74) were significantly higher than in normotensive subjects (3.00 ± 0.09 μM, *n*=162) (Lacy *et al.*, 2000). High levels of $H_2O_2$ (>0.5 mM) have been reported to cause tissue injury in organ bath experiments (Ellis *et al.*, 2003; Walia *et al.*, 2000), however the role of endothelial Nox4-derived $H_2O_2$ remains contradictory as both protective (Ray *et al.*, 2011; Schroder *et al.*, 2012) and damaging effects on vascular function have been reported (Montezano & Touyz, 2012). Therefore, further understanding of the mechanism of action of $H_2O_2$ may be beneficial for the development of new

strategies in treatment or prevention of diseases related to oxidative stress (Burgoyne *et al.*, 2013).

Studies of $H_2O_2$ in a variety of different vessels and species have demonstrated that $H_2O_2$ acts as a vasorelaxant via activation of potassium channels on the vascular smooth muscle (Barlow & White, 1998; Ellis *et al.*, 2003; Hayabuchi *et al.*, 1998; Matoba *et al.*, 2002; Matoba *et al.*, 2003; Matoba *et al.*, 2000; Miura *et al.*, 2003; Ohashi *et al.*, 2012; Rogers *et al.*, 2007; Rogers *et al.*, 2006; Thengchaisri & Kuo, 2003; Wheal *et al.*, 2012). However, inconsistencies in results have been reported when more specific potassium channel blockers were used. For example, use of iberiotoxin, charybdotoxin and/or apamin to inhibit large, intermediate and small-conductance calcium activated potassium channels significantly reduce the $H_2O_2$-induced vasorelaxation in porcine coronary arteries (Hayabuchi *et al.*, 1998) and human coronary arterioles (Miura *et al.*, 2003) but not in murine small mesenteric arteries (Ellis *et al.*, 2003). The other discrepancy in results is the role of cGMP in the $H_2O_2$-mediated relaxation where some studies (Burke & Wolin, 1987; Hayabuchi *et al.*, 1998) have demonstrated that blocking the guanylyl cyclase pathway inhibits $H_2O_2$-induced vasorelaxation but this is not universally supported (Barlow & White, 1998; Ellis *et al.*, 2003; Miura *et al.*, 2003; Thengchaisri & Kuo, 2003).

The aim of this chapter was to investigate the mechanism of action of exogenously applied $H_2O_2$ on PCAs, and specifically the involvement of potassium channels. This was then extended to investigate the role of the ouabain-sensitive $3Na^+/2K^+$-pump in the $H_2O_2$-induced vasorelaxation in PCAs.

## 3.2 Materials and Methods

### 3.2.1 Preparation of rings of distal PCAs

Tissues were set up as previously described in Chapter 2.

### 3.2.2 Wire myograph study

As previously described in Chapter 2, after 30 min of equilibration, the tissue response to 60 mM KCl was determined twice. The vascular tone was then raised to about 50-90% of the second KCl contraction with U46619 (1 nM - 50 μM), a thromboxane $A_2$-mimetic, or with KCl (60 mM) to examine the role of $H_2O_2$ as a factor for EDH. Once stable tone was achieved, concentration-response curves to $H_2O_2$ (1 μM - 1 mM), bradykinin (0.01 nM - 1 μM), sodium nitroprusside (SNP) (10 nM - 10 μM) or verapamil (1 nM - 10 μM) were constructed. In some experiments where the vascular tone could not be maintained due to the effects of the inhibitors and slow response of the test drug, a single concentration response was examined instead (100 μM $H_2O_2$ or 300 nM forskolin). Vasorelaxation to $H_2O_2$ was studied in the presence of $N^G$-nitro-L-arginine methyl ester (L-NAME) (300 μM), a NO synthase inhibitor and indomethacin (10 μM), a cyclooxygenase inhibitor to define EDH-type response. To study the role of the endothelium in $H_2O_2$-induced vasorelaxation, the endothelium of the vessels was removed mechanically by rubbing the lumen gently with stainless-steel forceps. PEG-catalase (300 Uml$^{-1}$) was added to eliminate intracellular $H_2O_2$ and carbenoxolone (100 μM) (Harris *et al.*, 2002; Tang & Vanhoutte, 2008) was used as a non-selective gap junction inhibitor to examine the role of gap junctions. To inhibit potassium ($K^+$) channels, tetraethylammonium (TEA) (10 mM) (Ellis *et al.*, 2003;

McCulloch *et al.*, 1997; Rogers *et al.*, 2007; Uhiara *et al.*, 2009) was used. Glibenclamide (1 μM) (Miura *et al.*, 2003) was used as an ATP-sensitive $K^+$ channel ($K_{ATP}$) inhibitor and 4-aminopyridine (4-AP) (1 mM) (Ellis *et al.*, 2003) was used as a voltage-gated $K^+$ channel ($K_V$) inhibitor. Barium chloride (30 μM) (Edwards *et al.*, 1998) was used as an inwardly rectifying $K^+$ channel ($K_{ir}$) inhibitor. Apamin (500 nM) (Weston *et al.*, 2005), TRAM-34 (10 μM) (Gluais *et al.*, 2005a) and iberiotoxin (100 nM) (Edwards *et al.*, 2000; Rogers *et al.*, 2007), small ($SK_{Ca}$), intermediate ($IK_{Ca}$) and large ($BK_{Ca}$) conductance calcium-activated potassium channel inhibitors respectively were used to study the role of selective $K^+$ channels in the $H_2O_2$-induced vasorelaxation. In some preparations, paxilline (300 nM or 1 μM) (Wilson *et al.*, 2000) was used as a potent inhibitor of the $BK_{Ca}$ channels. Ouabain (500 nM) (Beny & Schaad, 2000) was used to inhibit the sodium-potassium pump activity and 1H-[1,2,4] Oxadiazolo[4,3-a]quinoxalin-1-one (ODQ) (10 μM) (Ellis *et al.*, 2003; Hayabuchi *et al.*, 1998; Li *et al.*, 1998) was used to selectively inhibit soluble guanylyl cyclase activity. 2,4-dichlorobenzamil (DCB) (10 μM) was used as a $Na^+/Ca^{2+}$ exchanger inhibitor while KB-R7943 (10 μM) was used as a selective inhibitor of the reverse mode of the $Na^+/Ca^{2+}$ exchanger (Coleman & Khalil, 2002).

The concentration of U46619 used was significantly lower in the presence of L-NAME, indomethacin with ouabain ± barium (P<0.0001) or in endothelium denuded vessels (P<0.05) whereas the U46619 concentration used was significantly higher in the presence of glibenclamide (P<0.01) or KB-R7943 (P<0.01) the in PCAs from females (Table 3.1A). The level of tone achieved with U46619 was the same under all conditions in PCAs from female

pigs except for in the presence of ouabain ± barium (P<0.05) or in the presence of KB-R7943 or 100 μM DCB (P<0.05) (Table 3.1A). The concentration of U46619 used was significantly lower in the presence of L-NAME, indomethacin with ouabain (P<0.0001) or 4-AP (P<0.05) in PCAs from males (Table 3.1B). The level of tone achieved with U46619 was the same under all conditions in PCAs from male pigs except for in the presence of high $K^+$ (P<0.01) (Table 3.1B).

As $K^+$ has been previously reported to be a factor responsible for EDH, acting via activation of the $3Na^+/2K^+$ ATPase (Edwards *et al.*, 1998), the effect of 100 μM and 1 mM $H_2O_2$, 500 nM ouabain and endothelium denudation on KCl-induced vasorelaxation (0 – 20 mM KCl added at the interval of 2 - 5 min) in $K^+$-free Krebs'-Henseleit solution substituted with equimolar NaCl (Gallo *et al.*, 2010; Harris *et al.*, 2000) were examined. At the end of each experiment, successful removal of the endothelium was confirmed by 100 nM Substance P. All inhibitors were added 1 h before pre-contraction with U46619.

To further examine the effects of $H_2O_2$ on the KCl-induced contraction, vessels were pre-incubated with 100 μM or 1 mM $H_2O_2$ for 30 min or 1 h followed by washing out with Krebs'-Henseleit solutions for 1 h before being subjected to the third 60 mM KCl response. To study the effects of ouabain and $H_2O_2$ on $Ca^{2+}$-induced contraction, calcium-free Krebs'-Henseleit solutions were used. Vessels were pre-incubated with 500 nM ouabain or 100 μM $H_2O_2$ for 1 h followed by the addition of 60 mM KCl. Once stable tone was achieved, concentration-response curves to calcium re-introduction (1 μM – 10 mM) were constructed.

| A Female | | U46619-induced tone (% KCl response) | Concentration of U46619 (nM) |
|---|---|---|---|
| | Control | 69.0 ± 5.2 | 20.0 ± 3.0 |
| | Barium | 63.6 ± 7.2 | 13.0 ± 2.6 |
| L-NAME, indomethacin | Ouabain | 100 ± 6* | 3.83 ± 1.96**** |
| | Barium, ouabain | 106 ± 10* | 0.33 ± 0.21**** |
| | Endothelium denuded | 82.4 ± 15.9 | 10.0 ± 0* |
| | Control | 71.7 ± 3.0 | 16.7 ± 3.3 |
| L-NAME, indomethacin | High $K^+$ | 105 ± 6.7 | 60 mM KCl |
| | TEA | 90.8 ± 16.7 | 7.7 ± 1.5 |
| | Glibenclamide | 68.5 ± 4.8 | 32.5 ± 4.4** |
| | Control | 67.3 ± 6.7 | 17.5 ± 3.2 |
| | Iberiotoxin | 97.5 ± 5.4 | 13.8 ± 2.4 |
| | ODQ | 65.3 ± 8.1 | 16.3 ± 2.4 |
| | Iberiotoxin, ODQ | 67.8 ± 9.0 | 17.0 ± 3.7 |
| | Control | 56.3 ± 1.7 | 16.8 ± 0.2 |
| | 300nM Paxilline | 61.3 ± 10.8 | 14.7 ± 1.5 |
| | Control | 54.2 ± 2.1 | 10.6 ± 1.9 |
| | 1µM Paxilline | 61.0 ± 6.6 | 10.4 ± 1.6 |
| | Control | 72.8 ± 4.0 | 18.2 ± 4.2 |
| L-NAME, indomethacin | 10 µM DCB | 71.4 ± 5.6 | 17.8 ± 1.4 |
| | 10 µM KB-R7943 | 53.8 ± 2.1* | 94.0 ± 26.0** |
| | 500 nM ouabain | 87.6 ± 5.9 | 0.60 ± 0.24 |
| L-NAME, indomethacin | Control | 71.0 ± 6.5 | 35.0 ± 6.3 |
| | 100 µM DCB | 43.0 ± 5.5* | 3074 ± 1339 |

| B Male | | U46619-induced tone (% KCl response) | Concentration of U46619 (nM) |
|---|---|---|---|
| | Control | 69.7 ± 6.1 | 16.7 ± 2.3 |
| L-NAME, indomethacin | Ouabain | 83.0 ± 5.1 | 0.83 ± 0.54**** |
| | 4-AP | 64.0 ± 9.9 | 8.4 ± 1.9* |
| | High $K^+$ | 103 ± 2.0** | 60 mM KCl |

**Table 3.1** Summary of U46619 concentration used (nM) and the levels of tone achieved with U46619 expressed in percentage to the second KCl-induced tone in porcine coronary arteries from (A) female and (B) male pigs. Data are expressed as mean ± S.E.M. of 3-9 experiments. *P<0.05, **P<0.01, ****P<0.0001; one-way ANOVA followed by Bonferroni's *post hoc* test or 2-tailed, paired Student's *t*-test.

### 3.2.3 Atomic absorption spectrophotometric determination of $3Na^+/2K^+$ ATPase activity

The methodology for measuring rubidium-uptake using atomic absorption spectrophotometry (Perkin-Elmer, Coventry, UK) to study the sodium-potassium pump activity was adapted from Longo *et al.,* (1991). Finely dissected PCAs, cleaned of adherent connective and fatty tissues, were cut open longitudinally. PCA segments were then cut into 1.0 - 1.5 cm in length and placed into 6-well plates pre-filled with 3 ml Krebs'-Henseleit solution previously gassed with 5% $CO_2$ and 95% $O_2$. Test agents (500 nM or 10 mM ouabain, 10 μM, 100 μM or 1 mM $H_2O_2$) were added into the respective wells and plates were incubated at 37°C in a shaker for 30 min. After 30 min, Krebs'-Henseleit solution was replaced with $K^+$-free Krebs'-Henseleit solution containing 4 mM RbCl with respective inhibitors and incubated at 37°C in a shaker for an additional 30 min. Arteries were then rapidly washed three times with ice-cold 0.2 M $MgSO_4$ then stored at -20°C until further assay. Frozen segments were fixed with 2 mL fixative (containing 50% ethanol, 49% distilled water and 1% acetic acid) and left to evaporate in a fume hood overnight. Intracellular $Rb^+$ was then extracted in 2 mL of distilled water and the $Rb^+$ content was determined with flame photometry on an atomic absorption spectrometer using wavelength of 780 nm. $Rb^+$-uptake levels were interpolated from a standard $Rb^+$ curve and individual PCA reading was divided by the wet weight of the respective artery segment.

### 3.2.4 Statistical analysis

Data for the functional studies were presented and analysed as described in Chapter 2. In data where the $R_{max}$ were not achieved, data were analysed using the response generated at the highest concentration of vasorelaxant or at each individual concentration of vasorelaxant. Results of the $Rb^+$-uptake experiments were analysed using one-way ANOVA followed by Dunnett's multiple comparison test against the control.

### 3.2.5 Drugs and chemicals

All drugs were purchased from Sigma-Aldrich (Poole, Dorset, UK) unless otherwise indicated. Apamin, KB-R7943, paxilline and forskolin were purchased from Tocris Bioscience (Bristol, UK) and 2,4-dichlorobenzamil (DCB) from Enzo Life Sciences (Exeter, UK). All drugs were dissolved in distilled water except for indomethacin which was dissolved in absolute ethanol and TRAM-34, glibenclamide, DCB and KB-R7943 were dissolved in DMSO. TEA was dissolved directly into Krebs'-Henseleit solution. Stock solutions of bradykinin and U46619 were made to 10 mM and $H_2O_2$ to 100 mM with distilled water. All further dilutions of the stock solutions were made using distilled water.

## 3.3 Results

### 3.3.1 The effects of L-NAME, indomethacin, carbenoxolone and PEG-catalase on $H_2O_2$–induced vasorelaxation in PCAs from female pigs

$H_2O_2$ (1 μM–1 mM) produced concentration-dependent vasorelaxations in PCAs from females with an $R_{max}$ of 100 ± 16% (pEC$_{50}$ = 4.18 ± 0.20, *n*=4) under control conditions. The presence of PEG-catalase significantly reduced the $R_{max}$ for relaxation to $H_2O_2$ to 41.2 ±14.5% (pEC$_{50}$ = 4.00 ± 0.48, *n*=4) (P<0.05) but did not affect the potency (Figure 3.1). Relaxations to $H_2O_2$ were unaffected by the presence of L-NAME and indomethacin (pEC$_{50}$ = 4.00 ± 0.05, *n*=6) or carbenoxolone  (pEC$_{50}$ = 4.08 ± 0.12, *n*=4) (Figure  3.1).
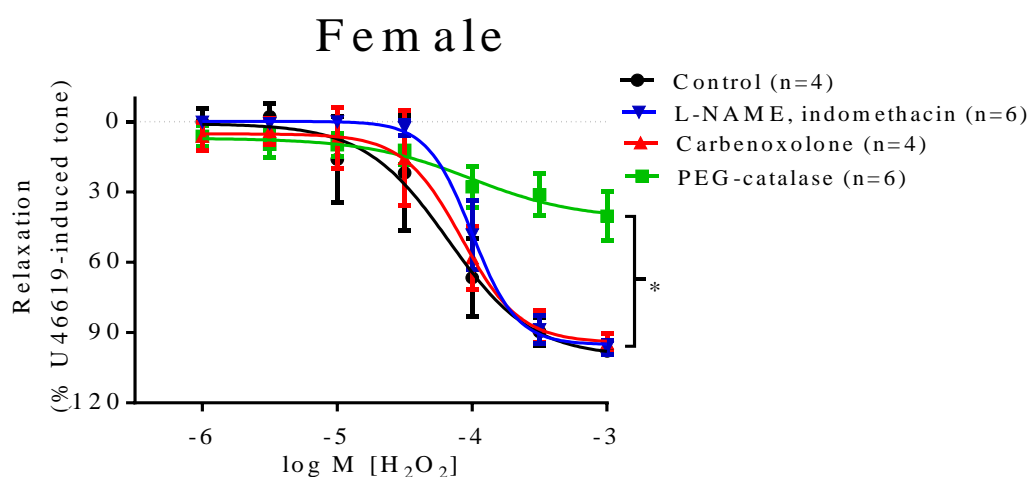


**Figure 3.1** Log concentration-response curves for the vasorelaxant effects of $H_2O_2$ in the absence or presence of 300 μM L-NAME, 10 μM indomethacin, 100 μM carbenoxolone or 300 Uml$^{-1}$ PEG-catalase in U46619 pre-contracted porcine coronary arteries from female pigs. Data are expressed as a percentage change from U46619-induced tone and are mean ± S.E.M. of 4-6 experiments. * P<0.05; one-way ANOVA followed by Bonferroni's *post hoc* test.

**3.3.2 The effects of potassium channel inhibitors on hydrogen peroxide –
induced vasorelaxation in PCAs from male or female pigs**

In PCAs from female pigs, in the presence of L-NAME and indomethacin,
removal of the endothelium or pre-treatment of vessels with 30 μM barium
chloride had no effect on the $H_2O_2$-induced vasorelaxation ($n$=5) (Figure
3.2A). The presence of 500 nM ouabain significantly inhibited the $H_2O_2$-
induced vasorelaxation ($n$=6) (P<0.0001) and this was not significantly altered
by the additional presence of barium chloride ($n$=5) (Figure 3.2A). In the
presence of L-NAME and indomethacin, 10 mM TEA significantly inhibited
the relaxation at 100 μM $H_2O_2$ (P<0.05) ($n$=6) (Figure 3.2B). High
extracellular KCl (60 mM) essentially abolished the relaxation to $H_2O_2$ at
concentrations up to 300 μM ($n$=5) (Figure 3.2B). The presence of 1 μM
glibenclamide had no effect on the $H_2O_2$-induced vasorelaxation ($n$=6) (Figure
3.2B).

In Chapter 2, sex differences in the role of endogenous $H_2O_2$ in PCA in
bradykinin-induced vasorelaxation were reported, therefore, here the effects of
$H_2O_2$-induced vasorelaxation in PCAs from male pigs were examined. Under
control conditions there were no sex differences between the $H_2O_2$-induced
vasorelaxation where the relaxation produced at 1 mM of $H_2O_2$ in male PCAs
was 98 ± 2% ($n$=9) (Figure 3.2C). Again, the presence of ouabain or 60 mM
KCl significantly inhibited the $H_2O_2$-induced vasorelaxation producing a
relaxation of 32 ± 5% ($n$=6) and 52 ± 9% ($n$=5) respectively at 1 mM $H_2O_2$
(P<0.0001). Pre-treatment with 1 mM 4-AP had no effect on the
vasorelaxation ($n$=4) (Figure 3.2C). For original trace see Figure 3.2D.

**Figure 3.2** Log concentration-response curves for the vasorelaxant effects of $H_2O_2$ in the presence of 300 μM L-NAME, 10 μM indomethacin with (A) removed endothelium, 30 μM barium chloride and/or 500 nM ouabain (B) 60 mM KCl, 10 mM TEA or 1 μM glibenclamide in U46619 pre-contracted porcine coronary arteries from female pigs and (C) 500 nM ouabain, 1 mM 4-AP or 60 mM KCl in PCAs from male pigs. Data are expressed as a percentage change from U46619-induced tone and are mean ± S.E.M. of 4-9 experiments. *P<0.05, ****P<0.0001; one-way ANOVA followed by Bonferroni's *post hoc* test.
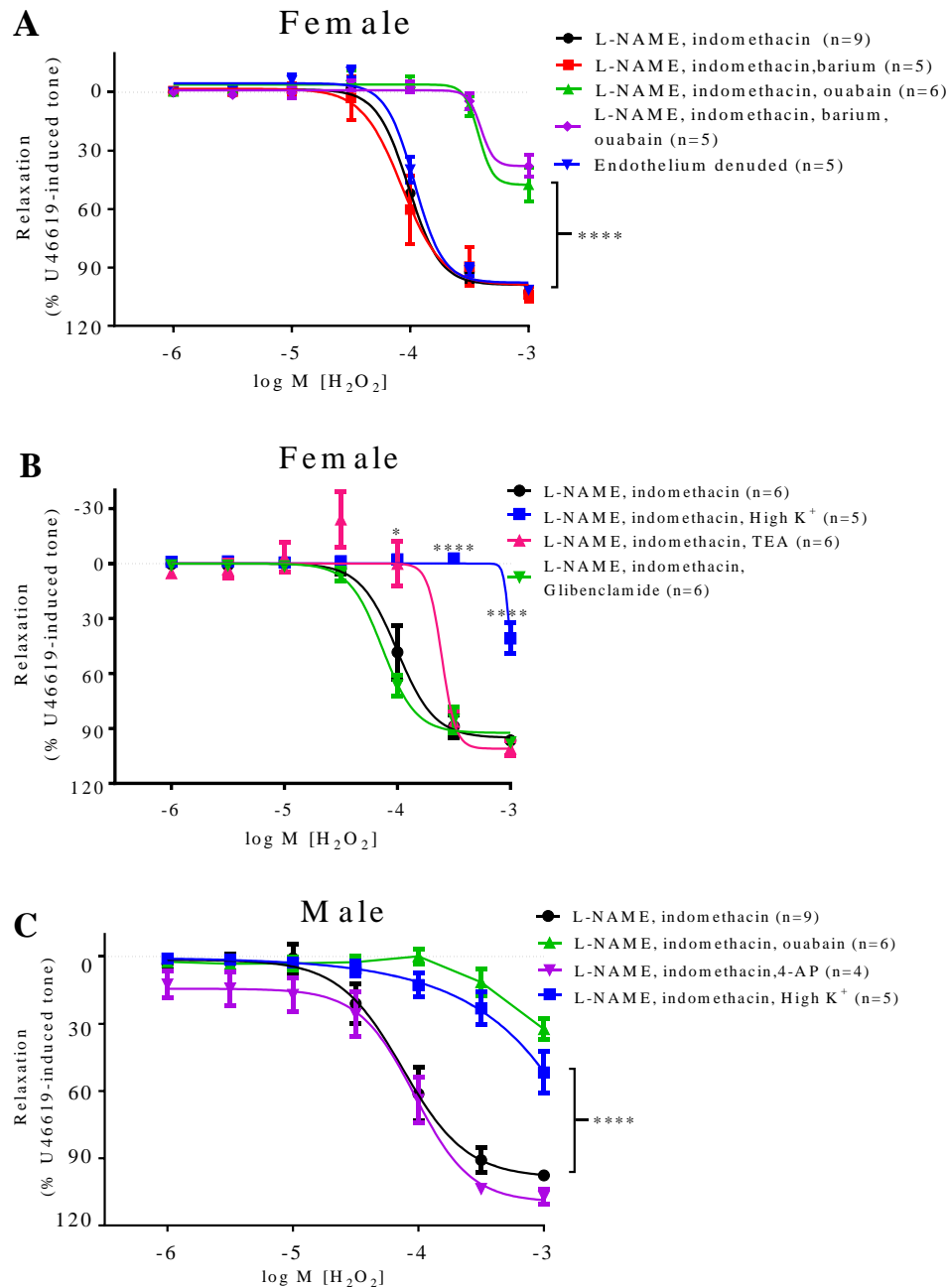
**D**
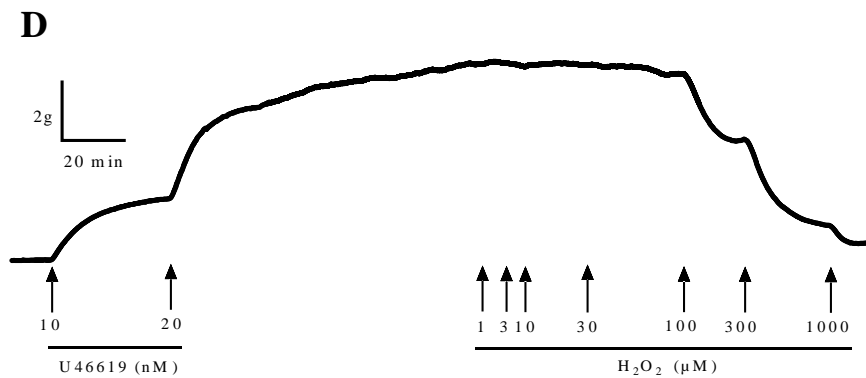


**Figure 3.2** (D) Original traces showing the responses to U46619 pre-contracted porcine coronary arteries and responses to increasing concentration of hydrogen peroxide.

### 3.3.3 The effects of soluble guanylyl cyclase inhibitor (ODQ) and selective $BK_{Ca}$ channel inhibitors on hydrogen peroxide ($H_2O_2$)–induced vasorelaxation in PCAs from female pigs

In PCAs from females, the soluble guanylyl cyclase inhibitor 10 µM ODQ had no effect on the $H_2O_2$-induced vasorelaxation ($n$=4) (Figure 3.3A). As no effect was observed in the presence of ODQ, a further experiment to examine the effects of ODQ was carried with a concentration-response curve to sodium nitroprusside (SNP). At 10 µM SNP, the relaxation was significantly reduced from 104 ± 2% to 18.5 ± 10.3% ($n$=3) in the presence of 10 µM ODQ (P<0.01) (Figure 3.3B).

The presence of 100 nM iberiotoxin, an inhibitor of the $BK_{Ca}$ channels alone ($n$=4) or in combination with ODQ ($n$=5) had no effect on the $H_2O_2$-induced vasorelaxation (Figure 3.3A). Further experiments with paxilline (300 nM or 1 µM), a potent $BK_{Ca}$ inhibitor, similarly had no effects on the $H_2O_2$-induced vasorelaxation ($n$=3-5) (Figure 3.3C and D respectively).
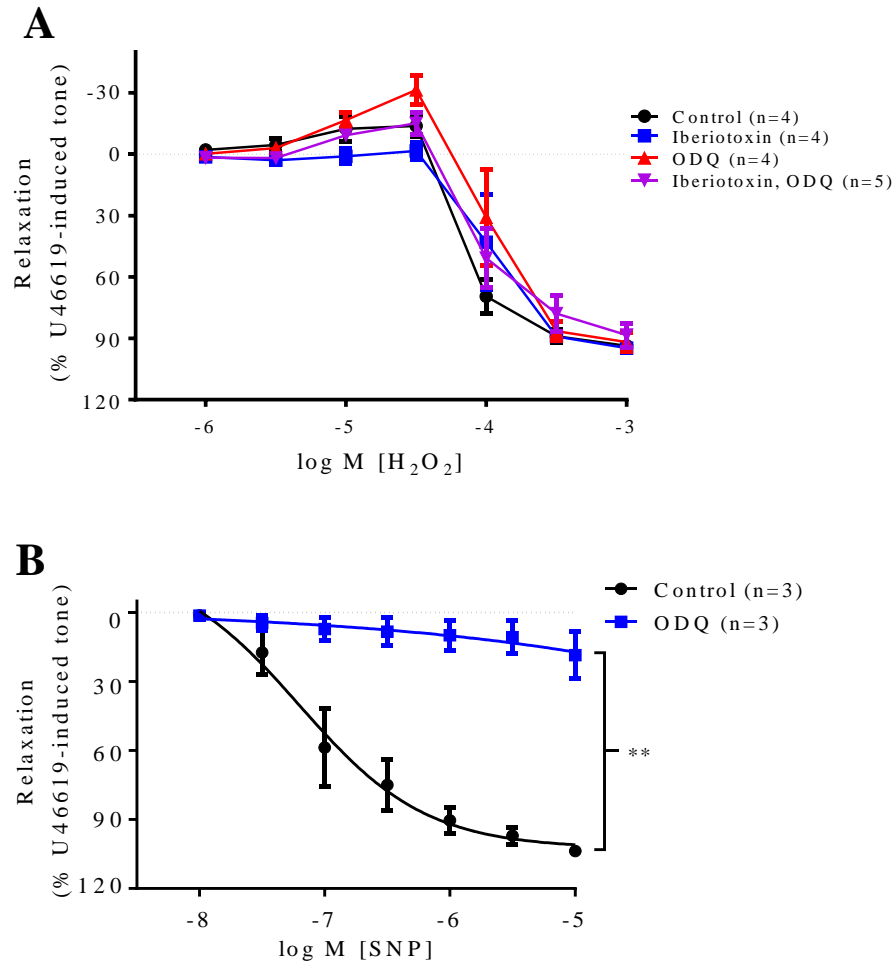
115

**Figure 3.3** Log concentration-response curves for the vasorelaxant effects of $H_2O_2$ in the absence or presence of (A) 100 nM iberiotoxin and/or 10 μM ODQ in U46619 pre-contracted porcine coronary arteries (PCAs) from female pigs. (B) Log concentration-response curves for the vasorelaxant effects of SNP in the absence or presence of 10 μM ODQ in PCAs from female pigs. Data are expressed as a percentage change from U46619-induced tone and are mean ± S.E.M. of 3-5 experiments. ** $P < 0.01$; 2-tailed, paired Student's $t$-test.
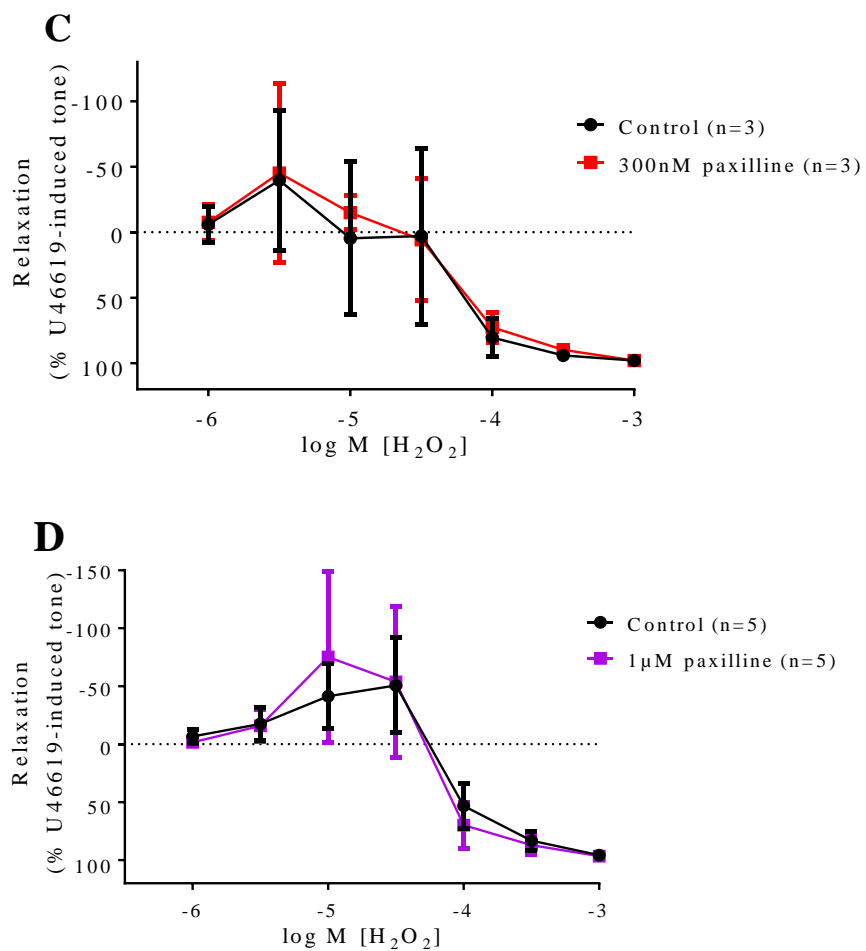
**C**



**D**

**Figure 3.3** Log concentration-response curves for the vasorelaxant effects of $H_2O_2$ in the absence or presence of (C) 300 nM paxilline or (D) 1μM paxilline in U46619 pre-contracted porcine coronary arteries from female pigs. Data are expressed as a percentage change from U46619-induced tone and are mean ± S.E.M. of 3-5 experiments.

### 3.3.4 The effects of selective $SK_{Ca}$ and $IK_{Ca}$ channel inhibitors on hydrogen peroxide ($H_2O_2$)–induced vasorelaxation in PCAs from female pigs

To examine the effects of $IK_{Ca}$ and $SK_{Ca}$ channels on $H_2O_2$-induced vasorelaxation in the presence of L-NAME and indomethacin, 10 μM TRAM-34 and 500 nM apamin were used as their respective inhibitors (Figure 3.4). Here, presence of TRAM-34 and/or apamin had no effects on the $H_2O_2$-induced vasorelaxation (*n*=6) (Figure 3.4).
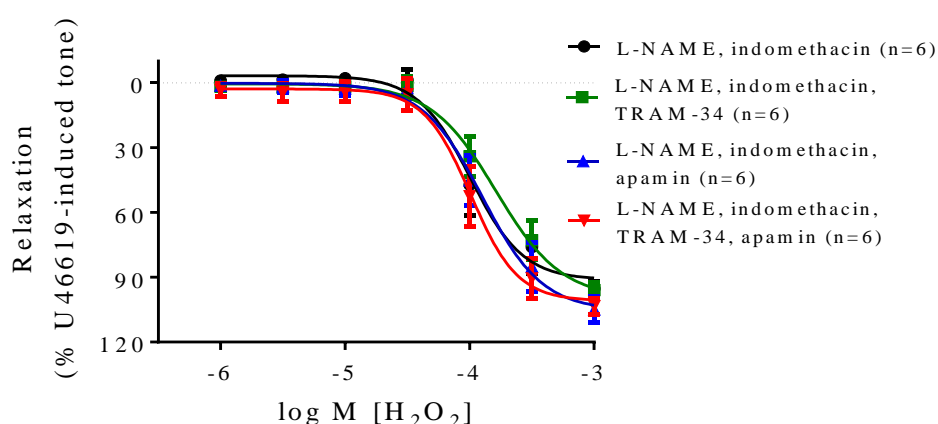


**Figure 3.4** Log concentration-response curves for the vasorelaxant effects of $H_2O_2$ in the presence of 300 μM L-NAME, 10 μM indomethacin, 10 μM TRAM-34 and/or 500 nM apamin in U46619 pre-contracted porcine coronary arteries from female pigs. Data are expressed as a percentage change from U46619-induced tone and are mean ± S.E.M. of 6 experiments.

### 3.3.5 The effects of L-NAME and indomethacin in the absence or presence of sodium-calcium exchangers (DCB or KB-R7943) on $H_2O_2$ –induced vasorelaxation in PCAs from either sex

Next, the role of $Na^+/Ca^{2+}$ exchanger (NCX) in the $H_2O_2$–induced vasorelaxation was investigated as Hinata *et al.* (2007) have previously reported that $H_2O_2$ activates NCX in isolated guinea-pig cardiac ventricular myocytes. Here, in the presence of L-NAME and indomethacin, neither 10

μM DCB nor 10 μM KB-R7943 had any effect on the responses to a single concentration of $H_2O_2$ (100 μM) ($n=5$) (Figure 3.5A) in PCAs. The presence of 500 nM of ouabain significantly inhibited the relaxation to 100 μM $H_2O_2$ (relaxation at 100 μM $H_2O_2$ = 82.7 ± 12.2%, control; 5.03 ± 3.3%, ouabain, $n=5$) (P<0.05) (Figure 3.5A). Increasing the concentration of DCB to 100 μM did not alter the relaxation to 100 μM $H_2O_2$ ($n=5$) (Figure 3.5B).
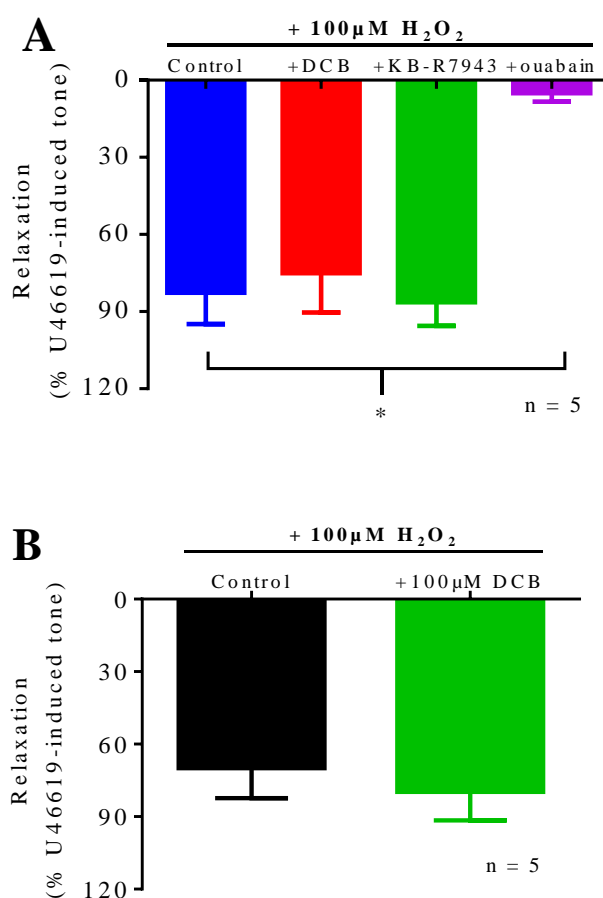


**Figure 3.5** Single concentration-responses to 100 μM $H_2O_2$ in the presence of 300 μM L-NAME, 10 μM indomethacin and (A) 10 μM DCB or KB-R7943 using 500 nM ouabain as a positive control and (B) higher concentration of DCB (100 μM) in U46619 pre-contracted porcine coronary arteries from either sex. Data are expressed as a percentage change from U46619-induced tone and are mean ± S.E.M. of 5 experiments. *P<0.05; one-way ANOVA followed by Bonferroni's *post hoc* test.

**3.3.6 The effects of ouabain in the absence or presence of L-NAME and indomethacin on bradykinin-induced vasorelaxation in PCAs from male or female pigs**

Next, the effects of ouabain on U46619 pre-contracted porcine coronary arteries PCAs from males and females against concentration-response curve to bradykinin were examined as a previous study has reported that bradykinin stimulate release of $H_2O_2$ in PCAs (Matoba *et al.*, 2003). In PCAs from females, the presence of L-NAME and indomethacin significantly reduced the relaxation at 1 μM bradykinin (relaxation at 1 μM bradykinin = 101 ± 1%, control; 70.1 ± 10.8%, L-NAME, indomethacin, *n*=7) (P<0.01) (Figure 3.6A). The presence of ouabain, both in the absence and presence of L-NAME and indomethacin essentially abolished the bradykinin-induced vasorelaxation (*n*=7) (P<0.0001) (Figure 3.6A).

Similarly in PCAs from males, L-NAME and indomethacin significantly reduced the relaxation at 1 μM bradykinin (relaxation at 1 μM bradykinin = 90.2 ± 5.6%, control; 61.0 ± 13.1%, L-NAME, indomethacin, *n*=5) (P<0.05). The presence of ouabain in the absence or presence of L-NAME and indomethacin abolished the bradykinin-induced vasorelaxation (*n*=5) (P<0.001) (Figure 3.6B).
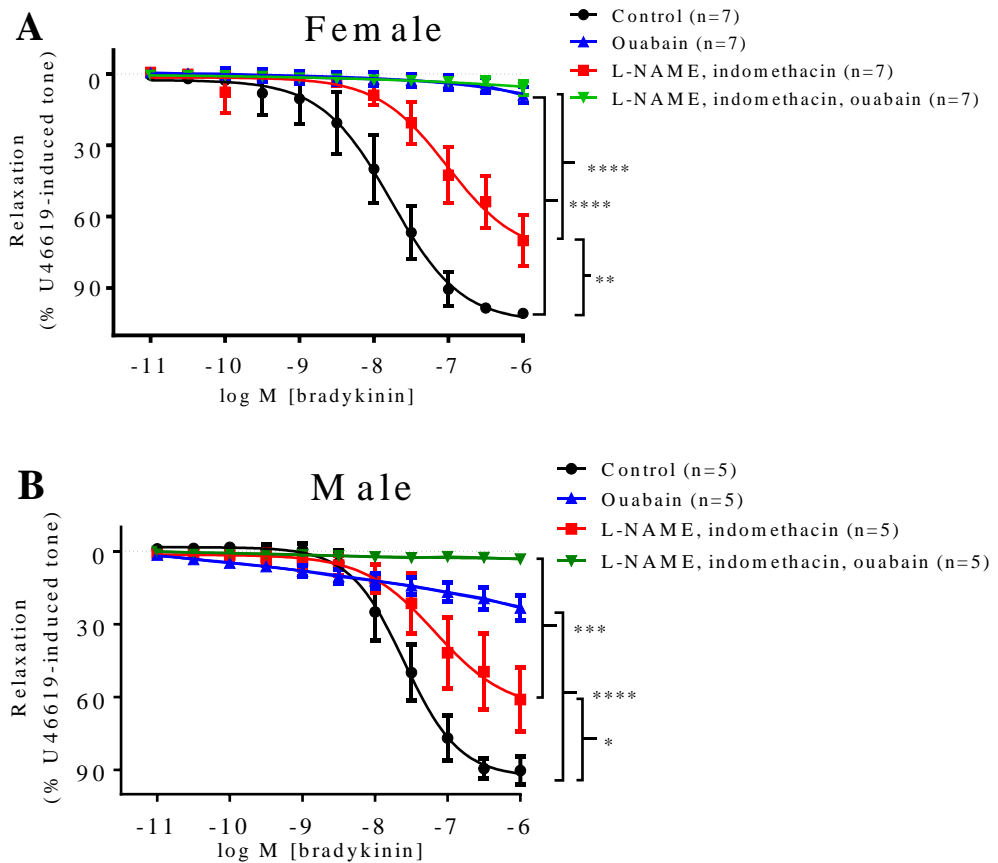
**Figure 3.6** Log concentration-response curves for the vasorelaxant effects of bradykinin in the presence or absence of 300 μM L-NAME, 10 μM indomethacin and/or 500 nM ouabain in U46619 pre-contracted porcine coronary arteries from (A) female or (B) male pigs. Data are expressed as a percentage change from U46619-induced tone and are mean ± S.E.M. of 5-7 experiments. *P<0.05, **P<0.01 ***P<0.001 and ****P<0.0001; one-way ANOVA followed by Bonferroni's *post hoc* test.

### 3.3.7 The effects of ouabain on responses to endothelium-independent vasorelaxants in PCAs from female pigs

To investigate the selectivity of 500 nM ouabain on vasorelaxation, responses to verapamil, were determined in its presence. Ouabain did not affect the verapamil-induced vasorelaxation ($n$=5) (Figure 3.7A). On the other hand, in the presence of L-NAME and indomethacin, 500 nM ouabain significantly inhibited the SNP-induced vasorelaxation ($n$=6) (P<0.05) (Figure 3.7B). Using a single concentration of forskolin (300 nM), the presence of 500 nM ouabain significantly inhibited the vasorelaxation after 2 h (relaxation to 300 nM forskolin = 93.6 ± 12.2%, without ouabain; 62.9 ± 10.2%, with ouabain, $n$=5) (P<0.05) (Figure 3.7C).
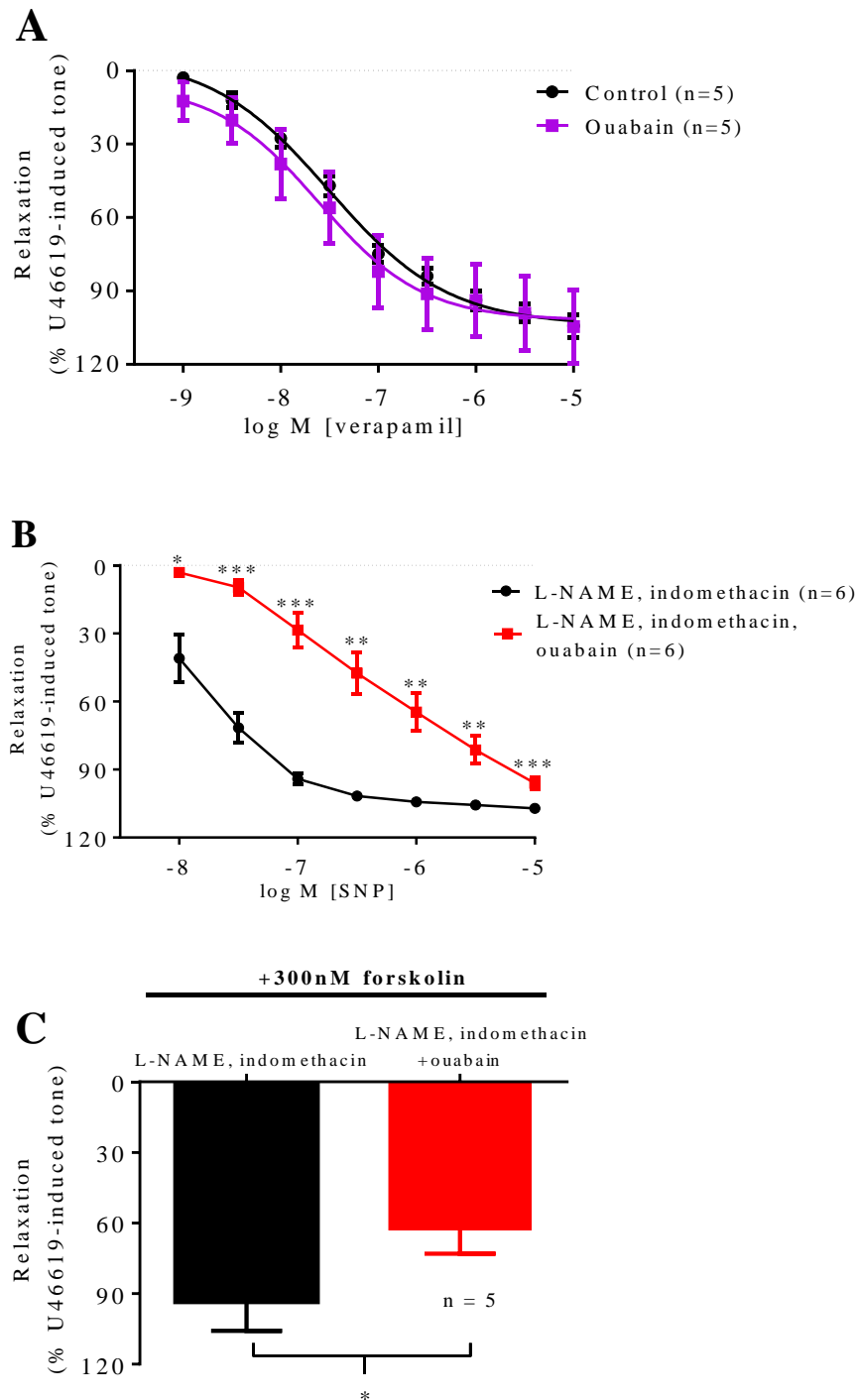
**Figure 3.7** Log concentration-response curves for the vasorelaxant effects of (A) verapamil (B) SNP and (C) a single concentration response to 300 nM forskolin in the absence or presence of 500 nM ouabain in U46619 pre-contracted porcine coronary arteries from female pigs. Data are expressed as a percentage change from U46619-induced tone and are mean ± S.E.M. of 5-6 experiments. *P<0.05, **P<0.01, ***P<0.001; 2-tailed, paired Student's *t*-test.

### 3.3.8 $3Na^+/2K^+$ pump activity as assessed by atomic absorption spectrophotometry in PCAs from female pigs

Measurement of the $3Na^+/2K^+$ ATPase activity using atomic absorption spectrophotometry in PCAs from female pigs showed that the presence of 10 μM ouabain significantly reduced the rubidium ($Rb^+$)-uptake in PCAs from $13.9 \pm 1.0$ μmol $mg^{-1}$ of tissue wet weight to $3.1 \pm 0.3$ μmol $mg^{-1}$ of tissue wet weight ($n$=9-10) (P<0.0001) (Figure 3.8A). The presence of 10 μM or 100 μM $H_2O_2$ had no effect on $Rb^+$-uptake, but at 1 mM $H_2O_2$, $Rb^+$-uptake was significantly reduced to $8.2 \pm 0.6$ μmol $mg^{-1}$ of tissue wet weight ($n$=7-9) (P<0.0001). The addition of 500 nM ouabain further reduced the $Rb^+$-uptake to $3.6 \pm 0.4$ μmol $mg^{-1}$ of tissue wet weight ($n$=9) (P<0.0001) (Figure 3.8A).

In a separate experiment, $Rb^+$-uptake was significantly reduced by 1 mM of $H_2O_2$ from $12.9 \pm 1.5$ μmol $mg^{-1}$ of tissue wet weight under control conditions to $7.1 \pm 0.7$ μmol $mg^{-1}$ of tissue wet weight ($n$=10) (P<0.01). A lower concentration of ouabain (500 nM) also significantly inhibited the $Rb^+$-uptake to $3.8 \pm 0.5$ μmol $mg^{-1}$ of tissue wet weight ($n$=10) (P<0.001) (Figure 3.8B).
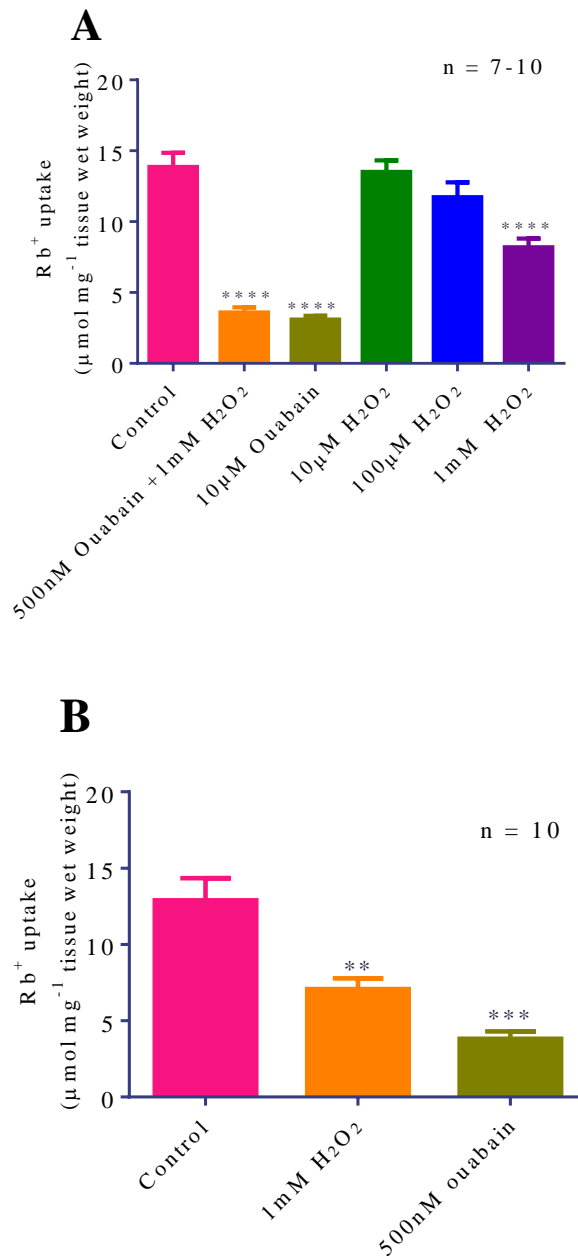
**Figure 3.8** Measurement of rubidium ($Rb^+$)-uptake (30 min incubation time) in PCAs from female pigs to determine the activity of $Na^+/K^+$ pump in the presence of (A) 500 nM or 10 μM ouabain, various concentrations of $H_2O_2$ (10 μM, 100 μM or 1 mM) and (B) 1 mM $H_2O_2$ or 500 nM ouabain using atomic absorption spectrophotometer used in a flame emission mode. Data are expressed as rubidium-uptake in μmol $mg^{-1}$ of tissue wet weight and are mean ± S.E.M. of 7-10 experiments. ** $P<0.01$, *** $P<0.001$ and **** $P<0.0001$; one-way ANOVA followed by Dunnett's multiple comparison test compared to the control.

### 3.3.9 The effects of 100 μM or 1 mM $H_2O_2$ on KCl-induced contraction in PCAs from either sex

To examine if the exposure of $H_2O_2$ impaired the ability of PCAs to contract again to 60 mM KCl, different concentrations of $H_2O_2$ (100 μM or 1 mM) were incubated with the vessels. Exposure to 100 μM $H_2O_2$ for 1 h had no effect on the KCl-induced contraction ($n$=6) (Figure 3.9A). On the other hand, exposure to 1 mM $H_2O_2$ for 1 h (7.48 ± 0.96g, control; 4.33 ± 0.83g, 1 mM $H_2O_2$, $n$=5) (Figure 3.9B), but not 30 min ($n$=4) (Figure 3.9C), significantly reduced the 60 mM KCl-induced contraction (P<0.01). Figure 3.10A and B show the responses of PCAs on exposure to 100 μM $H_2O_2$ and 1 mM $H_2O_2$ respectively under basal tone.
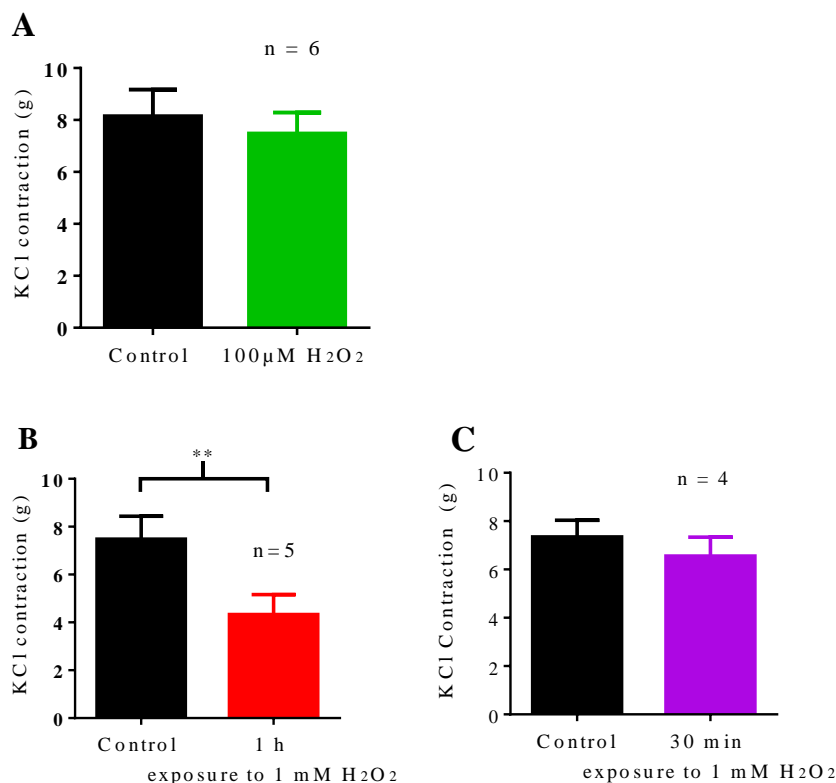


**Figure 3.9** The effects of (A) 100 μM $H_2O_2$ or 1 mM $H_2O_2$ for 1 h or 30 min on KCl-induced contraction in PCAs from either sex. Data are expressed as absolute KCl-induced contraction and are mean ± S.E.M. of 4-6 experiments. **P<0.01; 2-tailed, paired Student's $t$-test.
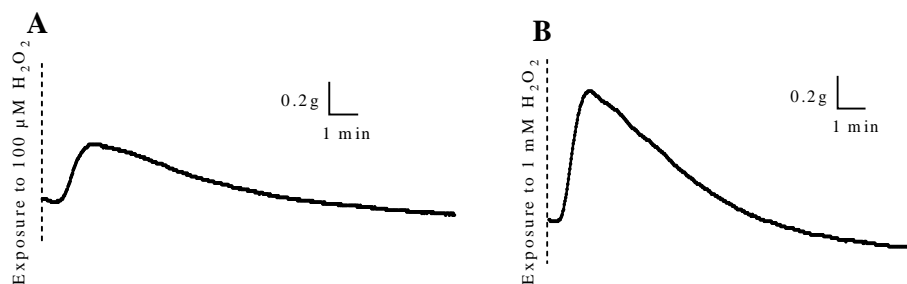
**Figure 3.10** Original traces showing the responses to exposure of (A) 100 μM $H_2O_2$ and (B) 1 mM $H_2O_2$ on PCAs under basal tone.

### 3.3.10 The effects of 500 nM ouabain, 100 μM $H_2O_2$ on $Ca^{2+}$ re-introduction in PCAs from either sex

As previous studies have reported that ouabain induces intracellular calcium oscillations in rat proximal tubule cells and increases calcium concentrations in rat cardiac myocytes (Aizman *et al.*, 2001; Kennedy *et al.*, 2006), the present study examined the effects 500 nM ouabain and 100 μM $H_2O_2$ in the presence of L-NAME and indomethacin on calcium-induced contraction in calcium-free Krebs'-Henseleit solutions. The presence of 100 μM $H_2O_2$ had no effect on the calcium-induced contraction whereas 500 nM ouabain significantly shifted the curve 10.7-fold to the right ($pEC_{50}$ = 3.88 ± 0.08, control; 2.85 ± 0.06, ouabain, *n*=4) (P<0.0001) (Figure 3.11A) (See Figure 3.11B and C for original traces).
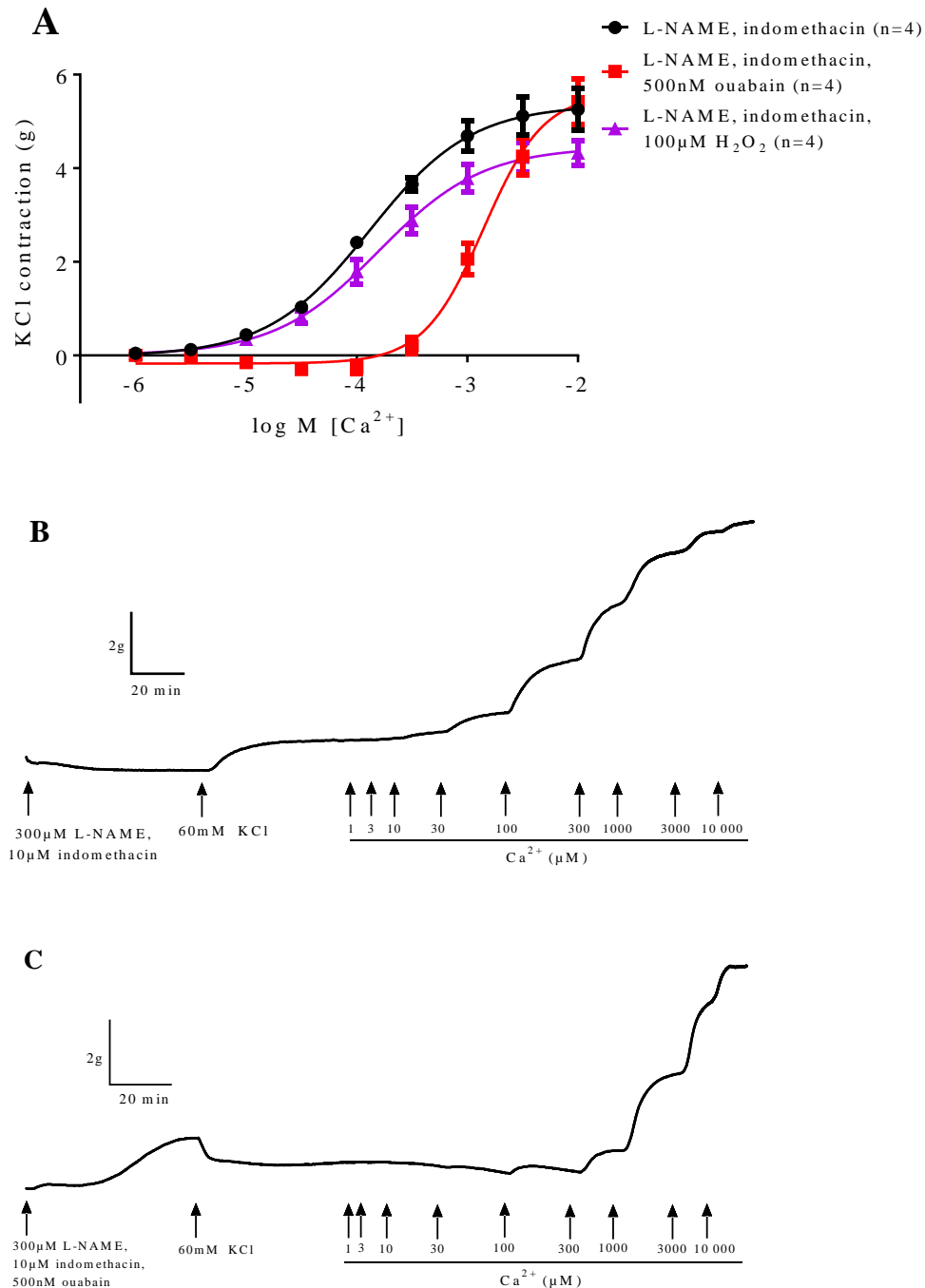
**Figure 3.11** (A) Log concentration-response curves for the contractile effects of reintroduction of $Ca^{2+}$ in KCl-depolarised porcine coronary arteries in the presence of 300 μM L-NAME, 10 μM indomethacin, 500 nM ouabain or 100 μM $H_2O_2$. Data are expressed as the absolute KCl-induced contraction and are mean ± S.E.M. of 4 experiments. Original traces showing the responses to increasing concentration of $Ca^{2+}$ in $Ca^{2+}$-free Krebs'-Henseleit solution in the presence of (B) 300 μM L-NAME, 10 μM indomethacin and (C) addition of 500 nM ouabain.

### 3.3.11 The effects of ouabain, $H_2O_2$ or removal of endothelium on KCl-induced response in PCAs from either sex

To examine the effects of ouabain and $H_2O_2$ on $3Na^+/2K^+$-pump activity, small gradual increases in extracellular $K^+$ were used (Edwards *et al.*, 1998; Harris *et al.*, 2000). Addition of KCl to PCAs precontracted with U46619 caused a biphasic response with a maximum relaxation at 5.0 mM KCl, followed by contraction at 20 mM KCl under control conditions. 100 μM $H_2O_2$ (*n*=5) (Figure 3.12A) or removal of the endothelium (*n*=4) (Figure 3.12B) had no effect on the potassium-induced vasorelaxation compared to the control conditions.

The presence of 500 nM ouabain essentially abolished the $K^+$-induced vasorelaxation at low concentrations of KCl and contractile responses at high concentrations of KCl (*n*=6) (Figure 3.12C). The presence of 1 mM $H_2O_2$ significantly inhibited the $K^+$-induced vasorelaxation producing a maximum relaxation of 63 ±3% (*n*=6) at 5 mM KCl (P<0.01) compared to 99 ± 3% (*n*=6) under control conditions. At concentrations >15 mM KCl, 1 mM $H_2O_2$ significantly inhibited the KCl-induced vasocontraction (P<0.05) (Figure 3.12C). Here, relaxation to KCl under control conditions was transient (See control curve of Figure 3.12A and C).
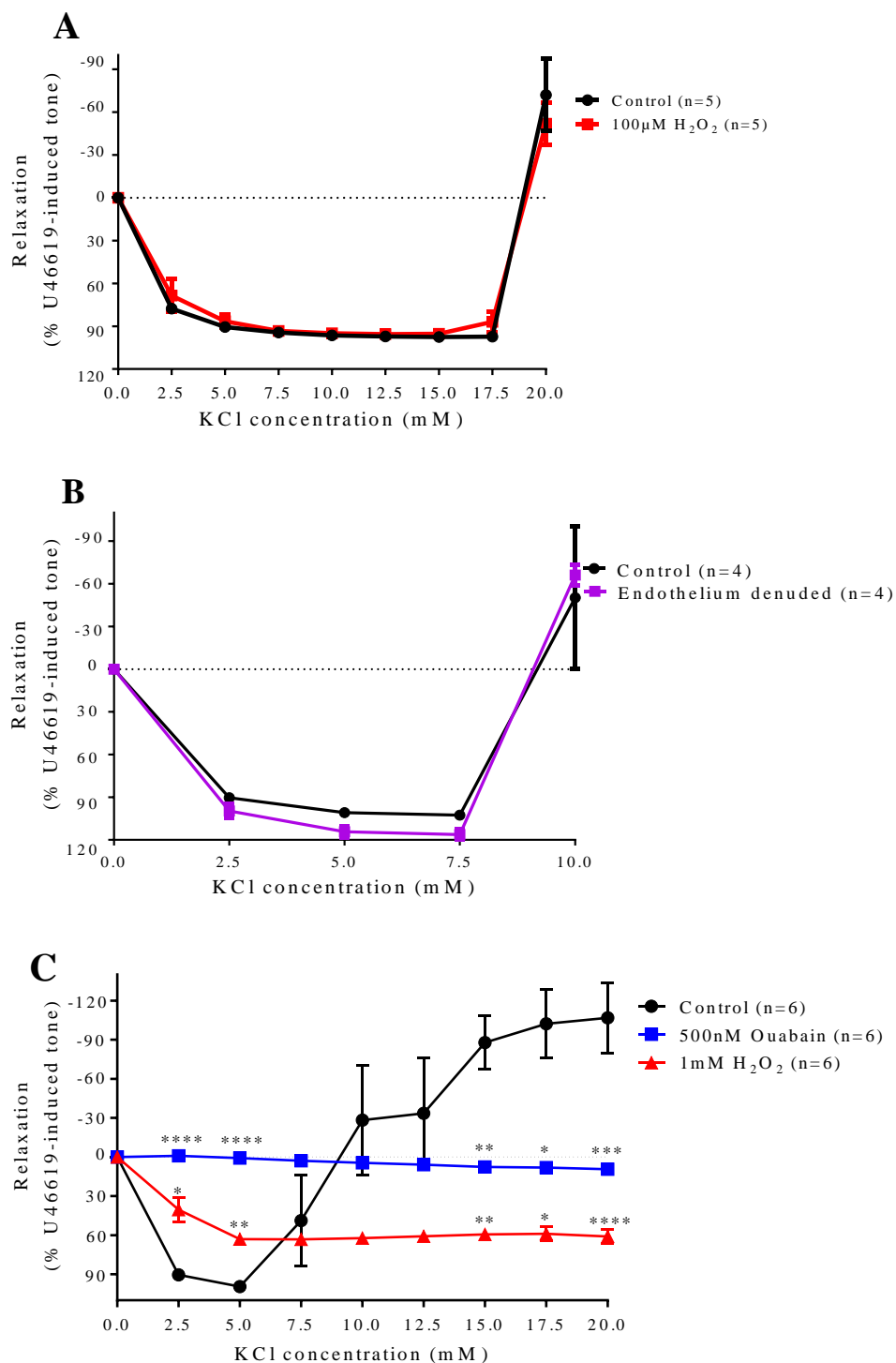
**Figure 3.12** Concentration-response curves to KCl in the presence of (A) 100 μM $H_2O_2$, (B) denuded endothelium and (C) 500 nM ouabain or 1 mM $H_2O_2$ in U46619 pre-contracted porcine coronary arteries from either sex. Data are expressed as a percentage change from U46619-induced tone and are mean ± S.E.M. of 4-6 experiments. *P<0.05, **P<0.01, ***P<0.001 and ****P<0.0001; one-way ANOVA followed by Bonferroni's *post hoc* test.

130

## 3.4 Discussion

This chapter has clearly shown that $H_2O_2$ causes complex vasorelaxant effects which are ouabain-sensitive in PCAs. The vascular effects are concentration-dependent such that at concentrations up to 100 µM, $H_2O_2$ appears to be selective and sensitive to ouabain. However, at higher concentrations, the responses appear non-selective where 1 mM $H_2O_2$ has been shown to inhibit the sodium-pump activity and produce vasorelaxation concurrently. Here, no sex differences in the $H_2O_2$-induced vasorelaxation were observed, therefore subsequent experiments were conducted using PCAs from either sex.

In contrast to a previous study where removal of the endothelium or presence of indomethacin significantly reduced the $H_2O_2$-induced vasorelaxation in PCAs (Thengchaisri & Kuo, 2003), the present study demonstrated that neither the endothelium nor nitric oxide and cyclo-oxygenase play a role in the $H_2O_2$-mediated relaxations. However, results from this chapter are in agreement with those of Rogers *et al.* (2006) and Miura *et al.* (2003) in canine coronary arteries and in human coronary arterioles (HCAs). The differences in findings in the present study with those of Thengchaisri & Kuo (2003) could be due to the age of the pigs used, as the present study used pigs from 4-6 months old while Thengchaisri & Kuo used younger pigs (8-12 weeks old). Apart from that, the vessel size used in this study was 8-17 times larger than Thengchaisri & Kuo's paper and results from the present study are consistent with a previous study using PCAs from larger vessels (2-4 mm diameter) (Barlow & White, 1998). Indeed, Rogers *et. al.* (2006) mentioned that coronary microvessels could be more sensitive to $H_2O_2$

than larger vessels, therefore it is possible that mechanism of action of $H_2O_2$ differs between vessel size (Ohashi *et al.*, 2012; Shimokawa, 2010).

Experiments with elevated extracellular potassium (Edwards *et al.*, 1998; Ellis *et al.*, 2003; Miura *et al.*, 2003; Ray *et al.*, 2011; Rogers *et al.*, 2006; Wheal *et al.*, 2012) or non-selective inhibition of $K^+$ channels with TEA (Ellis *et al.*, 2003; Gao *et al.*, 2004; Rogers *et al.*, 2006) in the present study significantly inhibited the $H_2O_2$-induced vasorelaxation demonstrating that potassium channels are involved in the $H_2O_2$-induced vasorelaxation in PCAs. These findings are consistent with previous studies (as summarized in Table 3.1), except for one study where it was reported that TEA alone or in combination with 4-AP had no effect on $H_2O_2$-induced vasorelaxation in mouse small mesenteric arteries (Ellis *et al.*, 2003), a finding that could be due to species difference.

As $H_2O_2$ has been proposed to be a factor for EDH-type relaxation, the effects of $H_2O_2$ acting through the 'classical' EDH pathway involving the $SK_{Ca}$, $IK_{Ca}$ and barium-sensitive $K_{ir}$ channels were examined. 500 nM apamin and/or 10 μM TRAM-34 or 30 μM barium chloride had no effect on the $H_2O_2$-induced vasorelaxation. The presence of 1 mM 4-AP also failed to inhibit the $H_2O_2$-induced vasorelaxation in the present study suggesting that inhibiting $SK_{Ca}$, $IK_{Ca}$, $K_{ir}$ and $K_V$ channels separately had no effect on the $H_2O_2$-mediated response (For similar effects with previous studies see Table 3.1).

Next, the role of guanylyl cyclase and large-conductance calcium activated potassium channels in $H_2O_2$-mediated relaxations were investigated as previous studies have reported that inhibition of these pathways

| Vascular bed of study | References | Significantly reduced $H_2O_2$ relaxation | No effects on $H_2O_2$ relaxation |
|---|---|---|---|
| Porcine coronary arteries | Present study | 60 mM KCl, 10 mM TEA, 500 nM ouabain | 500 nM apamin±10 μM TRAM-34, 1 μM glibenclamide, 30 μM barium, 1 mM 4-AP, 300 nM/1 μM paxilline |
| Porcine coronary arteries | Hayabuchi et al., 1998 | 100 nM ChTx | 20 μM glibenclamide, 1 mM 4-AP |
| Porcine coronary arteries | Barlow & White, 1998 | 80 mM KCl | |
| Porcine coronary arteries | Thengchaisri & Kuo, 2003 | 35 mM KCl | 5 μM glibenclamide |
| Porcine coronary microvessels | Matoba et al., 2003 | 40-60 mM KCl, 1 mM TBA | |
| Mouse mesenteric arteries and aortae | Ohashi et al., 2012 | 1 mM TBA | |
| Mouse small mesenteric arteries | Matoba et al., 2000 | 20-60 mM KCl, 1 mM TBA | 100 nM ChTx+1 μM apamin |
| Mouse small mesenteric arteries | Ellis et al., 2003 | 60 mM KCl | 10 mM TEA±1 mM 4-AP, 100 μM ouabain+ 30 μM barium, 100 nM ChTx+1 μM apamin |
| Human mesenteric arteries | Matoba et al., 2002 | 40-60 mM KCl | |
| Human coronary arterioles | Miura et al., 2003 | 40 mM KCl, 100 nM ChTx+ 1 μM apamin | 1 μM glibenclamide, |
| Canine coronary arteries | Rogers et al., 2006 | 60 mM KCl, 10 mM TEA, 3 mM 4-AP | |

**Table 3.1** A comparison of effects of various potassium channels inhibitors on $H_2O_2$-induced vasorelaxation in different arteries and species examined in the present and previous studies. **ChTx** charybdotoxin; **TEA** tetraethylammonium; **TBA** tetrabutylammonium; **4-AP** 4-aminopyridine.

significantly attenuate the $H_2O_2$-induced vasorelaxation (Burke & Wolin, 1987; Hayabuchi *et al.*, 1998). However, in the present study, the lack of effect of ODQ, iberiotoxin or paxilline would rule out the involvement of cGMP or $BK_{Ca}$ in $H_2O_2$-mediated relaxations in PCAs (Barlow & White, 1998; Ellis *et al.*, 2003; Rogers *et al.*, 2007; Rogers *et al.*, 2006; Thengchaisri & Kuo, 2003).

The ability of raised KCl to inhibit responses to $H_2O_2$ could be consistent with EDH-type responses being involved. Therefore, the effects of ouabain on $H_2O_2$-induced vasorelaxation were examined as EDH-responses have been reported to be inhibited by ouabain, an inhibitor of the $Na^+/K^+$-ATPase pump (Edwards *et al.*, 1998). Here, the presence of 500 nM ouabain significantly inhibited the $H_2O_2$-induced vasorelaxation and bradykinin-stimulated EDH-type responses, suggesting a role of the $Na^+/K^+$-ATPase pump.

To further characterize the effects of ouabain on PCAs, endothelium-dependent and -independent vasorelaxants were examined. Here, using bradykinin, an endothelium-dependent vasorelaxant, demonstrated that the $Na^+/K^+$-pump is involved in both the endothelium-dependent and EDH-mediated (non-nitric oxide, non-cyclooxygenase products) vasorelaxation, where the vasorelaxation was essentially abolished in PCAs from male and female pigs. Findings from the present study differ slightly from Matoba *et al.* (2003) in porcine coronary microvessels where they have reported that, in the presence of L-NAME and indomethacin, barium plus ouabain significantly shifted the bradykinin curve to the right but had no effect on the maximum relaxation. Again, these differences could be due to the size of the vessel used.

The present study demonstrated that the ouabain-sensitive $Na^+/K^+$-pump plays a role in mediating endothelium-dependent vasorelaxation in distal PCAs.

Next, the effects of ouabain against other vasorelaxants, verapamil, sodium nitroprusside, and forskolin were examined where ouabain significantly reduced the responses to SNP- and cAMP-induced vasorelaxation, but not relaxation associated with L-type calcium channel inhibition. Although ouabain significantly affected responses to both SNP and forskolin, the relaxations to SNP and forskolin were not abolished. Here, it is possible that ouabain has non-selective effects on the vasorelaxation. The fact that verapamil-induced responses were unaffected demonstrates that the effects of ouabain on the $H_2O_2$ relaxation are not due to non-specific effects on smooth muscle relaxation responses.

As previous studies have reported a role for the $Na^+/Ca^{2+}$ exchanger in increasing calcium influx following inhibition of the $Na^+/K^+$-pump (Barry $et$ $al.$, 1985) and activation of the $Na^+/K^+$-pump subsequently stimulates the activation of the forward mode $Na^+/Ca^{2+}$ exchanger in mouse aortae (Kim $et$ $al.$, 2005), present study hypothesized that the $Na^+/Ca^{2+}$ exchanger could play a role in the $H_2O_2$-mediated response. $H_2O_2$ has also been reported to activate the $Na^+/Ca^{2+}$ exchanger in isolated guinea-pig cardiac ventricular myocytes (Hinata $et$ $al.$, 2007). However, the present study using DCB and KB-R7943, an inhibitor of the $Na^+/Ca^{2+}$ exchanger and a selective inhibitor of the reverse mode of the $Na^+/Ca^{2+}$ exchanger respectively, had no effect on the $H_2O_2$-induced vasorelaxation.

To further examine the effects of $H_2O_2$ on $Na^+/K^+$-pump activity in intact tissue, atomic absorption spectrophotometry measuring $Rb^+$-uptake (replacing $K^+$) (Longo *et al.*, 1991) was used. Here, using 500 nM ouabain as a positive control, present study demonstrated that 100 μM $H_2O_2$ did not affect the $Na^+/K^+$-pump activity. However, at higher concentration of $H_2O_2$ (1 mM) the pump activity was significantly inhibited. This inhibition could be a possible explanation for the biphasic effects observed in some vessels (Gao *et al.*, 2004; Lucchesi *et al.*, 2005) where exogenously applied $H_2O_2$ causes initial contraction (Figure 3.10A and B) possibly through inhibition of the pump followed by relaxation through hyperpolarization of the vascular smooth muscle cells (Beny & von der Weid, 1991; Matoba *et al.*, 2003; Ohashi *et al.*, 2012). Alternatively, it could also be possible that exposure to high oxidant stress (1 mM) damages the pump (Elmoselhi *et al.*, 1994; Ingbar & Wendt, 1997; Kim & Akera, 1987). Similar to a previous study (Ellis *et al.*, 2003), the present study demonstrated that 1 mM $H_2O_2$ may have irreversibly damaged vascular smooth muscle cell contraction in that incubation with 1 mM $H_2O_2$, followed by wash out, caused inhibition of the contraction to 60 mM KCl. Ellis *et al.* (2003) suggested that 1 mM $H_2O_2$ causes vasorelaxation (or loss in tone) through impairment of smooth muscle contractile response. However the present study using 100 μM $H_2O_2$ (a concentration which produces about 60% of relaxation in PCAs) showed that smooth muscle contraction to KCl was not impaired. The data demonstrate that low concentrations of $H_2O_2$ (below 100 μM) produce a relaxation of the porcine coronary artery through an ouabain-sensitive mechanism, whereas at higher concentrations, $H_2O_2$ inhibits the $Na^+/K^+$-pump itself, which may be due to irreversible damage.

A previous study has suggested that $H_2O_2$ produces a relaxation through alteration of calcium-induced contractions, possibly at the level of calcium signalling (Ellis *et al.*, 2003). One possible explanation for the inhibition of $H_2O_2$ relaxation by ouabain is that it inhibits influx of extracellular calcium through calcium channels. If $H_2O_2$ does the same, or acts to inhibit calcium signalling downstream of calcium influx, this could explain why ouabain inhibits the $H_2O_2$ relaxation. Although it was found that ouabain does inhibit calcium-induced contractile responses, $H_2O_2$ did not inhibit this calcium-induced contraction. These data, therefore, demonstrate that $H_2O_2$ does not produce a relaxation through inhibition of calcium influx or signalling downstream of calcium influx.

To demonstrate that ouabain was affecting the sodium-pump mediated vasorelaxation, exogenous $K^+$ was applied to U46619 precontracted PCAs in potassium free Krebs'-Henseleit solution (Ding *et al.*, 2000; Edwards *et al.*, 1998; Harris *et al.*, 2000). Here, reintroduction of $K^+$ to U46619 precontracted PCAs produced a biphasic response (with almost 100% relaxation at 5 mM KCl followed by >100% contraction at 20 mM KCl). This response was endothelium-independent and was essentially abolished in the presence of 500 nM ouabain. This indicates that exogenous $K^+$ ions can mimic the EDH-mediated response on smooth muscle cells acting through $Na^+/K^+$ pump. Similar findings using $K^+$ ions as a factor for EDH in PCAs and rat hepatic arteries (Beny & Schaad, 2000; Edwards *et al.*, 1999) have previously been reported. Incubating PCAs with 1 mM $H_2O_2$ significantly reduced the $K^+$-induced vasorelaxation up to 5 mM KCl and significantly inhibited the contraction induced by >15 mM KCl. This indicates that $H_2O_2$ could possibly

be inhibiting the $Na^+/K^+$-pump as a previous study in PCAs reported similar finding whereby $H_2O_2$ and superoxide reduced the $Na^+/K^+$-pump activity in the KCl-induced vasorelaxation assay (Elmoselhi *et al.*, 1994) and this observation is consistent with the effects on rubidium-uptake. Exposure to 100 μM $H_2O_2$ had no effect on the KCl-induced relaxation which is consistent with the spectrophotometry experiment where 100 μM $H_2O_2$ had no effect on the rubidium-uptake level.

In summary (Figure 3.13), this chapter established that $H_2O_2$ acts in an ouabain-sensitive manner (a property also shared by EDH responses) at concentrations up to 100 μM and that only at higher concentrations (1 mM) does it inhibit the $Na^+/K^+$ pump, possibly due to dysfunction of the $Na^+/K^+$-pump (Elmoselhi *et al.*, 1994; Kim & Akera, 1987). The mechanisms and effects of different concentrations of $H_2O_2$ presented here may provide a better understanding of the vascular functions during oxidative stress where different levels of $H_2O_2$ have been detected in disease (Burgoyne *et al.*, 2013).
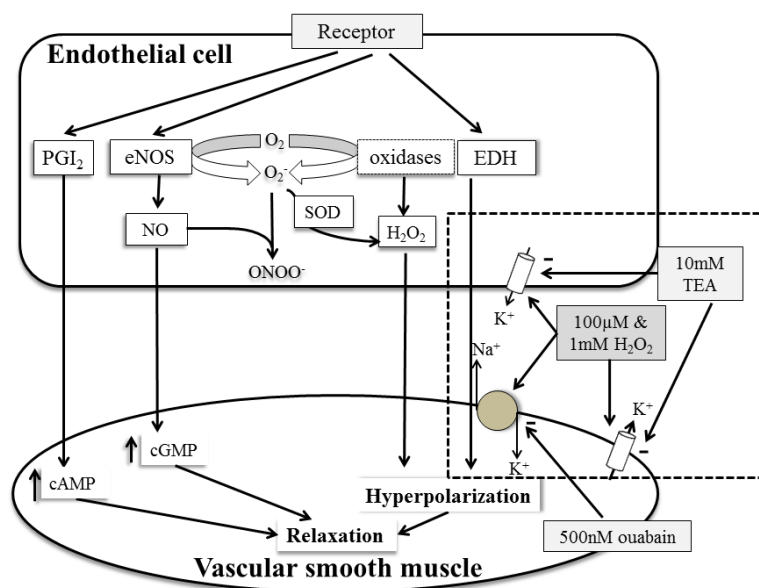


**Figure 3.13** Summary of mechanism of action of hydrogen peroxide on porcine isolated coronary arteries.

# *Chapter 4*

**Hyperoxic gassing with Tiron[®] enhances bradykinin-induced endothelium-dependent and EDH-type relaxation through generation of hydrogen peroxide**

## 4.1 Introduction

To date, almost all of the isometric tension studies use 95% oxygen with 5% $CO_2$ for the oxygenation of buffers. However, hyperoxic gassing conditions may affect tissue responses, particularly in studies which involved reactive oxygen species (ROS). In the 1980s when endothelium-derived relaxing factor (EDRF) was first reported, the effect of oxygen tension on the endothelium-dependent relaxation was also studied, demonstrating that under anoxic conditions, relaxations to acetylcholine were abolished (Furchgott & Zawadzki, 1980). EDRF was later confirmed to be NO and Palmer *et al.,* (1987) reported that NO reacts readily with superoxide anions ($O_2^-$) to form peroxynitrite ($ONOO^-$) thereby reducing NO bioavailability (Palmer *et al.*, 1987). It has also been reported that the synthesis of NO is inhibited under low oxygen tensions ($PO_2$ values about 15-25 mmHg) (Kim *et al.*, 1993).

In Chapter 2, using porcine isolated coronary arteries (PCAs), the involvement of NO and endothelium-dependent hyperpolarization (EDH)-type relaxation in bradykinin-induced vasorelaxation has been demonstrated. The EDH-type pathway is defined as the remaining proportion of endothelium-dependent relaxation which is insensitive to NO synthase inhibition and cyclooxygenase inhibition (Edwards *et al.*, 2010; Weston *et al.*, 2005).

In the endothelium, superoxide anions ($O_2^-$) can be generated from sources such as eNOS, NADPH oxidases or cytochrome P450 epoxygenases (Shimokawa, 2010). These superoxide anions will in turn form $H_2O_2$ either by spontaneous dismutation or by dismutation by SOD (Faraci & Didion, 2004). Superoxide dismutase (SOD) has been shown to enhance endothelium-dependent relaxation by increasing the bioavailability of NO (Gryglewski *et*

*al.*, 1986; Palmer *et al.*, 1987). Tiron[®], a drug marketed as a cell permeable superoxide scavenger, has previously been used as a cell-permeable SOD mimetic in organ chamber studies involving bradykinin-induced vasorelaxation in porcine isolated coronary microvessels and human mesenteric arteries (Matoba *et al.*, 2003; Morikawa *et al.*, 2004). In these studies, they have concluded that $H_2O_2$ is a factor for EDH-type responses and that Tiron[®] acts as a superoxide scavenger which facilitates the formation of $H_2O_2$ in the endothelium (Matoba *et al.*, 2003; Morikawa *et al.*, 2004). Previous studies and Chapter 3 of the present study have shown that exogenously applied $H_2O_2$ produces concentration-dependent vasorelaxation in human, porcine, rat and mice vessels (Barlow & White, 1998; Hayabuchi *et al.*, 1998; Matoba *et al.*, 2002; Matoba *et al.*, 2000; Miura *et al.*, 2003; Wheal *et al.*, 2012).

Given the possibility that superoxide anions can be generated in well-oxygenated Krebs'-Henseleit buffer, this chapter examined if hyperoxic gassing conditions could alter the relaxation responses to bradykinin through effects on NO. Here, the effects of different gassing conditions (95% $O_2$/5% $CO_2$ and 95% air/5% $CO_2$) on endothelium-dependent relaxation in distal PCAs were investigated. As studies in Chapter 2 have shown sex differences in endothelial function, whereby intracellular $H_2O_2$ plays a role in PCAs from female, but not male pigs, the present chapter also examined the effects of cell permeable superoxide scavenger, Tiron[®] on endothelium-dependent relaxation in PCAs from male and female pigs.

## 4.2 Materials and methods

### 4.2.1 Preparation of rings of distal PCAs

Tissues were set up as previously described in Chapter 2.

### 4.2.2 Wire myography

As previously described in Chapter 2, after 30 min of equilibration, contractile responses to 60 mM KCl were determined twice. The vascular tone was then raised to about 50 - 80% of the second KCl contraction tone by the addition of the thromboxane $A_2$ mimetic, U46619 (1 nM - 90 nM). Once stable tone was achieved, concentration-response curves to an endothelium-dependent vasorelaxant, bradykinin (0.01 nM - 1 μM) or $H_2O_2$ (1 μM - 1 mM) were constructed. Tiron® (1 mM) (Matoba *et al.*, 2003) was used as a cell permeable superoxide scavenger and catalase (1000 UmL$^{-1}$) (Wheal *et al.*, 2012) was used to breakdown $H_2O_2$. In some preparations, $N^G$-nitro-L-arginine methyl ester (L-NAME) (300 μM) (Randall & Griffith, 1991) was used as a NO synthase inhibitor and indomethacin (10 μM) was used to inhibit the synthesis of prostanoids. There were no differences in the concentration of U46619 used to pre-contract the tissue when gassed with either 95% $O_2$/5% $CO_2$ or 95% air/5% $CO_2$ (Table 4.1A) or in the presence of Tiron®, with or without catalase compared to the control (Table 4.1B) or in the presence of L-NAME and indomethacin (Table 4.1C). However, in the presence of 100 μM $H_2O_2$, a higher concentration of U46619 (on average 2-fold) was required to achieve a similar level of tone compared to the controls (P<0.05) (Table 4.2). The presence of 1 mM Tiron® had no effect on the pH of the Krebs'-Henseleit solution when gassed with either 95% $O_2$/5% $CO_2$ or 95% air/5% $CO_2$.

| A | Concentration of U46619 (nM) | | | | U46619-induced tone (% KCl response) | | | |
|---|---|---|---|---|---|---|---|---|
| | Control ($O_2$) | Tiron ($O_2$) | Control (air) | Tiron (air) | Control ($O_2$) | Tiron ($O_2$) | Control (air) | Tiron (air) |
| Male | 2.58 ± 0.27 | 2.00 ± 0.52 | 3.17 ± 0.49 | 2.25 ± 0.48 | 56.0 ± 1.1 | 61.2 ± 2.9 | 61.5 ± 6.7 | 72.8 ± 11.2 |
| Female | 12.3 ± 1.8 | 11.3 ± 2.3 | 13.4 ± 5.3 | 10.8 ± 2.9 | 67.3 ± 2.9 | 67.1 ± 5.2 | 61.8 ± 3.5 | 62.6 ± 3.1 |

| B | Concentration of U46619 (nM) | | | U46619-induced tone (% KCl response) | | |
|---|---|---|---|---|---|---|
| | Control | Tiron | Tiron, catalase | Control | Tiron | Tiron, catalase |
| Male | 7.42 ± 2.73 | 4.67 ± 1.21 | 5.17 ± 3.03 | 60.2 ± 3.72 | 65.5 ± 3.66 | 77.7 ± 7.24 |
| Female | 10.9 ± 1.4 | 10.3 ± 1.1 | 34.8 ± 10.8 | 56.0 ± 1.0 | 61.1 ± 4.2 | 65.6 ± 6.6 |

| C | Concentration of U46619 (nM) | | U46619-induced tone (% KCl response) | |
|---|---|---|---|---|
| | L-NAME, indomethacin | L-NAME, indomethacin, Tiron | L-NAME, indomethacin | L-NAME, indomethacin, Tiron |
| Male | 15 ± 2.6 | 15 ± 2.7 | 62 ± 6.9 | 58.67 ± 5.4 |
| Female | 18.2 ± 4.4 | 17.9 ± 2.6 | 55.8 ± 2.6 | 55.4 ± 4.2 |

**Table 4.1** Summary of U46619 concentration used (nM) and the level of tone induced by U46619 expressed in the percentage to second KCl-induced tone when (A) gassed with either 95% $O_2$/5% $CO_2$ or 95% air/5% $CO_2$ or (B) in the presence of 1 mM Tiron[®] with or without 1000 UmL[-1] catalase compared to the control or (C) in the presence of 300μM L-NAME, 10 μM indomethacin with or without 1 mM Tiron in porcine coronary arteries from male and female pigs. Data are expressed as mean ± S.E.M. of 5-11 experiments.

| Female | Control | 100 μM H$_2$O$_2$ | L-NAME, indomethacin | |
|---|---|---|---|---|
| | | | Control | 100 μM H$_2$O$_2$ |
| **Concentration of U46619 (nM)** | 10.9 ± 1.1 | 21.6 ± 4.0 | 12.6 ± 1.6 | 20.7 ± 1.9* |
| **U46619-induced tone (% KCl response)** | 77.4 ± 7.8 | 65.0 ± 9.6 | 60 ± 4.8 | 63.6 ± 6.3 |

**Table 4.2** Summary of U46619 concentration used (nM) and the level of tone induced by U46619 expressed in the percentage to second KCl-induced tone in the absence or presence of 300 μM L-NAME, 10 μM indomethacin with or without 100 μM H$_2$O$_2$ in porcine coronary arteries from female pigs. Data are expressed as mean ± S.E.M. of 5-7 experiments. *P<0.05, 2-tailed, paired Student's *t*-test.

**4.2.3 Biochemical assay to detect hydrogen peroxide using Amplex Red**

Krebs'-Henseleit solution (300 μL) was collected before and after the pharmacological studies and placed in a 96-well plate (Garry *et al.*, 2009). Amplex Red (10 μM) and horseradish peroxidase (0.6 UmL$^{-1}$) were added into each well and the plate incubated in the dark at room temperature for 15 min. Absorbance was read at 590 nm with excitation of 530 nm using FLUOstar Galaxy (BMG Labtech Ltd, Aylesbury, Bucks, UK). Experiments were performed in the absence or presence of Tiron$^{®}$ and/or catalase with or without tissue in Krebs'-Henseleit solution maintained at 37°C gassed with either 95% $O_2$/5% $CO_2$ or 95% air/5% $CO_2$.

**4.2.4 Biochemical assay to detect superoxide anion using Nitrotetrazolium Blue (NBT) reduction assay**

To determine if superoxide is generated in the Krebs'-Henseleit solution, NBT (1 mg/mL) reduction assay was performed in the absence of tissue (Dehne *et al.*, 2001). In the presence of superoxide, NBT is reduced to monoformazan (NBT$^{+}$) forming a blue precipitate which is insoluble in aqueous solutions (Goto *et al.*, 2004; Tarpey & Fridovich, 2001). To detect the amount of superoxide formed in the Krebs'-Henseleit solution, the decrease in intensity of the absorbance of NBT was measured at 560 nm (Goto *et al.*, 2004; Tarpey & Fridovich, 2001) using a SpectraMAX 340 PC microplate reader (Molecular Devices, Wokingham, Berkshire, UK). NBT (1 mg/ml) was dissolved in Krebs'-Henseleit solution, maintained at 37°C in the myograph. Krebs'-Henseleit solution was either not gassed or gassed with 95% $O_2$/5% $CO_2$ for

4 h (the duration of the pharmacological responses). 200 μL of Krebs'-Henseleit solution was then collected from the myograph chamber and placed into a 96-well plate followed by reading of the absorbance of NBT at 560 nm.

### 4.2.5 Statistical analysis

Data for the functional studies were presented and analysed as described in Chapter 2. Data for the $H_2O_2$ determinations are presented as the mean of arbitrary fluorescence units with standard error of the mean (S.E.M.) and $n$ being the number of separate animals.

### 4.2.6 Drugs and reagents

All drugs were purchased from Sigma-Aldrich (Poole, Dorset, UK) and were dissolved in distilled water except for catalase and NBT (N6876) which were dissolved directly in the Krebs'-Henseleit solution. Stock solutions of bradykinin and U46619 were made to 10 mM in water and ethanol respectively while stock solution of $H_2O_2$ was made up to 100 mM in water. All further dilutions of the stock solutions were made using distilled water.

## 4.3 Results

### 4.3.1 The effects of Tiron[®] on bradykinin-induced vasorelaxation in PCAs from male and female pigs under different gassing conditions (95% $O_2$/5% $CO_2$ or 95% air/5% $CO_2$ )

In PCAs from males under control conditions, gassing with 95% air/5% $CO_2$ had no effect on the relaxation to bradykinin compared to gassing with 95% $O_2$/5% $CO_2$. The presence of Tiron[®] had no effect on the $R_{max}$ of the bradykinin-induced vasorelaxation in either gassing condition, but caused a 11.7-fold leftward shift in the concentration-response curve when gassed with 95% $O_2$/5% $CO_2$ (P<0.001) such that there was an increase in potency ($pEC_{50}$ = 8.74 ± 0.13 compared to 7.67 ± 0.13 in the controls, $n$=6) (Figure 4.1A). On the other hand, the presence of Tiron[®] had no effect on the bradykinin responses when gassed with air ($pEC_{50}$ = 7.80 ± 0.11, control; 7.73 ± 0.23, Tiron[®], $n$=6) (Figure 4.1A).

Similarly in PCAs from females, gassing with 95% air/5% $CO_2$ had no effect on the relaxation to bradykinin compared to gassing with 95% $O_2$/5% $CO_2$. The presence of Tiron[®] did not affect the maximum relaxation under either gassing condition (Figure 4.1B) but again significantly increased the potency of bradykinin 5.1-fold (P<0.001) ($pEC_{50}$ = 8.10 ± 0.06, control; 8.81 ± 0.07, Tiron[®], $n$=9) when gassed with 95% $O_2$/5% $CO_2$ and not with 95% air/5% $CO_2$ ($pEC_{50}$ = 8.09 ± 0.12, control; 8.42 ± 0.13, Tiron[®], $n$=9).
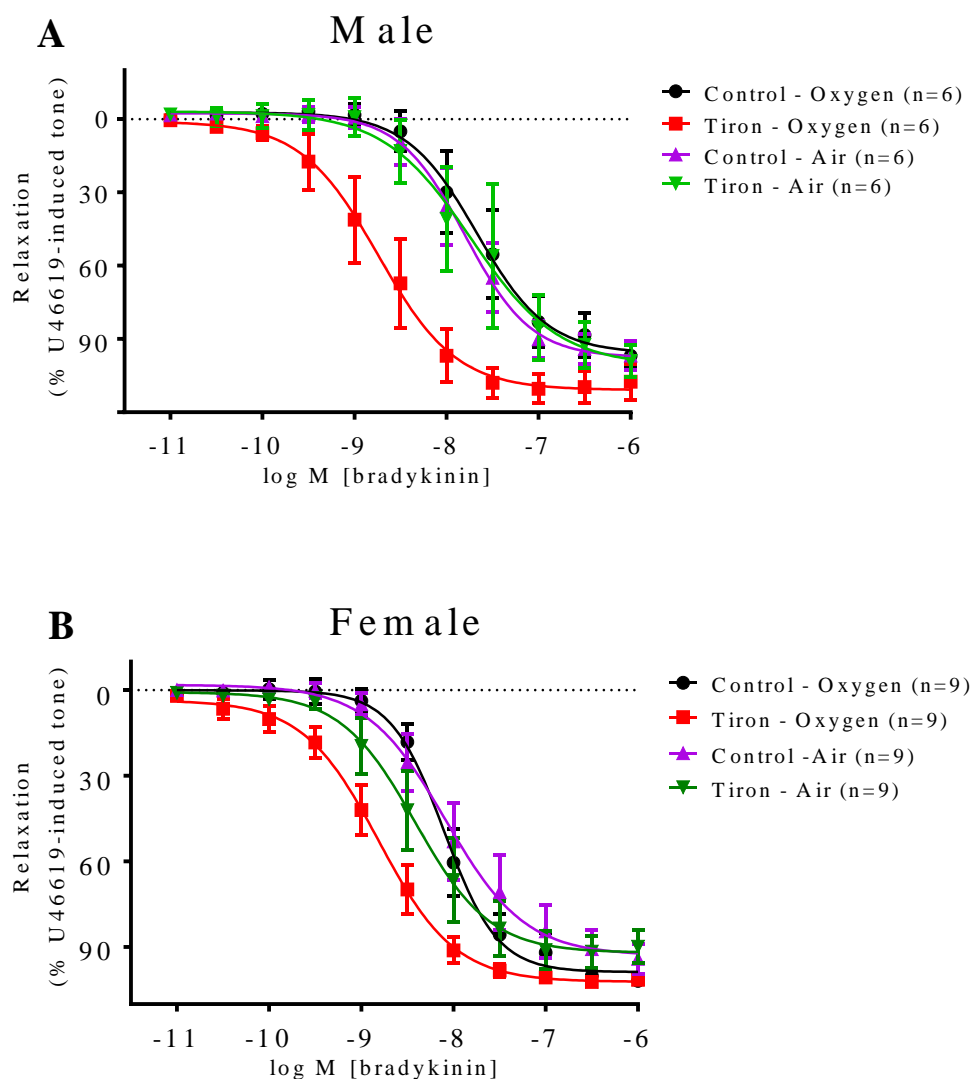
**Figure 4.1** Log concentration-response curves for the vasorelaxant effects of bradykinin in the absence or presence of 1 mM Tiron$^{®}$ in U46619 pre-contracted porcine coronary arteries from (A) male and (B) female pigs gassed with either 95% $O_2$/5% $CO_2$ or 95% air/5% $CO_2$. Data are expressed as a percentage change from U46619-induced tone and are mean $\pm$ S.E.M. of 6-9 experiments.

**4.3.2 The effects of Tiron[®] in the presence or absence of catalase on bradykinin-induced vasorelaxation in PCAs from male and female pigs gassed with 95% $O_2$/5% $CO_2$**

As Tiron[®], a superoxide dismutase mimetic, significantly increased the potency of bradykinin when gassed with 95% $O_2$/5% $CO_2$, the effects of catalase on Tiron[®] were examined to determine if Tiron[®] is generating $H_2O_2$. In PCAs from males oxygenated with 95% $O_2$/5% $CO_2$, treatment with Tiron[®] alone or in the additional presence of catalase had no effect on the $R_{max}$ (Figure 4.2A). However, the presence of Tiron[®] significantly increased the potency of bradykinin (P<0.05) ($pEC_{50}$ = 8.09 ± 0.08, control; 8.56 ± 0.09, Tiron[®], $n$=6), which was prevented by the presence of catalase ($pEC_{50}$ = 8.02 ± 0.13, Tiron[®], catalase, $n$=6) (Figure 4.2A).

In the presence of 95% $O_2$/5% $CO_2$, in PCAs from females, the presence of Tiron[®] significantly shifted the curve 3.7-fold to the left ($pEC_{50}$ = 8.37 ± 0.04, control; 8.94 ± 0.04, Tiron[®], $n$=8-9) (P<0.001) and this was prevented by catalase ($pEC_{50}$ = 8.08 ± 0.15, Tiron[®], catalase, $n$=9) (Figure 4.2B). Furthermore, treatment with catalase reduced the $R_{max}$ significantly from 103 ± 2% in the presence of Tiron[®] to 87.4 ± 6.37% ($n$=8) with the addition of catalase ($n$=9) (P<0.05) (Figure 4.2B).
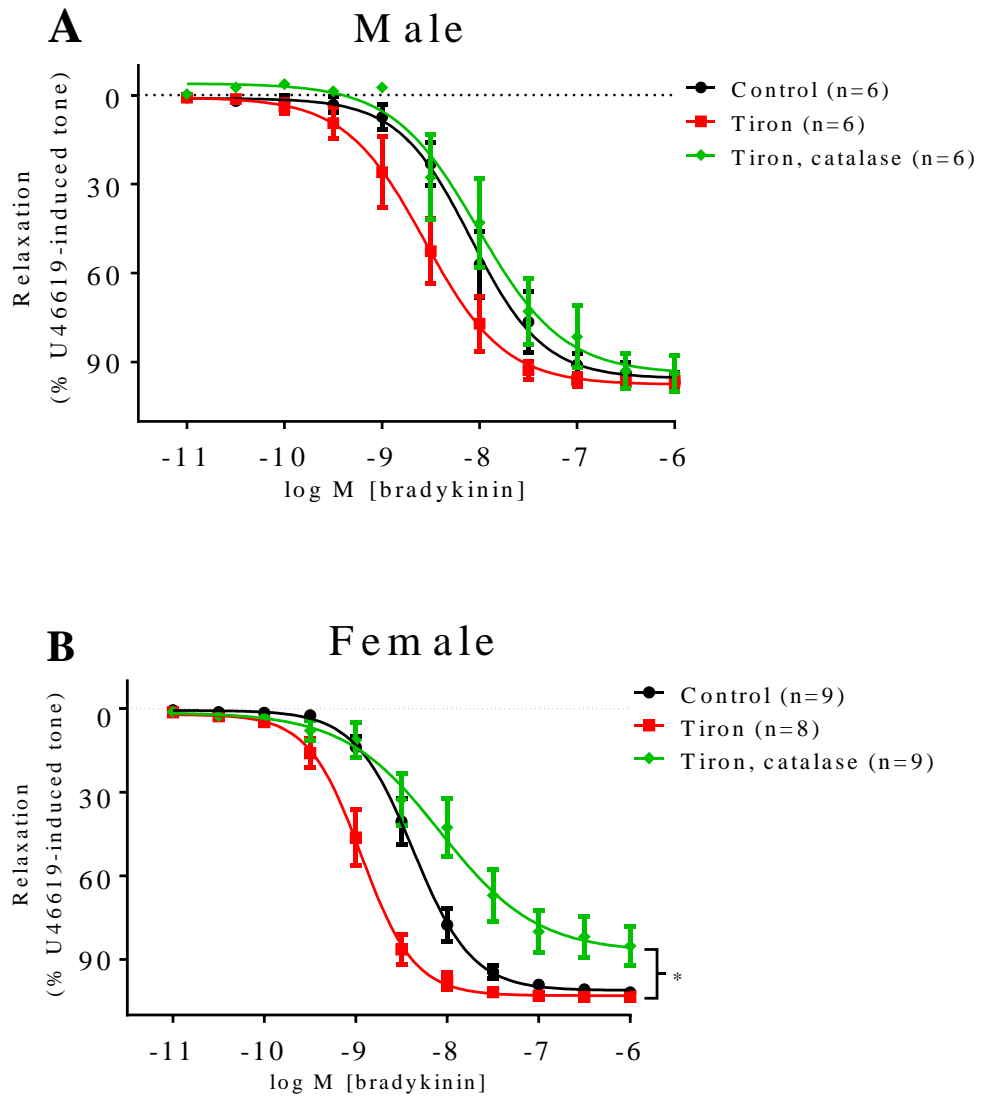
**Figure 4.2** Log concentration-response curves for the vasorelaxant effects of bradykinin in the absence or presence of 1 mM Tiron® with or without 1000 UmL$^{-1}$ catalase in U46619 pre-contracted porcine coronary arteries from (A) male and (B) female pigs gassed with 95% $O_2$/5% $CO_2$. Data are expressed as a percentage change from U46619-induced tone and are mean ± S.E.M. of 6-9 experiments. *P<0.05; one-way ANOVA followed by Bonferroni's *post hoc* test.

### 4.3.3 Biochemical assay on the effects of Tiron® under different gassing conditions (95% $O_2$/5% $CO_2$ or 95% air/5% $CO_2$) in the absence or presence of PCAs from female pigs using Amplex Red

The presence of 1 mM Tiron® significantly increased the fluorescence signals to Amplex Red in Krebs'-Henseleit solution when gassed with 95% $O_2$/5% $CO_2$ in the presence of arterial rings before bradykinin (Figure 4.3A) (P<0.0001) and after bradykinin (Figure 4.3B) (P<0.0001) response. This was prevented by catalase, indicating that the increase in Amplex Red fluorescence was due to production of $H_2O_2$ (Figure 4.4). A similar effect was seen in the absence of arterial segments (Figure 4.3A & B), indicating that the increase in $H_2O_2$ was from the buffer and not the tissues. On the other hand, there was no detectable change in $H_2O_2$ levels detected by Amplex Red when the Krebs'-Henseleit buffer was gassed with 95% air/5% $CO_2$ (Figure 4.3A and B).

In the presence of tissue under control condition after the bradykinin response, the concentration of $H_2O_2$ accumulated in the Krebs'-Henseleit buffer determined using the Amplex Red assay was ~80 µM (gassed with 95% $O_2$/5% $CO_2$). In the presence of Tiron® after the bradykinin response (~2.45 h after the addition of Tiron®), the concentration of $H_2O_2$ was ~3.6 M when gassed with 95% $O_2$/5% $CO_2$. The accumulation of $H_2O_2$ was almost abolished in the additional presence of 1000 $UmL^{-1}$ catalase (Figure 4.4).
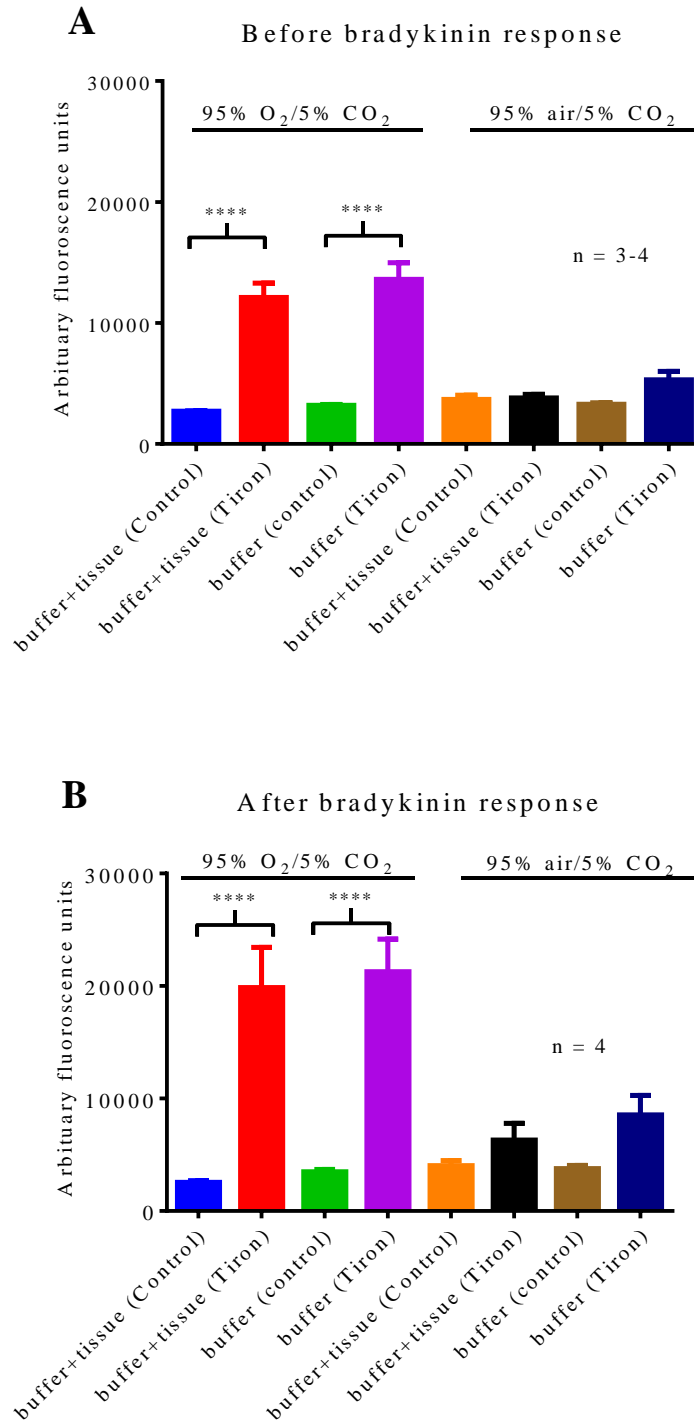
**Figure 4.3** Measurement of $H_2O_2$ levels in the Krebs'-Henseleit solution in the absence or presence of 1 mM Tiron[®] with or without tissue in 95% $O_2$/5% $CO_2$ or 95% air/5% $CO_2$ (A) before or (B) after bradykinin response. Data are expressed as arbitrary fluorescence units and are mean ± S.E.M. of 3-4 experiments. \*\*\*P<0.001, \*\*\*\*P<0.0001; one-way ANOVA followed by Bonferroni's *post hoc* test.
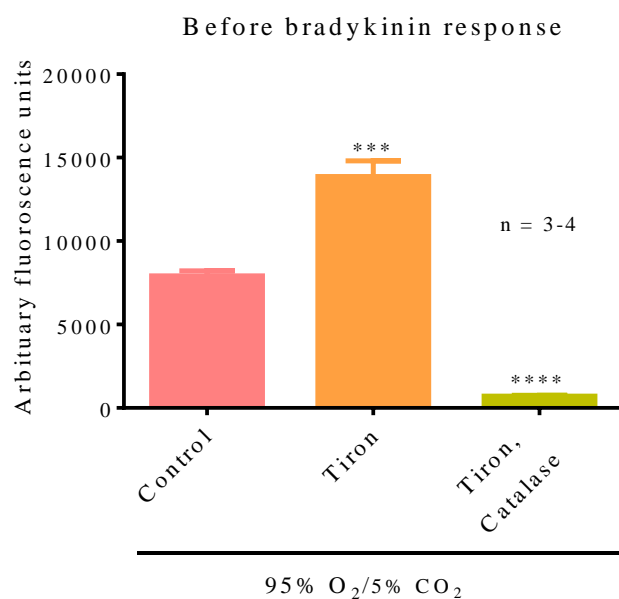
**Figure 4.4** Measurement of $H_2O_2$ level in the Krebs'-Henseleit solution in the absence or presence of 1 mM Tiron® with or without 1000 UmL$^{-1}$ catalase gassed with 95% $O_2$/5% $CO_2$. Data are expressed as arbitrary fluorescence units and are mean ± S.E.M. of 3-4 experiments. \*\*\*P<0.001, \*\*\*\*P<0.0001; one-way ANOVA followed by Bonferroni's *post hoc* test.

## 4.3.4 Detection of superoxide anion in the Krebs'-Henseleit solutions in the absence of PCAs using Nitrotetrazolium Blue (NBT)

In the absence of tissue, gassing of the Krebs'-Henseleit solutions with 95% $O_2$/5% $CO_2$ significantly reduced the intensity of the NBT solution compared to the control (Figure 4.5) ($P<0.001$). This indicates that superoxide anions are generated in the Krebs'-Henseleit solutions when gassed with 95% $O_2$/5% $CO_2$.
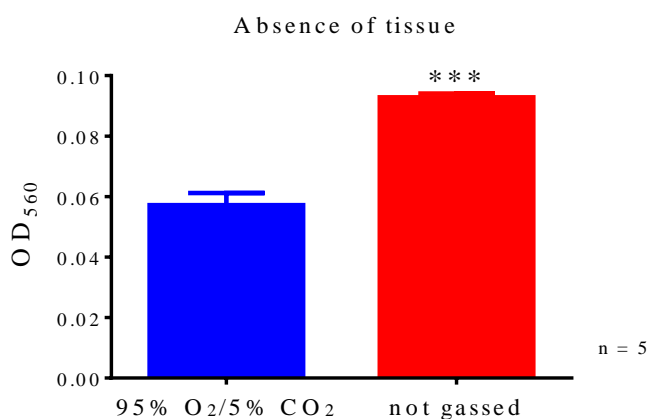


**Figure 4.5** Assessment of the superoxide levels in the Krebs'-Henseleit solution in the absence of tissue gassed with 95% $O_2$/5% $CO_2$ using 1 mg/ml NBT; where a decrease in absorbance indicates increased level of superoxide. Data are expressed as the optical density measured at absorbance of 560 nm and are mean ± S.E.M. of 5 replicates. ***$P<0.001$; 2-tailed, paired Student's $t$-test.

**4.3.5 The effects of L-NAME and indomethacin on bradykinin-induced vasorelaxation in PCAs from female pigs under different gassing conditions (95% $O_2$/5% $CO_2$ or 95% air/5% $CO_2$) or with the additional presence of Tiron® in PCAs from male and female pigs gassed with 95% $O_2$/5% $CO_2$**

As Tiron® significantly enhanced the bradykinin-induced vasorelaxation when gassed with 95% $O_2$/5% $CO_2$, the effects of different gassing conditions on the non-nitric oxide, non-cyclooxygenase products, (EDH)-type response using L-NAME and indomethacin were then investigated. Figure 4.6A demonstrates that under control conditions different gassing conditions had no effect on the $R_{max}$ or the $pEC_{50}$ values of bradykinin-induced vasorelaxation. Similarly in the presence of L-NAME and indomethacin, the bradykinin-induced vasorelaxation showed no differences in the $R_{max}$ or the $pEC_{50}$ values of when gassed with either 95% air/5% $CO_2$ ($pEC_{50} = 7.32 \pm 0.17$, $n=4$) or 95% $O_2$/5% $CO_2$ ($pEC_{50} = 7.02 \pm 0.28$, $n=7$ ).

Next, the effects of 1 mM Tiron® in the presence of L-NAME and indomethacin on bradykinin-induced vasorelaxation in the presence of 95% $O_2$/5% $CO_2$ were examined. Here, the presence of 1 mM Tiron® significantly enhanced the potency of the bradykinin-induced vasorelaxation in PCAs from male pigs by shifting the curve 4.1-fold to the left (Figure 4.6B) ($P<0.01$) ($pEC_{50} = 7.42 \pm 0.11$; without Tiron®, $8.03 \pm 0.10$; with Tiron®, $n=11$) and in female pigs by shifting the curve 6.2-fold to the left (Figure 4.6C) ($P<0.05$,) ($pEC_{50} = 7.59 \pm 0.10$; without Tiron®, $8.38 \pm 0.06$; with Tiron®, $n=5$).
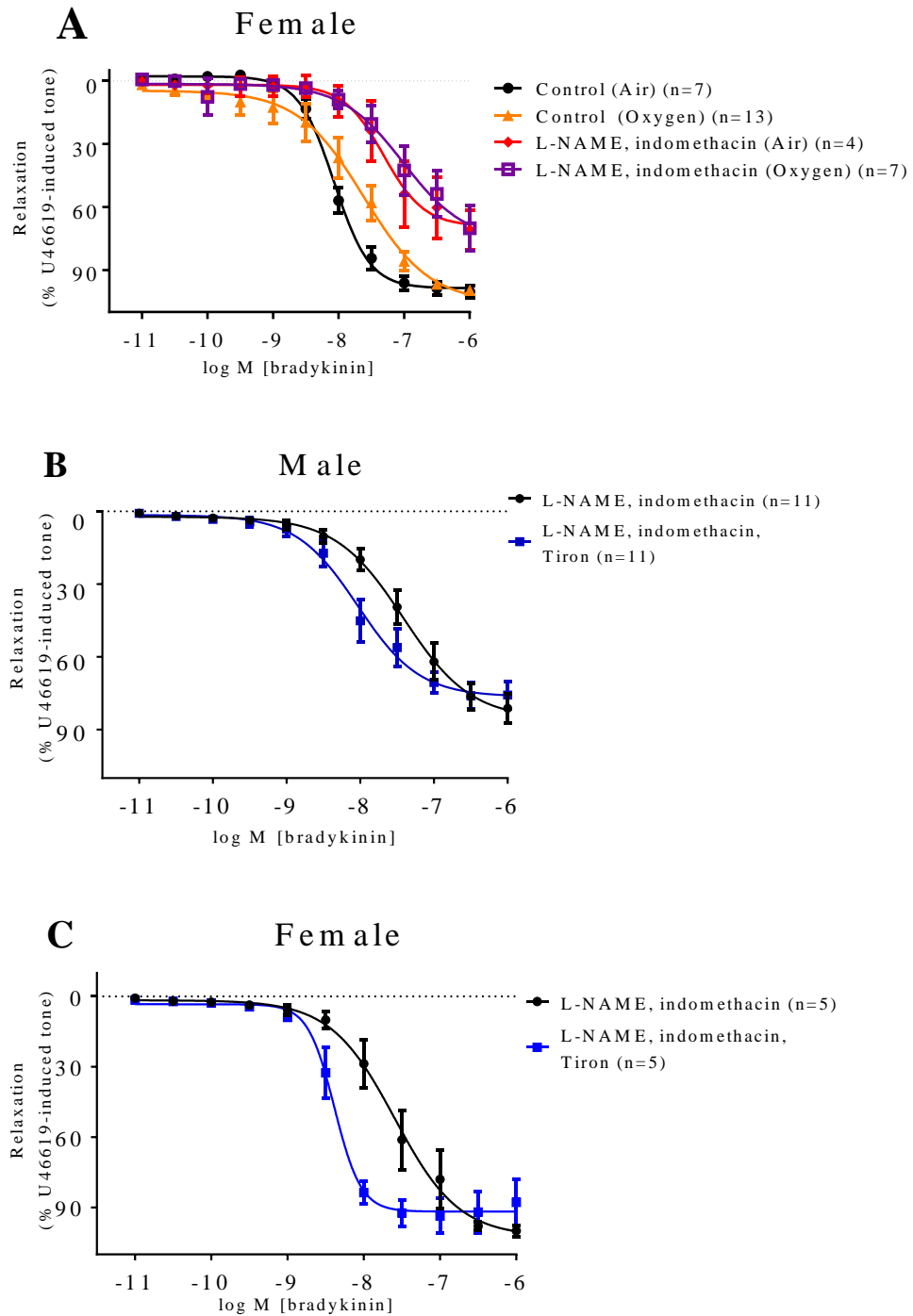
**Figure 4.6** Log concentration-response curves for the vasorelaxant effects of bradykinin in the absence or presence of 300 μM L-NAME and 10 μM indomethacin (A) under different gassing conditions (95% $O_2$/5% $CO_2$ or 95% air/5% $CO_2$) and with the additional presence of 1 mM Tiron® in U46619 pre-contracted porcine coronary arteries from (B) male and (C) female pigs gassed with 95% $O_2$/5% $CO_2$. Data are expressed as a percentage change from U46619-induced tone and are mean ± S.E.M. of 4-13 experiments.

**4.3.6 The effects of different gassing conditions (95% $O_2$/5% $CO_2$ or 95% air/5% $CO_2$) on $H_2O_2$-induced vasorelaxation in PCAs from female pigs**

As Tiron® generates $H_2O_2$ and enhances the bradykinin-induced vasorelaxation only when gassed with 95% $O_2$/5% $CO_2$ and not with 95% air/5% $CO_2$, the effects of different gassing conditions on $H_2O_2$-induced vasorelaxation were then investigated. As some of the individual curves did not achieve a maximum relaxation, data were analysed using the relaxation generated at the highest concentration of $H_2O_2$ used. Here, 1 mM of $H_2O_2$ produced a comparable relaxation in the presence of 95% $O_2$/5% $CO_2$ and 95% air/5% $CO_2$ (Figure 4.7).
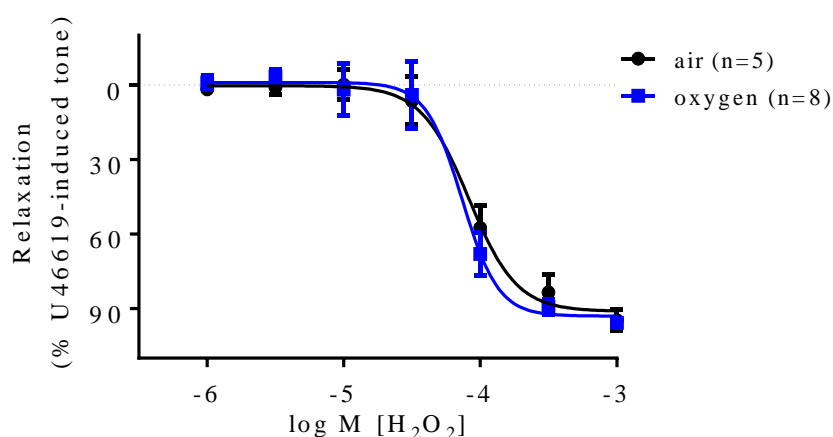


**Figure 4.7** Log concentration-response curves for the vasorelaxant effects of $H_2O_2$ in U46619 pre-contracted porcine coronary arteries from female pigs under different gassing conditions (95% $O_2$/5% $CO_2$ or 95% air/5% $CO_2$). Data are expressed as a percentage change from U46619-induced tone and are mean ± S.E.M. of 5-8 experiments.

**4.3.7 The effects of 100 µM $H_2O_2$ in the absence or presence of L-NAME and indomethacin on bradykinin-induced vasorelaxation (gassed with 95% $O_2$/5% $CO_2$) in PCAs from female pigs**

As the presence of Tiron® significantly enhanced the potency of bradykinin-induced vasorelaxation and increased formation of $H_2O_2$, the effects of exogenously applied $H_2O_2$ (100 µM) on bradykinin-induced vasorelaxation were examined. Here, the presence of 100 µM $H_2O_2$ had no effect on the $R_{max}$ or $pEC_{50}$ ($pEC_{50}$ = 8.28 ± 0.09, control; 8.18 ± 0.05, $H_2O_2$, $n$=5) of the bradykinin-induced vasorelaxation (Figure 4.8A). On the other hand, in the presence of L-NAME and indomethacin, 100 µM $H_2O_2$ significantly enhanced the bradykinin-induced vasorelaxation at 10 nM and 30 nM (P<0.05) of bradykinin (Figure 4.8B).
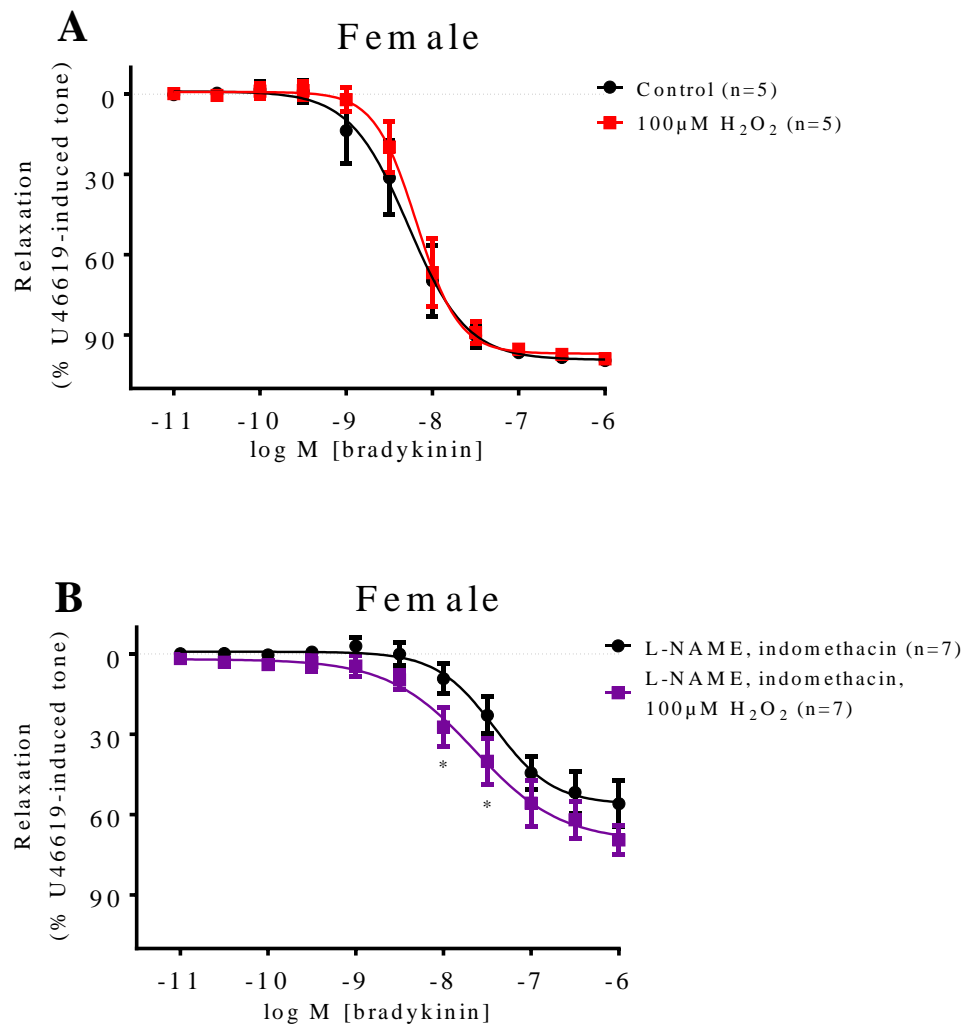
**Figure 4.8** Log concentration-response curves for the vasorelaxant effects of bradykinin in the presence of 100 μM $H_2O_2$ in U46619 pre-contracted porcine coronary arteries from female pigs in the (A) absence or (B) presence of 300 μM L-NAME and 10 μM indomethacin, gassed with 95% $O_2$/5% $CO_2$. Data are expressed as a percentage change from U46619-induced tone and are mean ± S.E.M. of 5-7 experiments. *P<0.05; 2-tailed, paired Student's *t*-test.

## 4.4 Discussion

This chapter clearly shows that the level of oxygenation significantly influences the local environment for endothelium-dependent vasorelaxations, such that under hyperoxic conditions, the antioxidant Tiron[®] enhances endothelium-dependent and EDH-type relaxations through generation of $H_2O_2$ in the Krebs'-Henseleit solution. A previous study measuring the partial pressure of oxygen in Krebs'-Henseleit solution has shown that when gassed with 95% $O_2$/5% $CO_2$ the partial pressure of $O_2$ was $619 \pm 17$ mmHg (*n*=3) while when gassed with 95% air/5% $CO_2$ the partial pressure of $O_2$ was $140 \pm 4$ mmHg (*n*=3) (White, 2012).

This chapter has demonstrated that bradykinin produced a comparable relaxation in the presence of either 95% air/5% $CO_2$ or 95% $O_2$/5% $CO_2$ in PCAs from both male and female pigs. However, under hyperoxic conditions, the superoxide dismutase mimetic Tiron[®] caused a substantial increase in the potency of bradykinin as an endothelium-dependent vasorelaxant in PCAs from male and female pigs. This was not seen under lower levels of oxygenation and suggests that hyperoxia may be associated with an increase in superoxide production which suppresses endothelium-dependent relaxations. As superoxide anion ($O_2^-$) readily reacts with NO forming peroxynitrite (Gryglewski *et al.*, 1986; Kerr *et al.*, 1999), it is possible that Tiron[®] acting as a superoxide scavenger reduces the superoxide levels in the PCAs or in the Krebs'-Henseleit buffer thereby increasing NO bioavailability improving endothelium-dependent vasorelaxation. The effects of Tiron[®] were more pronounced in the male arteries in which, as shown in Chapter 2, NO plays a more prominent role in endothelium-dependent relaxations. However, if this

was the case, one would expect the relaxations to bradykinin to be greater in the presence of 95% air/5% $CO_2$, compared to 95% $O_2$/5% $CO_2$ due to the lower superoxide level generated in buffer gassed with 95% air/5% $CO_2$. An alternative explanation is that Tiron[®] scavenges superoxide in the Krebs'-Henseleit buffer converting it into $H_2O_2$, which then enhances the endothelium-dependent relaxations. Indeed, in the absence of NO (in the presence of L-NAME), Tiron[®] also enhanced the bradykinin-induced vasorelaxation (further discussion below).

Previous studies and present study in Chapter 3 have demonstrated that $H_2O_2$ itself causes vasorelaxations in PCAs (Barlow & White, 1998; Matoba *et al.*, 2003). A higher concentration of superoxide in the presence of 95% $O_2$/5% $CO_2$ would mean that there is a greater concentration of $H_2O_2$ in the presence of Tiron[®]. As confirmation of this, the effects of Tiron[®] in enhancing endothelium-dependent vasorelaxation when gassed with 95% $O_2$/5% $CO_2$ were abolished by catalase which breaks down $H_2O_2$. The presence of catalase significantly reduced the maximum relaxation in PCAs from female, but not male pigs, indicating that $H_2O_2$ plays a role in the endothelium-dependent vasorelaxation induced by bradykinin, as previously reported in Chapter 2. In the presence of Tiron[®], there was an increase in Amplex Red fluorescence in the Krebs'-Henseleit solution in the presence of 95% $O_2$/5% $CO_2$, but not 95% air/5% $CO_2$. Again, the increase in Amplex Red fluorescence was prevented by catalase, confirming that Tiron[®] is producing $H_2O_2$ under hyperoxic conditions. Here, the generation of $H_2O_2$ by Tiron[®] (acting as a superoxide scavenger) in the Krebs'-Henseleit solution was independent of the presence of tissues and the level of $H_2O_2$ produced was two- to three fold greater than when

gassed with 95% $O_2$/5% $CO_2$ compared to 95% air/5% $CO_2$. This observation is comparable with a previous study using the same biochemical assay to determine the $H_2O_2$ level in the presence of 1 mM ascorbic acid (Garry *et al.*, 2009). Further study using the NBT reduction assay to detect the superoxide level in the Krebs'-Henseleit solution confirm that in the absence of tissue, gassing with 95% $O_2$/5% $CO_2$ generated superoxide in the buffer.

In this chapter, no increase in vasorelaxation was observed before the addition of bradykinin in the presence of Tiron[®], although it was hypothesized that Tiron[®] generated $H_2O_2$ in the buffer. One possible explanation for this observation is that the level of $H_2O_2$ generated in the Krebs'-Henseleit solution appears to be increasing over time (comparing Figure 4.3A and B, before and after bradykinin response). Furthermore, there could be a potentiation through the bradykinin receptor or signal transduction, as bradykinin produced a concentration-dependent vasorelaxation.

Next, the effects of different gassing conditions on the EDH-type responses induced by bradykinin were examined as $H_2O_2$ has previously been reported to be a factor for the EDH-type response (Garry *et al.*, 2009; Matoba *et al.*, 2002; Matoba *et al.*, 2003; Matoba *et al.*, 2000; Miura *et al.*, 2003). Here, the EDH-type response is defined as the remaining proportion of bradykinin-induced vasorelaxation which is insensitive to L-NAME and indomethacin, the non-nitric oxide, non-cyclooxygenase products mediated response. Previous studies in porcine coronary microvessels and human mesenteric arteries have demonstrated that in the presence of L-NAME and indomethacin, bradykinin caused an endothelium-dependent hyperpolarization (Matoba *et al.*, 2003; Morikawa *et al.*, 2004). The present study demonstrated

that different gassing conditions had no effect on the bradykinin-induced vasorelaxation in the absence or presence of L-NAME and indomethacin. This suggests that the oxygen levels do not affect the bradykinin-induced EDH-type vasorelaxation in PCAs. However, under hyperoxic gassing conditions, the presence of Tiron significantly enhanced the bradykinin-induced vasorelaxation in the EDH-type response in PCAs from both male and female pigs. This observation is similar to previous studies using porcine coronary microvessels from male pigs and human mesenteric arteries from male and female subjects (Matoba *et al.*, 2003; Morikawa *et al.*, 2004). In Chapter 2, it was reported that the EDH-type response is greater in PCAs from female compared to male pigs. In this chapter, the presence of Tiron seems to have generated a greater enhancement in bradykinin-induced EDH-type vasorelaxation in PCAs from female pigs, 6.2-fold in females compared to 4.1-fold in males. The enhancement of the bradykinin response under hyperoxic gassing condition is not specific for Tiron as a previous study from another laboratory using iliac arteries from male rabbit has demonstrated that when gassed with 95% $O_2$/5% $CO_2$, other antioxidants such as ascorbic acid (AA) and tetrahydrobiopterin ($BH_4$) also enhanced the EDH-type relaxation induced by cyclopiazonic acid (CPA) and acetylcholine which was sensitive to catalase (Garry *et al.*, 2009). In the presence of AA and $BH_4$, measurement of the $H_2O_2$ level using Amplex Red assay demonstrated that there is an increase in the $H_2O_2$ level in the Krebs'-Henseleit solution (Garry *et al.*, 2009). In their study, vessels were pre-contracted with phenylephrine and relaxed with CPA and acetylcholine. Here, similar effects were seen using U46619 as the pre-

contracting agent and bradykinin as the endothelium-dependent vasorelaxant, suggesting that the effects seen are independent of agonists used.

Since the enhanced bradykinin-induced vasorelaxation in the presence of Tiron was thought to be due to production of $H_2O_2$ when gassed with 95% $O_2$/5% $CO_2$, the effects of different gassing conditions on $H_2O_2$-induced vasorelaxation were investigated. Different gassing conditions (95% $O_2$/5% $CO_2$ or 95% air/5% $CO_2$) had no effect on the $H_2O_2$-induced vasorelaxation. This suggests that the effects of exogenously applied $H_2O_2$ on PCAs are not affected by the oxygen level in the buffers and possibly that the superoxide generated in hyperoxic buffer does not interact with the exogenous $H_2O_2$.

Lastly, the effects of exogenously applied $H_2O_2$ (100 μM) on bradykinin-induced vasorelaxation were examined since Tiron generating $H_2O_2$ significantly enhanced the relaxation. This chapter demonstrates that the presence of $H_2O_2$ increased the potency of bradykinin slightly in the EDH-type responses but had no effect on the overall endothelium-dependent relaxation. Similar observations have been previously reported in iliac arteries from rabbit where presence of 100 μM $H_2O_2$ significantly enhanced the EDH-type responses induced by CPA and acetylcholine (Garry *et al.*, 2009). This is consistent with the results as discussed above where the presence of Tiron significantly enhanced the bradykinin-induced vasorelaxation in the presence of 95% $O_2$/5% $CO_2$ through the formation of $H_2O_2$ from superoxide generated in the Krebs'-Henseleit solution. In the study conducted by Garry *et al.* (2009), they suggested that the enhanced vasorelaxation to ACh in the presence of $H_2O_2$ is due to mobilisation of intracellular $Ca^{2+}$ from the endoplasmic

reticulum store through formation of $InsP_3$ where $H_2O_2$ sensitize $InsP_3$ receptor leading to increase in intracellular $Ca^{2+}$ release.

In summary, this chapter demonstrates that in the presence of 95% $O_2$ /5% $CO_2$, Tiron, a superoxide scavenger is likely to have converted superoxide generated in the Krebs'-Henseleit solution into $H_2O_2$ and enhances the bradykinin-induced vasorelaxation in both PCAs from male and female pigs (Figure 4.9). This provides strong evidence that hyperoxic gassing conditions could alter the environment, generating superoxide within the Krebs-Henseleit buffer, which may, in turn, influence the *in vitro* pharmacological responses.
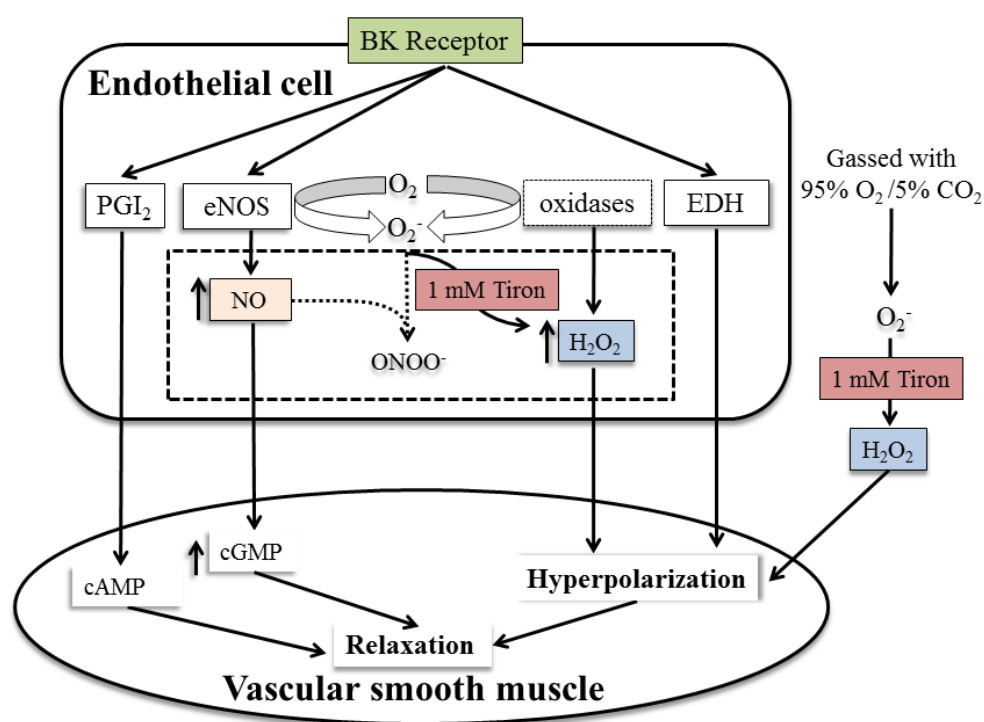


**Figure 4.9** Summary of results where hyperoxic gassing (95% $O_2$/5% $CO_2$) with 1 mM Tiron enhances bradykinin-induced endothelium-dependent and EDH-type relaxation through generation of hydrogen peroxide.

# *Chapter 5*

**Sex differences in the role of NADPH oxidases in endothelium-dependent vasorelaxation in porcine isolated coronary arteries**

## 5.1 Introduction

Reactive oxygen species (ROS), including superoxide and hydrogen peroxide ($H_2O_2$) have been reported to play a role in causing oxidative stress in cardiovascular diseases such as hypertension and atherosclerosis (Lacy *et al.*, 2000; Streeter *et al.*, 2013; Wind *et al.*, 2010a; Wingler *et al.*, 2011). In Chapter 2 and in a previous study, clear sex differences in endothelial function, where the EDH-type response plays a greater role in females compared to males have been reported (McCulloch & Randall, 1998). Other studies in young, healthy human subjects, rat aortae, and rat cerebral arteries demonstrated that males exhibit greater oxidative stress compared to females (Borras *et al.*, 2003; Brandes & Mugge, 1997; Ide *et al.*, 2002; Miller *et al.*, 2007). In rat aortae and cerebral arteries, NADPH-stimulated superoxide generated in males was significantly higher compared to females (Brandes & Mugge, 1997; Miller *et al.*, 2007).

Sex differences in the role of endogenous $H_2O_2$ on endothelium-dependent vasorelaxation have been demonstrated in Chapter 2. Therefore, this chapter tested the hypothesis that the sex differences in endothelial function could be related to vascular ROS generated by Nox as other studies have reported that $H_2O_2$ is a factor for EDH-type response in human, mouse and porcine arteries (Matoba *et al.*, 2002; Matoba *et al.*, 2003; Matoba *et al.*, 2000; Miura *et al.*, 2003). In previous studies, apocynin and Diphenyliodonium chloride (DPI) have been widely used as Nox inhibitors. However, there is increasing evidence that these inhibitors are non-selective (Miller *et al.*, 2007; Wind *et al.*, 2010b; Wingler *et al.*, 2011). Therefore, newer more selective Nox inhibitors, ML-171, a phenothiazine derivative (Gianni *et al.*, 2010) and

VAS2870, a derivative of triazolopyrimidine (Kleinschnitz *et al.*, 2010; Wind *et al.*, 2010a) were used in this chapter to examine the role of Nox-generated ROS in the coronary artery.

No previous study has specifically examined whether sex differences influence the functional role of Nox using small molecule Nox inhibitors in coronary artery. Therefore, the aim of this chapter was to compare the role of vascular Nox as a source of ROS in porcine isolated coronary arteries from male and female pigs using selective Nox inhibitors, ML-171(Gianni *et al.*, 2010) and VAS2870 (Kleinschnitz *et al.*, 2010; Wind *et al.*, 2010a; Wind *et al.*, 2010b). Activity and protein expression of Nox enzymes were also investigated in this chapter. This chapter demonstrated that Nox-generated ROS play a role in the EDH-type responses in PCAs from male but not female pigs and this could be attributed to the higher expression of Nox1 and Nox2 proteins in males.

## 5.2 Materials and methods

### 5.2.1 Preparation of rings of distal PCAs

Tissues were set up as previously described in Chapter 2.

### 5.2.2 Wire myography

As previously described in Chapter 2, after 30 min of equilibration, contractile responses to 60 mM KCl were determined twice. The vascular tone was then raised to about $50 - 90\%$ of the second KCl contraction tone by the addition of the thromboxane $A_2$ mimetic, U46619 (0.3 pM $-$ 100 nM). Once stable tone was achieved, concentration-response curves to bradykinin, an endothelium-dependent vasorelaxant (0.1 nM $-$ 1 μM), forskolin, a cell permeable adenylyl cyclase activator (0.1 nM $-$ 1 μM) or pinacidil, a $K_{ATP}$ channel activator (1 nM $-$ 30 μM) were constructed to investigate the effects of NADPH oxidase inhibitor on relaxation mediated through other pathways. In some experiments, the effects of NADPH oxidase inhibitors on U46619$-$induced tone (0.1 fM $-$ 1 μM) were examined. To examine the non-nitric oxide and non-cyclooxygenase products relaxation pathway, $N^G$-nitro-L-arginine methyl ester (L-NAME) (300 μM) was used to inhibit the synthesis of NO and indomethacin (10 μM) was used to inhibit the synthesis of prostanoids. Diphenyliodonium chloride (DPI) (10 μM) (Fleming *et al.*, 2001) was used as a non-selective NADPH oxidase inhibitor while 2-acetylphenothiazine (ML-171) (10 μM or 100 μM) (Gianni *et al.*, 2010) and VAS2870 (10 μM) (Kleinschnitz *et al.*, 2010) were used as selective NADPH oxidase inhibitors. Allopurinol (30 μM) (Qamirani *et al.*, 2005) was used as a xanthine oxidase inhibitor. To examine the role of cytochrome P450 (CYP450) enzymes on bradykinin-induced vasorelaxation, proadifen hydrochloride (10 μM) (Martinkova *et al.*, 2012) was used to inhibit

CYP450, 1-aminobenzotriazole (1-ABT) (Martinkova *et al.*, 2012) (100 μM) was used as a suicide inhibitor of CYP450 and sulfaphenazole (10 μM) (Fleming *et al.*, 2001; Matoba *et al.*, 2003) was used as a specific CYP450 inhibitor. All inhibitors were incubated with the vessels for 1 h before pre-contraction with U46619.

The level of tone achieved with U46619 was the same under all conditions except for in the presence of proadifen (with L-NAME and indomethacin) in females where a significantly lower U46619-induced tone ($P<0.05$) was achieved (Table 5.1B). The concentration of U46619 required to achieve similar level of tone to the control was significantly higher in the presence of 100 μM ML-171 in both male (only in the absence of L-NAME and indomethacin) ($P<0.01$) and females (in the absence and presence of L-NAME and indomethacin) ($P<0.05$) (Table 5.1A). The concentration of U46619 required was also significantly higher in the presence of L-NAME and indomethacin with 1-ABT or proadifen in males ($P<0.05$) (Table 5.1A). The presence of VAS2870, allopurinol and sulfaphenazole had no effect on either the level of tone or the concentration of U46619 required.

| A Concentration of U46619 (nM) | | Control | Inhibitor | L-NAME, indomethacin | |
|---|---|---|---|---|---|
| | | | | Control | Inhibitor |
| ML-171 | Male | 8.67 ± 1.31 | 17.8 ± 2.2** | 15.2 ± 1.53 | 20.2 ± 1.685 |
| | Female | 10.1 ± 1.5 | 16.6 ± 1.9* | 15.9 ± 1.9 | 26.8 ± 1.3** |
| VAS2870 | Male | 0.14 ± 0.09 | 0.16 ± 0.10 | 12.8 ± 3.4 | 15.2 ± 3.7 |
| | Female | 0.30 ± 0.03 | 0.39 ± 0.06 | 7.50 ± 1.11 | 7.92 ± 1.20 |
| Allopurinol | Male | | | 14.1 ± 2.1 | 15.2 ± 3.2 |
| | Female | | | 10.0 ± 1.7 | 11.0 ± 1.3 |
| Proadifen | Male | | | 6.69 ± 0.70 | 33.1 ± 10.3* |
| | Female | | | 3.14 ± 2.40 | 23.7 ± 10.3 |
| 1-ABT | Male | | | 7.4 ± 1.0 | 14.2 ± 1.9* |
| Sulfaphenazole | Male | | | 12.1 ± 1.0 | 14.2 ± 1.0 |
| | Female | | | 10.6 ± 1.6 | 10.6 ± 0.4 |

**Table 5.1** Summary of (A) U46619 concentration used (nM) in the absence or presence of 300 μM L-NAME, 10 μM indomethacin with or without 100 μM ML-171, 10 μM VAS2870, 30 μM allopurinol, 10μM proadifen, 100 μM 1-ABT or 10 μM sulfaphenazole in porcine coronary arteries from male and female pigs. Data are expressed as mean ± S.E.M. of 5-8 experiments. *P<0.05, **P<0.01, 2-tailed, paired Student's *t*-test.

| **B** U46619-induced tone (% KCl response) | | Control | Inhibitor | L-NAME, indomethacin | |
|---|---|---|---|---|---|
| | | Control | Inhibitor | Control | Inhibitor |
| ML-171 | Male | 79.0 ± 7.9 | 66.5 ± 7.3 | 65.8 ± 6.0 | 65.0 ± 6.1 |
| | Female | 71.3 ± 4.8 | 74.6 ± 6.7 | 53.3 ± 0.6 | 52.3 ± 0.8 |
| VAS2870 | Male | 64.0 ± 4.3 | 60.0 ± 7.0 | 58.8 ± 3.0 | 60.8 ± 7.7 |
| | Female | 69.2 ± 7.5 | 60.0 ± 4.5 | 64.8 ± 6.4 | 62.0 ± 6.3 |
| Allopurinol | Male | | | 53.8 ± 1.4 | 55.2 ± 1.1 |
| | Female | | | 52.8 ± 1.1 | 55.1 ± 2.0 |
| Proadifen | Male | | | 57.7 ± 3.1 | 51.7 ± 0.6 |
| | Female | | | 67.2 ± 5.9 | 51.7 ± 0.6* |
| 1-ABT | Male | | | 57.1 ± 1.6 | 55.6 ± 3.5 |
| Sulfaphenazole | Male | | | 66.1 ± 5.6 | 58.0 ± 2.6 |
| | Female | | | 63.4 ± 7.3 | 59.8 ± 4.7 |

**Table 5.1** Summary of (B) the level of U46619-induced tone expressed in percentage to second KCl-induced tone in the absence or presence of 300 μM L-NAME, 10 μM indomethacin with or without 100 μM ML-171, 10 μM VAS2870, 30 μM allopurinol, 10μM proadifen, 100 μM 1-ABT or 10 μM sulfaphenazole in porcine coronary arteries from male and female pigs. Data are expressed as mean ± S.E.M. of 5-8 experiments. *P<0.05, 2-tailed, paired Student's *t*-test.

### 5.2.3 Measurement of NADPH oxidase activity

NADPH oxidase activity of PCAs was measured using lucigenin-enhanced chemiluminescence method (adapted from Wind *et. al.,* 2010 and Guzik & Channon, 2005). Briefly, fresh PCAs were finely dissected and cut into segments of ~2 cm then gassed with 95% $O_2$/5% $CO_2$ at 37°C for 1 h in the myograph. Segments were then stored at -80°C until biochemical determinations were carried out. PCAs were homogenized in Krebs'-HEPES buffer (pH 7.4) consisting 99 mM NaCl, 4.7 mM KCl, 1.9 mM $CaCl_2$, 1.2 mM $MgSO_4$, 1 mM $KH_2PO_4$, 25 mM $NaHCO_3$, 11.1 mM glucose, 20 mM HEPES and protease inhibitor cocktail Set I (Calbiochem, VWR International Ltd, Lutterworth, Leicestershire, UK) (Guzik & Channon, 2005) in a glass-glass homogenizer. Homogenates were then centrifuged at 1,000x g for 10 min at 4°C to remove cell debris. Protein concentrations of the supernatants were determined by the Bradford method as described in Chapter 2. In duplicate, 50 µg of protein homogenates were incubated at 37°C for 20 min in the absence or presence of 300 µM L-NAME, 10 µM indomethacin, 10 µM DPI, 100 µM ML-171 or 10 µM VAS2870 with a final concentration of 5 µM lucigenin. 100 µM NADPH substrate (total volume of 100 µL) was added into each well to start the reaction and samples were allowed to equilibrate in a semi-dark environment for 5 min. Photon emission was measured using TopCount NXT (PerkinElmer, Cambridge, Cambridgeshire, UK) set to single photon-counting mode for 10 s per well. Readings were divided by background single photon counts. Mean chemiluminescence readings obtained were divided by the background single photon counts (in the absence of tissue homogenates) to

normalize the results. Results were expressed in basal fold to the background photon count.

## 5.2.4 Western Blotting

Western Blot studies were carried out to determine the relative expression levels of Nox1, 2 and 4 proteins in PCAs from male and female pigs. Similar to Chapter 2, the method described below is the result of substantial method development including different batches of antibodies and different lysis buffers. Results of these developments are included in Appendix C for future reference. Methods were as described in Chapter 2. Samples in this chapter were homogenised on ice in lysis buffer (20 mM Tris, 1 mM EGTA, 320 mM sucrose, 0.1% Triton X100, 1 mM sodium fluoride, 10 mM sodium β-glycerophosphate, pH 7.6) containing protease inhibitor cocktail Set I (Calbiochem, VWR International Ltd, Lutterworth, Leicestershire, UK) followed by centrifugation at 3,000x g for 5 min at 4°C. Supernatants of the samples were then solubilised in 6x solubilisation buffer and diluted to 1 mg/ml of protein with 1x solubilisation buffer

15 or 20 μg of PCAs samples, 15 μg HepG2 cell lysate (positive control for Nox1 protein) or 15 μg pig brain lysate (positive control for Nox2 and 4 protein) were used in this chapter. The primary antibodies used in this chapter are rabbit polyclonal anti-NOX1 antibody (ab137603 Abcam®, Cambridge, UK) (1:500), rabbit polyclonal anti-gp91-phox antibody (sc-20782 Santa Cruz Biotechnology, Insight Biotechnology Ltd, Wembley, Middlesex, UK) (1:500), rabbit monoclonal anti-NOX4 [UOTR1B492] antibody

(ab109225 Abcam®) (1:1000) and mouse monoclonal anti-β-actin antibody (A2228 Sigma-Aldrich) (1:100,000). The secondary antibodies used in this chapter are IRDye 800CW Goat anti-rabbit IgG (1:10,000) for anti-rabbit antibody and IRDye® 680LT Goat anti-mouse IgG (1:10 000) (LI-COR Biosciences, Cambridge, UK) for anti-mouse antibody. The immunoblot was then visualised using a LI-COR Odyssey Infrared Imaging Scanner. Densities of bands were determined using Image Studio (Version 3.1 LI-COR Biosciences, Cambridge, UK).

### 5.2.5 Statistical analysis

Data for functional studies were presented and analysed as described in Chapter 2. In data where the $R_{max}$ was not achieved, data were analysed using the response generated at the highest concentration of vasorelaxant. NADPH oxidase activity assay was analysed using one-way ANOVA followed by a Dunnett's multiple comparison test against the control. For Western blot, expression levels of Nox1, 2 and 4 proteins in PCAs from male and female pigs were normalised to β-actin level then analysed using 2-tailed, unpaired Mann-Whitney U-test.

### 5.2.6 Drugs and chemicals

All drugs were purchased from Sigma-Aldrich (Poole, Dorset, UK) unless otherwise indicated. ML-171, DPI and forskolin were purchased from Tocris Bioscience (Bristol, UK) and VAS2870 from VWR (Nottingham, UK). All drugs were dissolved in distilled water except for indomethacin which was

dissolved in absolute ethanol and ML-171, DPI, VAS2870, allopurinol, pinacidil and forskolin were dissolved in DMSO. Stock solutions of bradykinin, pinacidil, forskolin and U46619 thromboxane $A_2$-agonist were made to 10 mM. All further dilutions of the stock solutions were made using distilled water.

## 5.3 Results

### 5.3.1 The effects of DPI and ML-171 on bradykinin-induced vasorelaxation in PCAs from male and female pigs

In PCAs from female pigs, the presence of 10 μM DPI, a non-selective NADPH oxidase inhibitor, had no effect on bradykinin-induced vasorelaxation ($pEC_{50}$ = 7.86 ± 0.11; control, 7.63 ± 0.12; DPI, $n$=8-9) (Figure 5.1A). Similarly neither 10 μM nor 100 μM ML-171 affected the bradykinin-induced vasorelaxation (Figure 5.1A). On the other hand, in PCAs from male pigs, treatment with 10 μM DPI significantly shifted the curve 2.8-fold to the right ($P$<0.01), but did not affect the $R_{max}$ such that in controls $R_{max}$ was 103 ± 4% ($pEC_{50}$ = 8.00 ± 0.07, $n$=6) and after treatment with DPI was 93.2 ± 4.9% ($pEC_{50}$ = 7.55 ± 0.08, $n$=6) (Figure 5.1B). Treatment with 100 μM ML-171 had no effect on the $R_{max}$ or $EC_{50}$ values where the $R_{max}$ = 95.7 ± 4.1% ($pEC_{50}$ = 8.27 ± 0.09, $n$=6) compared to the controls (Figure 5.1B).
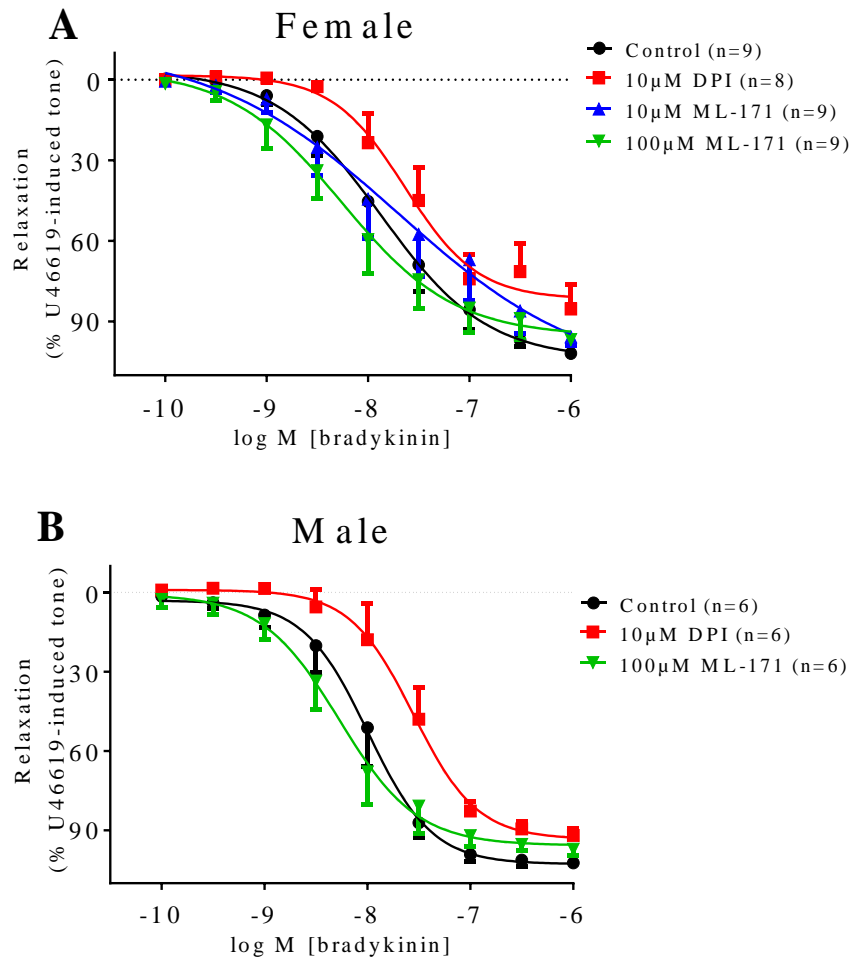
**Figure 5.1** Log concentration-response curves for the vasorelaxant effects of bradykinin in the presence of 10 μM DPI, 10 μM or 100 μM ML-171 in U46619 pre-contracted porcine coronary arteries from (A) female or (B) male pigs. In PCAs from male pigs, treatment with 10 μM DPI significantly shifted the curve 2.8-fold to the right (P<0.01; one-way ANOVA followed by Bonferroni's *post hoc* test). Data are expressed as a percentage change from U46619-induced tone and are mean ± S.E.M. of 6-9 experiments.

## 5.3.2 The effects of DPI and ML-171 in the presence of L-NAME, indomethacin on bradykinin-induced vasorelaxation in PCAs from male and female pigs

In the presence of L-NAME and indomethacin, again treatment with 10 μM DPI did not affect the bradykinin-induced vasorelaxation in PCAs from female pigs such that the $R_{max}$ in the presence of L-NAME and indomethacin was 73.3 ± 6.3% ($pEC_{50}$ = 7.72 ± 0.15, $n$=6) compared to a response of 78.6 ± 8.0% ($pEC_{50}$ = 7.80 ± 0.19, $n$=6) in the presence of 10 μM DPI (Figure 5.2A). Similarly, treatment with 100 μM ML-171 in the presence of L-NAME and indomethacin did not affect the bradykinin-induced vasorelaxation producing an $R_{max}$ of 68.2 ± 8.9% ($pEC_{50}$ = 7.90 ± 0.25, $n$=6) (Figure 5.2A).

Conversely, in PCAs from male pigs, treatment with 10 μM DPI or 100 μM ML-171 in the presence of L-NAME and indomethacin significantly shifted the curve 2.5-fold and 3.2-fold to the left ($P<0.0001$) respectively with no effect on the $R_{max}$ values such that the $R_{max}$ in the presence of L-NAME and indomethacin was 88.3 ± 5.16% ($pEC_{50}$ = 7.43 ± 0.09, $n$=5) and additional treatment with 10 μM DPI produced an $R_{max}$ of 83.5 ± 5.7% ($pEC_{50}$ = 7.83 ± 0.12, $n$=5) while 100 μM ML-171 was 92.4 ± 4.0% ($pEC_{50}$ = 7.93 ± 0.08, $n$=5) (Figure 5.2B).
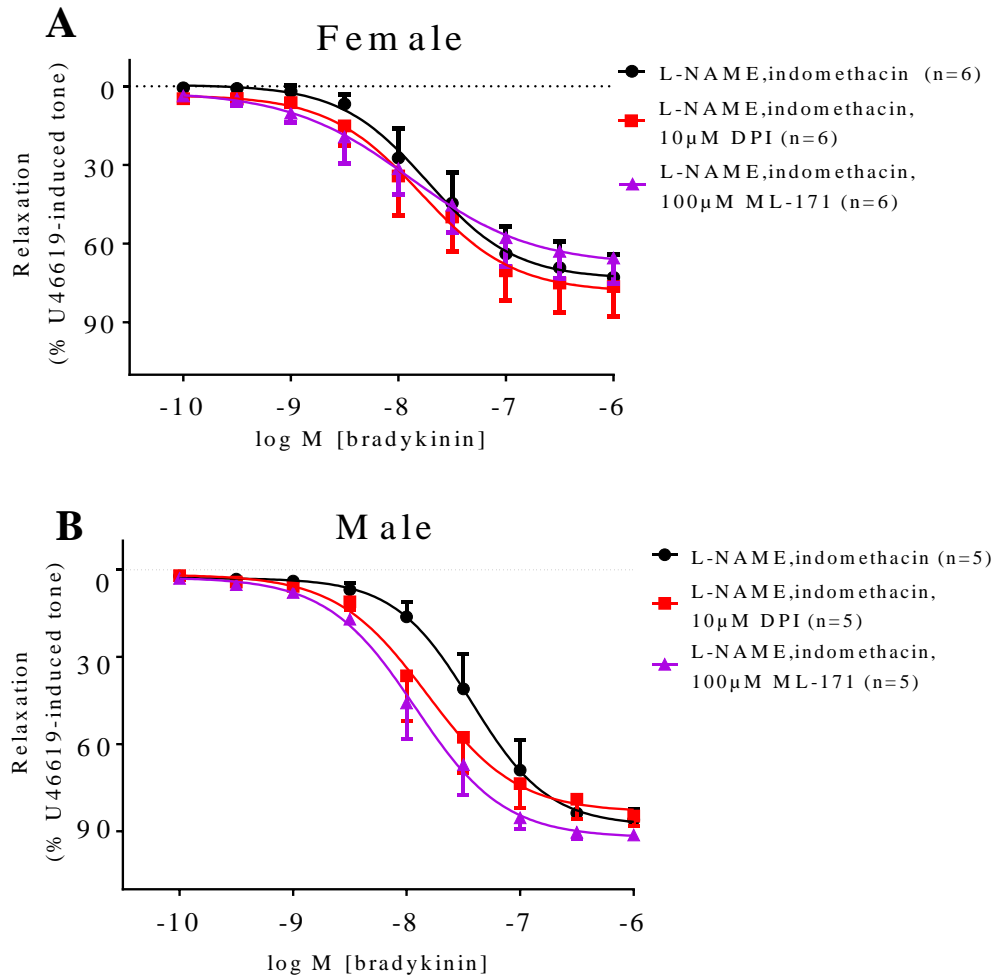
**Figure 5.2** Log concentration-response curves for the vasorelaxant effects of bradykinin in the presence 300 μM L-NAME and 10 μM indomethacin with or without 10 μM DPI or 100 μM ML-171 in U46619 pre-contracted porcine coronary arteries from (A) female and (B) male pigs. In PCAs from male pigs, presence of 10μM DPI or 100μM ML-171 in L-NAME and indomethacin significantly shifted the bradykinin-induced response curve 2.5-fold and 3.2-fold to the left respectively (P<0.0001; one-way ANOVA followed by Bonferroni's *post hoc* test). Data are expressed as a percentage change from U46619-induced tone and are mean ± S.E.M. of 5-6 experiments.

## 5.3.3 The effects of L-NAME, indomethacin and ML-171 on responses to endothelium-independent vasorelaxants (forskolin) in PCAs from male pigs

To examine if the enhanced bradykinin-induced vasorelaxation effect in the presence of ML-171 in males is selective for bradykinin, or if it is due to an effect on the pre-contractile response, the effects of forskolin, a cell permeable adenylyl cyclase activator were examined. In PCAs from male pigs, treatment with 100 μM ML-171 in the presence of L-NAME and indomethacin did not affect the forskolin-induced vasorelaxation such that $R_{max}$ was $128 \pm 18\%$ ($pEC_{50} = 7.64 \pm 0.22$, $n=8$) compared to a response of $121 \pm 15\%$ ($pEC_{50} = 8.13 \pm 0.25$, $n=8$) in the presence of 100 μM ML-171 (Figure 5.3).
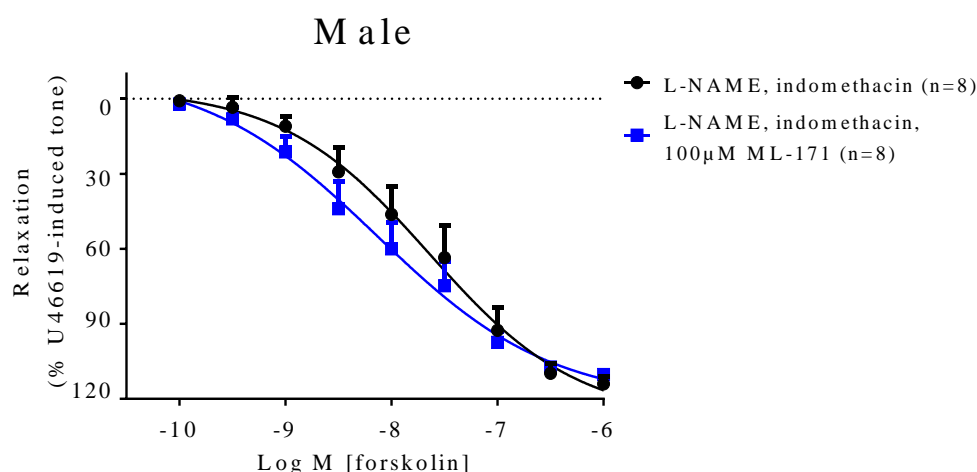


**Figure 5.3** Log concentration-response curves for the vasorelaxant effects of forskolin in the presence of 300 μM L-NAME, 10 μM indomethacin with or without 100 μM ML-171 in U46619 pre-contracted porcine coronary arteries from male pigs. Data are expressed as a percentage change from U46619-induced tone and are mean $\pm$ S.E.M. of 8 experiments.

**5.3.4 The effects of L-NAME, indomethacin and ML-171 on responses to endothelium-independent vasorelaxants (pinacidil) in PCAs from male pigs**

Treatment with 100 μM ML-171 in the presence of L-NAME and indomethacin did not affect the $R_{max}$ or $EC_{50}$ values of the pinacidil-induced vasorelaxation such that the $R_{max}$ was 131 ± 8% ($pEC_{50} = 6.12 ± 0.09$, $n=9$) in the presence of L-NAME, indomethacin and additional presence of ML-171 produced an $R_{max}$ of 122 ± 8% ($pEC_{50} = 6.46 ± 0.11$, $n=9$) (Figure 5.4). When the pinacidil-induced vasorelaxation was analysed at individual concentrations, the presence of ML-171 significantly enhanced the relaxation at 3 - 300 nM of pinacidil ($P<0.05$) (Figure 5.4).
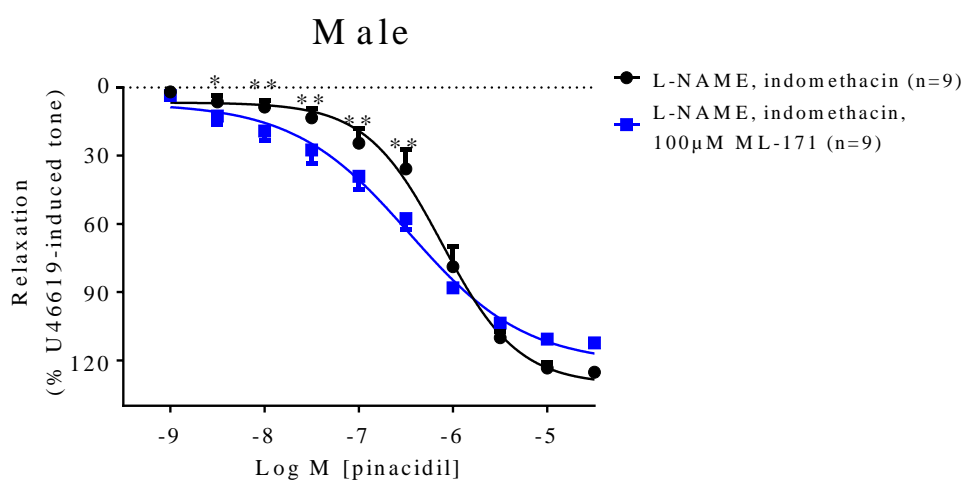


**Figure 5.4** Log concentration-response curves for the vasorelaxant effects of pinacidil in the presence of 300 μM L-NAME and 10 μM indomethacin with or without 100 μM ML-171 in U46619 pre-contracted porcine coronary arteries from male pigs. Data are expressed as a percentage change from U46619-induced tone and are mean ± S.E.M. of 9 experiments. *P<0.05 and **P<0.01; 2-tailed, paired Student's *t*-test.

**5.3.5 The effects of L-NAME, indomethacin and ML-171 on U46619-induced contraction in PCAs from male and female pigs with or without endothelium**

In PCAs from male pigs with intact endothelium, as the contraction to U46619 curves did not fit to a sigmoidal curve, the maximum contractions were constrained to 145% and data were analysed based on each individual U46619 concentrations (Figure 5.5A). Treatment with ML-171 significantly reduced the U46619-induced contractions (P<0.05) (Figure 5.5A). In endothelium-denuded PCAs from male pigs, the presence of ML-171 significantly reduced the maximum contraction induced by U46619 (P<0.01) from $143 \pm 4\%$ ($pEC_{50}$ $= 7.86 \pm 0.06$, $n$=6) in the presence of L-NAME and indomethacin to $125 \pm 2\%$ ($pEC_{50}$ $= 7.54 \pm 0.02$, $n$=6) with the additional presence of ML-171 (Figure 5.5B). The presence of ML-171 significantly shifted the curve 2.1-fold to the right (P<0.05) (Figure 5.5B).

In PCAs from female pigs with intact endothelium, treatment with ML-171 did not affect the maximum contraction to U46619, but significantly shifted the curve 2.6-fold to the right (P<0.01) ($pEC_{50} = 8.1 \pm 0.07$; without ML-171 compared to $7.68 \pm 0.04$; with ML-171 $n$=6) (Figure 5.6A). In endothelium-denuded vessels in PCAs from female pigs, treatment with ML-171 in the presence of L-NAME and indomethacin significantly reduced the maximum U46619-induced contraction (P<0.05) reducing the contraction from $139 \pm 2\%$ in the presence of L-NAME and indomethacin to $128 \pm 3\%$ with the additional presence of ML-171 (Figure 5.6B). The curve was significantly shifted 3.2-fold to the right in the presence of ML-171 ($pEC_{50} = 8.11 \pm 0.03$ compared to $7.61 \pm 0.04$, $n$=6) (P<0.001) (Figure 5.6B).

184

**A** Male: endothelium-intact

Top curve constraint to 145%

- L-NAME,indomethacin (n=6)
- L-NAME,indomethacin, 100µM ML-171 (n=6)

Contraction (% KCl)

Log M [U46619]

**B** Male: endothelium-denuded

- L-NAME,indomethacin (n=6)
- L-NAME,indomethacin, 100µM ML-171 (n=6)

Contraction (% KCl)

Log M [U46619]
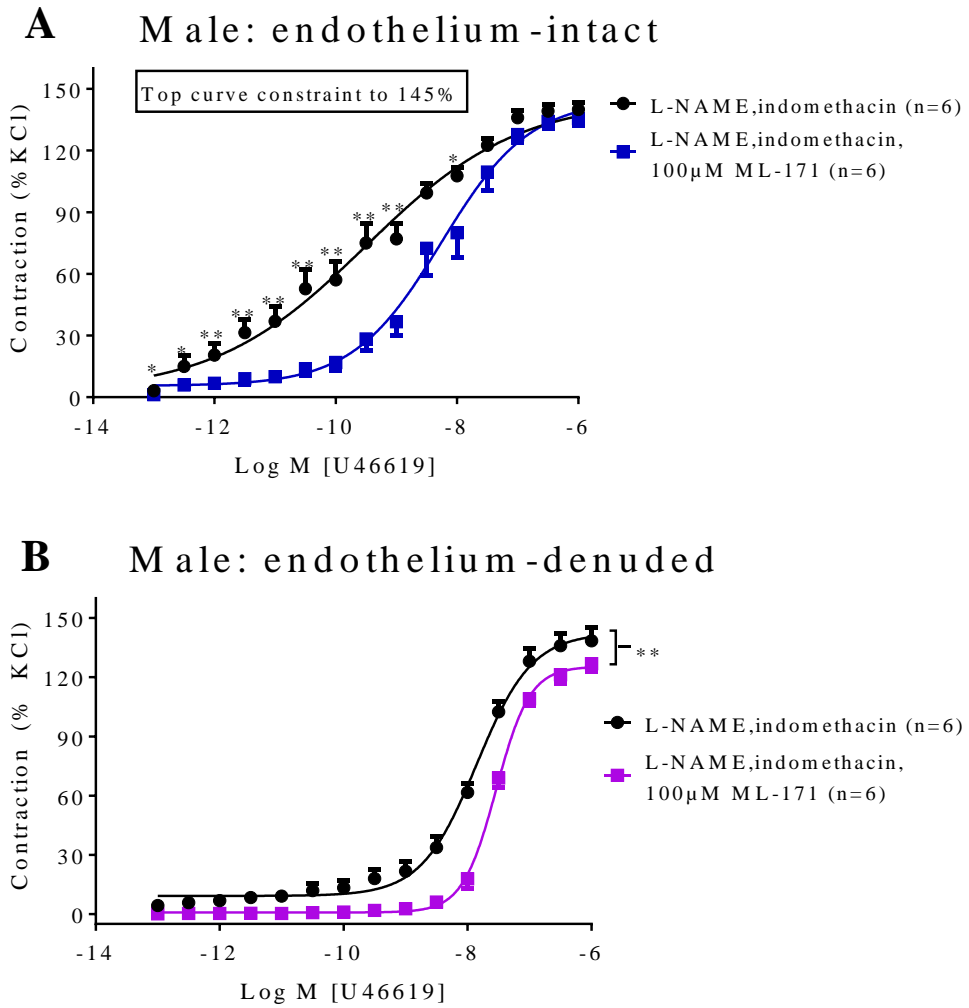
**Figure 5.5** Log concentration-response curves for the contractile effects of U46619 in the presence of 300 μM L-NAME and 10 μM indomethacin with or without 100 μM ML-171 in porcine coronary arteries from male pigs with (A) intact endothelium or (B) denuded endothelium. (A) In PCAs from male pigs, contraction to U46619 curves did not fit in to a sigmoidal curve therefore the maximum contraction were constraint to 145% and data were analysed based on each individual point of U46619 concentration. Data are expressed as a percentage change from the second KCl-induced tone and are mean ± S.E.M. of 6 experiments. *P<0.05 and **P<0.01; 2-tailed, paired Student's *t*-test.
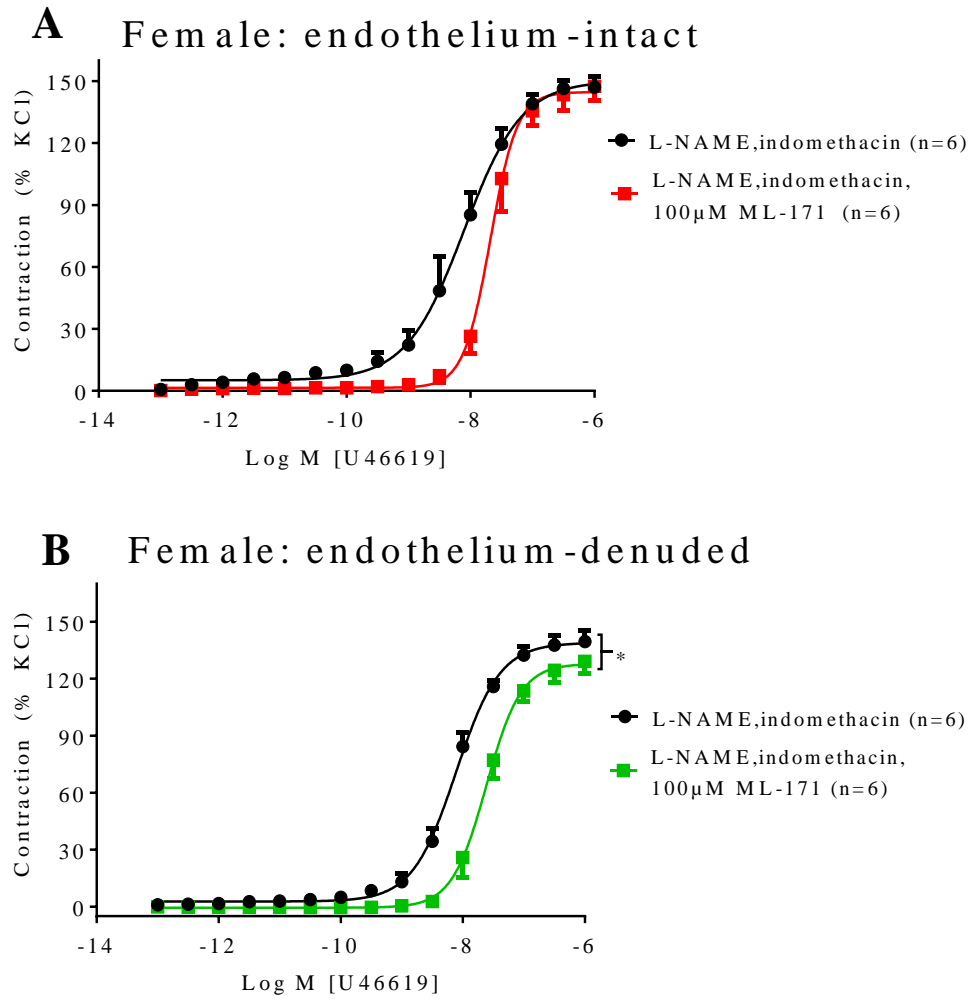
**Figure 5.6** Log concentration-response curves for the contractile effects of U46619 in the presence of 300 μM L-NAME and 10 μM indomethacin with or without 100 μM ML-171 in porcine coronary arteries from female pigs with (A) intact endothelium or (B) denuded endothelium. Data are expressed as a percentage change from the second KCl-induced tone and are mean ± S.E.M. of 6 experiments. *P<0.05; 2-tailed, paired Student's *t*-test.

### 5.3.6 The effects of VAS2870 on bradykinin-induced vasorelaxation in PCAs from male and female pigs

In PCAs from male pigs, using a different Nox inhibitor 10 μM VAS2870 had no effect on the bradykinin-induced vasorelaxation such that under control conditions the $R_{max}$ was 114 ± 3% ($pEC_{50}$ = 8.79 ± 0.05, $n$=5) compared to a response of 108 ± 2% ($pEC_{50}$ = 8.63 ± 0.04, $n$=5) in the presence of 10 μM VAS2870 (Figure 5.7A).

Similarly in PCAs from female pigs VAS2870 did not affect the bradykinin-induced vasorelaxation such that the $R_{max}$ was 99.9 ± 3.7% ($pEC_{50}$ = 8.26 ± 0.08, $n$=6) under control conditions and $R_{max}$ of 92.9 ± 4.3%, $pEC_{50}$ = 8.30 ± 0.10, $n$=6) in the presence of VAS2870 (Figure 5.7B).

### 5.3.7 The effects of VAS2870 in the presence L-NAME and indomethacin on bradykinin-induced vasorelaxation in PCAs from male and female pigs

In PCAs from male pigs, treatment with 10 μM VAS2870 in the presence of L-NAME and indomethacin significantly inhibited the bradykinin-induced vasorelaxation such that the $R_{max}$ was 76.3 ± 2.7% ($pEC_{50}$ = 7.85 ± 0.07, $n$=6) under control conditions and in the presence of VAS2870 the $R_{max}$ was 54.3 ± 4.1% ($pEC_{50}$ = 8.09 ± 0.20, $n$=6) (P<0.05) (Figure 5.8A).

On the other hand, in PCAs from female pigs, treatment with VAS2870 had no effect on the bradykinin-induced vasorelaxation in the presence of L-NAME and indomethacin (Figure 5.8B).
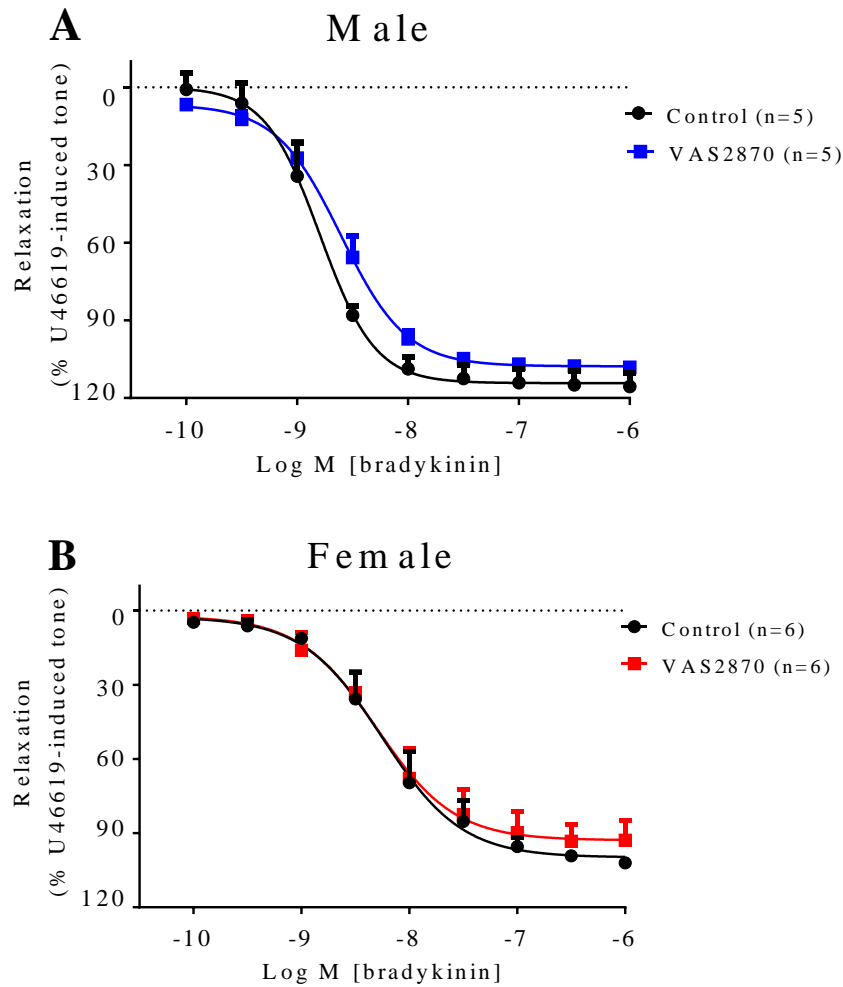
**Figure 5.7** Log concentration-response curves for the vasorelaxant effects of bradykinin in the presence or absence of 10 μM VAS2870 in U46619 pre-contracted porcine coronary arteries from (A) male or (B) female pigs. Data are expressed as a percentage change from U46619-induced tone and are mean ± S.E.M. of 5-6 experiments.
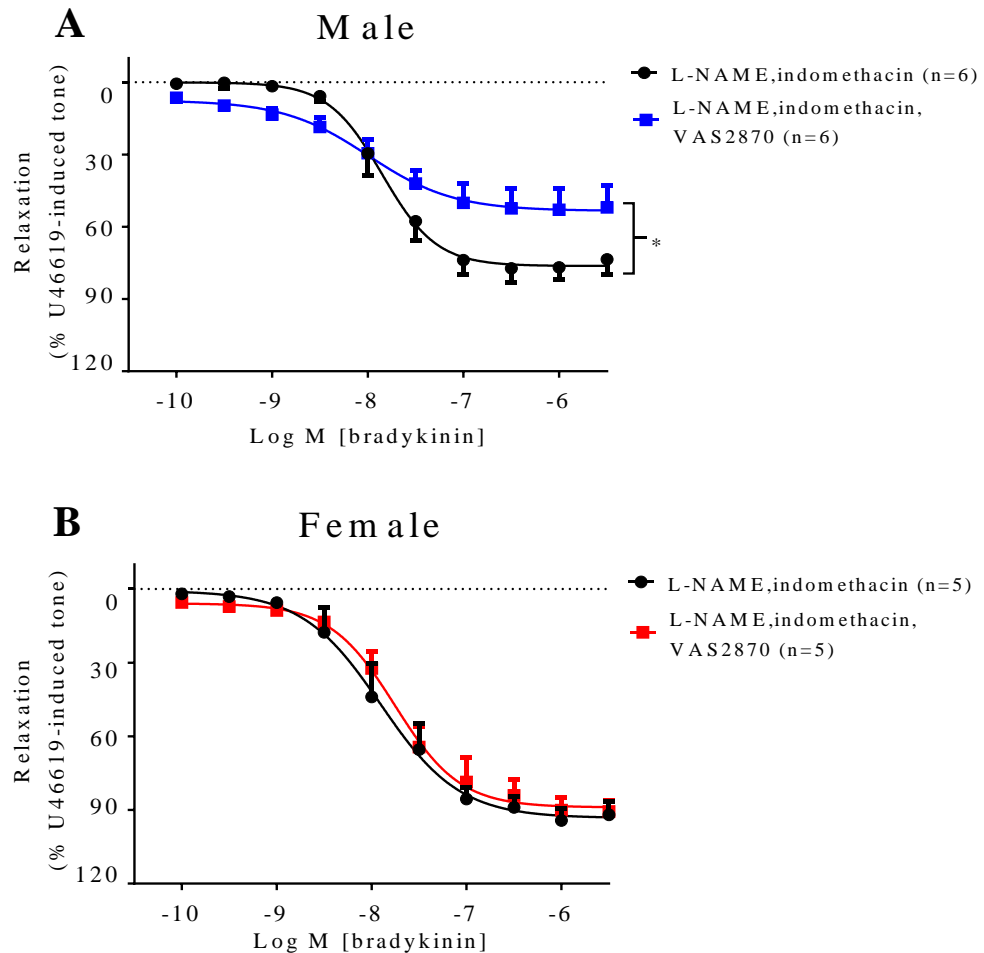
**Figure 5.8** Log concentration-response curves for the vasorelaxant effects of bradykinin in the presence 300 μM L-NAME and 10 μM indomethacin with or without 10 μM VAS2870 in U46619 pre-contracted porcine coronary arteries from (A) male or (B) female pigs. Data are expressed as a percentage change from U46619-induced tone and are mean ± S.E.M. of 5-6 experiments. *P<0.05; 2-tailed, paired Student's *t*-test.

**5.3.8 The effects of VAS2870 in the presence L-NAME and indomethacin on U46619-induced contraction in PCAs from male pigs**

Further experiments to examine the effects of VAS2870 on U46619-induced contraction showed that VAS2870 had no effect on the U46619-induced contraction producing an $R_{max}$ of $130 \pm 8\%$ ($pEC_{50} = 7.63 \pm 0.16$, $n=6$) in the presence of L-NAME and indomethacin and an $R_{max}$ of $135 \pm 8\%$ ($pEC_{50} = 8.35 \pm 0.16$, $n=6$) in the additional presence of VAS2870 (Figure 5.9).
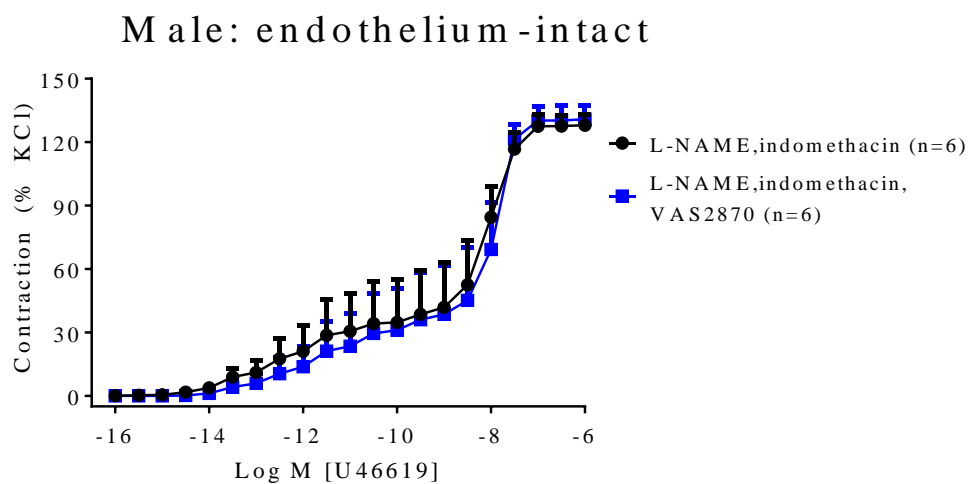


**Figure 5.9** Log concentration-response curves for the contractile effects of U46619 in the presence of 300 μM L-NAME and 10 μM indomethacin with or without 10 μM VAS2870 in porcine coronary arteries from male pigs with intact endothelium. Data are expressed as a percentage change from the second KCl-induced tone and are mean $\pm$ S.E.M. of 6 experiments.

**5.3.9 The effects of L-NAME, indomethacin and xanthine oxidase inhibitor (allopurinol) on bradykinin-induced vasorelaxation in PCAs from male and female pigs**

As reactive oxygen species are also generated by xanthine oxidase, the effects of 30 μM allopurinol, a xanthine oxidase inhibitor were examined in the presence of L-NAME and indomethacin on bradykinin-induced vasorelaxation in PCAs from male and female pigs. Here, allopurinol had no effect on the $R_{max}$ or $EC_{50}$ (Table 5.2) of the bradykinin-induced EDH-type vasorelaxation in either PCAs from male or female pigs (Figure 5.10A & B).

| Gender | L-NAME, indomethacin | Maximal relaxation (%), $pEC_{50}$ | | $n$ |
|---|---|---|---|---|
| | | **Control** | **Inhibitor** | |
| **Male** | **30 μM allopurinol** | 83.7 ± 6.5, 7.75 ± 0.13 | 91.8 ± 8.5, 7.34 ± 0.13 | 8 |
| **Female** | | 88.2 ± 8.9, 7.42 ± 0.17 | 83.5 ± 16.7, 7.06 ± 0.30 | 6 |
| **Male** | **100 μM 1-ABT** | 79.2 ± 5.6, 7.73 ± 0.12 | 68.8 ± 6.8, 7.84 ± 0.17 | 5 |
| **Male** | **10 μM sulfaphenazole** | 72.7 ± 4.4, 7.73 ± 0.10 | 85.3 ± 4.4, 7.94 ± 0.10 | 9 |
| **Female** | | 99.6 ± 6.6, 7.53 ± 0.11 | 98.5 ± 6.4, 7.85 ± 0.11 | 5 |

**Table 5.2** Summary of the effects of different CYP450 inhibitors (100 μM 1-ABT or 10 μM sulfaphenazole) or xanthine oxidase (30 μM allopurinol) in the presence of 300 μM L-NAME and 10 μM indomethacin on the maximal relaxations and $pEC_{50}$ values of the bradykinin-induced vasorelaxation in U46619 precontracted PCAs from male and female pigs.
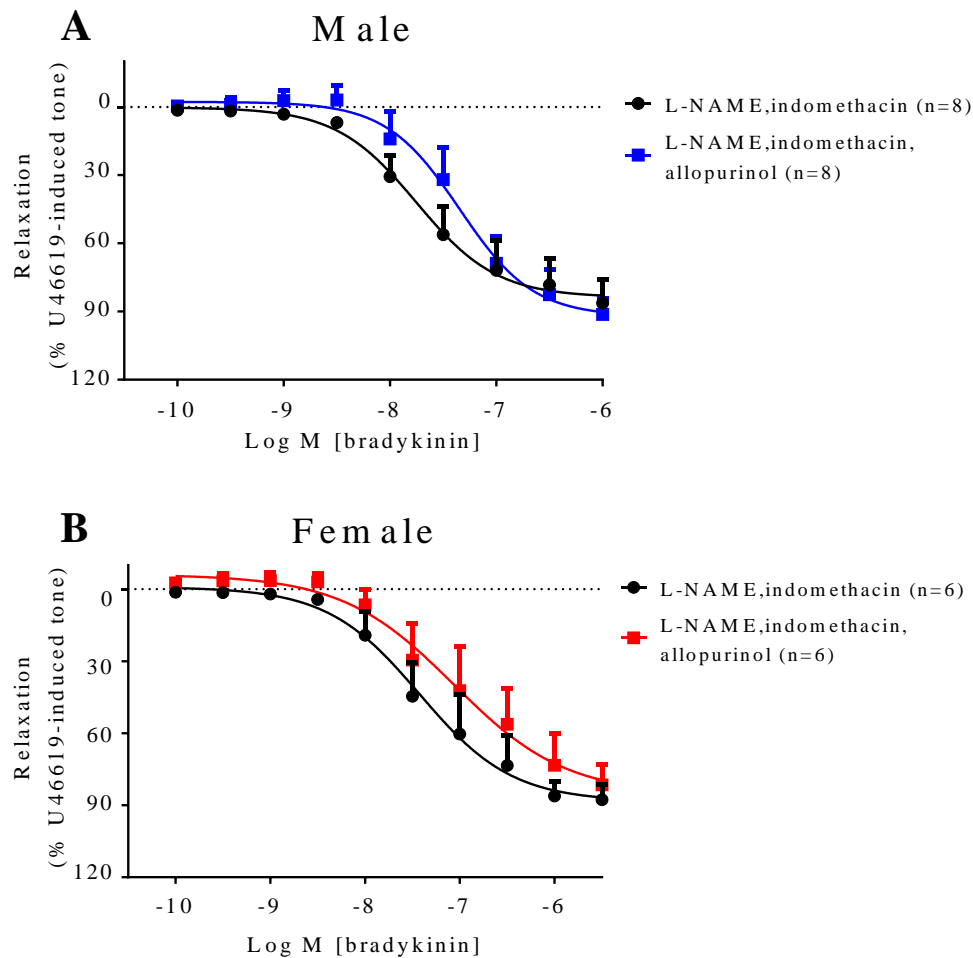
**Figure 5.10** Log concentration-response curves for the vasorelaxant effects of bradykinin in the presence 300 μM L-NAME, 10 μM indomethacin with or without 30 μM allopurinol in U46619 pre-contracted porcine coronary arteries from (A) male or (B) female pigs. Data are expressed as a percentage change from U46619-induced tone and are mean ± S.E.M. of 6-8 experiments.

**5.3.10 The effects of cytochrome P450 inhibitors, proadifen in the presence of L-NAME and indomethacin on bradykinin-induced vasorelaxation in PCAs from male and female pigs**

As cytochrome P450 (CYP450) enzymes are a source of superoxide production, further studies to examine the role of ROS using CYP450 inhibitors on bradykinin-induced vasorelaxation were conducted. As some of the individual curves did not achieve a maximum relaxation, data were analysed using the relaxation achieved at 1 μM bradykinin. In PCAs from male pigs, treatment with 10 μM proadifen in the presence of L-NAME and indomethacin significantly inhibited the bradykinin-induced vasorelaxation such that the relaxation at 1 μM bradykinin was $98.8 \pm 2.7\%$ ($n=7$) in the presence of L-NAME and indomethacin compared to $71.2 \pm 12.8\%$ ($n=7$) in the presence of proadifen (P<0.05) (Figure 5.11A).

Similarly in PCAs from female pigs, treatment with proadifen in the presence of L-NAME and indomethacin significantly inhibited the vasorelaxation where the relaxation at 1 μM bradykinin was inhibited from $94.4 \pm 7.4\%$ ($n=6$) in the presence of L-NAME and indomethacin to $49.4 \pm 11.4\%$ ($n=6$) with the additional presence of proadifen (P<0.01) (Figure 5.11B).

**Figure 5.11** Log concentration-response curves for the vasorelaxant effects of bradykinin in the presence 300 μM L-NAME, 10 μM indomethacin with or without 10 μM proadifen in U46619 pre-contracted porcine coronary arteries from (A) male or (B) female pigs. Data are expressed as a percentage change from U46619-induced tone and are mean ± S.E.M. of 6-7 experiments. *P<0.05 and **P<0.01; 2-tailed, paired Student's *t*-test.

## 5.3.11 The effects of suicide inhibitor of cytochrome P450, 1-aminobenzotriazole in the presence of L-NAME and indomethacin on bradykinin-induced vasorelaxation in PCAs from male pigs

On the other hand, a suicide inhibitor of CYP450, 100 μM 1-aminobenzotriazole (1-ABT) (Figure 5.12) in the presence of L-NAME and indomethacin had no effect on the $R_{max}$ and $EC_{50}$ of the bradykinin-induced vasorelaxation in PCAs from male pigs (Table 5.2).
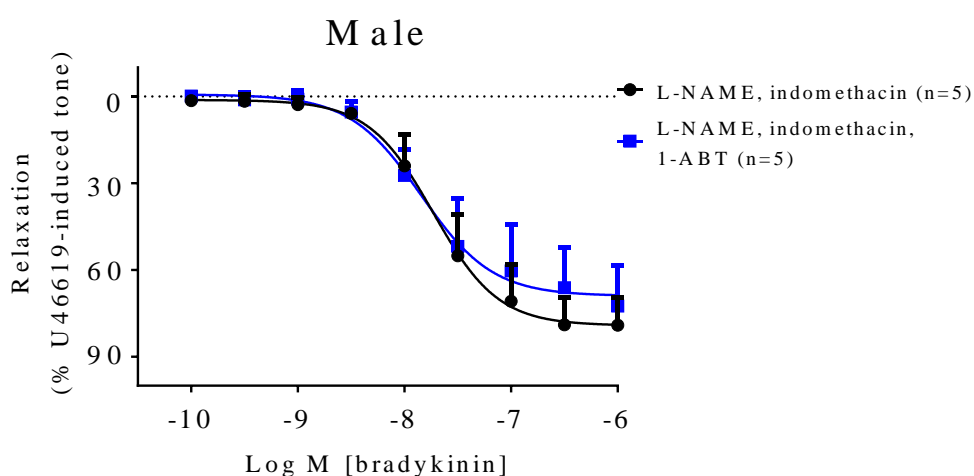


**Figure 5.12** Log concentration-response curves for the vasorelaxant effects of bradykinin in the presence 300 μM L-NAME and 10 μM indomethacin with or without 100 μM 1-ABT in U46619 pre-contracted porcine coronary arteries from male pigs. Data are expressed as a percentage change from U46619-induced tone and are mean ± S.E.M. of 5 experiments.

**5.3.12 The effects of specific cytochrome P450 inhibitor, sulfaphenazole in the presence of L-NAME and indomethacin on bradykinin-induced vasorelaxation in PCAs from male and female pigs**

Similarly, a specific CYP450 inhibitor, 10 μM sulfaphenazole (Figure 5.13A and B) in the presence of L-NAME and indomethacin had no effect on the $R_{max}$ of $EC_{50}$ of the bradykinin-induced vasorelaxation in PCAs from male and female pigs (Table 5.2).
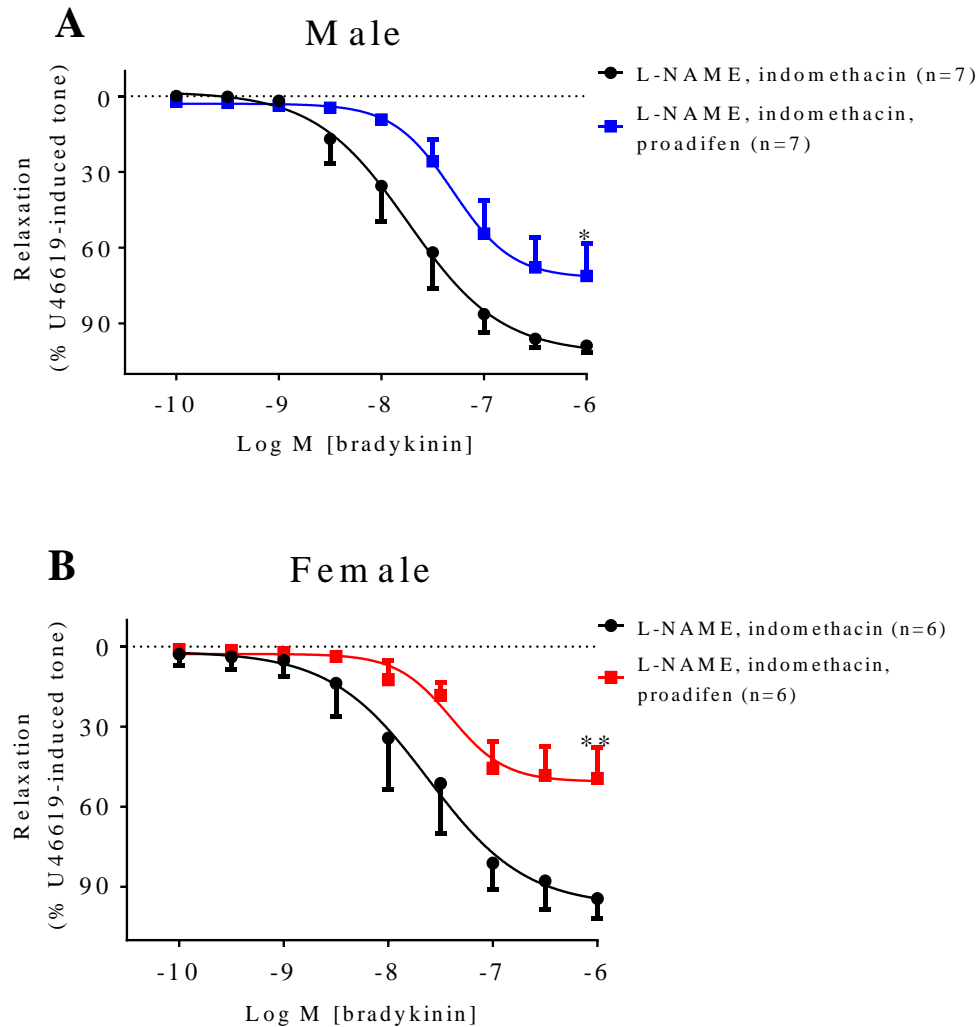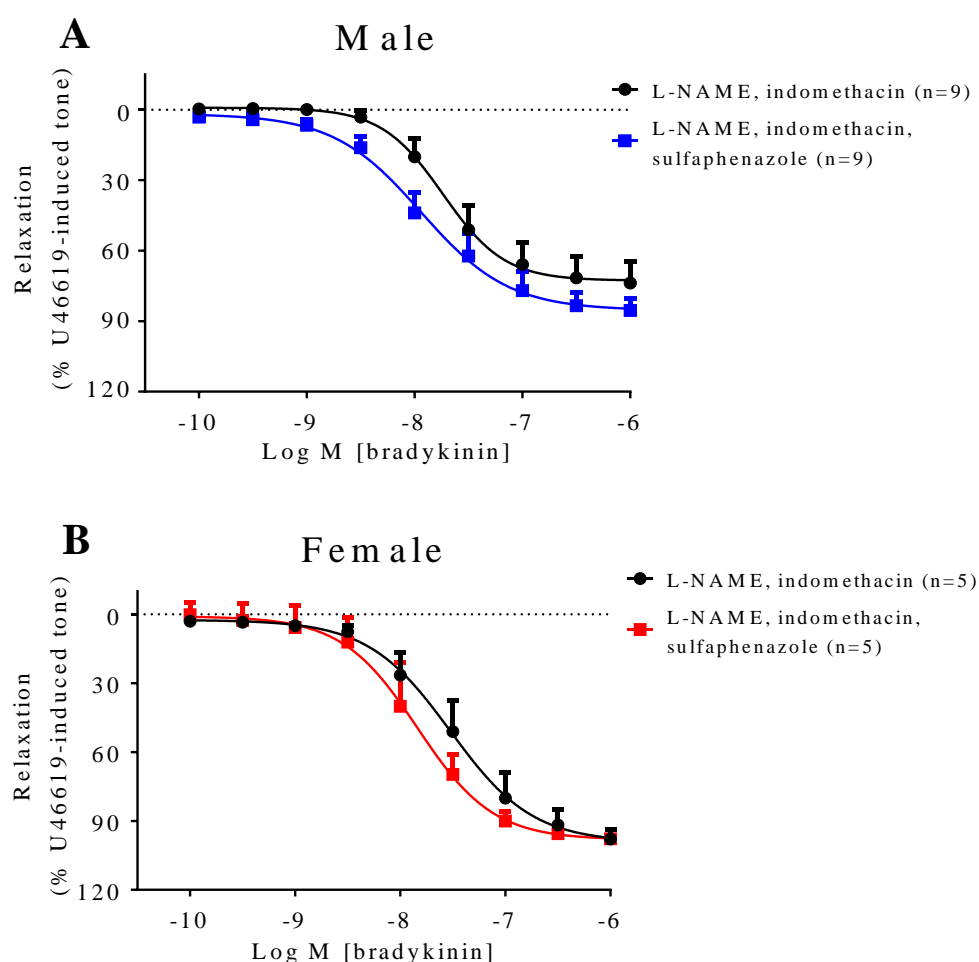


**Figure 5.13** Log concentration-response curves for the vasorelaxant effects of bradykinin in the presence 300 μM L-NAME, 10 μM indomethacin with or without 10 μM sulfaphenazole in U46619 pre-contracted porcine coronary arteries from (A) male or (B) female pigs. Data are expressed as a percentage change from U46619-induced tone and are mean ± S.E.M. of 5-9 experiments.

### 5.3.13 NADPH oxidase activity in PCAs from male and female pigs

Having demonstrated that DPI and ML-171 enhanced the EDH-type response induced by bradykinin in PCAs from male, but not female pigs, the effects of these inhibitors were then further examined by measuring NADPH oxidase activity in homogenates from PCAs using the lucigenin-enhanced chemiluminescence method. Here, in the presence of L-NAME and indomethacin, DPI and ML-171 significantly reduced the NADPH oxidase activity level in PCAs from male and female pigs compared to their respective controls (0.1% DMSO) (Figure 5.14). On the other hand, VAS2870 had no effect on the NADPH oxidase activity in either PCAs from male or female pigs.
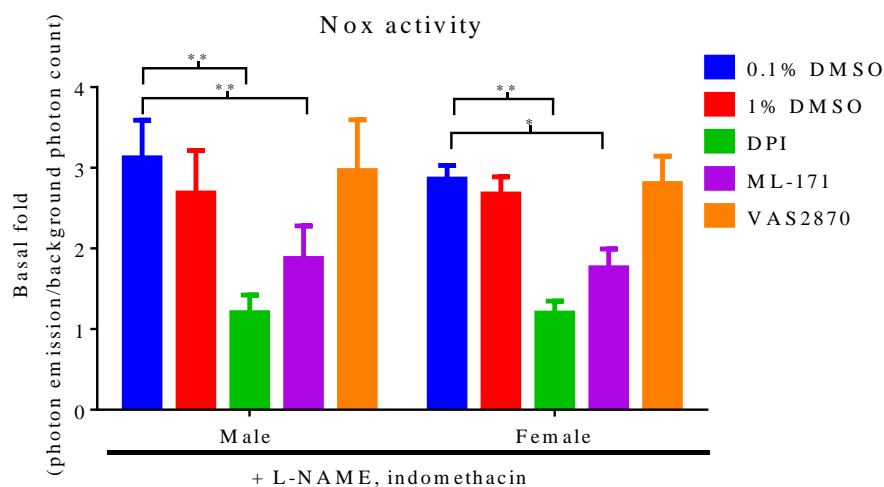


**Figure 5.14** NADPH oxidase activities using lucigenin-enhanced chemiluminescence method in tissue homogenates in the presence of 300 μM L-NAME, 10 μM indomethacin, 10 μM DPI, 100 μM ML-171, or 10 μM VAS2870 in porcine coronary arteries from male and female pigs. After 20 min incubation with inhibitors, 100 μM NADPH was added and measurements were taken in an interval of 10 s per well. Data are expressed as a basal fold from tissue blank and are mean ± S.E.M. of 6 experiments. *P<0.05 and **P<0.01; one-way ANOVA followed by a Dunnett's multiple comparison test.

**5.3.14 Determination of expression of Nox1, Nox2 and Nox4 proteins in PCAs from male and female pigs via Western blotting**

Western blotting confirmed the expression of Nox1 (65 kDa) (Figure 5.15A), Nox2 (~60 kDa) (Figure 5.16A) and Nox4 (~63 kDa) (Figure 5.17A) proteins in PCAs from male and female pigs. Further quantitative analysis of the expression level of the Nox protein based on the ratio of the protein band intensities to β-actin (42 kDa) as a loading control showed higher level of expression of Nox1 ($P<0.05$) and Nox2 ($P<0.01$) proteins in PCAs from males compared to females (Figure 5.15B & 5.16B). In contrast, the expression level of Nox4 ($P<0.05$) protein was higher in PCAs from female compared to male pigs (Figure 5.17B).

**A**

MW
150 kDa —
100 kDa —
75 kDa —
50 kDa —
37 kDa —
25 kDa —

← Nox 1 (65 kDa)
← β-actin (42 kDa)

M1  M2  M3  M4  M5  F1  F2  F3  F4  F5  HepG2

**B**

Nox1

Ratio of Nox 1:β-actin expression levels

*

n = 4-5

Male PCAs        Female PCAs
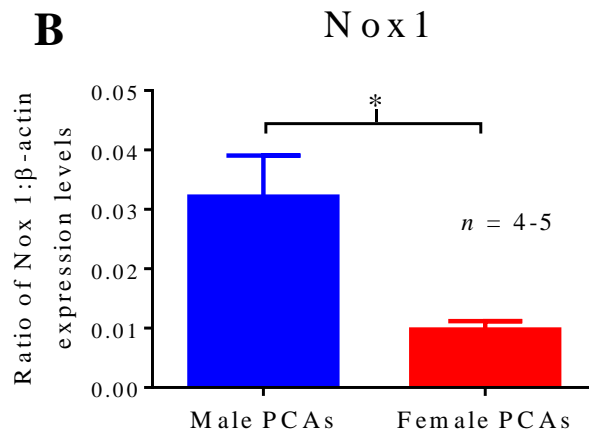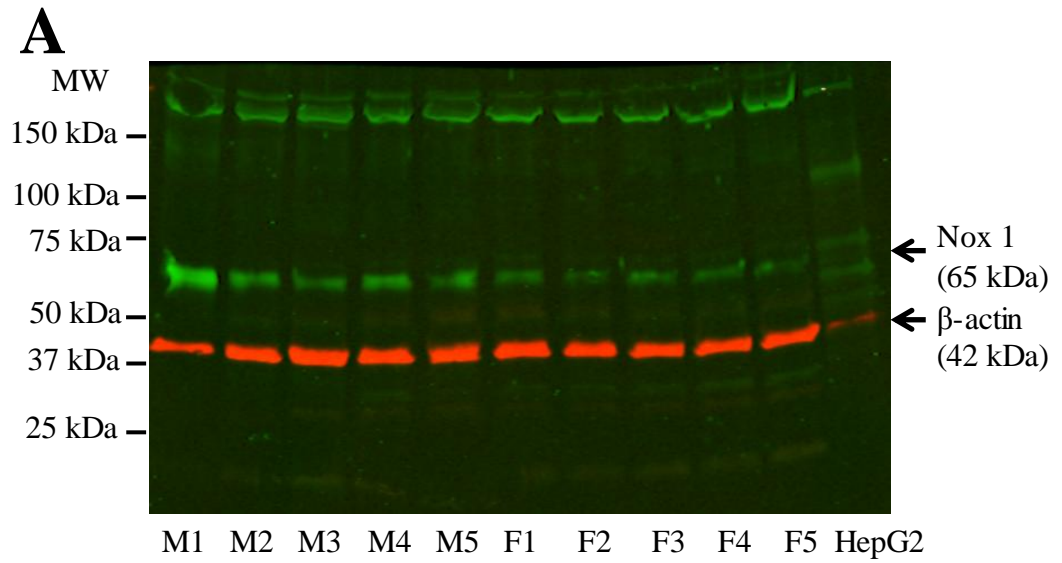
**Figure 5.15** (A) Nox1 (65 kDa) and β-actin (42 kDa) protein expression levels in 20 μg of porcine coronary arteries (PCAs) homogenates from male (M1-M5) and female (F1-F5) pigs with HepG2 cells as positive control. (B) Ratio of the expression levels of Nox1 to β-actin in male and female PCAs based on the intensities of their bands. Data are expressed in the ratio of Nox1 to β-actin intensities bands and are mean ± SEM of 4-5 PCAs. *P<0.05; 2-tailed, unpaired Mann-Whitney U-test.
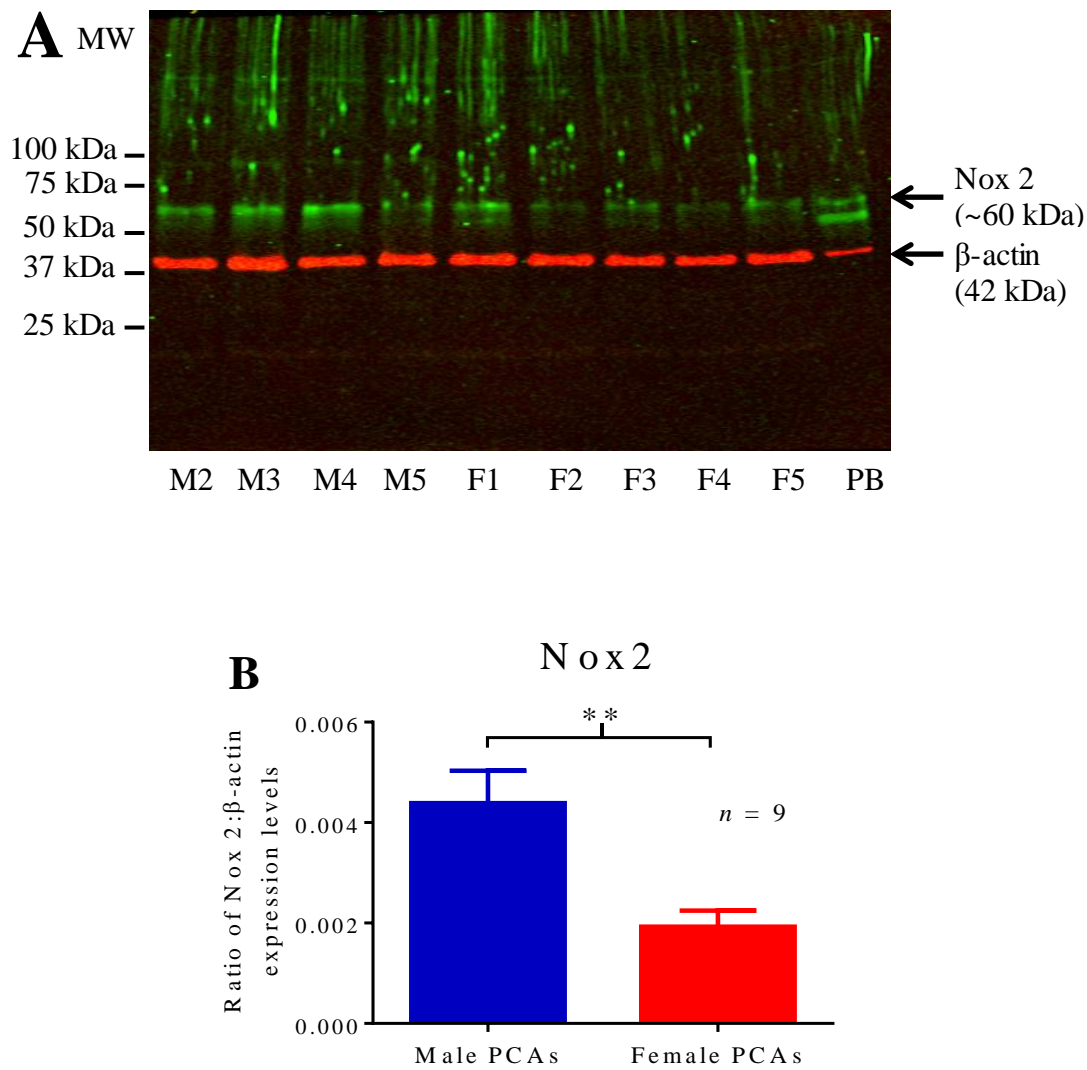
**Figure 5.16** (A) Nox2 (~60 kDa) and β-actin (42 kDa) protein expression levels in 15 μg of porcine coronary arteries (PCAs) homogenates from male (M1-M5) and female (F1-F5) pigs with pig brain (PB) as positive control. (B) Ratio of the expression levels of Nox2 to β-actin in male and female PCAs based on the intensities of their bands. Data are expressed in the ratio of Nox2 to β-actin intensities bands and are mean ± SEM of 9 PCAs. **P<0.01; 2-tailed, unpaired Mann-Whitney U-test.
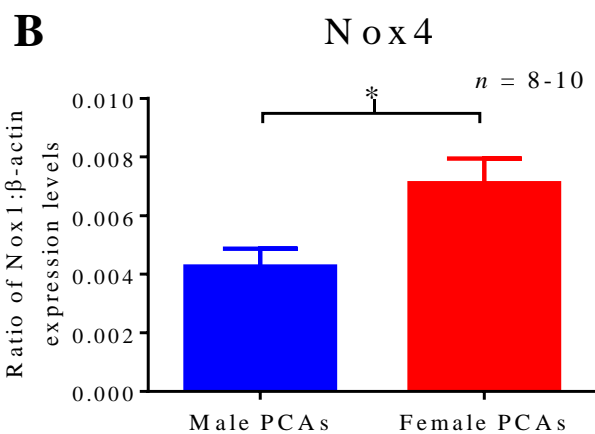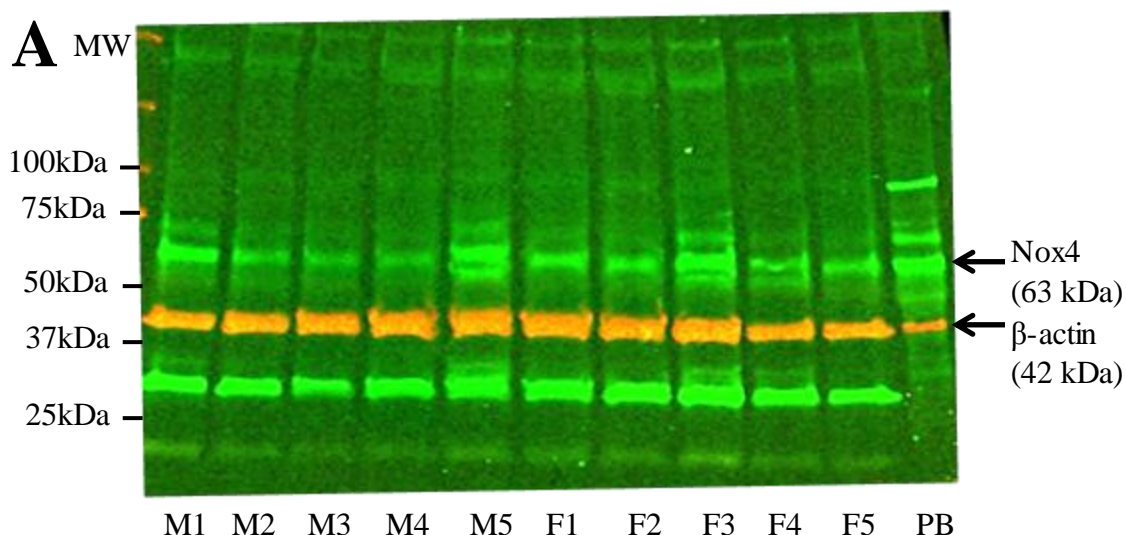
**Figure 5.17**(A) Nox4 (~63 kDa) and β-actin (42 kDa) protein expression levels in 20μg of porcine coronary arteries (PCAs) homogenates from male (M1-M5) and female (F1-F5) pigs with pig brain (PB) as positive control. (B) Ratio of the expression levels of Nox4 to β-actin in male and female PCAs based on the intensities of their bands. Data are expressed in the ratio of Nox4 to β-actin intensities bands and are mean ± SEM of 8-10 PCAs. *P<0.05; 2-tailed, unpaired Mann-Whitney U-test.

## 5.4 Discussion

This chapter has demonstrated sex differences in the expression and function of NADPH oxidases (Nox) in porcine isolated coronary arteries. Here, using two Nox inhibitors, ML-171 and VAS2870, the role of Nox-generated ROS in the EDH-type responses in PCAs from male, but not female pigs were shown. The functional role of Nox-generated ROS in PCAs from male pigs observed in this chapter could be related to the higher expression level of Nox1 and Nox2 proteins in males.

In the present study, bradykinin, an endothelium-dependent vasorelaxant, produced a concentration-dependent vasorelaxation in PCAs from male and female pigs. A previous study in human coronary arterioles demonstrated that bradykinin produces endothelial ROS through activation of Nox (Larsen *et al.*, 2009). Here, the presence of ML-171, a selective Nox1 inhibitor (Gianni *et al.*, 2010) had no effect on the bradykinin-induced vasorelaxation in both PCAs from male and female pigs. 100 μM ML-171 was used in the present study as a previous study in HEK293-Nox1 reconstitute cell system demonstrated that ML-171 inhibited Nox1-dependent ROS generation with an $IC_{50}$ of 0.25 μM (Gianni *et al.*, 2010). Here, a higher concentration of inhibitor was required for penetration of the inhibitor into the multiple cell layers of the blood vessels. On the other hand, DPI, a commonly used yet non-selective Nox inhibitor (Shi *et al.*, 2001; Wind *et al.*, 2010a; Wind *et al.*, 2010b) significantly reduced the potency of bradykinin by 2.8-fold in PCAs from male, but not female pigs. The inhibition by DPI could possibly be due to the inhibition of eNOS (Wind *et al.*, 2010b). As previously reported in Chapter 2, NO plays a greater role in PCAs from male pigs. In the EDH-type response,

inhibiting Nox with DPI and ML-171 significantly enhanced the bradykinin-induced vasorelaxation in PCAs from male pigs, but not from female pigs. These data further support the theory that in the absence of L-NAME, DPI acts as a NOS inhibitor in the bradykinin-mediated response because when NOS is inhibited by L-NAME, the inhibitory response by DPI is turned into an enhancement. The enhancement in the EDH-type vasorelaxation observed in coronary arteries from male pigs and not from female pigs suggests that there may be greater Nox activity in arteries from male pigs compared to female pigs, which may be indicative of greater ROS production in males. This is in agreement with previous studies in isolated aortae from rats (Brandes & Mugge, 1997; Kerr *et al.*, 1999), cerebral arteries from rats (Miller *et al.*, 2007) and in young healthy human subjects (Ide *et al.*, 2002) where there generation superoxide is greater in males compared to females.

In transfected HEK293, ML-171 produced an $IC_{50}$ of 0.25, 5, 3, 5 and 5.5 μM whereas DPI produced and $IC_{50}$ of 1.2, 0.5, 0.75, 1.1 and 0.005 μM for Nox1, 2, 3, 4 and xanthine oxidase respectively (Gianni *et al.*, 2010). To eliminate the possibility that ML-171 inhibits xanthine oxidase, the present study examined the role of xanthine oxidase-generated ROS by using allopurinol, a xanthine oxidase inhibitor. Here, allopurinol had no effect on the bradykinin-induced EDH-type response, indicating that the enhanced vasorelaxation to bradykinin in the presence of ML-171 in PCAs from male pigs was not due to inhibition of xanthine oxidase. Previous studies in aortic abdominal aneurysmal segments from human (Guzik *et al.*, 2013), aortic segments of normotensive and hypertensive rats (Beswick *et al.*, 2001; Wind *et al.*, 2010a), and aortae from male and female rats (Brandes & Mugge, 1997)

similarly demonstrated no role of xanthine oxidase in ROS production. To eliminate the possibility that ML-171 or VAS2870 inhibit other ROS-generating enzymes such as CYP450 epoxygenases, studies using CYP450 inhibitors were conducted. The lack of effects on the EDH-type response when more selective CYP450 inhibitors (1-ABT and sulfaphenazole) were used in the present study showed that the CYP450 enzymes do not play a role in the ROS generation in PCAs from male or female pigs.

Alternatively, the enhanced relaxation to bradykinin could be explained by an inhibitory effect on the pre-contraction, rather than enhancement of the relaxation *per se*. In PCAs with intact endothelium from both male and female pigs, ML-171 reduced the potency of the U46619-induced contraction at low concentrations of U46619, but had no effect on the maximum contraction. In endothelium denuded vessels, the presence of ML-171 significantly reduced the potency and maximum contraction to U46619 in PCAs from both sexes. The fact that ML-171 inhibited the U46619-induced contraction indicates that activation of thromboxane receptors increases ROS production and may be the source of ROS that influences the bradykinin response. Indeed, a previous study in human vascular smooth muscle cells (hVSMCs) demonstrated that incubation with 100 nM U46619 significantly increase the thromboxane $A_2$ synthase mRNA and protein level which was inhibited by apocynin, a Nox inhibitor (Muzaffar *et al.*, 2011). Further studies using siRNA demonstrated that Nox1 but not Nox4 upregulated the thromboxane $A_2$ synthase expression and activity (Muzaffar *et al.*, 2011). These authors concluded that the upregulation of thromboxane $A_2$ synthase and Nox1 expression represent a self-amplifying cascade (Muzaffar *et al.*, 2011).

The effect of ML-171 on the U46619-induced contraction appears to be greater in endothelium intact vessels from male pigs, compared to female pigs. This may explain why ML-171 and DPI enhanced the EDH-type relaxation in coronary arteries from male pigs, but not from female pigs. Furthermore, in the absence of ML-171, the U46619-induced contraction appears to be greater in PCAs with intact endothelium in males compare to females but upon removal of the endothelium in PCAs from males, the potency of U46619 decrease to a level similar to females. Indeed, a previous study in rat aortae has demonstrated that endothelium-intact aortic rings from males generate a higher amount of superoxide compared to females, and removal of the endothelium reduced the superoxide production (Brandes & Mugge, 1997). This would explain why the effect of ML-171 on the U46619-induced contraction in the absence of the endothelium was not as great as that seen in the presence of the endothelium.

To further investigate the effects of ML-171 on relaxation mediated through other pathways, forskolin, a cell-permeable adenylyl cyclase activator, and pinacidil, an ATP-sensitive potassium channel activator, were used. The presence of ML-171 had no effect on the maximum relaxation and $pEC_{50}$ of both the forskolin-induced and pinacidil-induced vasorelaxation, therefore the possibility that the enhancement of the bradykinin-mediated relaxation is due to inhibition of the U46619-induced contraction can be ruled out. At low concentrations of pinacidil, the presence of ML-171 significantly enhanced the vasorelaxation. At a low concentration, pinacidil causes vascular smooth muscle relaxation through activation of the $K_{ATP}$ channel, decreasing $[Ca^{2+}]_i$ (Anabuki *et al.*, 1990). Superoxide production has been shown to inhibit $K_{ATP}$

channel activity (Armstead, 1999), therefore, the reduction in superoxide production by ML-171 would enhance the vasorelaxation induced by pinacidil.

The differential effect of ML-171 and DPI on PCAs from males compared to females may be due to different levels of Nox activity. However, a biochemical assay using lucigenin-enhanced chemiluminescence to measure Nox activity showed that DPI and ML-171 significantly reduced superoxide production in PCAs from both male and female pigs and no sex differences in total Nox activity were detected. This result differs slightly from that of Miller *et al.* (2007) where they have reported that superoxide generated by Nox in rat cerebral arteries were approximately 50% higher in males compared to females. However, this assay measured Nox activity in both smooth muscle and endothelium. As ML-171 enhanced the endothelium-dependent EDH-type relaxation, the difference in Nox activity may only be seen within the endothelial cells.

As no sex differences were detected in the total Nox activity stimulated by NADPH, the possibility that the differences in the pharmacological responses may be related to the differential expression of Nox isoforms were then explored. Indeed, there was a higher level of Nox1 and Nox2 proteins expressed in PCAs from male pigs, but in contrast, a higher level of Nox4 protein was expressed in female pigs. This result is consistent with a previous study in porcine coronary microvessels from female pigs where Nox1 and Nox2 proteins have been reported to be poorly expressed while the expression of Nox4 was abundant (Xie *et al.*, 2012). The higher expression level of Nox1 and Nox2 in PCAs from males could be a possible explanation for the effects of the Nox inhibitors, ML-171 and DPI observed in PCAs from male, but not

female pigs. A previous *in vivo* study in mice reported that transgenic mice overexpressing endothelial Nox4 are associated with an increased production of $H_2O_2$ which enhances endothelium-dependent vasorelaxation compared to wild-type mice (Ray *et al.*, 2011). Here, the higher expression level of Nox4 protein in PCAs from female pigs correlates with the results from Chapter 2 and 4 where endogenous $H_2O_2$ plays a role in the bradykinin-induced vasorelaxations in PCAs from female, but not male pigs. In the present study, although a higher expression level of Nox4 protein was detected in females, the lack of response in the EDH-type relaxation in the presence of Nox inhibitor suggest that the Nox pathway does not play a role in PCA from females or that other compensatory pathways may be involved. For instance, Chapter 2 of the present study has demonstrated that gap junction communication and $IK_{Ca}$ channels play a role in the bradykinin-induced EDH-type vasorelaxation in PCAs from female but not male pigs.

To further confirm the role of Nox in PCAs, the effects of a different Nox inhibitor, VAS2870 (Wind *et al.*, 2010a; Wingler *et al.*, 2012) were then investigated. Previous studies have reported that VAS2870 inhibits activity of all Nox isoforms including Nox1, Nox2 and Nox4 (Kleinschnitz *et al.*, 2010; Wind *et al.*, 2010a; Wingler *et al.*, 2012), improving endothelial functions of spontaneously hypertensive rat aortae (Wind *et al.*, 2010a) and protecting mice from brain damage after cerebral ischaemia (Kleinschnitz *et al.*, 2010). Similar to ML-171, VAS2870 had no effects on the bradykinin-induced endothelium-dependent vasorelaxation in PCAs from both male and female pigs in the absence of L-NAME and indomethacin. These results differ slightly from a previous study using aortic rings from WKY and SHR male rats, where

the presence of VAS2870 significantly enhanced the acetylcholine-induced vasorelaxation (Wind *et al.*, 2010a). This could be due to species or vascular bed differences. In contrast to ML-171 and DPI, VAS2870 inhibited the EDH-type relaxation induced by bradykinin in PCAs from male, but not female pigs. The fact that VAS2870 had no effect on the U46619-induced tone indicates that ML-171 and VAS2870 may be acting on different pathways. This is supported by the finding that VAS2870 had no effect on Nox activity in PCAs. Here, it should be noted that all previous studies that exhibit the protective effects of VAS2870 have been conducted in rodent and the present study conducted in PCAs demonstrated detrimental effects. Therefore, further studies on the effects of VAS2870 in vessels from human subject of specified sex are required.

In summary, inhibition of Nox with DPI and ML-171 enhances, while VAS2870 inhibited the EDH-type response in PCAs from male, but not female pigs. This indicates that Nox-generated ROS regulates the EDH-type response in males, but not in females. The sex differences in EDH-type response could be attributed to the differential expression of Nox isoforms. This may underlie the greater oxidative stress observed in men, whereby increased ROS production through Nox1 and Nox2 leads to a reduction in the EDH-type response.

# *Chapter 6*

**Sex differences in the role of Transient Receptor Potential (TRP) channels in endothelium-dependent vasorelaxation in porcine isolated coronary arteries**

## 6.1 Introduction

The transient receptor potential (TRP) channel superfamily is a diverse group of non-selective cation-permeable channels which are divided into six subfamilies based on the protein sequence identity (Earley & Brayden, 2010). TRP channels have been detected in endothelial cells and vascular smooth muscle cells, playing a role in the regulation of vascular tone (Bubolz *et al.*, 2012; Earley & Brayden, 2010; Huang *et al.*, 2011). Three subfamilies of the TRP proteins, TRPM (TRP melastatin), TRPC (TRP canonical) and TRPV (TRP vanilloid) channels, have been reported as mediators of oxidative stress (Balzer *et al.*, 1999; Bubolz *et al.*, 2012; Kraft *et al.*, 2004; Poteser *et al.*, 2006). Specifically, the TRPM2 channel has been demonstrated to be activated by $H_2O_2$ (Bari *et al.*, 2009; Hecquet *et al.*, 2008), whereas endothelial TRPC3 and TRPC4 channels have been reported to be redox-sensitive cation channels (Balzer *et al.*, 1999; Poteser *et al.*, 2006).

Previous studies have reported that TRPM2 channels play a role in the $H_2O_2$-mediated calcium influx in human pulmonary arterial endothelial cells (Hecquet *et al.*, 2008) and in cultured microglial cells (Kraft *et al.*, 2004). Increased levels of $H_2O_2$ have been detected in various pathological diseases including essential hypertension in human subjects (Lacy *et al.*, 2000) and ischaemia and reperfusion of rat brain (Hyslop *et al.*, 1995). Therefore, further understanding of the mechanism of action of $H_2O_2$ and the role of TRP channels in vascular function may benefit the development of new strategies in treatment and prevention of diseases related to $H_2O_2$ (Burgoyne *et al.*, 2013).

Other vasoactive substances which regulate vascular tone include endothelium-derived relaxing factor (NO), prostacyclin and endothelium-

derived hyperpolarization (EDH)-type responses (Edwards *et al.*, 2010; Furchgott & Zawadzki, 1980; Taylor & Weston, 1988). A previous study in rat mesenteric arterial bed and the present study (Chapter 2 and 5) in PCAs have demonstrated clear sex differences in endothelial function and it was concluded that this could be a possible explanation for the higher cardiovascular risk observed in men and postmenopausal women compared to premenopausal women (McCulloch & Randall, 1998). However, most of the current studies on endothelial function are conducted on arteries from either males only or from either sexes and conclusions from these results may be biased and inconsistent as previously discussed in Chapter 2.

Previous studies on TRP channels have demonstrated sex differences in other tissues, where inhibition of TRPM2 channels and knockdown of TRPM2 expression in mice have significantly protected male neurons from cell death, but had no effect in females (Jia *et al.*, 2011). In the mouse bladder, a higher gene expression level of TRPV1 has been reported in female compared to male mice (Kobayashi *et al.*, 2009). To date, no-one has yet investigated if there are sex differences in the role of endothelial TRP channels in vascular control. In Chapter 2, sex differences in the endothelium-dependent relaxations to bradykinin in the PCAs have been demonstrated. Therefore, using pharmacological antagonists, this chapter examined whether TRP channels contribute to these sex differences in bradykinin-induced vasorelaxation specifically the role of TRPC3 and TRPV4 channels and also the roles of TRP channels in $H_2O_2$-mediated vasorelaxation in PCAs.

## 6.2 Materials and methods

### 6.2.1 Preparation of rings of distal PCAs

Tissues were set up as previously described in Chapter 2.

### 6.2.2 Wire myography

As described in Chapter 2, after 30 min of equilibration, responses to 60 mM KCl were determined twice. The vascular tone was then raised to about 40-90% of the second KCl contraction tone by the addition of the thromboxane $A_2$ mimetic, U46619 (1 nM - 400 nM). Once stable tone was achieved, concentration-response curves to an endothelium-dependent vasorelaxant, bradykinin (0.01 nM - 1 μM), A23187 (1 nM - 3 μM) or $H_2O_2$ (1 μM - 1 mM) were constructed in the presence of various inhibitors. $N^G$-nitro-L-arginine methyl ester (L-NAME) (300 μM) was used as a NO synthase inhibitor and indomethacin (10 μM) was used to inhibit the synthesis of prostanoids. To examine the role of TRP channels in $H_2O_2$-induced vasorelaxation and on endothelium-dependent vasorelaxation, the following inhibitors were used; 2-diphenylboranyloxyethanamine (2-APB) (10 μM or 100 μM) (Hagenston *et al.*, 2009; Li *et al.*, 2005; Togashi *et al.*, 2008) and 2-[3-(4-pentylphenyl)prop-2-enoylamino]benzoic acid (ACA) (20 μM or 100 μM) (Bari *et al.*, 2009; Kraft *et al.*, 2006; Togashi *et al.*, 2008) as non-selective TRP channels blockers. 1-[2-(4-methoxyphenyl)-2-[3-(4-methoxyphenyl)propoxy]ethyl] imidazole (SKF96365) (10 μM) (Huang *et al.*, 2011) was used to inhibits TRPC channels whereas ethyl-1-(4-(2,3,3-trichloroprop-2-enoylamino) phenyl]-5-(trifluoromethyl)pyrazole-4-carboxylate (Pyr3) (3 μM) (Huang *et al.*, 2011) and 2,4-dichloro-N-propan-2-yl-N-[2-(propan-2-ylamino)ethyl] benzenesulfonamide (RN1734) (30 μM) (Bagher *et al.*, 2012; Bubolz *et al.*,

2012) were used as selective TRPC3 and TRPV4 antagonist respectively. All inhibitors were added into the bath 1 h before pre-contraction with U46619. In the majority of cases, a higher concentration of U46619 was required to induce tone in the presence of TRP antagonists and in some cases the level of tone achieved with U46619 was slightly less than vehicle controls. Table 6.1A and B summarises the concentration of U46619 used and the level of tone induced under these conditions.

### 6.2.3 Western Blotting

The relative expression levels of TRPC3 and TRPV4 in PCAs from male and female pigs were compared using Western blotting. PCAs were finely dissected and cut into segments of approximately 1.5 cm in length. PCAs were then gassed with 5% $CO_2$ and 95% $O_2$ at 37°C for 1 h in Krebs'-Henseleit solution as previously described in Chapter 2 (Samples in this chapter were solubilised in 6x solubilisation buffer). Again, the method described below is the result of substantial method development using antibodies from different companies, different batches of antibodies and different dilutions of antibody. Results of these developments are included in Appendix D. For quantification of TRPC3 protein, 35 μg of PCA samples with 25 μg of pig brain lysates used as positive control were incubated with rabbit polyclonal anti-TRPC3 antibody (ab70603 Abcam®, Cambridge, UK) (1:500). For quantification of TRPV4 protein, 15 μg of PCA samples with 15 μg of human β-cell lysates used as positive control were incubated with rabbit polyclonal anti-TRPV4 antibody (ab94868 Abcam®) (1:1000).

| A Concentration of U46619 (nM) | | Control | Antagonist | L-NAME, indomethacin | | Indomethacin | |
|---|---|---|---|---|---|---|---|
| | | | | Control | Antagonist | Control | Antagonist |
| 2-APB | Male | 12.3 ± 1.2 | 40.2 ± 6.3** | 21.5 ± 3.7 | 99.0 ± 26.9* | | |
| | Female | 11.8 ± 1.1 | 31.8 ± 2.4*** | 13.2 ± 1.7 | 40.7 ± 4.7** | | |
| SKF96365 | Male | 6.9 ± 1.1 | 153 ± 41* | 12.2 ± 1.3 | 80.0 ±20.5* | | |
| | Female | 10.0 ± 1.7 | 258 ± 53** | 10.2 ± 0.9 | 181 ± 38** | | |
| Pyr3 | Male | | | 13.8 ± 1.3 | 17.7 ± 1.1* | 20.0 ± 1.1 | 19.9 ± 0.9 |
| | Female | | | 18.7 ± 2.0 | 17.7 ± 1.6 | 30.5 ± 1.9 | 28.8 ± 1.8 |
| RN1734 | Male | 9.17 ± 0.70 | 28.0 ± 7.8 | 10.5 ± 0.8 | 47.7 ± 5.8** | 28.3 ± 4.5 | 185 ± 40* |
| | Female | 8.57 ± 1.33 | 35.6 ± 6.6** | 12.0 ± 1.3 | 49.4 ± 4.8*** | 28.5 ± 4.8 | 111 ± 12*** |

| B U46619-induced tone (% KCl response) | | Control | Antagonist | L-NAME, indomethacin | | Indomethacin | |
|---|---|---|---|---|---|---|---|
| | | | | Control | Antagonist | Control | Antagonist |
| 2-APB | Male | 76.7 ± 7.0 | 53.3 ± 0.4* | 60.0 ± 5.2 | 52.2 ± 0.7 | | |
| | Female | 70.0 ± 5.5 | 58.7 ± 4.3 | 62.0 ± 5.1 | 54.3 ± 1.0 | | |
| SKF96365 | Male | 62.0 ± 10.3 | 51.0 ± 5.6 | 67.6 ± 8.0 | 56.4 ± 3.1 | | |
| | Female | 67.0 ± 6.5 | 47.2± 3.2** | 63.1 ± 4.3 | 56.5 ± 3.9* | | |
| Pyr3 | Male | | | 53.3 ± 1.2 | 60.2 ± 3.7 | 67.6 ± 5.6 | 67.0 ± 5.7 |
| | Female | | | 62.3 ± 4.8 | 59.7 ± 4.2 | 63.5 ± 6.7 | 70.3 ± 6.6 |
| RN1734 | Male | 72.8 ± 6.1 | 56.7 ± 2.3* | 60.8 ± 4.3 | 50.7 ± 1.1 | 63.5 ± 7.3 | 53.5 ± 1.3 |
| | Female | 71.9 ± 5.6 | 53.6 ± 0.8* | 62.7 ± 4.4 | 51.9 ± 0.5* | 80.3 ± 6.3 | 54.2 ± 1.3** |

**Table 6.1** Summary of (A) U46619 concentration used (nM) and (B) the level of U46619-induced tone expressed in percentage to second KCl-induced tone. Data are expressed as mean ± S.E.M. of 3-11 experiments. *P<0.05, **P<0.01, ***P<0.001; 2-tailed, paired Student's *t*-test.

Mouse monoclonal anti-GAPDH antibody (G8795 Sigma-Aldrich, Poole, Dorset, UK) (1:40,000) was used as loading control for both quantification. Secondary antibodies, IRDye® 680LT Goat anti-mouse IgG (1:10 000) (LI-COR Biosciences, Cambridge, UK) was used for anti-mouse antibody and IRDye® 800CW Goat anti-rabbit IgG (1:10 000) (LI-COR Biosciences, Cambridge, UK) for anti-rabbit antibody. LI-COR Odyssey Infrared Imaging Scanner was used to visualise the immunoblots and densities of the bands were determined using Image Studio Analysis Software Version 3.1 (LI-COR).

### 6.2.4 Statistical analysis

Data for functional studies were presented and analysed as described in Chapter 2. For Western blot, expression levels of TRPC3 and TRPV4 proteins in PCAs from male and female pigs were normalised to GAPDH level then analysed using 2-tailed, unpaired Mann-Whitney U-test.

### 6.2.5 Drugs and reagents

All drugs were purchased from Sigma-Aldrich (Poole, Dorset, UK) except for SKF96365, Pyr3 and RN1734 from Tocris Bioscience (Bristol, UK) and ACA from Calbiochem (VWR International Ltd, Lutterworth, Leicestershire, UK). Stock solutions of L-NAME and SKF96365 were dissolved in distilled water while 2-APB, ACA, Pyr3 and RN1734 were dissolved in DMSO. Stock solution of indomethacin was dissolved in absolute ethanol. Stock solution of A23187 was made up to 1 mM in absolute ethanol and $H_2O_2$ was made up to 100 mM in distilled water. All further dilutions of the stock solutions were made using distilled water.

## 6.3 Results

### 6.3.1 The effects of 2-APB on bradykinin-induced vasorelaxation in PCAs from male and female pigs

In PCAs from males, the presence of 100 μM 2-APB significantly inhibited the $R_{max}$ to bradykinin from $104 \pm 4\%$ under control conditions to $66 \pm 6\%$ in the presence of 2-APB ($n=6$) (P<0.01), but had no effect on the $pEC_{50}$ ($8.35 \pm 0.09$, control; $8.12 \pm 0.18$, 2-APB, $n=6$) (Figure 6.1A).

Similarly, in PCAs from females, the presence of 100 μM 2-APB significantly inhibited the $R_{max}$ of the bradykinin-induced vasorelaxation compared to the control and had no effects on the $pEC_{50}$ ($8.22 \pm 0.07$, control; $7.94 \pm 0.14$, 2-APB, $n=6$) (Figure 6.1B). The $R_{max}$ was significantly reduced from $98.8 \pm 3.6\%$ under control conditions to $75.4 \pm 5.6\%$ in the presence of 2-APB ($n=6$) (P<0.001) (Figure 6.1B).

### 6.3.2 The effects of 2-APB on bradykinin-induced vasorelaxation in the presence of L-NAME and indomethacin in PCAs from male and female pigs

In the presence of L-NAME and indomethacin, the additional presence of 100 μM 2-APB essentially abolished the bradykinin-induced vasorelaxation in PCAs from both male and female pigs (Figure 6.2A and B respectively). The $R_{max}$ in the presence of L-NAME and indomethacin was $74.3 \pm 13.0\%$ for PCAs from male pigs and $60.7 \pm 18.2\%$ for PCAs from female pigs ($n=6$).
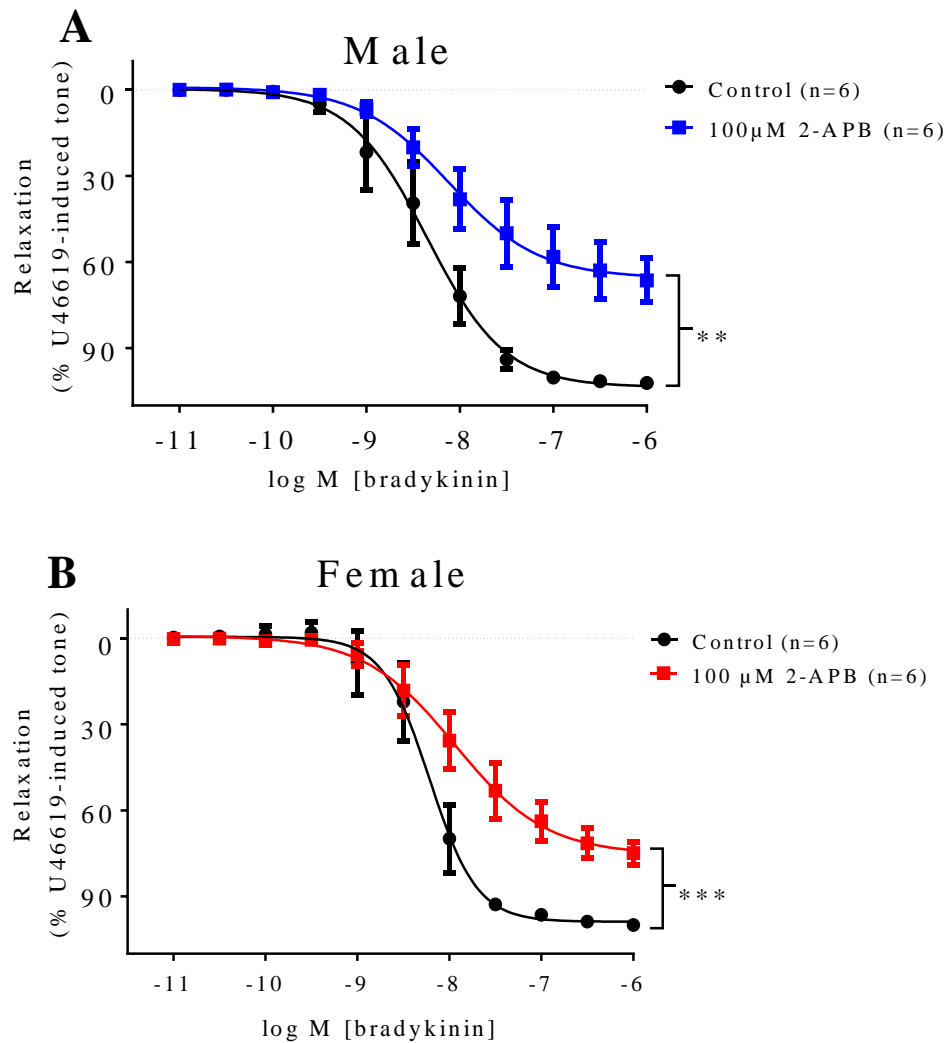
**Figure 6.1** Log concentration-response curves for the vasorelaxant effects of bradykinin in the presence of 100 μM 2-APB in U46619 pre-contracted porcine coronary arteries from (A) male and (B) female pigs. Data are expressed as a percentage change from U46619-induced tone and are mean ± S.E.M. of 6 experiments. **P<0.01, ***P<0.001, 2-tailed; paired Student's *t*-test.

**Figure 6.2** Log concentration-response curves for the vasorelaxant effects of bradykinin in the presence of 300 μM L-NAME and 10 μM indomethacin with or without 100 μM 2-APB in U46619 pre-contracted porcine coronary arteries from (A) male and (B) female pigs. Data are expressed as a percentage change from U46619-induced tone and are mean ± S.E.M. of 6 experiments.

### 6.3.3 The effects of SKF96365 on bradykinin-induced vasorelaxation in PCAs from male and female pigs

SKF96365, a non-selective TRPC channel inhibitor, significantly reduced the $R_{max}$ ($P<0.05$) of the bradykinin-induced vasorelaxation in PCAs from male pigs from $104 \pm 4\%$ under control conditions to $90 \pm 3\%$ in the presence of SKF96365, but had no effect on the $pEC_{50}$ ($8.80 \pm 0.10$, control; $8.92 \pm 0.10$, SKF96365, $n=5$) (Figure 6.3A).

On the other hand, in PCAs from females, SKF96365 had no effect on the $R_{max}$ or $pEC_{50}$ of the bradykinin-induced vasorelaxation ($7.71 \pm 0.08$, control; $7.65 \pm 0.08$, SKF96365, $n=6$) (Figure 6.3B).
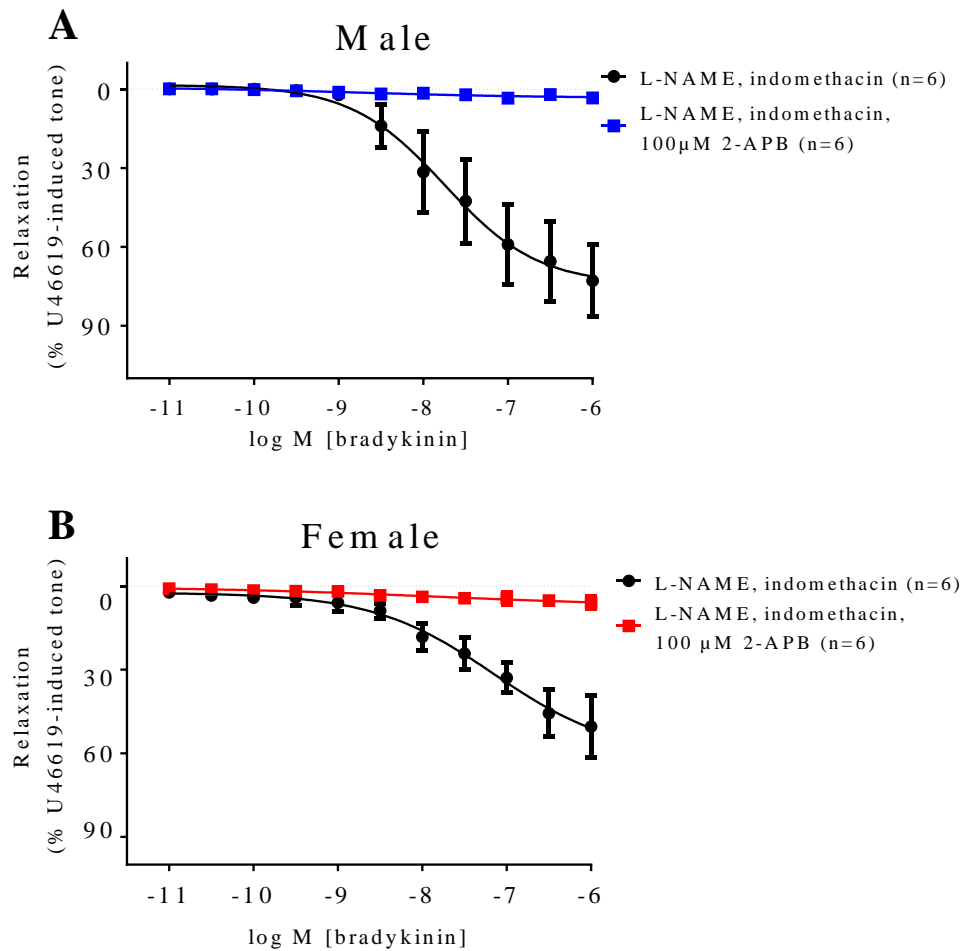
### 6.3.4 The effects of SKF96365 on bradykinin-induced vasorelaxation in the presence of L-NAME and indomethacin in PCAs from male and female pigs

In the presence of L-NAME and indomethacin, the presence of SKF96365 significantly reduced the $R_{max}$ of the bradykinin-induced vasorelaxation in PCAs from both male (Figure 6.4A) and female pigs (Figure 6.4B) ($P<0.05$). In male PCAs, the $R_{max}$ was reduced ($P<0.05$) from $95.0 \pm 3.4\%$ in the presence of L-NAME and indomethacin to $69.7 \pm 3.0\%$ ($n=5$) in the additional presence of SKF96365. In female PCAs, the $R_{max}$ was reduced ($P<0.05$) from $84.0 \pm 6.4\%$ in the presence of L-NAME and indomethacin to $62.3 \pm 5.8\%$ ($n=10$) in the additional presence of SKF96365.

In contrast, the presence of SKF96365 had no effect on the $pEC_{50}$ of the bradykinin-induced EDH-type response in PCAs from both male and

female pigs (in males; 8.07± 0.07, without SKF96365; 8.18 ± 0.09, with SKF96365) (in females; 7.56 ± 0.12, without SKF96365; 7.69 ± 0.16, with SKF96365).
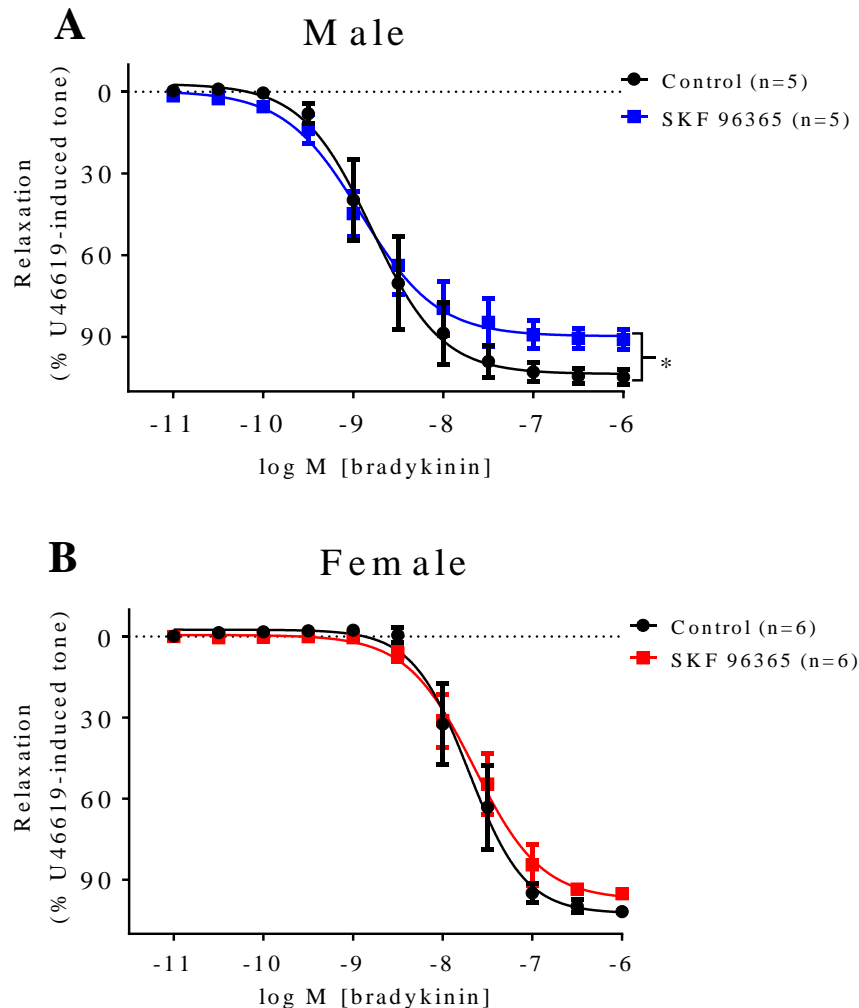


**Figure 6.3** Log concentration-response curves for the vasorelaxant effects of bradykinin in the presence of 10 μM SKF96365 in U46619 pre-contracted porcine coronary arteries from (A) male and (B) female pigs. Data are expressed as a percentage change from U46619-induced tone and are mean ± S.E.M. of 5-6 experiments. *P<0.05; 2-tailed, paired Student's *t*-test.

**Figure 6.4** Log concentration-response curves for the vasorelaxant effects of bradykinin in the presence of 300 μM L-NAME and 10 μM indomethacin with or without 10 μM SKF96365 in U46619 pre-contracted porcine coronary arteries from (A) male and (B) female pigs. Data are expressed as a percentage change from U46619-induced tone and are mean ± S.E.M. of 5-10 experiments. *P<0.05; 2-tailed, paired Student's *t*-test.

## 6.3.5 The effects of 2-APB or SKF96365 on A23187-induced vasorelaxation in the presence of L-NAME and indomethacin in PCAs from male pigs
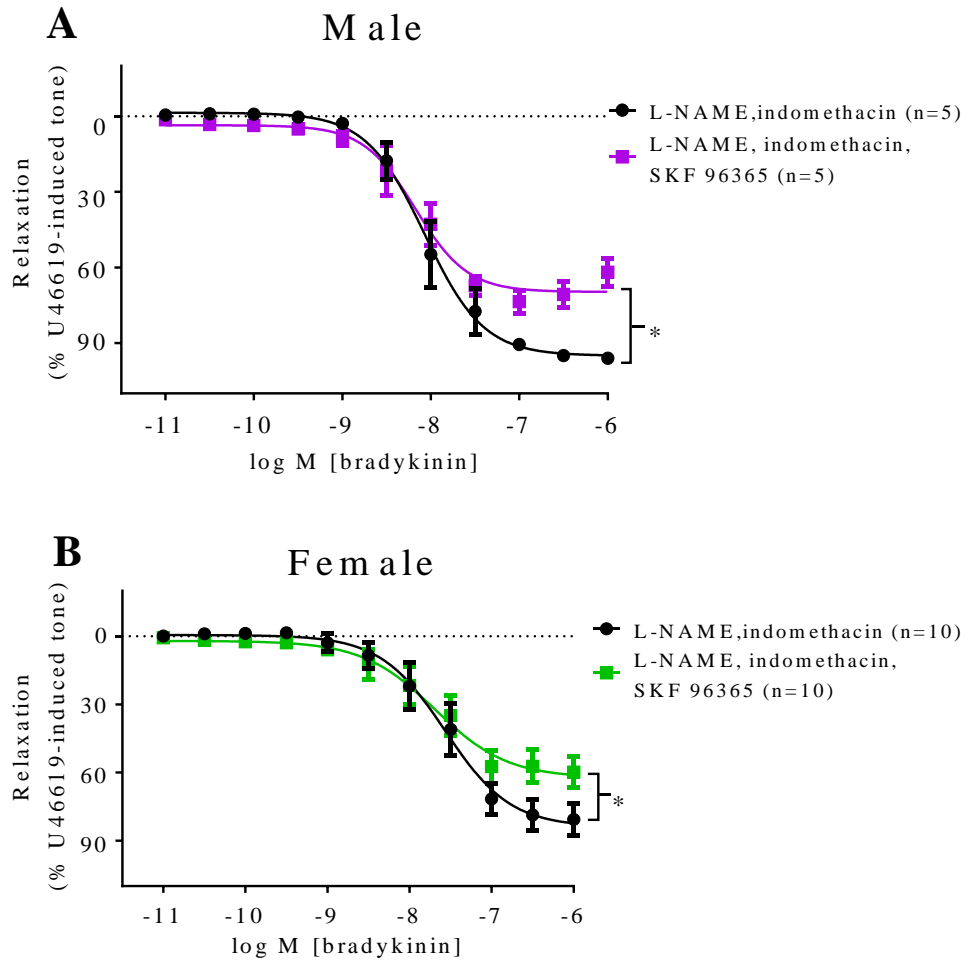
As 100 μM 2-APB essentially abolished the bradykinin-induced vasorelaxation in the presence of L-NAME and indomethacin, the effects of 2-APB on

relaxations to A23187, a calcium ionophore which causes endothelium-dependent relaxations were examined. In PCAs from male pigs, the presence of 2-APB (*n*=6) (Figure 6.5A), but not SKF96365 (*n*=8) (Figure 6.5B) significantly inhibited (P<0.01) the A23187-induced EDH-type vasorelaxations.



**Figure 6.5** Log concentration-response curves for the vasorelaxant effects of A23187 in the presence of 300 μM L-NAME, 10 μM indomethacin and (A) 100 μM 2-APB or (B) 10 μM SKF96365 in U46619 pre-contracted porcine coronary arteries from male pigs. Data are expressed as a percentage change from U46619-induced tone and are mean ± S.E.M. of 6-8 experiments. **P<0.01; 2-tailed, paired Student's *t*-test.
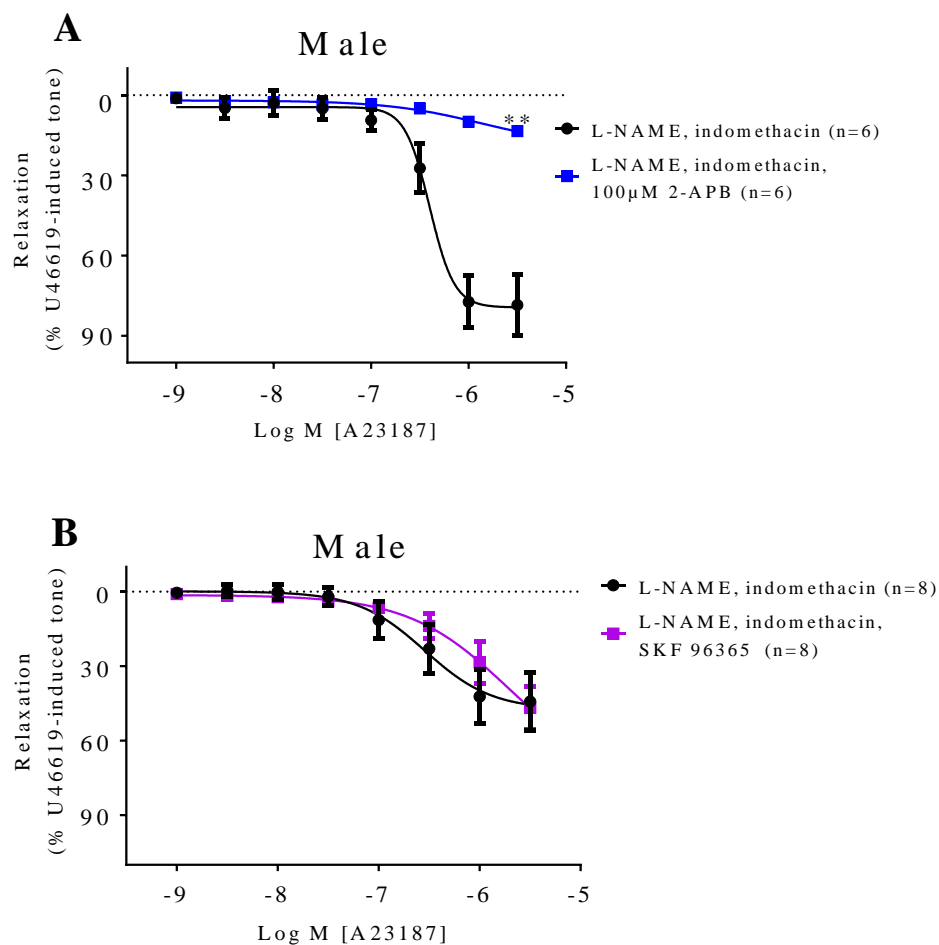
**6.3.6 The effects of Pyr3 in the presence of indomethacin on bradykinin-induced vasorelaxation in PCAs from male and female pigs**

Next, the effects of Pyr3, a selective TRPC3 antagonist, on bradykinin-induced vasorelaxation in the NO-mediated response in PCAs from male and female pigs were examined as previous studies have reported that TRPC3 channels play a role in the NO-mediated vasorelaxation (Chen *et al.*, 2009; Huang *et al.*, 2011). In the presence of indomethacin, 3 $\mu$M Pyr3 in PCAs from male pigs had no effect on the $R_{max}$ of the bradykinin-induced vasorelaxation, but significantly reduced the potency of bradykinin by 4.2-fold from $pEC_{50}$= 8.29 ± 0.10 to $pEC_{50}$= 7.67 ± 0.06 (*n*=10) (P<0.05) (Figure 6.6A).

In contrast, in PCAs from females, Pyr3 (in the presence of indomethacin) had no effect on the $R_{max}$ or $pEC_{50}$ of the bradykinin-induced vasorelaxation ($pEC_{50}$= 7.88 ± 0.06, control, *n*=5; 7.77 ± 0.05, Pyr3, *n*=6) (Figure 6.6B).

**6.3.7 The effects of Pyr3 on bradykinin-induced vasorelaxation in the presence of L-NAME and indomethacin in PCAs from male and female pigs**

Similarly in the presence of both L-NAME and indomethacin, Pyr3 significantly reduced the bradykinin-induced vasorelaxation at 30 nM bradykinin in males (*n*=11) (P<0.05) (Figure 6.7A), whereas in PCAs from females, Pyr3 had no effect on the bradykinin-induced vasorelaxation (*n*=6) (Figure 6.7B).
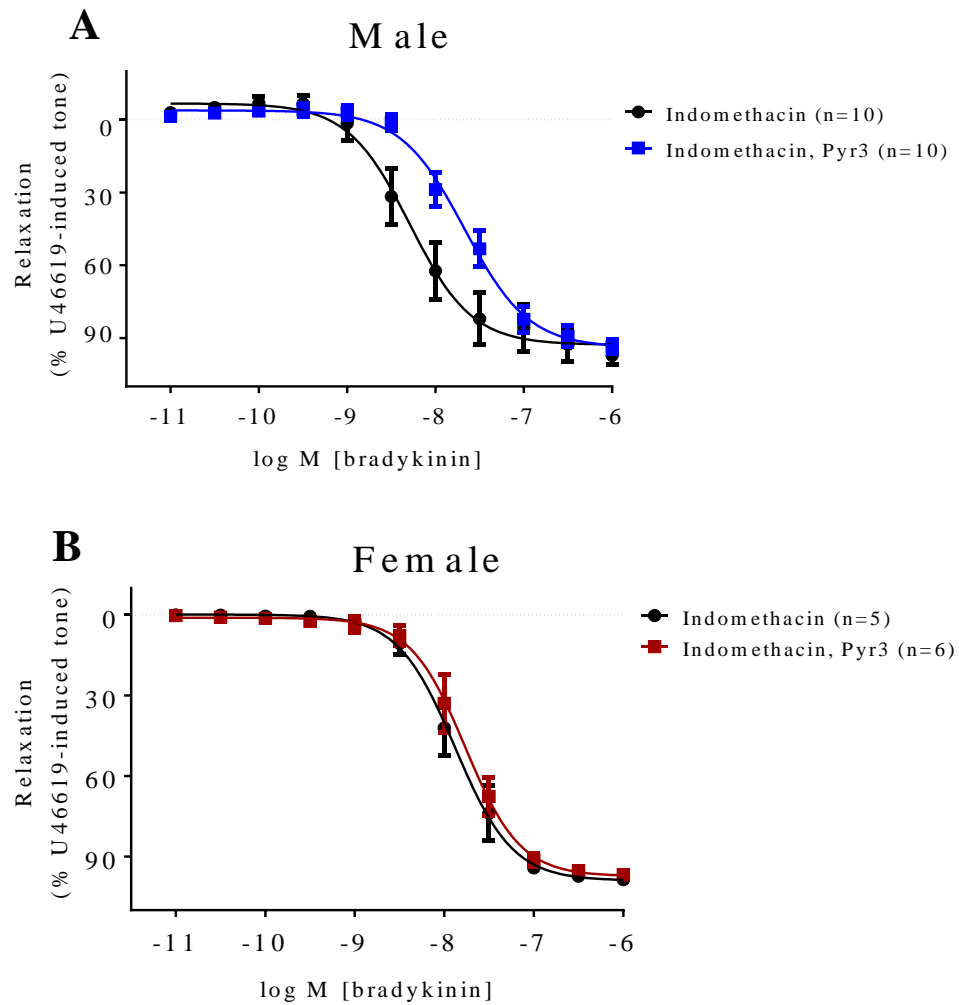
**Figure 6.6** Log concentration-response curves for the vasorelaxant effects of bradykinin in the presence of 10 μM indomethacin and 3 μM Pyr3 in U46619 pre-contracted porcine coronary arteries from (A) male or (B) female pigs. Data are expressed as a percentage change from U46619-induced tone and are mean ± S.E.M. of 5-10 experiments.
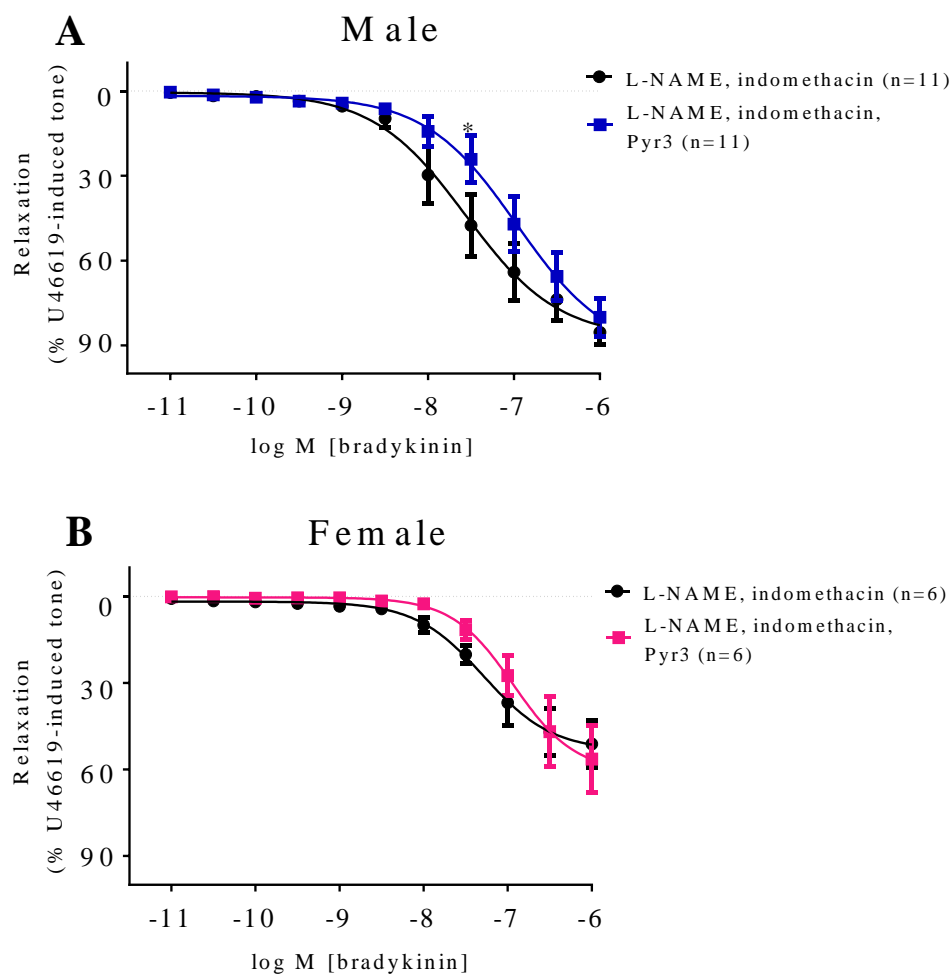
**Figure 6.7** Log concentration-response curves for the vasorelaxant effects of bradykinin in the presence of 300 μM L-NAME and 10 μM indomethacin with or without 3 μM Pyr3 in U46619 pre-contracted porcine coronary arteries from (A) male or (B) female pigs. Data are expressed as a percentage change from U46619-induced tone and are mean ± S.E.M. of 6-11 experiments. *P<0.05; 2-tailed, paired Student's *t*-test.

### 6.3.8 The effects of RN1734 on bradykinin-induced vasorelaxation in PCAs from male and female pigs

A previous study has reported that TRPV4 and $IK_{Ca}$ channels cluster within the endothelial cells' projection towards the smooth muscle cells (Bagher *et al.*, 2012). In Chapter 2, sex differences in the role of $IK_{Ca}$ channels in PCAs have been reported where $IK_{Ca}$ plays a role in the EDH-type response to bradykinin in female, but not male pigs. Therefore, sex differences in the role of TRPV4 on bradykinin-induced vasorelaxation in PCAs from male and female pigs were investigated. In PCAs from males, the presence of RN1734, a selective TRPV4 antagonist ($pEC_{50}= 8.18 \pm 0.04$), had no effect on the bradykinin-induced vasorelaxation compared to the control ($pEC_{50}= 8.33 \pm 0.05$) ($n=6$) (Figure 6.8A).

Interestingly, in PCAs from females, the presence of RN1734 significantly reduced ($P<0.05$) the potency of bradykinin by 4.4-fold ($pEC_{50}= 8.36 \pm 0.05$, control; $7.72 \pm 0.11$, RN1734, $n=7$), but had no effect on the $R_{max}$ (Figure 6.8B).

### 6.3.9 The effects of RN1734 on bradykinin-induced vasorelaxation in the presence of indomethacin with or without L-NAME in PCAs from male and female pigs

In the presence of indomethacin, RN1734 had no effect on the bradykinin-induced vasorelaxation in PCAs from male pigs (Figure 6.9A), but significantly reduced the potency of bradykinin in PCAs from female pigs by

226

4.9-fold (P<0.05) (pEC$_{50}$= 8.63 ± 0.03, indomethacin; 7.94 ± 0.08, indomethacin and RN1734, $n$=6) (Figure 6.9B).

In the EDH-type response, in the presence of L-NAME and indomethacin, RN1734 inhibited the R$_{max}$ (P<0.05) of both PCAs from male (Figure 6.10A) and female pigs (Figure 6.10B), but had no effect on the pEC$_{50}$ of the bradykinin-induced vasorelaxation. (R$_{max}$ in males = 77.6 ± 17.6%, without RN1734; 55.6 ± 6.0%, with RN1734, $n$=6, in females = 73.2 ± 7.0%, without RN1734; 55.4 ± 5.4%, with RN1734, $n$=7).
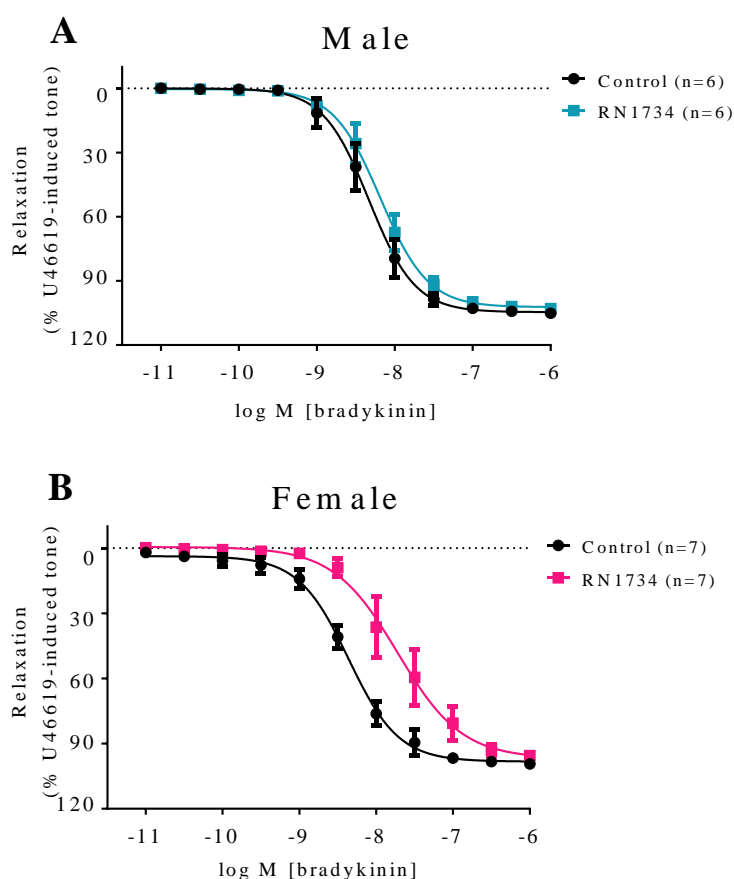


**Figure 6.8** Log concentration-response curves for the vasorelaxant effects of bradykinin in the presence of 30 μM RN1734 in U46619 pre-contracted porcine coronary arteries from (A) male and (B) female pigs. Data are expressed as a percentage change from U46619-induced tone and are mean ± S.E.M. of 6-7 experiments.
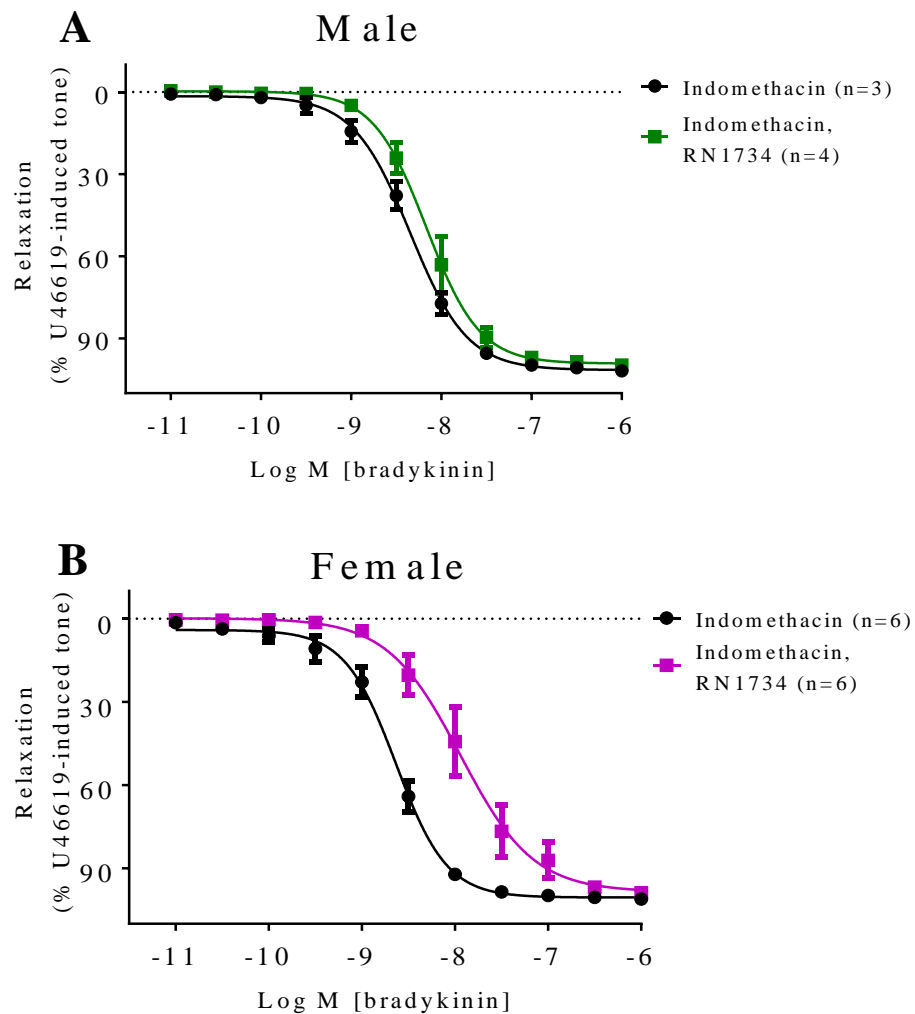
**Figure 6.9** Log concentration-response curves for the vasorelaxant effects of bradykinin in the presence of 10 μM indomethacin with or without 30 μM RN1734 in U46619 pre-contracted porcine coronary arteries from (A) male and (B) female pigs. Data are expressed as a percentage change from U46619-induced tone and are mean ± S.E.M. of 3-6 experiments.
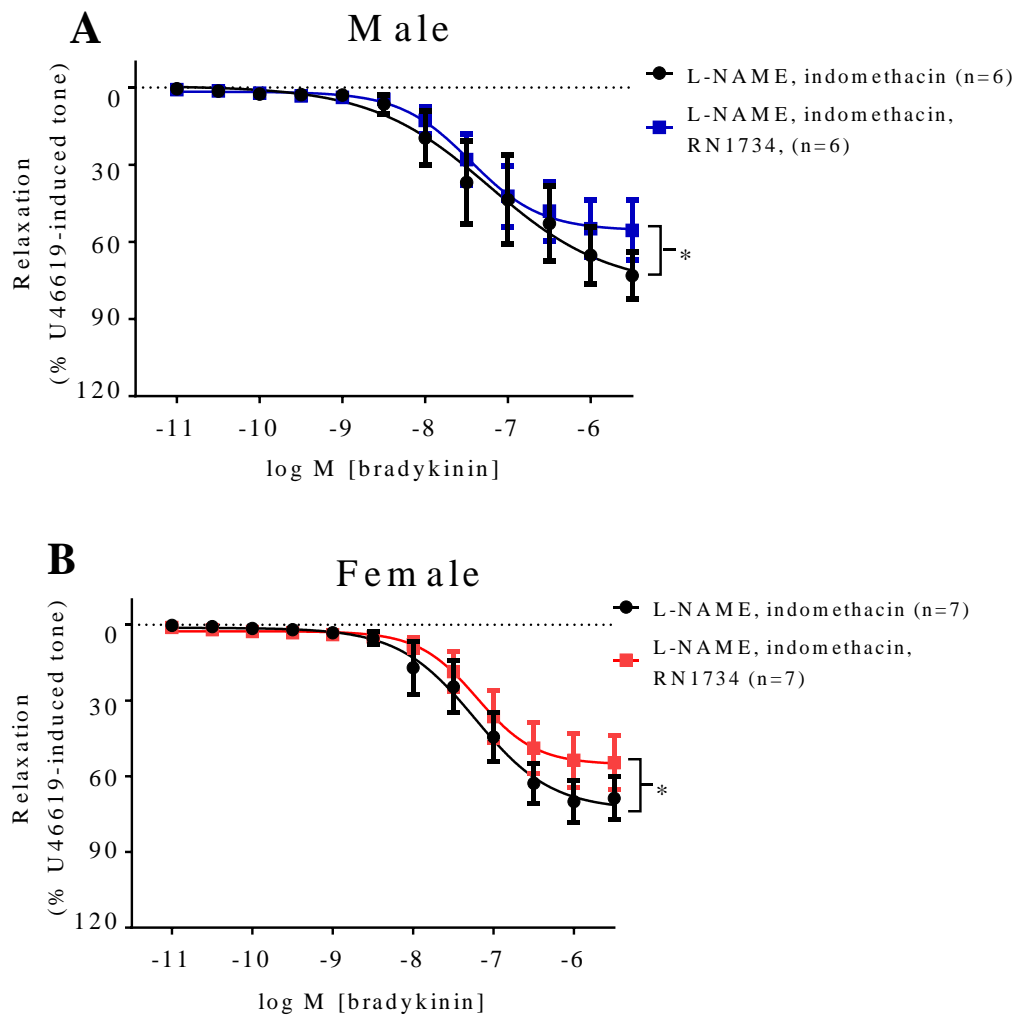
**Figure 6.10** Log concentration-response curves for the vasorelaxant effects of bradykinin in the presence of 300 μM L-NAME and 10 μM indomethacin with or without 30 μM RN1734 in U46619 pre-contracted porcine coronary arteries from (A) male and (B) female pigs. Data are expressed as a percentage change from U46619-induced tone and are mean ± S.E.M. of 6-7 experiments. *P<0.05; 2-tailed, paired Student's *t*-test.

**6.3.10 The effects of TRPMs and TRPCs (2-APB and ACA) antagonists in the presence of L-NAME and indomethacin on $H_2O_2$-induced vasorelaxation in PCAs from female pigs**

Next, the effects of various TRP channel antagonists on $H_2O_2$-induced vasorelaxation were studied as a previous study demonstrated a role for the TRPM2 channels in $H_2O_2$-induced calcium influx (Kraft *et al.*, 2004). Previous studies have also demonstrated that $H_2O_2$ is a factor for EDH-type responses (Matoba *et al.*, 2002; Matoba *et al.*, 2003; Matoba *et al.*, 2000; Miura *et al.*, 2003). Therefore, in the present study, relaxations were conducted in the presence of L-NAME and indomethacin. As Chapter 2 has demonstrated a role for $H_2O_2$ in bradykinin-induced vasorelaxation in PCAs from female but not male pigs, the present chapter only investigated the effects of TRP antagonists on $H_2O_2$-induced vasorelaxation in PCAs from female pigs only.

At 10 μM, 2-APB an antagonist of TRPMs and TRPCs channels, had no effect on the $H_2O_2$-induced vasorelaxation ($pEC_{50}= 3.77 \pm 0.07$) compared to the control ($pEC_{50}= 3.71 \pm 0.08$, *n*=8) (Figure 6.11A). However, at 100 μM, 2-APB significantly (P<0.001) shifted the curve 2.5-fold to the right ($pEC_{50} = 3.32 \pm 0.05$, *n*=8) (Figure 6.11A). As the data for 100 μM 2-APB did not achieve an $R_{max}$, all curves in Figure 6.11A were constrained to an $R_{max}$ of 100%.

ACA (20 μM), an antagonist of TRPMs and TRPCs channels, had no effect on the single concentration of $H_2O_2$-induced (100 μM) vasorelaxation (*n*=5) (Figure 6.11B). Here, a single concentration of $H_2O_2$ was used because the U46619-induced tone could not be maintained in the presence of 20 μM ACA, whereas at 100 μM ACA, U46619 failed to induce tone.

**Figure 6.11** Log concentration-response curves for the vasorelaxant effects of $H_2O_2$ in the presence of 300 μM L-NAME and 10 μM indomethacin, with or without (A) 10 μM or 100 μM 2-APB or (B) 20 μM ACA in U46619 pre-contracted porcine coronary arteries from female pigs. Data are expressed as a percentage change from U46619-induced tone and are mean ± S.E.M. of 5-8 experiments.
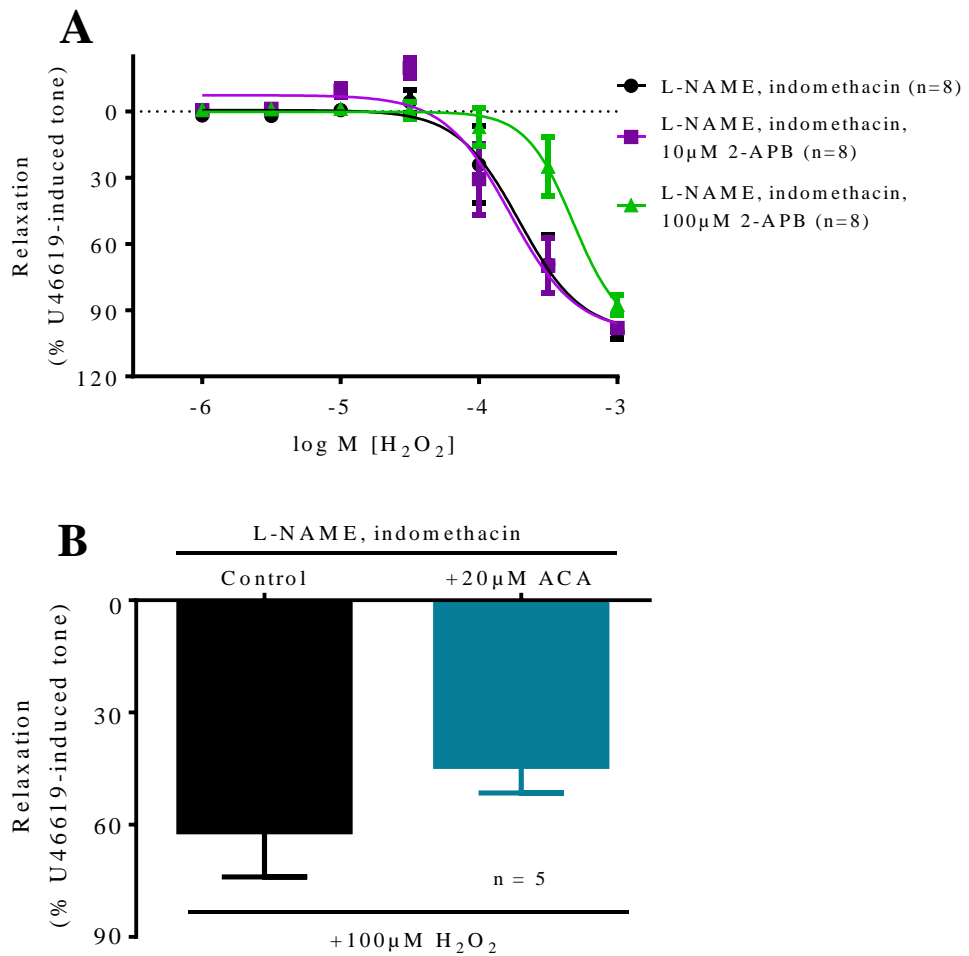
**6.3.11 The effects of selective TRPCs (SKF96365), TRPC3 (Pyr3) and TRPV4 (RN1734) antagonists in the presence of L-NAME and indomethacin on $H_2O_2$-induced vasorelaxation in PCAs from female pigs**

SKF96365 (10 μM), a non-selective TRPC channels antagonist, significantly inhibited the $R_{max}$ (P<0.01), but had no effect on the $pEC_{50}$ of the $H_2O_2$-induced vasorelaxation compared to the control ($pEC_{50}$= 4.01 ± 0.06, control; 4.04 ± 0.07, SKF96365, $n$=5) (Figure 6.12A). The $R_{max}$ of the $H_2O_2$-induced vasorelaxation under control conditions was significantly reduced (P<0.01) from 104 ± 7% to 84 ± 6% in the presence of SKF96365 ($n$=5).

Pyr3, a selective TRPC3 antagonist, had no effect on the $R_{max}$ or $pEC_{50}$ of the $H_2O_2$-induced relaxation in PCAs from female pigs ($n$=6) (Figure 6.12B). Whereas, 30 μM RN1734, a selective TRPV4 antagonist, significantly reduced (P<0.05) the $H_2O_2$-induced relaxation at 100 μM-1 mM $H_2O_2$ ($n$=5) (Figure 6.12C). Here, TRPV4 channels were examined because a previous study in human coronary arterioles reported that activation of TRPV4 channels with 4α-PDD increased superoxide and $H_2O_2$ formation (Bubolz *et al.*, 2012) and in human coronary artery endothelial cells, exogenously applied $H_2O_2$ sensitises TRPV4 to channel agonist (Zheng *et al.*, 2013a).
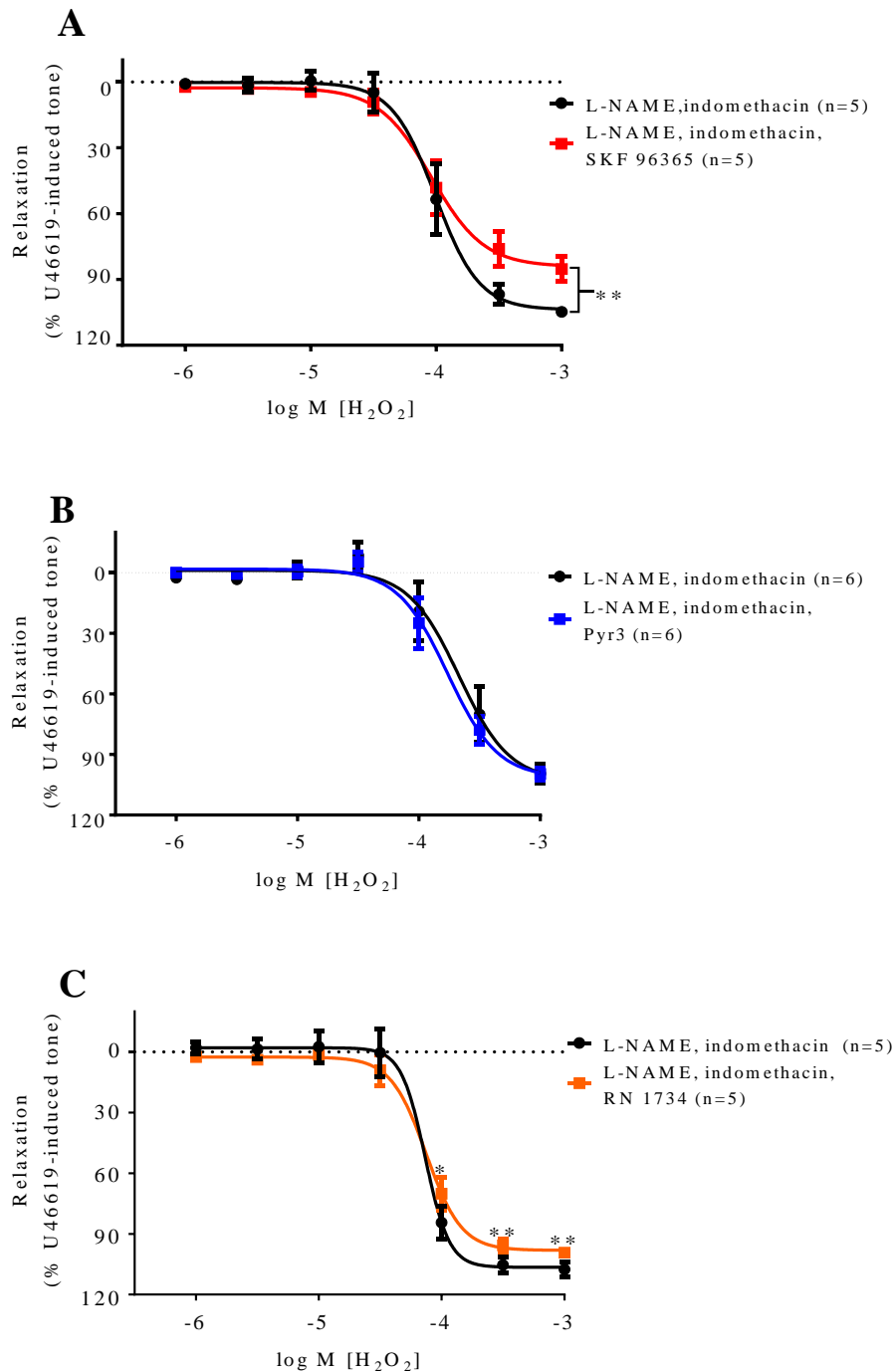
**Figure 6.12** Log concentration-response curves for the vasorelaxant effects of $H_2O_2$ in the presence of 300 μM L-NAME and 10 μM indomethacin with or without (A) 10 μM SKF96365, (B) 3 μM Pyr3 or (C) 30 μM RN1734 in U46619 pre-contracted porcine coronary arteries from female pigs. Data are expressed as a percentage change from U46619-induced tone and are mean ± S.E.M. of 5-6 experiments. *P<0.05, **P<0.01; 2-tailed, paired Student's *t*-test.

## 6.3.12 Determination of expression of TRPC3 and TRPV4 proteins in PCAs from male and female pigs via Western blotting

Western blot analysis of TRPC3 (Figure 6.13A) and TRPV4 (Figure 6.14A) protein expression levels demonstrated no differences between PCAs from male and female pigs. Quantification of the TRPC3 (Figure 6.13B) and TRPV4 (Figure 6.14B) proteins were analysed based on ratio of the protein band intensities to their respective loading control (GAPDH) within each lane.
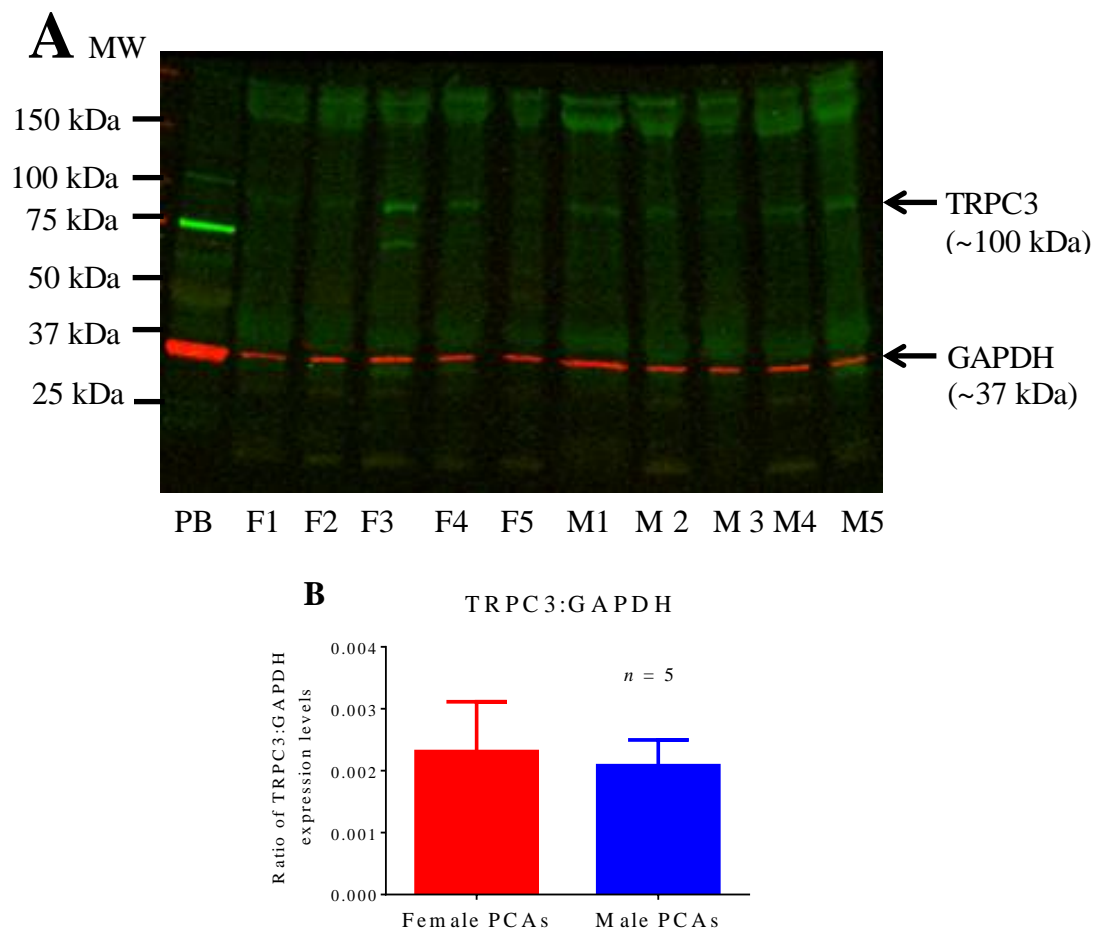


**Figure 6.13** (A) TRPC3 (~100 kDa) and GAPDH (~37 kDa) expression levels in 35 μg of porcine coronary artery homogenates (PCAs) from female (F1-F5) and male (M1-M5) pigs using 25 μg of pig brain (PB) lysates as positive control. (B) Ratio of expression levels of TRPC3 to GAPDH in PCAs from male and female pigs based on the intensities of the bands. Data are expressed in the ratio of protein to GAPDH intensities bands and are mean ± S.E.M. of 5 PCAs.
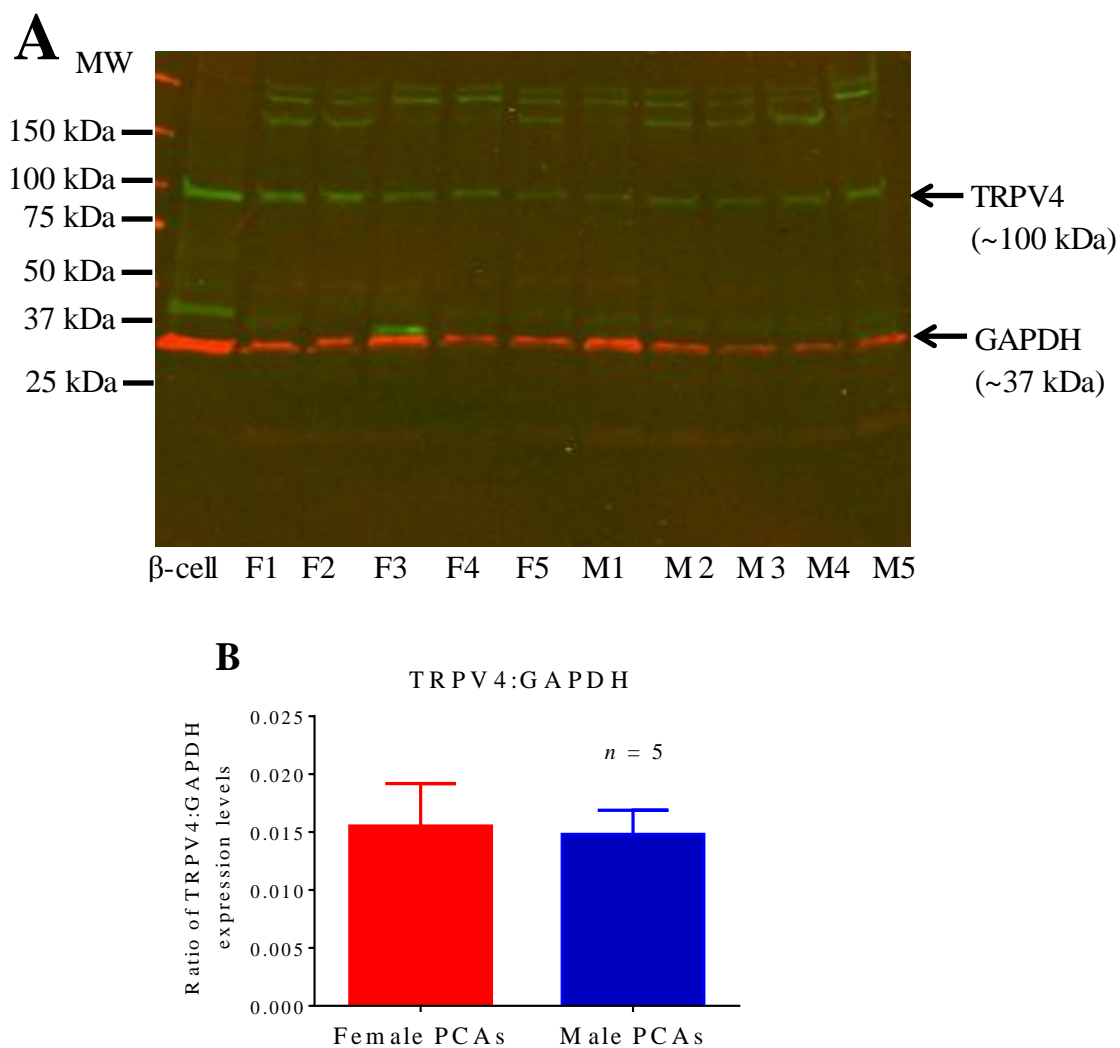
**Figure 6.14** (A) TRPV4 (~100 kDa) and GAPDH (~37 kDa) expression levels in 15 μg of porcine coronary artery homogenates (PCAs) from female (F1-F5) and male (M1-M5) pigs using 15 μg of human β-cell lysates as positive control. (B) Ratio of expression levels of TRPV4 to GAPDH in PCAs from male and female pigs based on the intensities of the bands. Data are expressed in the ratio of protein to GAPDH intensities bands and are mean ± S.E.M. of 5 PCAs.

## 6.4 Discussion

This chapter provides evidence for a functional role of TRP channels in endothelium-dependent and $H_2O_2$-mediated vasorelaxation in distal PCAs. Here, clear sex differences in the role of TRPC3 and TRPV4 channels in PCAs induced by bradykinin were demonstrated, where TRPC3 plays a role in the NO- and EDH-type response only in males, whereas TRPV4 plays a role in the endothelium-dependent vasorelaxation only in females.

Initial experiments in this chapter were performed using the commonly-used, but non-selective TRP channel inhibitor 2-APB. 2-APB significantly reduced the bradykinin-induced vasorelaxation and abolished the EDH-type response in PCAs from both male and female pigs. Using A23187, a calcium ionophore to examine the effects of 2-APB on the EDH-type responses demonstrated consistent results with the bradykinin-induced vasorelaxation, where the EDH-type response was abolished. These data suggest a role for TRP channels in the EDH-type response in the porcine coronary artery. However, 2-APB has been suggested to inhibit other channels including multiple voltage and $Ca^{2+}$-dependent $K^+$ conductance in pyramidal neurons (Hagenston *et al.*, 2009). This could explain the effects seen (where the EDH-type response was abolished) as $K_{Ca}$ channels on the endothelial cells play a role in the 'classical' EDH-type responses (Edwards *et al.*, 2010; Gluais *et al.*, 2005a).

2-APB (100 μM) reduced the potency of the $H_2O_2$-mediated vasorelaxation, suggesting a role for TRP channels in this response as well, although, again, an effect on $K^+$ channels cannot be ruled out. Another study has also demonstrated that 2-APB inhibits gap junctions (Bai *et al.*, 2006).

236

However, the effects of gap junctions in the $H_2O_2$-mediated response can be ruled out as the study from Chapter 3 has shown that a gap junction inhibitor has no effect on the $H_2O_2$-induced vasorelaxation. 2-APB can inhibit TRPM2 channels (Togashi *et al.*, 2008), therefore the effects of a purported inhibitor of TRPM2 channel inhibitor, ACA (Kraft *et al.*, 2006; Togashi *et al.*, 2008), were investigated. In $H_2O_2$-mediated vasorelaxation, 20 μM ACA had no effect on the $H_2O_2$-induced vasorelaxation in PCAs. This lack of effect could be due to the concentrations of inhibitor used. In previous studies using HEK293 cells transfected with human TRPM2 channels, 10 μM 2-APB and 20 μM ACA have been shown to completely inhibit whole cell current (Kraft *et al.*, 2006; Togashi *et al.*, 2008). In the present study, a higher concentration of inhibitors may be required due to lower penetration of the inhibitors into the multiple cell layers in blood vessels. However, with 100 μM ACA, PCAs failed to develop any U46619-induced tone and therefore the effect of higher concentrations of this compound on the $H_2O_2$ relaxation could not be studied. The shift in the potency of $H_2O_2$-mediated response in the presence of 2-APB may indicate a role for TRPM and TRPC channels in the $H_2O_2$-induced vasorelaxation. As a selective TRPM2 antagonist is currently unavailable, the functional roles of TRPM2 in $H_2O_2$-mediated and endothelium-dependent vasorelaxation remain to be explored.

As the data obtained with the non-selective TRP channel inhibitor, 2-APB indicated a potential role for TRP channels, the effects of a TRPC channels antagonist, SKF96365 (Huang *et al.*, 2011) on endothelium-dependent and $H_2O_2$-induced vasorelaxation were examined. In the bradykinin-induced endothelium-dependent vasorelaxation, the presence of SKF96365

reduced the $R_{max}$ in PCAs from male, but not female pigs. This could be due to differential regulation of the release of NO through TRPC channel activation. The role of NO playing a more prominent role in PCAs from male pigs compared to female pigs has been previously demonstrated in Chapter 2 and a previous study in PCAs demonstrated that inhibition of TRPC3 channels reduces the amount of endothelial NO released (Huang *et al.*, 2011). Here, it is possible that a significant reduction in the relaxation was not seen in PCAs from female pigs owing to the greater role that EDH plays in the endothelium-dependent vasorelaxation (McCulloch & Randall, 1998; White *et al.*, 2000). In the EDH-type responses, the presence of SKF96365 significantly reduced the $R_{max}$ in PCAs from both sexes indicating that TRPC channels play a role in the bradykinin-induced EDH-type response in both male and female pigs. It is possible that the reduction in EDH-type response is due to the reduction in increased $[Ca^{2+}]_i$ level due to the inhibition of SOCE by SKF96365 (Chen *et al.*, 2013) as endothelial $[Ca^{2+}]_i$ ions are required for activation of $SK_{Ca}$ and $IK_{Ca}$ channels in the EDH-type response (Edwards *et al.*, 2010). This possibility is further supported by the A23187 data where SKF96365 had no effect on the A23187-induced vasorelaxation in the EDH-type pathway. SKF96365 reduced the $R_{max}$ of the $H_2O_2$-induced vasorelaxation suggests that TRPC channels may also play a role in the $H_2O_2$-induced vasorelaxation.

To further study the role of TRPC channels, the effects of a selective TRPC3 antagonist, Pyr3 were investigated. The presence of Pyr3 reduced the potency of bradykinin in the NO- and EDH-type response in PCAs from male, but not female pigs and these differences are not due to the expression level of the protein as shown in the Western blot study. However, it is possible that

there are differences in the activation of the receptor, or downstream signalling. Interestingly, a previous study in porcine aortic endothelial cells suggested that TRPC3 channels can be activated by oxidative stress (Balzer *et al.*, 1999) and Chapter 5 of the present study demonstrated that NADPH oxidase generated reactive oxygen species play a role in PCAs from males but not females. Other studies have also reported that there is a greater oxidative stress observed in men compared to premenopausal women (Ide *et al.*, 2002) and higher superoxide anion generated in aortae from male rats compared to female rats (Brandes & Mugge, 1997). It is therefore possible that TRPC3 channels play a role in the endothelium-dependent and EDH-type vasorelaxation activated by reactive oxygen species in males. Furthermore, as discussed above, Huang *et al.,* (2011) reported that endothelial TRPC3 channel contributes to the bradykinin-induced NO release.

In contrast, the present study demonstrated that TRPC3 do not play a role in the $H_2O_2$-induced vasorelaxation suggesting that TRPC3 may not be activated by oxidative stress and this finding differ to that of Balzer *et al.* (1999) as mentioned above. The differences in finding could be due to the differences in experimental condition as the study by Balzer *et al.* (1999) was conducted on endothelial cells whereas the present study was conducted on whole vessels. Chapter 3 of the present study demonstrated that $H_2O_2$-induced vasorelaxation is endothelium-independent, therefore it is possible that endothelial TRPC3 is activated by oxidative stress as demonstrated by Balzer *et al.* (1999) which also support the finding from the present study using bradykinin as an endothelium-dependent vasorelaxant. Whereas in the $H_2O_2$-

induced vasorelaxation, it is possible that $H_2O_2$ had a direct effect on the vascular smooth muscle causing vasorelaxation through a different pathway.

Lastly, the effects of a selective TRPV4 antagonist, RN1734 on bradykinin-induced and $H_2O_2$-induced vasorelaxation in PCAs from male and female pigs were examined. In the present study, Chapter 2 demonstrated a role for the $IK_{Ca}$ channel in female but not male pigs in the bradykinin-induced EDH-type response. A study from another laboratory reported that TRPV4 and $IK_{Ca}$ channels cluster within the endothelial cells' projection toward the smooth muscle cells (Bagher *et al.*, 2012). Therefore, this chapter also examined if TRPV4 contribute to sex differences in endothelial function. In the bradykinin-induced vasorelaxation, this chapter showed sex differences in the effects of RN1734, indicating that TRPV4 channels play a role only in PCAs from female pigs. Similarly, sex differences in the functional response to RN1734 are not due to the expression level of the TRPV4 proteins. A previous study measuring flow induced dilatation of human coronary arterioles (HCAs) reported that RN1734 had no effect on the bradykinin-induced vasorelaxation (Bubolz *et al.*, 2012). One possible explanation for this observation is that the HCA from male and female subjects were not investigated separately. This study also reported that in HCAs, activation of TRPV4 channels using 4α-PDD enhanced the production of mitochondrial ROS, examined using MitoSOX (Bubolz *et al.*, 2012). In their HCAs perfusion study, catalase significantly inhibited the 4α-PDD-induced vasorelaxation and further semi-quantitative analysis using DCFH and DHE demonstrated that 4α-PDD significantly increased the $H_2O_2$ and superoxide production (Bubolz *et al.*, 2012). Chapter 2 of the present study reported that endogenous $H_2O_2$ plays a role in the

bradykinin-induced, NO-mediated pathway in PCAs from female but, not male pigs. Taking together the results from these studies, it is possible that inhibition of TRPV4 channels in the NO-mediated pathway reduced the production of endogenous $H_2O_2$, therefore reducing the potency of the bradykinin-induced vasorelaxation only in female pigs. In the EDH-type response induced by bradykinin, the presence of RN1734 had little effect on the $R_{max}$ in PCAs from both male and female pigs. Again, the slight reduction in vasorelaxation could possibly be due to the decrease in $[Ca^{2+}]_i$ release following inhibition of TRPV4 channels (Bubolz *et al.*, 2012). In the $H_2O_2$-mediated response, RN1734 caused a modest inhibition at 100 μM-1 mM $H_2O_2$. In a previous study using overexpressed TRPV4 channels in human coronary artery endothelial cells, a high concentration of $H_2O_2$ (1 mM) produced a transient increase in $[Ca^{2+}]_i$ whereas at 10 μM $H_2O_2$, the effects of TRPV4 agonist 4α-PDD-induced increased in $[Ca^{2+}]_i$ was enhanced (Zheng *et al.*, 2013a). Therefore, in this chapter, inhibition of the endothelial TRPV4 may have reduced the release of endothelial $[Ca^{2+}]_i$.

In summary, this chapter demonstrates clear sex differences in the role of TRPC3 and TRPV4 channels in the bradykinin-induced vasorelaxation, where TRPC3 plays a role in the NO- and EDH-type response in PCA from male pigs only, whereas TRPV4 plays a role in the NO-mediated response in PCA from female pigs only. This chapter further demonstrates that gender-specific drug treatment may be a potential strategy in the treatment for cardiovascular diseases in the future.

# *Chapter 7*

**General Discussion**

## 7.1 Sex differences in the endothelium-dependent vasorelaxation

In the present study, sex differences in endothelial function in PCAs have been clearly demonstrated where different ion channels and Nox isoforms have been found to be involved in the bradykinin-induced vasorelaxation in male and female pigs. Preliminary studies in Chapter 2 demonstrated that bradykinin is an endothelium-dependent vasorelaxant which stimulates the release of NO- and EDH-type responses in PCAs from male and female pigs and this finding is in agreement with previous studies in PCAs (Matoba et al., 2003; Nagao & Vanhoutte, 1992). This study was then extended to examine if there are any sex differences in the EDH-type response, defined as the remaining proportion of vasorelaxation which is insensitive to NO synthase and cyclo-oxygenase inhibition. Chapter 2 demonstrated that the NO-mediated vasorelaxation is more prominent in PCAs from males whereas the EDH-type response plays a greater role in females and this is in agreement with previous studies in rat mesenteric arteries and eNOS/COX-1 double knockout mice (McCulloch & Randall, 1998; Scotland *et al.*, 2005; White *et al.*, 2000).

As $H_2O_2$ has previously been proposed to be a factor for EDH-type relaxation in human and mouse mesenteric arteries, human and porcine coronary arteries (Matoba *et al.*, 2002; Matoba *et al.*, 2003; Matoba *et al.*, 2000; Miura *et al.*, 2003), the present study examined the role of $H_2O_2$ in bradykinin-induced vasorelaxation in PCAs. Chapter 2 demonstrated that endogenous $H_2O_2$ plays a role in the bradykinin-induced vasorelaxation only in PCAs from female pigs and is not a factor for EDH-type response in PCAs from both sexes. Possible explanations for differences in the EDH-type

response between the present study and previous studies have been discussed in detail in Chapter 2.

Chapter 2 demonstrated that whilst $SK_{Ca}$ channels play a role in PCAs from both male and female pigs, $IK_{Ca}$ channels and gap junctional communication appear to be more important in the EDH-mediated pathway in PCAs from female pigs. These mechanisms could possibly be acting as compensation for the diminished response in the NO-mediated pathway in PCAs from female pigs. Indeed, previous studies in saphenous arteries from male obese rats and mesenteric arteries from male ZDF rats reported an up-regulation in expression and activity of $IK_{Ca}$ channels and gap junction communication to compensate for the loss of NO-mediated response (Chadha *et al.*, 2010; Schach *et al.*, 2014). However, Western blot study did not detect any differences in protein expression for Cx40, Cx43 and $IK_{Ca}$ channels in PCAs from male and female pigs. The upregulated EDH-type response in females may be a possible explanation for the lower cardiovascular risk observed in premenopausal women compared to age-matched men or postmenopausal women.

As $H_2O_2$ was shown to play a role in the endothelium-dependent vasorelaxation, Chapter 3 and Chapter 6 examined the mechanism of action of exogenously applied $H_2O_2$-induced vasorelaxation in PCAs from male and female pigs, specifically in the role of $K^+$ channels and TRP channels respectively. Furthermore, previous studies in human subjects have reported that the plasma level of $H_2O_2$ is significantly higher in subjects with essential hypertension compared to normotensive subjects (Lacy *et al.*, 2000) and during inflammation, activated macrophages may produce up to 100 μM of $H_2O_2$

locally (Droge, 2002). Therefore, further understanding on the mechanism of action of $H_2O_2$ may be beneficial for future drug development (Burgoyne *et al.*, 2013). Chapter 3 demonstrated that $H_2O_2$-induced vasorelaxation was unaffected by removal of the endothelium, inhibition of NOS, cyclo-oxygenase, gap junctions, $SK_{Ca}$, $IK_{Ca}$, $BK_{Ca}$, $K_{ir}$, $K_V$, $K_{ATP}$, cGMP or $Na^+/Ca^{2+}$ exchanger. However, the presence of ouabain significantly inhibited the $H_2O_2$-induced vasorelaxation at concentrations up to 100 μM. At higher concentrations of $H_2O_2$ (1 mM), a biochemical assay demonstrated that the $Na^+/K^+$ pump was inhibited, possibly due to dysfunction of the $Na^+/K^+$-pump (Elmoselhi *et al.*, 1994; Kim & Akera, 1987). On the other hand, it was demonstrated in Chapter 6 that TRP channels may also play a role in the $H_2O_2$−induced vasorelaxation as 2-APB (non-selective TRPM and TRPC antagonist), SKF96365 (TRPC antagonist) and RN1734 (TRPV4 antagonist) but not Pyr3 (TRPC3 antagonist), significantly inhibited the $H_2O_2$−induced vasorelaxation. However, future studies involving more selective antagonists or siRNAs may be required. Furthermore, the signalling pathway of the $H_2O_2$−mediated response was not examined in the present study. Therefore, the mechanism by which $H_2O_2$ alters TRP channel activity needs to be investigated. Nonetheless, previous studies using Rp-8-Br-cGMPS to inhibit protein kinase G1α (PKG1α) in porcine coronary arteries, human coronary arterioles and mouse mesenteric arteries demonstrated that dimerization of the PKG1α plays a role in the $H_2O_2$-induced vasorelaxation and hyperpolarization (Dou *et al.*, 2012; Ohashi *et al.*, 2012; Zhang *et al.*, 2012a). In these studies, 100 μM and 1 mM of $H_2O_2$ significantly increased the protein expression of PKG1 dimer (Dou *et al.*, 2012; Zhang *et al.*, 2012a). Due to the lack of effects

of ODQ on $H_2O_2$-induced vasorelaxation, Zhang *et al.* (2012) suggested that $H_2O_2$ acts on downstream signalling of sGC in human coronary arterioles. On the other hand, Ohashi *et al.* (2012) reported that the effect of Rp-8-Br-cGMPS is vascular bed dependent, where the PKG1$\alpha$ pathway only plays a role in the $H_2O_2$-induced vasorelaxation in mouse mesenteric arteries, but not aortae.

In Chapter 4, different gassing conditions (95% $O_2$/5% $CO_2$ or 95% air/5% $CO_2$) on bradykinin- and $H_2O_2$-induced vasorelaxation in PCAs from male and female pigs were examined as previous studies have demonstrated that low oxygen tension affects synthesis of NO and superoxide anions react readily with NO to form peroxynitrite (Kerr *et al.*, 1999; Kim *et al.*, 1993; Palmer *et al.*, 1987). Chapter 4 demonstrated that when gassed with 95%$O_2$/5% $CO_2$, Tiron[®], a superoxide scavenger is likely to have converted superoxide generated in the Krebs'-Henseleit solution into $H_2O_2$ and enhances the bradykinin-induced vasorelaxation in PCAs from both male and female pigs. Further Amplex Red assay confirmed the formation of $H_2O_2$ in the Krebs'-Henseleit buffer when gassed with 95%$O_2$/5% $CO_2$ in the presence of Tiron[®] independent of tissue. Hyperoxic gassing conditions may possibly be generating superoxide within the Krebs-Henseleit buffer and may affect *in vitro* pharmacological responses involving endothelium-dependent vasorelaxation. Therefore, *in vitro* organ studies involving reactive oxygen species should be interpreted with care. Gassing with 95% air/5% $CO_2$ should preferably be used in organ bath studies as it is more physiological relevant. Furthermore, Chapter 4 demonstrated that gassing with 95% air/5% $CO_2$ does not generate $H_2O_2$ in the Krebs-Henseleit buffer in the presence of Tiron[®].

Chapter 5 explored the possibility of sex differences in the Nox-generation of ROS pathway using Nox inhibitors, DPI, ML-171 and VAS2870 as previous studies have reported greater oxidative stress in males compared to females (Brandes & Mugge, 1997; Ide *et al.*, 2002; Kerr *et al.*, 1999) and Nox is a source of superoxide generation in the endothelial cells (Shimokawa & Morikawa, 2005). In this chapter, inhibition of Nox with DPI and ML-171 enhances while VAS2870 inhibited the EDH-type response only in PCAs from male, but not female pigs. This suggests that in vessels where the endothelial function of NO and $PGI_2$ is compromised, the role of Nox-generated ROS was uncovered only in PCAs from males but not females. Western blot analysis in this chapter demonstrated that a higher level of Nox1 and Nox2 proteins are expressed in PCAs from males compared to females. This may underlie the greater oxidative stress observed in men, whereby increased ROS production through Nox1 and Nox2 leads to a reduction in the EDH-type response. Putting together the results from Chapter 2 and Chapter 5, the present study demonstrated sex differences in the different pathways involved in the EDH-type mediated response where $IK_{Ca}$ and gap junctional communications are involved in PCAs from females while the Nox-generated ROS only plays a role in the EDH-type response in males. However, given the possibilities that ML-171 or VAS2870 may have non-selective effects on different Nox isoforms, future studies using siRNAs selective for Nox1 and Nox4 may be required for further verifications. Furthermore, as discussed in Chapter 1, Nox4-generated ROS may exert both protective (Ray *et al.*, 2011) and detrimental (Kleinschnitz *et al.*, 2010) effects depending on the species or vascular bed of study. Therefore, future studies involving *in vivo* work may

provide information about the overall effect on different vascular bed. Whereas, as for the opposing effects of VAS2870 observed in the present study compared to a previous study in mice where treatment with VAS2870 after ischaemia improve neurological functions (Kleinschnitz *et al.*, 2010), further studies involving vessels from human subjects of specified sex may be required.

Having demonstrated sex differences in oxidative stress in endothelial function in Chapter 5 and sex differences in the role of gap junctional communication and $IK_{Ca}$ channels in the EDH-type response in Chapter 2, Chapter 6 examined if there are any sex differences in the role of TRP channels in PCAs. TRPC and TRPV4 channels have previously been reported as mediators of oxidative stress in porcine aortic endothelial cells and human coronary arteries (Balzer *et al.*, 1999; Bubolz *et al.*, 2012; Poteser *et al.*, 2006). In PCAs, TRPC3 channels have been reported to be involved in NO release (Huang *et al.*, 2011) whereas in rat mesenteric arteries, TRPC3 channels have been reported to be highly expressed in the internal elastic lamina holes in close proximity with MEGJs and $IK_{Ca}$ channels (Senadheera *et al.*, 2012). Similarly in rat cremaster arterioles, TRPV4 channels and $IK_{Ca}$ channels have been reported to cluster within the endothelial cell projection microdomain (Bagher *et al.*, 2012). In the present study, Chapter 6 demonstrated sex differences in the role of TRPC3 and TRPV4 channels in the bradykinin-induced vasorelaxation, where TRPC3 plays a role in the NO- and EDH-type response in PCAs from male pigs only, whereas TRPV4 plays a role in the NO-mediated response in PCAs from female pigs only. However, the differences in the bradykinin-induced vasorelaxation were not attributed to the

differential expression of TRPC3 or TRPV4 proteins. As discussed in Chapter 6, it is possible that the bradykinin-induced NO release which is more prominent in males (Chapter 2) is affected by endothelial TRPC3 channels. Whereas in the EDH-type vasorelaxation, TRPC3 channels could have been activated by ROS (Balzer *et al.*, 1999) in PCAs from males only as previous studies and Chapter 5 of the present study have demonstrated greater oxidative stress in males compared to females (Brandes & Mugge, 1997; Ide *et al.*, 2002). As for the role of TRPV4 in the bradykinin-induced vasorelaxation observed only in PCAs from females, it is possible that activation of the TRPV4 channels stimulates the production of ROS (Bubolz *et al.*, 2012). Chapter 2 demonstrated that $H_2O_2$ plays a role only in PCAs from female pigs, therefore inhibition of TRPV4 channels could have reduced the production of endogenous $H_2O_2$. For further confirmation, again use of siRNA selective for TRPC3 and TRPV4 may be required. Furthermore, immunohistochemical studies to detect the distributions of these channels may provide further understanding of the roles of these channels in the vessels.

## 7.2 Seasonal variations in the EDH-type vasorelaxation

In general, although Figure 2.7A in Chapter 2 clearly demonstrated a greater EDH-type response in PCAs from females compared to males, it was noted that the EDH-type response varied from ~45% to 100% throughout the study. Here, the EDH-type response induced by bradykinin (Figure 7.1 A and B) or A23187 (Figure 7.2) in PCAs from male and female pigs appeared to be greater during summer compared to winter. It is therefore possible that there are seasonal variations in the EDH-type responses in the PCAs. Interestingly, a population based human study reported a significant seasonal variation of sudden death related to cardiovascular disease, particularly in patients over 65 (Arntz *et al.*, 2000). The number of sudden death events occurred highest during winter months (December to February, $n = 6493$) and lowest during summer months (June to August, $n = 5472$) (Arntz *et al.*, 2000). Here, the seasonal variations in the cardiovascular events could possibly be related to the vitamin D status through exposure to sunlight during summer, however further work measuring serum vitamin D levels during different seasons may be required. A previous study in haemodialysis patients reported that the risk of sudden cardiac death events in patients with severe vitamin D deficiency is 3-fold higher than those with sufficient vitamin D levels (Drechsler *et al.*, 2010). In an animal study, the mean arterial pressure and heart rate were significantly higher in vitamin D deficient male and female rats (Tare *et al.*, 2011). Further vascular functional studies in these rat mesenteric arteries demonstrated endothelial dysfunction in vitamin D deficient male and female rats (Tare *et al.*, 2011).
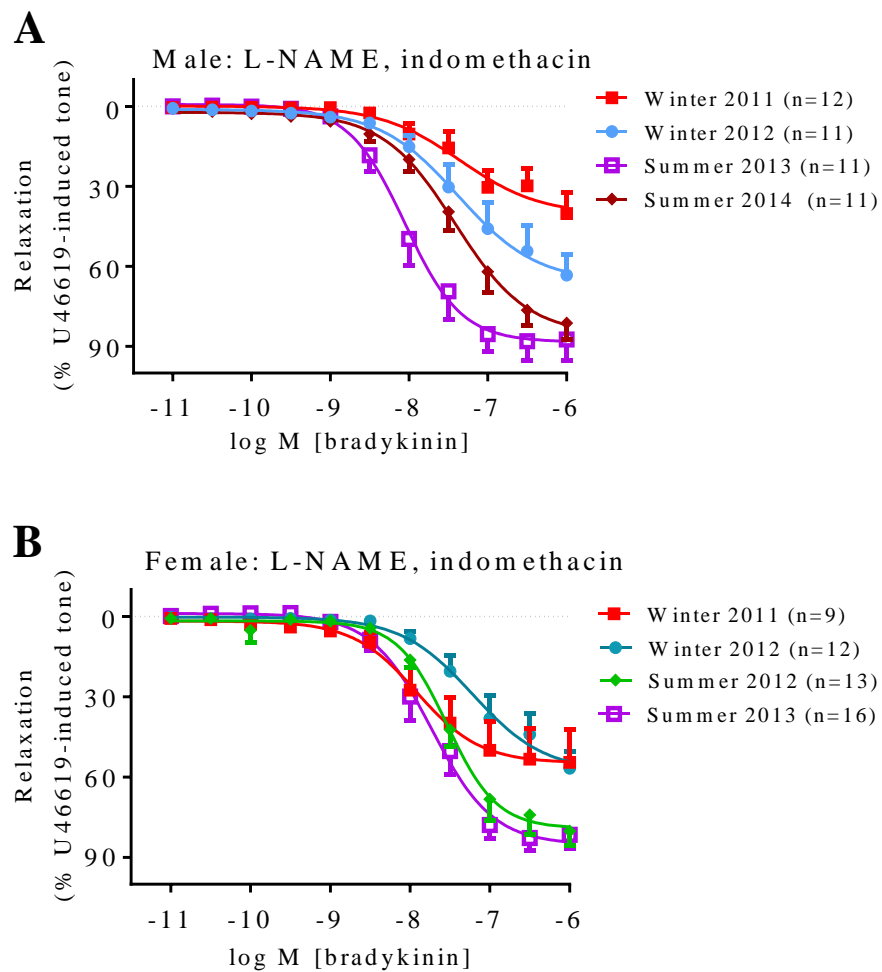
**Figure 7.1** Seasonal variations in the bradykinin-induced EDH-type response in porcine coronary arteries from (A) male and (B) female pigs. Data are expressed as a percentage change from U46619-induced tone and are mean ± S.E.M. of 9-16 experiments (Figures compiled from Chapters 2 - 6).
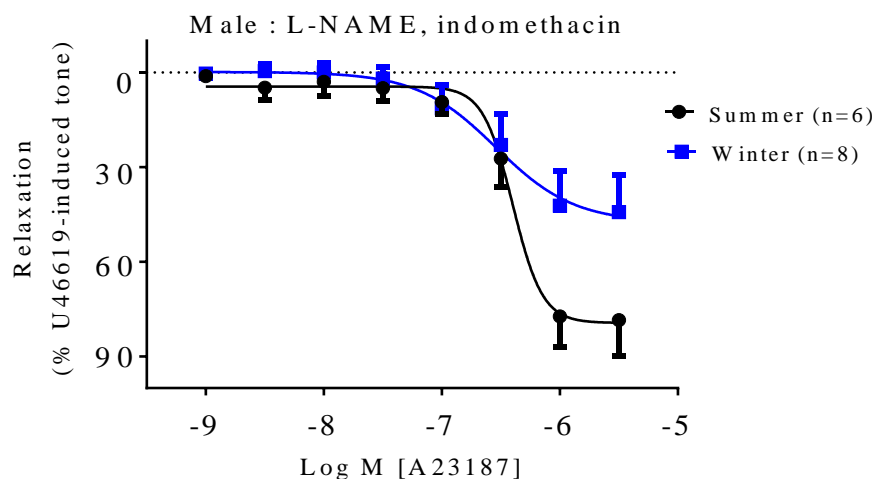
**Figure 7.2** Seasonal variations in the A23187-induced EDH-type response in porcine coronary arteries from male pigs. Data are expressed as a percentage change from U46619-induced tone and are mean ± S.E.M. of 6-8 experiments (Figure taken from Chapter 6).

Despite the fact that each set of data has been compared with their internal contemporaneous control and sex differences in the role of MEGJs, $IK_{Ca}$ channels, Nox-generated ROS and TRP channels have been demonstrated, limitations of the present study include the possibility of seasonal variation in the roles of these protein channels or Nox-generated ROS. Apart from that, oestrus cycle of the female pigs was not documented. However, this could also be a good representation of a randomised population group study and future work involving human arteries may be required due to the possibility of variations in species or vascular bed of study (Feletou & Vanhoutte, 2006).

## 7.3 Conclusions

The present study demonstrated clear sex differences in the endothelial function in PCAs and examined the effects of different gassing conditions (95% oxygen vs 95% air) on bradykinin-induced vasorelaxation in PCAs from male and female pigs. This study also investigated the mechanism of action of $H_2O_2$–induced vasorelaxation in PCAs, specifically the role of different $K^+$ channels. Chapter 2 demonstrated greater EDH-type response in PCAs from females compared to males and showed that $H_2O_2$ plays a role in the bradykinin-mediated response only in female pigs. Chapter 2 further demonstrated sex differences in the entity which regulates the EDH-type responses where MEGJs and $IK_{Ca}$ play a role in the bradykinin-induced vasorelaxation in PCAs from female but not male pigs.

Chapter 3 demonstrated a possible role for the sodium-pump in $H_2O_2$–induced vasorelaxation in PCAs, however further study involving the signalling pathway of $H_2O_2$ remains to be elucidated. Chapter 4 established that hyperoxic gassing conditions generated superoxide in the Krebs'-Henseleit buffer, which was then converted to $H_2O_2$ in the presence of Tiron® and subsequently enhanced the bradykinin-induced vasorelaxation. Chapter 5 and 6 further demonstrated sex differences in the endothelial function where oxidative stress plays a greater role in the EDH-type response in PCAs from male pigs which may possibly influenced the role of TRPC3 channels in bradykinin-induced response only in PCAs from male pigs. On the other hand, the role of $H_2O_2$ in PCAs from female pigs could be associated with endothelial TRPV4 channels. Therefore, gender-specific drug treatment may represent a potential strategy in the treatment for cardiovascular diseases.

# *Appendices*

# A. List of buffers and chemicals used for Western Blot

## 1. Lysis buffer

|  | Concentration |
| --- | --- |
| **Tris** | 20 mM |
| **EGTA** | 1 mM |
| **Sucrose** | 320 mM |
| **Triton X100** | 0.1% |
| **Sodium fluoride** | 1 mM |
| **β-glycerophosphate** | 10 mM |
| pH to 7.6 | |

**Table 1** List of materials in lysis buffer.

## 2. MAPK homogenisation buffer

|  | Concentration |
| --- | --- |
| **Sodium β-glycerophosphate** | 80 mM |
| **Imidazole** | 20 mM |
| **Dithiothreitol** | 1 mM |
| **Sodium fluoride** | 1 mM |
| pH to 7.6 | |

**Table 2** List of materials in MAPK homogenisation buffer.

## 3. Tris-buffered saline containing 0.1% Tween 20 (TBS-T)

|  | Concentration |
| --- | --- |
| **Tris** | 25 mM |
| **NaCl** | 125 mM |
| **Tween 20** | 0.1% |
| pH to 7.6 | |

**Table 3** List of materials in TBS-T.

## 4. 6x solubilisation buffer

|  | Concentration | |
| --- | --- | --- |
| **24% SDS** | 4% | 2.4 g |
| **30% Glycerol** | 5% | 3 mL |
| **β-mercaptoethanol** | 5% | 3 mL |
| **2.5% BPB** | 0.01% | 240 μL |
| **1.5 M Tris-HCl** | 0.0625 M | 2.5 mL |
| Make up to 10 mL (Store at -20C) | | |

**Table 4** List of materials in 6x solubilisation buffer.

**5. Protease Inhibitor Cocktail Set I (Calbiochem)**

| Product | Concentration | Target protease |
|---|---|---|
| **AEBSF hydrochloride** | 500 μM | Serine proteases |
| **Aprotinin, bovine lung, crystalline** | 150 nM | Serine proteases and esterases |
| **E-64 Protease inhibitor** | 1 μM | Cysteine proteases |
| **EDTA, disodium** | 0.5 mM | Metalloproteases |
| **Leupeptin, hemisulfate** | 1 μM | Cysteine and trypsin-like proteases |

**Table 5** List of materials in protease inhibitor cocktail Set I

**6. 10X electrophoresis buffer**

| | |
|---|---|
| **Tris** | **30.3 g** |
| **Glycine** | 144 g |
| **Dissolve in dH$_2$O** | 8 L |
| **Add methanol** | 2 L |
| **Store at 4°C** | |

**Table 6** List of materials in 10X electrophoresis buffer

**7. Transfer buffer**

| | |
|---|---|
| **Tris** | **30.3 g** |
| **Glycine** | 144 g |
| **SDS** | 10 g |
| **Make up to 1 L in dH$_2$O** | |

**Table 7** List of materials in transfer buffer

## B. Method development for Western Blot in Chapter 2

**1. Connexin 43 (C8093 Sigma-Aldrich, Poole, Dorset, UK)**
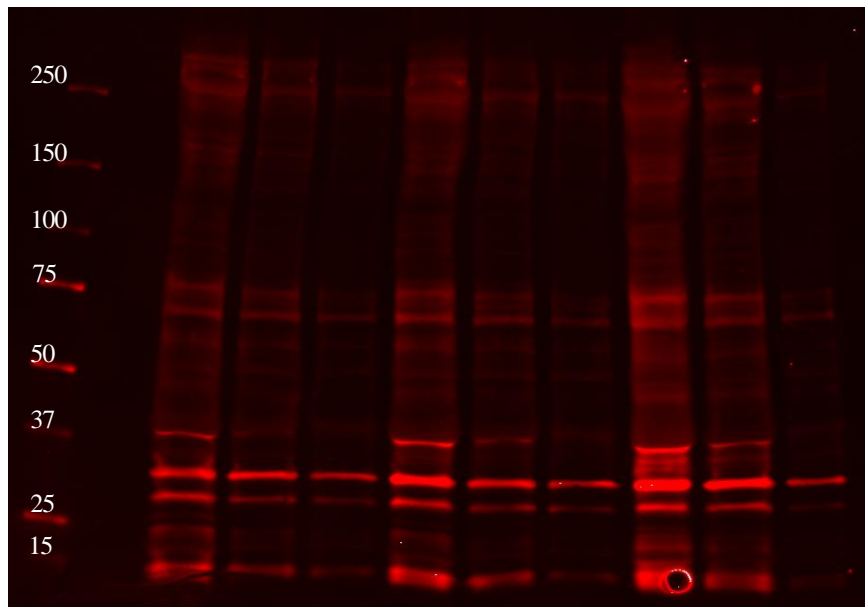


**Figure 1** Western blot analysis of connexin 43 protein for three different PCAs samples at 20 μg, 10 μg and 5 μg of protein concentration detected using rabbit polyclonal anti-Cx43 antibody (1:1000) from **Cell Signalling** blocked with 1.5% fish skin gelatine. Multiple bands were detected with no band detected at the molecular weight of Cx43 (~43 kDa).
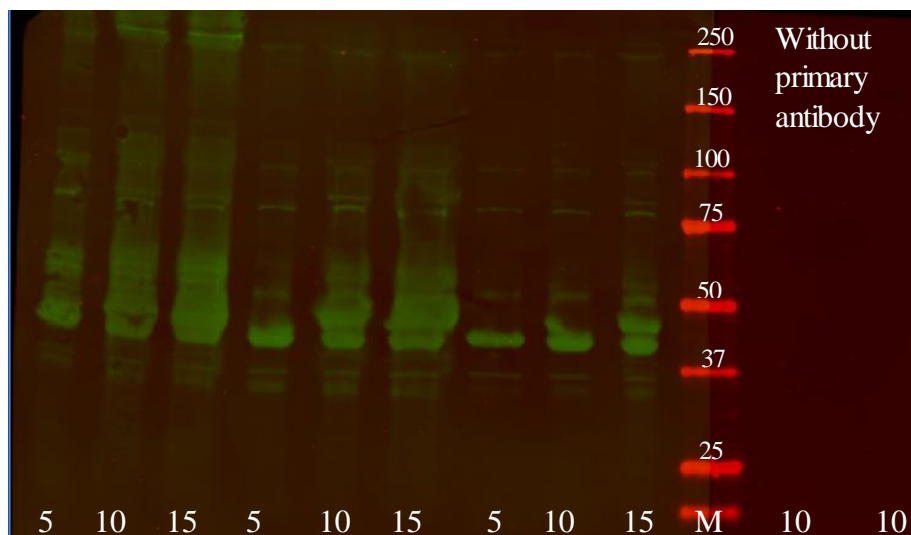


**Figure 2** Western blot analysis of connexin 43 protein for three different PCAs samples at 5 μg, 10 μg and 15 μg protein concentration using mouse monoclonal anti-Cx43 antibody (1:1000) from **Sigma-Aldrich** (lot no. of 080M4846) with 1.5% fish skin gelatine as blocking agent. Multiple bands were detected with strong band detected at the correct molecular weight (~43 kDa). Last two lanes were incubated with blocking agent in the absence of primary antibody.
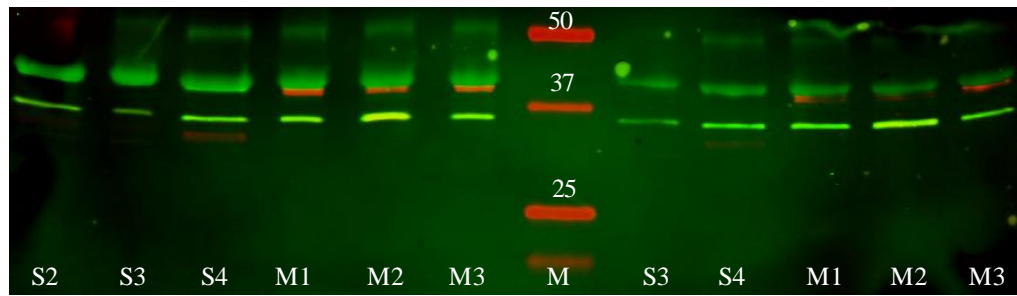
**Figure 3** Western blot analysis of connexin 43 (43 kDa) protein in PCAs from female (S2-S4) and male pigs (M1-M3) with the first six lanes loaded with 5 µg protein and the last five lanes with 2.5 µg protein concentrations. Using 5% milk as blocking agent, Cx43 proteins were incubated with anti-Cx43 antibody (1:1000) (green band) from Sigma-Aldrich (lot no. of 080M4846) and rabbit monoclonal anti-GAPDH antibody (36 kDa) (1:20,000) (red band).
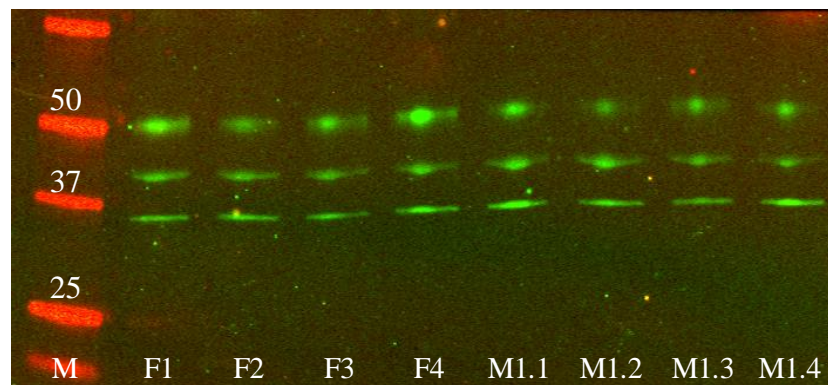


**Figure 4** Western blot analysis of connexin 43 (43 kDa) protein using 5% milk as blocking agent, incubating blot with anti-Cx43 antibody (1:1000) from Sigma-Aldrich (lot no. 080M4846) in 2.5µg PCAs from female (F1-F4) and male pigs (M1.1-M1.4). In an attempt to analyse the protein concentration between male and female PCAs, three bands were detected instead of one band (as specified by the manufacturer). A replacement antibody from a different batch was subsequently tested (lot no. 052M4834).
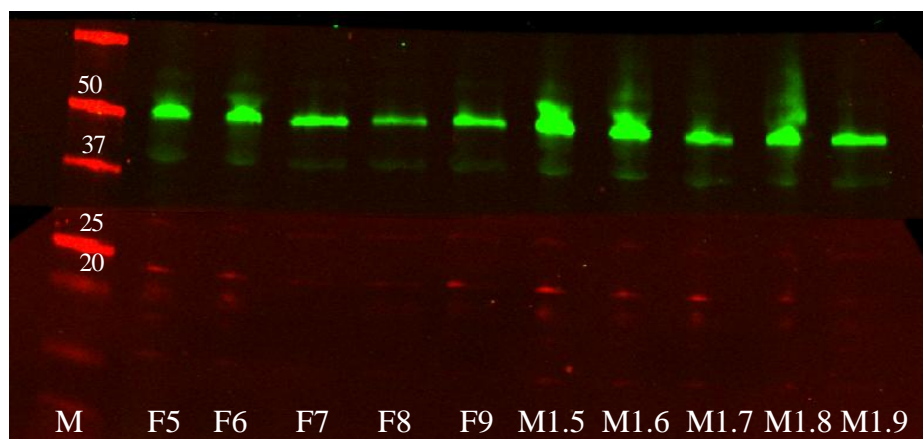
**Figure 5** Western blot analysis comparing expression level of Cx43 in 5 μg of PCAs from male (M1.5-M1.9) and female (F5-F9) pigs using a different batch of Cx43 antibody (lot no. 052M4834) (1:1000) and MLC (1:1000). Samples (not previously gassed) were homogenized in freshly prepared lysis buffer without triton-X. Results could not be analysed as a strong band was observed at 50 kDa instead of 43 kDa and MLC as the loading control band was too faint. A higher concentration of MLC antibody was used in further study.
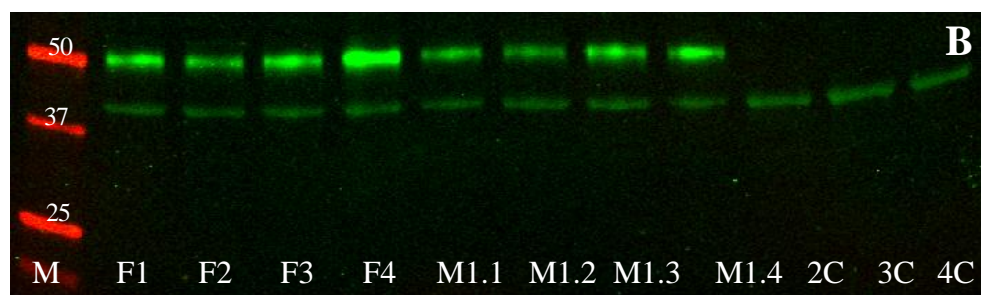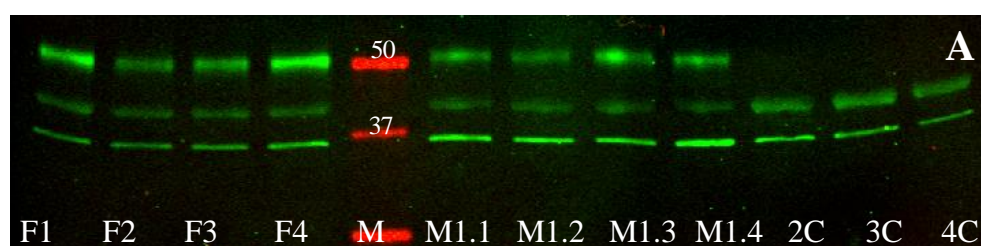


**Figure 6** Western blot analysis comparing two different batches of Cx43 antibody (1:1000) from Sigma-Aldrich using the same PCAs samples from male (M1.1-M1.4) and female (F1-F4, 2C-4C) pigs (6 μg proteins). Samples 2C-4C (homogenised in MAPK lysis buffer) were samples previously gassed with 95% $O_2$ at 37°C for other studies while the remaining samples were finely dissected tissues and stored at -80°C until further use. Here, comparing the results of the first batch of antibody (lot no. 080M4846) (A) with the replacement antibody (lot no. 052M4834) (B) demonstrated that the first batch of antibody detected one extra band at 37 kDa. Results also demonstrated that previously gassed samples (2C-4C) do not display the 50 kDa bands. Therefore, using the replacement antibody, further studies using PCAs samples treated under different conditions were conducted.
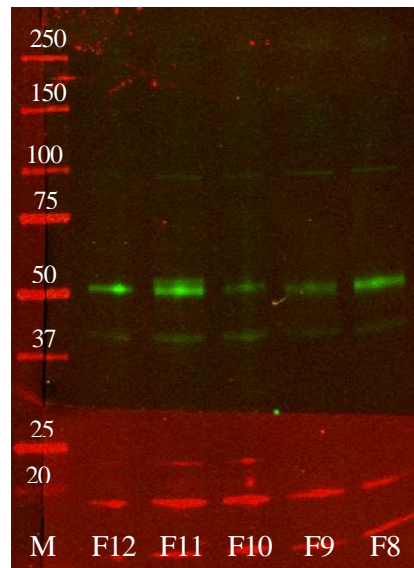
**Figure 7** Western blot analysis comparing samples homogenised in different lysis buffer using 5 µg PCAs from female pigs incubated overnight with Cx43 antibody (lot no. 052M4834) (1:1000) and MLC (1:500) (18 kDa). Samples (F10-F12) were homogenized in freshly prepared MAPK lysis buffer while samples F8 and F9 were same samples as Figure 8.5. Strong band was still detected at 50 kDa and no differences were observed between samples homogenised in different lysis buffer.
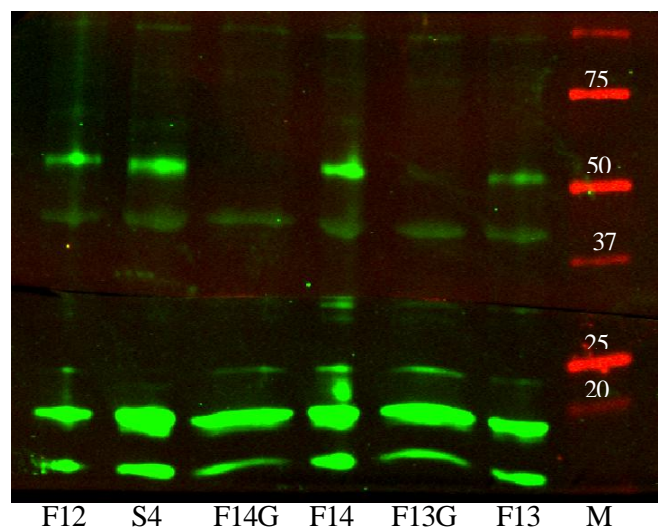


**Figure 8** Western blot analysis comparing samples prepared under different conditions using 5 µg PCAs from female pigs incubated overnight with Cx43 antibody (lot no. 052M4834) (1:1000) and MLC (1:500) (18 kDa). F12 and S4 were previously used sample as above while F13&F13G and F14&F14G are samples from the same PCAs. F13G and F14G were gassed with 95%$O_2$ at 37°C in the myograph subjected to tension, KCl, U46619 and bradykinin and a single band was form at ~43 kDa.
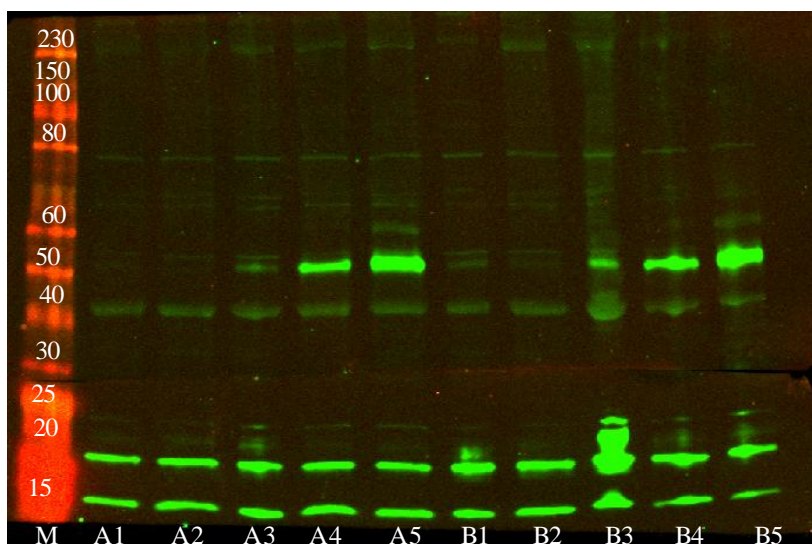
A1/B1 - No tension (at 37°C with 95% O$_2$)
A2/B2 - Tension (at 37°C with 95% O$_2$)
A3/B3 - RT with 95% O$_2$
A4/B4 - RT without oxygen
A5/B5 - fresh tissue finely dissected on the same day of delivery then stored at -80°C

**Figure 9** Western blot analysis comparing samples prepared under different conditions as described above using 5 μg PCAs from female pigs incubated overnight with Cx43 antibody (lot no. 052M4834) (1:1000) and MLC (1:500) (18 kDa). Samples A1-A5 and B1-B5 were from the same PCA. Samples A1-A4 and B1-B4 were samples stored overnight at 4°C in 2% w/v Ficoll Krebs'-Henseleit solution.
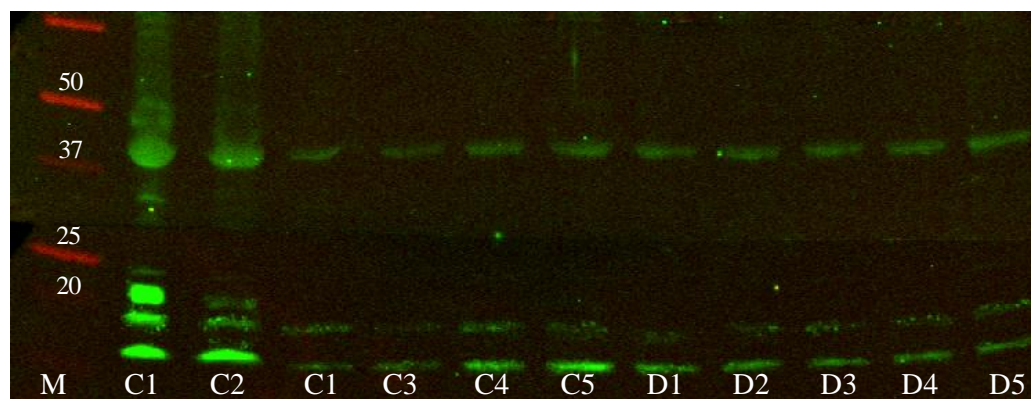


C1/D1 – Gas with 95% nitrogen at 37°C
C2/D2 - No gas at 37°C
C3/D3 - Gas with 95% O$_2$ at 37°C
C4/D4 – 1000 UmL$^{-1}$ catalase
C5/D5 – 1mM Tiron$^{®}$

**Figure 10** Western blot analysis comparing samples prepared under different conditions as described above using 5 μg PCAs from female pigs incubated overnight with Cx43 antibody (lot no. 052M4834) (1:1000) and MLC (1:500) (18 kDa). No band was observed at 50 kDa.

262

## 2. Connexin 40 (ab38580 Abcam®, Cambridge, UK)
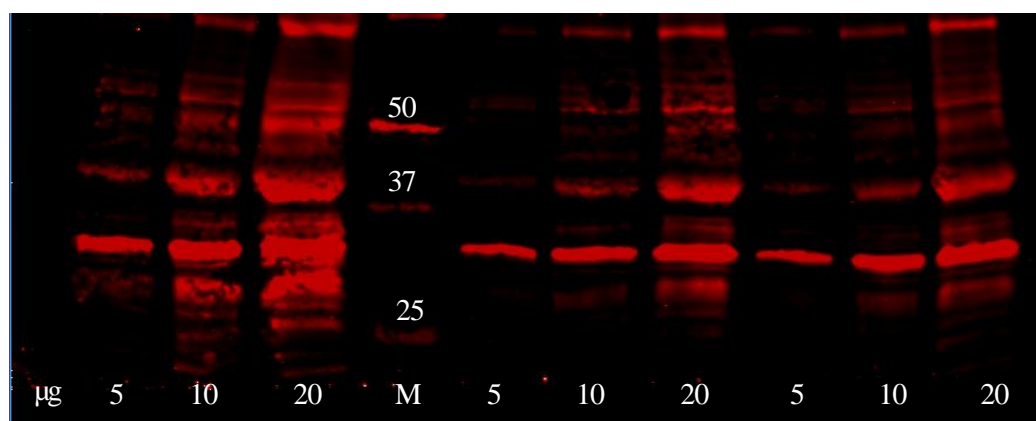


**Figure 11** Western blot analysis of Cx40 protein blocked with 1.5% fish skin gelatine, incubated with Cx40 antibody (1:500) (40 kDa) overnight with three different PCAs samples (5-20 μg protein). A strong band at about 40 kDa was observed with 20 μg protein, therefore further experiments were conducted using 20 μg of PCAs samples.
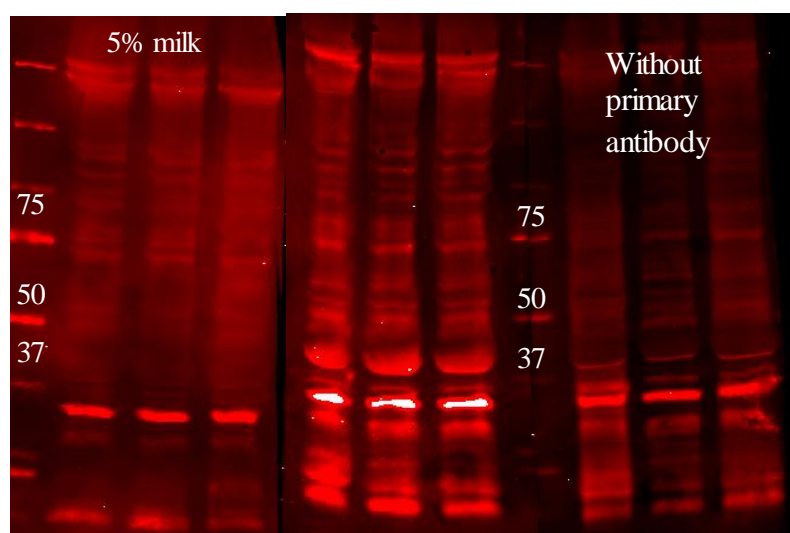


**Figure 12** Western blot analysis of Cx40 protein blocked with either 5% milk or 1.5% fish skin gelatine, with or without primary antibody (1:100) with 20 μg protein. The band slightly below 37 kDa is a non-specific band produced by the secondary antibody, IRDye® 680LT Goat anti-rabbit IgG.
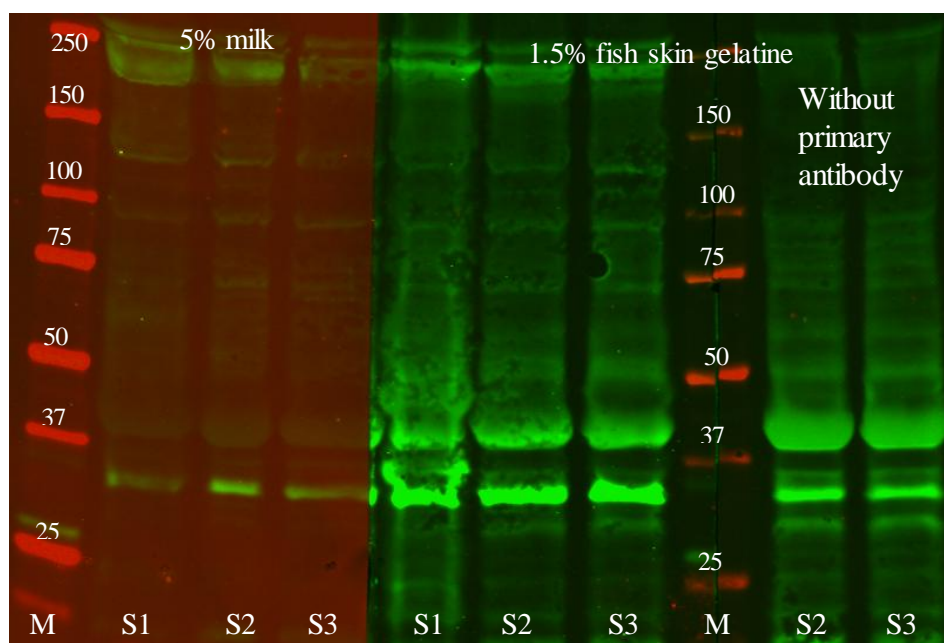
**Figure 13** Western blot analysis of Cx40 protein blocked with either 5% milk or 1.5% fish skin gelatine, with or without primary antibody (1:100) with 20 µg PCA proteins detected using IRDye® 800CW Donkey anti-rabbit IgG (secondary antibody). 5% milk appears to be a better blocking agent compared to fish skin gelatine, therefore further experiments were blocked with 5% milk.
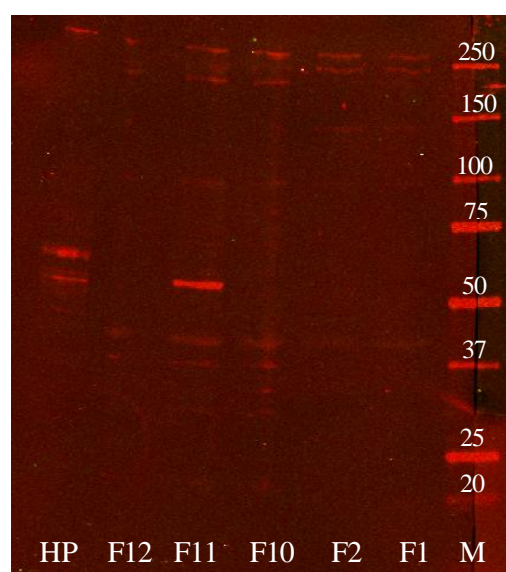


**Figure 14** Western blot analysis of Cx40 protein blocked with 5% milk, incubated with Cx40 antibody (1:100) using 5 µg human placenta (HP) lysate as positive control and 5 µg PCA samples from females prepared in different lysis buffer (F1-F2 lysis buffer, F10-F12 MAPK lysis buffer). Here, a lower concentration of protein was used to minimise detection of multiple bands. However, only a very faint band was detected at ~40 kDa, therefore subsequent experiments were conducted with higher concentration of protein.
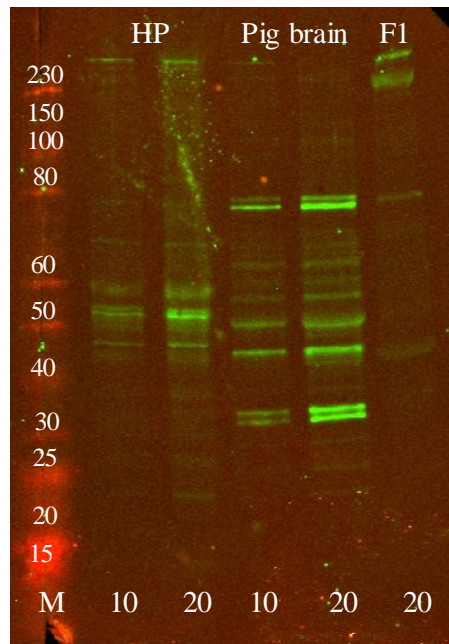
**Figure 15** Western blot analysis of Cx40 protein blocked with 5% milk, incubated with Cx40 antibody (1:100) using 10 or 20 μg human placenta (HP) or pig brain lysates as positive controls and 20 μg PCAs samples from female pigs (F1). A faint band was detected at ~40 kDa in PCA sample and a strong band was detected in 20 μg pig brain lysate.
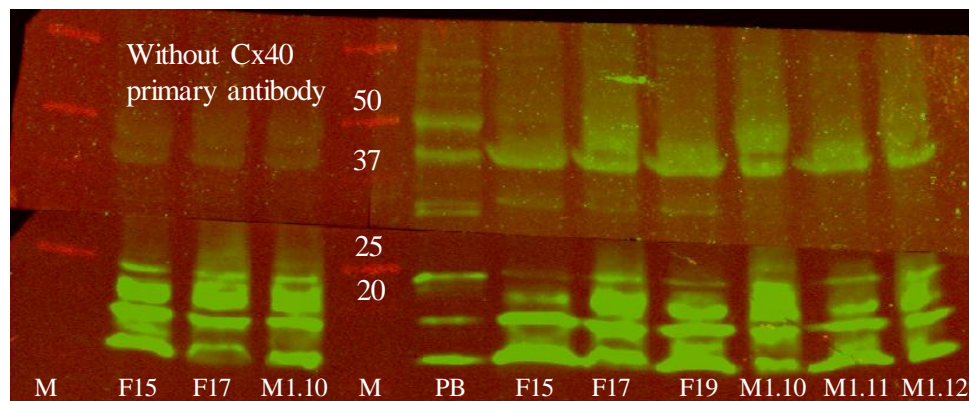


**Figure 16** Western blot analysis of Cx40 protein blocked with 5% milk, incubated with or without Cx40 antibody (1:100) (top half of the blot) using 20 μg pig brain lysate as positive control and 25 μg PCA samples from male (M1.10-M1.12) and female (F15, F17, F19) pigs. Lower half of the blot was incubated with MLC (1:1000) as the loading control. MLC bands detected were too strong, therefore lower concentration of MLC antibody was used in subsequent experiments. In the absence of Cx40 primary antibody, the band at 40 kDa was not detected.
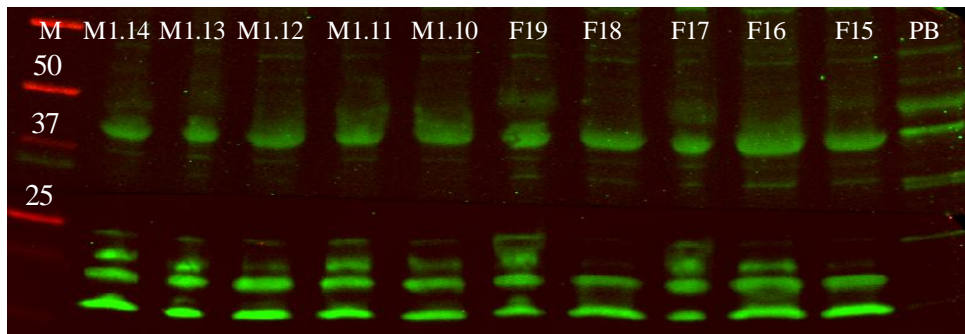
**Figure 17** Western blot analysis of Cx40 protein blocked with 5% milk, incubated with Cx40 antibody (1:100) (top half of the blot) using 20 μg pig brain lysate (PB) as positive control and 15 μg PCAs samples from male (M1.10-M1.14) and female (F15 - F19) pigs. Lower half of the blot was incubated with MLC (1:3000) as the loading control. No MLC band was detected in pig brain lysate, therefore GAPDH was used as loading control for subsequent experiments.
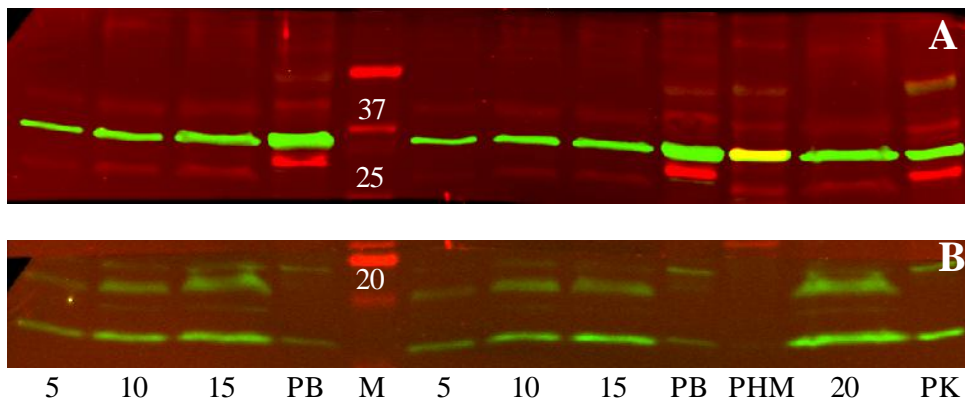


**Figure 18** Western blot analysis of Cx40 protein blocked with 5% milk, incubated with Cx40 antibody (1:100) (40 kDa) and GAPDH (1:40,000) (36 kDa) (A) using 20 μg pig brain (PB), pig heart membrane (PHM) and pig kidney (PK) lysates as positive controls and 5-20 μg PCAs samples from female pigs. MLC (1:3000) (18 kDa) used as loading control (B) was not detected in PB, PHM and PK samples. PCA samples in this blot were normalised to 1 mg/mL.
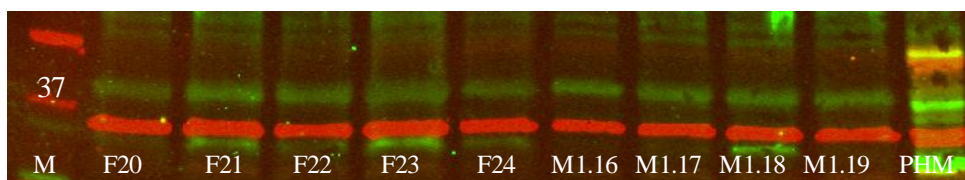


**Figure 19** Western blot analysis of Cx40 protein blocked with 5% milk, incubated with Cx40 antibody (1:100) (40 kDa) and GAPDH (1:40,000) (36 kDa) using 20 μg pig heart membrane (PHM) lysate as positive control and 10 μg PCAs samples from male (M1.16-M1.19) and female (F20-F24) pigs. PCA samples in this blot were normalised to 1 mg/mL.

## 3. Connexin 37 (C15878 Assay Biotech, Stratech Scientific Limited, Suffolk, UK)
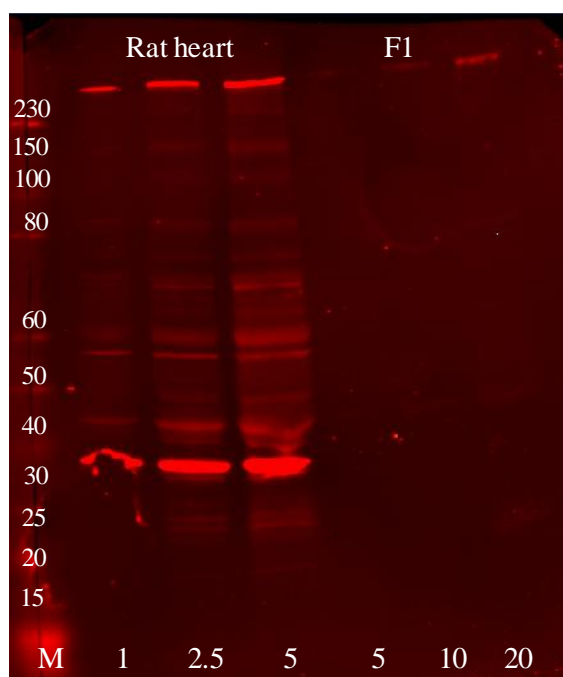


**Figure 20** Western blot analysis of Cx37 protein blocked with 5% milk, incubated with Cx37 antibody (1:500) (37 kDa) using rat heart lysate (1-5 μg) as positive control (first three lanes) and PCAs samples from female (5-20 μg) (F1) pigs (last three lanes).
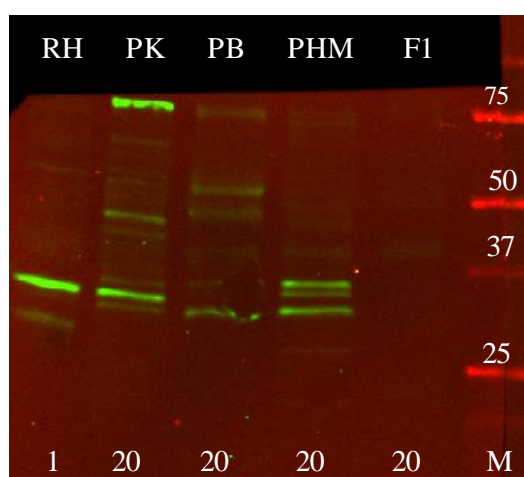


**Figure 21** Western blot analysis of Cx37 protein blocked with 5% milk, incubated with Cx37 antibody (1:500) (37 kDa) using 1μg rat heart (RH), 20 μg pig kidney (PK), pig brain (PB) and pig heart membrane (PHM) lysates as positive controls and 20 μg of PCA samples from female (F1) pigs.
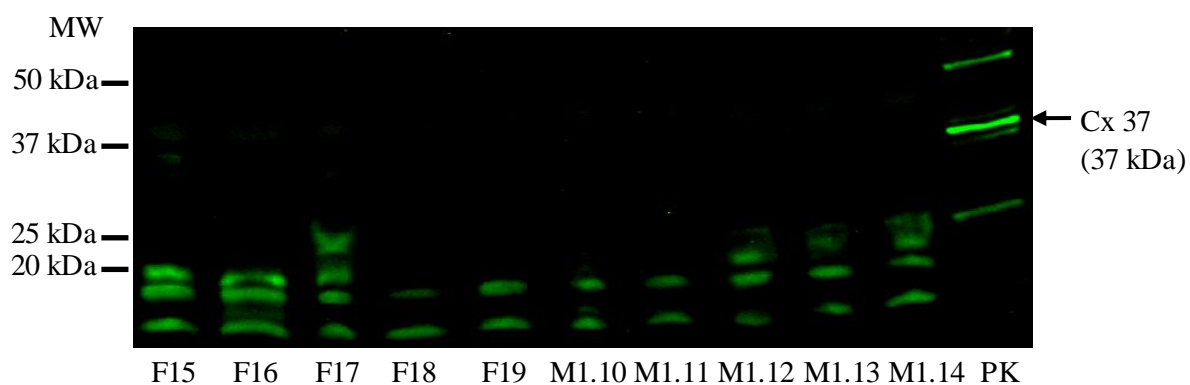
**Figure 22** Western blot analysis of Cx37 protein blocked with 5% milk, incubated with Cx37 antibody (1:500) (37 kDa) using 20 μg pig kidney (PK) lysate as positive control and 20 μg of PCA samples from male (M1.10-M1.14) and female (F15-F19) pigs with MLC (18 kDa) (1:5000) as the loading control (lower half of the blot). Cx37 protein was not detected in the PCA samples from both male and female pigs.

**4. Intermediate conductance calcium-activate potassium channel (IK$_{Ca}$) (H00003783-B01P Abnova, Taipei, Taiwan)**
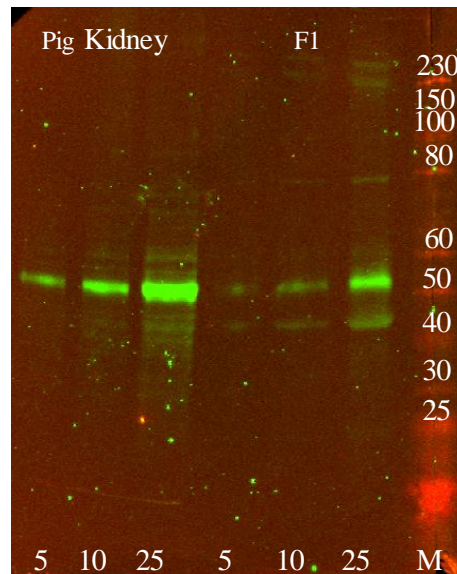


**Figure 23** Western blot analysis of IK$_{Ca}$ protein blocked with 5% milk, incubated with IK$_{Ca}$ antibody (1:500) (47.7 kDa) using different concentration of pig kidney (PK) lysate (5-25 μg) as positive control in the first three lanes and PCA samples from female (F1) (5-25 μg) pigs.
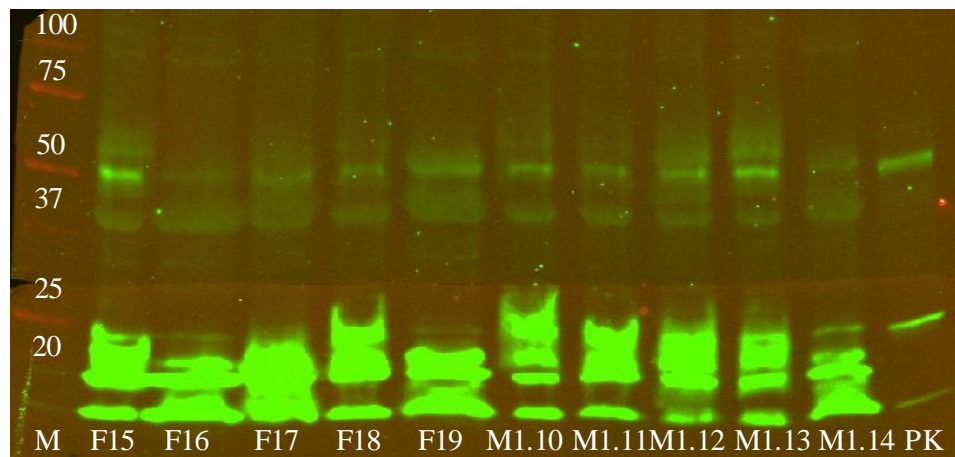


**Figure 24** Western blot analysis of IK$_{Ca}$ protein blocked with 5% milk, incubated with IK$_{Ca}$ antibody (1:500) (47.7 kDa) using 10 μg pig kidney (PK) lysate as positive control and 25 μg PCAs samples from male (M1.10-M1.14) and female (F15-F19) pigs. Concentration of MLC antibody (1:1000) used as loading control (lower half of the blot) was too high.
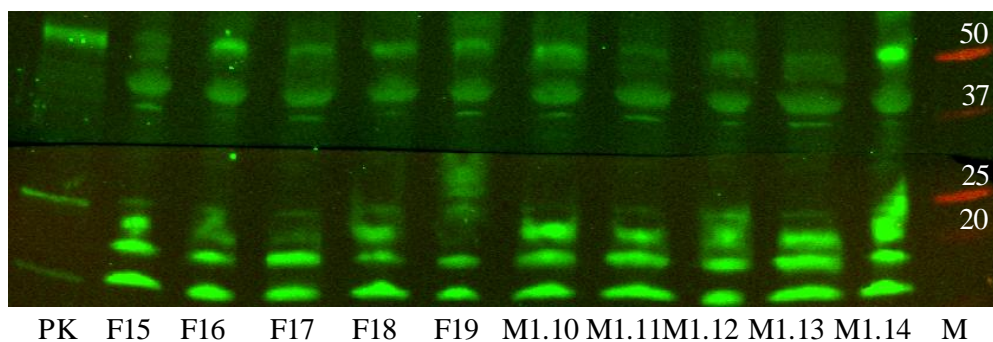
**Figure 25** Western blot analysis of IK$_{Ca}$ protein blocked with 5% milk, incubated with IK$_{Ca}$ antibody (1:250) (47.7 kDa) using 10 μg pig kidney (PK) lysate as positive control and 15 μg PCA samples from male (M1.10-M1.14) and female (F15-F19) pigs. MLC antibody (1:3000) was used as a loading control (lower half of the blot).

## C. Method development for Western Blot in Chapter 5

### 1. NADPH-oxidase 1 (ab55831 & ab137603 Abcam®, Cambridge, UK)
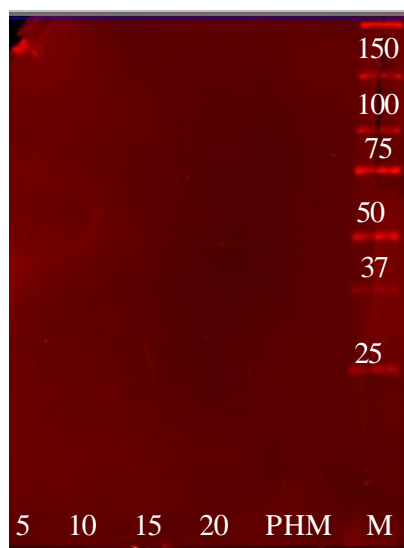


**Figure 26** Western blot analysis of Nox1 protein blocked with 5% milk, incubated with Nox1 antibody (ab55831 Lot GR132883-1) (1:1000) (65 kDa) using 10 μg pig heart membrane (PHM) lysate as positive control and 5-20 μg PCA samples from male (M1.13) pig. No band was dectected on the blot, further experiment with different positive controls and different secondary antibody was used.
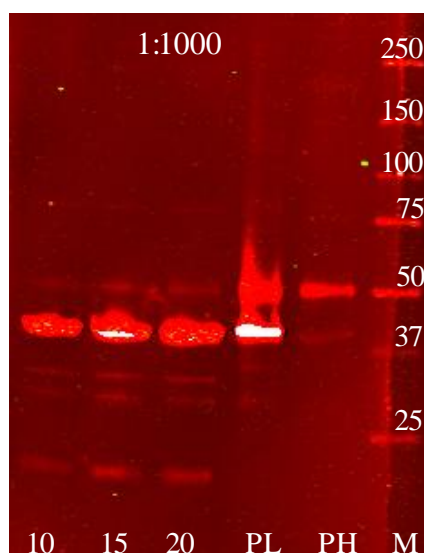


**Figure 27** Western blot analysis of Nox1 protein blocked with 5% milk, incubated with Nox1 antibody (ab55831 Lot GR132883-1) (1:1000) (65 kDa) using 10 μg pig heart (PH) and 15 μg pig lung (PL) lysates as positive controls and 10-20 μg PCAs samples from male pigs. Nox1 protein band was not detected on the blot (absence of green band - IRDye® 800CW Goat anti-rabbit IgG) while β-actin used as loading control (42 kDa) (red band- IRDye® 680LT Goat anti-mouse IgG) was detected.

271
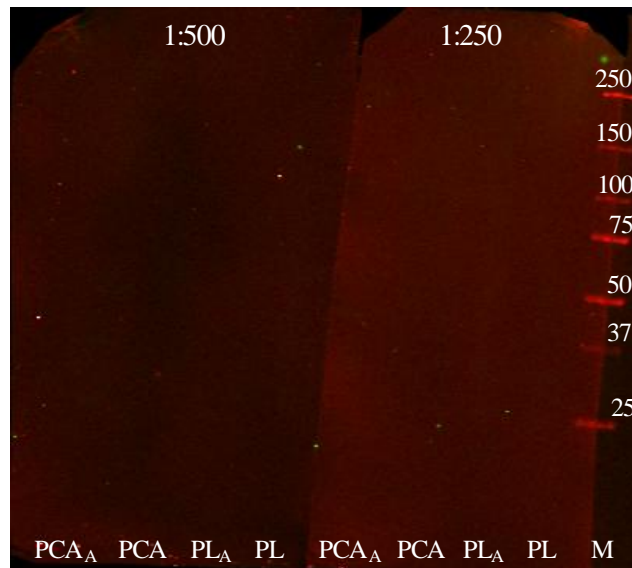
**Figure 28** Western blot analysis of Nox1 protein blocked with 5% milk, incubated with Nox1 antibody (ab55831 Lot GR132883-1) (1:500 or 1:250) (65 kDa) using samples homogenised in different lysis buffer. 15 μg pig lung (PL) lysate was used as positive control and 15 μg PCA samples from male pigs were loaded onto gel. PCA$_A$ and PL$_A$ samples were homogenised in 20 mM Tris-HCl, 50 mM NaCl, 0.1% Triton X-100, 3 mM EGTA buffer (Xie *et al.*, 2012) while PCA and PL samples were homogenised in lysis buffer (Table 8.1). Again, Nox1 protein band was not detected on the blot (absence of green band).



**Figure 29** Western blot analysis of Nox1 protein blocked with 5% milk, incubated with Nox1 antibody (ab55831 Lot GR132883-1) (1:250, 1:500 or 1:1000) (65 kDa) using 10μg pig lung (PL) and 12 μg mouse colon (MC) lysates as positive controls and 15-20 μg PCA samples from male pigs. Nox1 protein band was not detected (absence of green band) whereas β-actin (1:100,000) (42 kDa) used as loading control (red band) was detected on the blot.
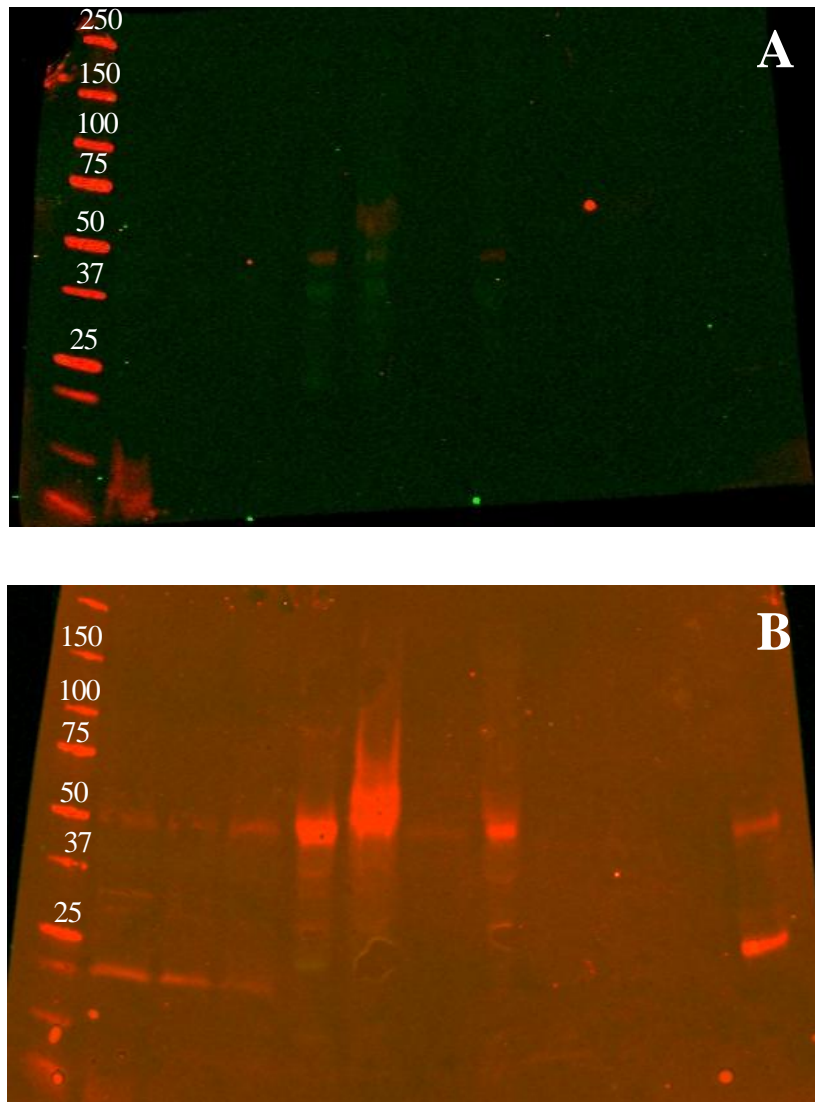
Lane 1 marker
Lane 2 male PCA (60 μg)
Lane 3 male PCA (60 μg)
Lane 4 male PCA (60 μg) same lysis buffer as Xie *et al.,* (2012) (Xie *et al.*, 2012)
Lane 5 Pig Lung (60 μg) same lysis buffer as Xie *et al.,* (2012)
Lane 6 Pig Lung (60 μg)
Lane 7 Pig Brain (20 μg)
Lane 8 Pig Heart (60 μg)
Lane 9 HL60 (20 μg)
Lane 10 Calu3 (15 μg)
Lane 11HepG2 (15 μg)
Lane 12 Mouse Colon (37 μg)

**Figure 30** Western blot analysis of Nox1 protein blocked with 5% milk, incubated with two different batches (A Lot GR76500-4 & B Lot GR76500-5) of Nox1 replacement antibodies (ab55831) (1:500) (65 kDa) using samples listed as above. Nox1 protein band was not detected in both blots (absence of green band - IRDye[®] 800CW Goat anti-rabbit IgG) whereas red bands detected were non-specific bands from the secondary antibody (IRDye[®] 680LT Goat anti-mouse IgG).
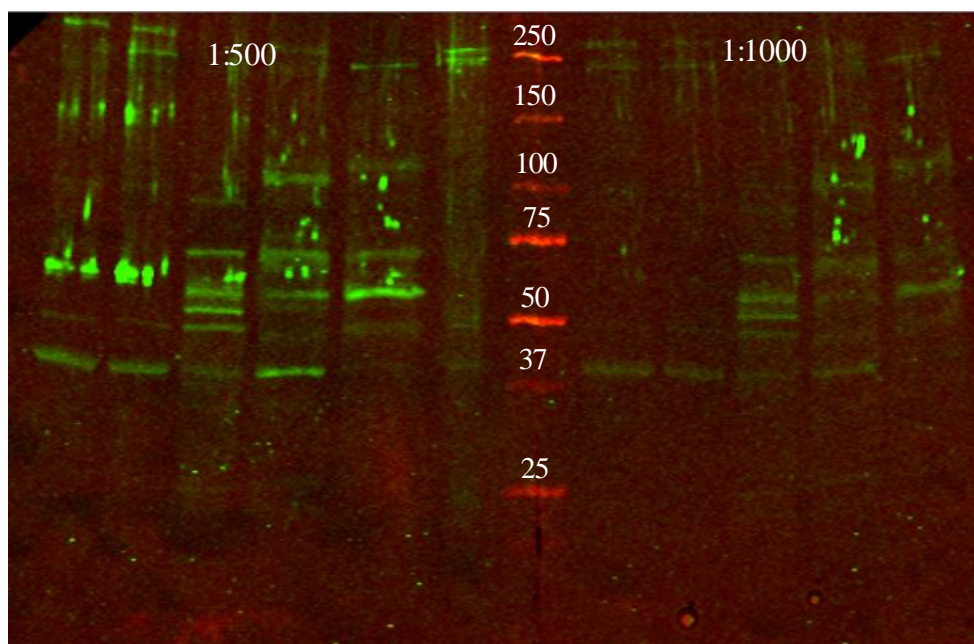
Lane 1 male PCA (20 μg)
Lane 2 male PCA (15 μg)
Lane 3 mouse colon (30 μg)
Lane 4 Calu3 (15 μg)
Lane 5 HepG2 (15 μg)
Lane 6 pig lung (15 μg)
Lane 7 marker
Lane 8 male PCA (20 μg)
Lane 9 male PCA (15 μg)
Lane 10 mouse colon (30 μg)
Lane 11 Calu3 (15 μg)
Lane 12 HepG2 (15 μg)

**Figure 31** Western blot analysis of Nox1 protein blocked with 5% milk, incubated with a different Nox1 antibody (~65 kDa) **(ab137603)** in two different dilution (1:500 or 1:1000) using a range of positive controls as listed above.

**2. NADPH-oxidase 2 (sc-20782 Santa Cruz Biotechnology, Insight Biotechnology Ltd, Wembley, Middlesex, UK)**
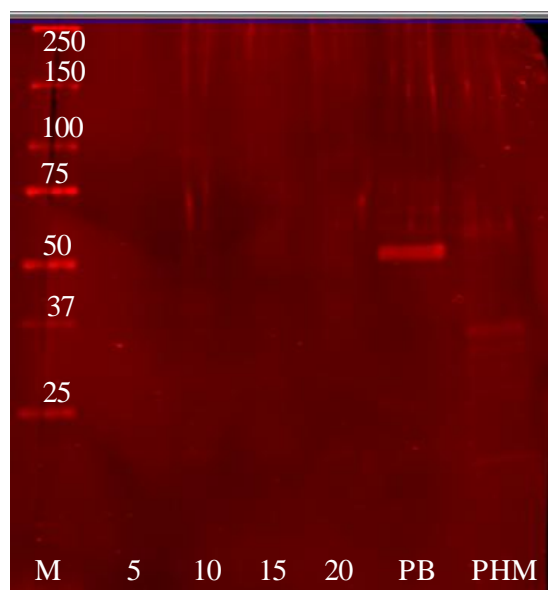


**Figure 32** Western blot analysis of Nox2 protein blocked with 5% milk, incubated with Nox2 antibody (1:500)(~60 kDa) using 10μg pig brain (PB) and pig heart membrane (PHM) lysates as positive controls and PCA from male pig (M1.13) (5-20 μg).
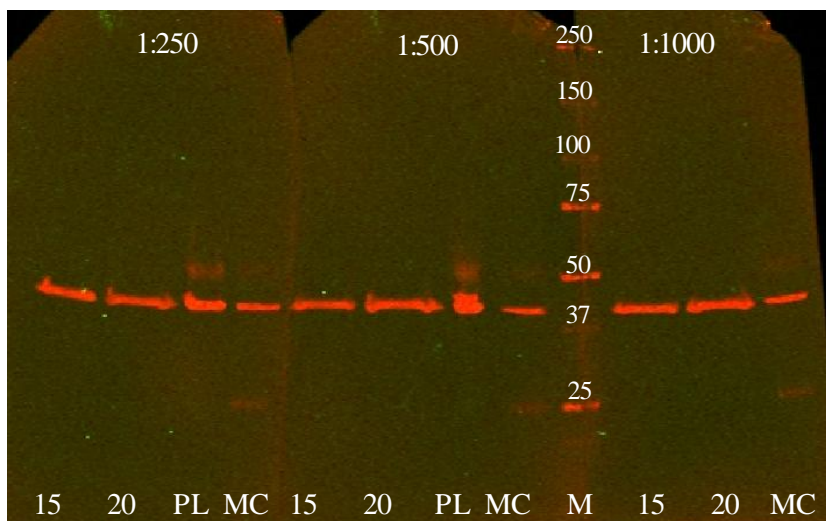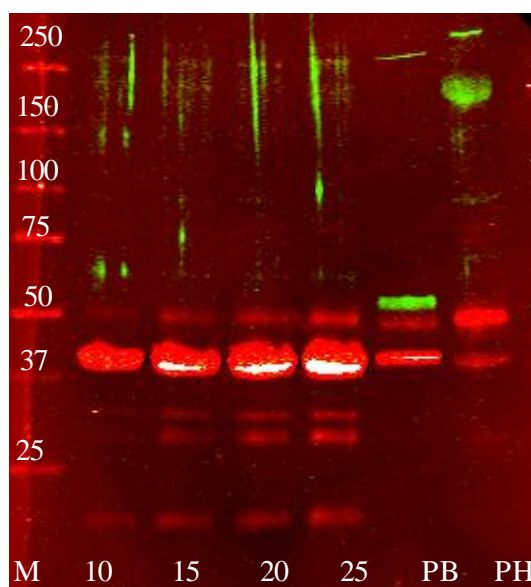


**Figure 33** Western blot analysis of Nox2 protein blocked with 5% milk, incubated with Nox2 antibody (1:500)(~60 kDa) using 10 μg pig brain (PB) and pig heart (PH) lysates as positive controls and PCA from male pig (M1.13) (10-25 μg). A single Nox2 band (~60 kDa) was detected in the pig brain lysate (green band) and only a very faint band was detected in the PCA samples. β-actin band used as loading control (42 kDa) (1:40,000) was too strong, therefore further dilution to 1:100,000 was used in subsequent experiments.
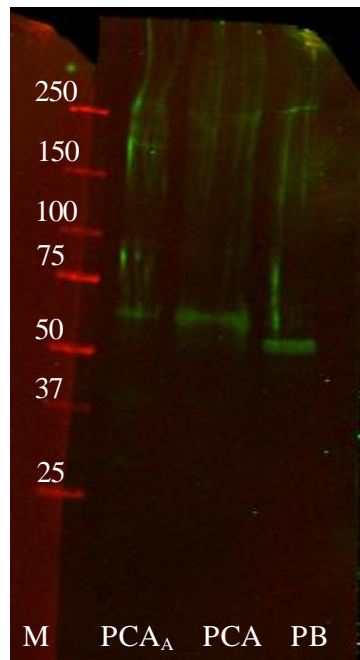
**Figure 34** Western blot analysis of Nox2 protein blocked with 5% milk, incubated with Nox2 antibody (1:500)(~60 kDa) using 10 μg pig brain (PB) lysate as positive control and 15 μg PCAs from male pigs homogenised in different lysis buffer (same samples as Figure 8.28).



**Figure 35** Western blot analysis of Nox2 protein blocked with 5% milk, incubated with Nox2 antibody (1:500)(~60 kDa) using 10μg pig brain (PB) lysate as positive control and 15 μg PCAs from five male ($M_A$- $M_E$) and five female ($F_A$- $F_E$) pigs. β-actin (1:100,000) (42 kDa) was used as a loading control (red band). As one of the β-actin bands ($F_D$) appears thinner than the others, Western Blot was repeated with more PCA samples from female pigs.

**Figure 36** Western blot analysis of Nox2 protein blocked with 5% milk, incubated with Nox2 antibody (1:500)(~60 kDa) using 10 μg pig brain (PB) lysate as positive control and 15 μg (first 5 lanes) or 20 μg (last 5 lanes) PCAs from five female pigs ($F_F$- $F_J$). β-actin (1:100,000) (42 kDa) was used as a loading control (red band).
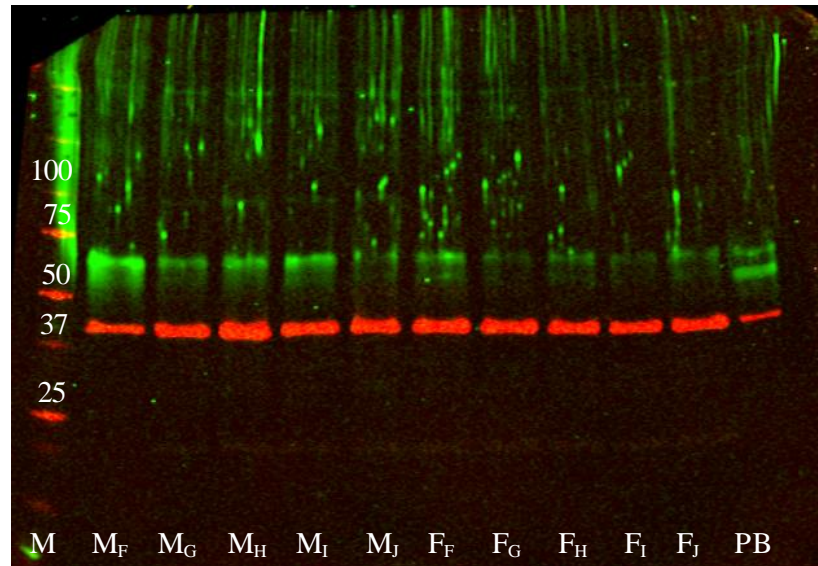


**Figure 37** Western blot analysis of Nox2 protein blocked with 5% milk, incubated with Nox2 antibody (1:500)(~60 kDa) using 10 μg pig brain (PB) lysate as positive control and 15 μg PCAs from five male ($M_F$- $M_J$) and five female ($F_F$- $F_J$) pigs. β-actin (1:100,000) (42 kDa) was used as a loading control (red band).

### 3. NADPH-oxidase 4 (ab109225 Abcam® Cambridge, UK)
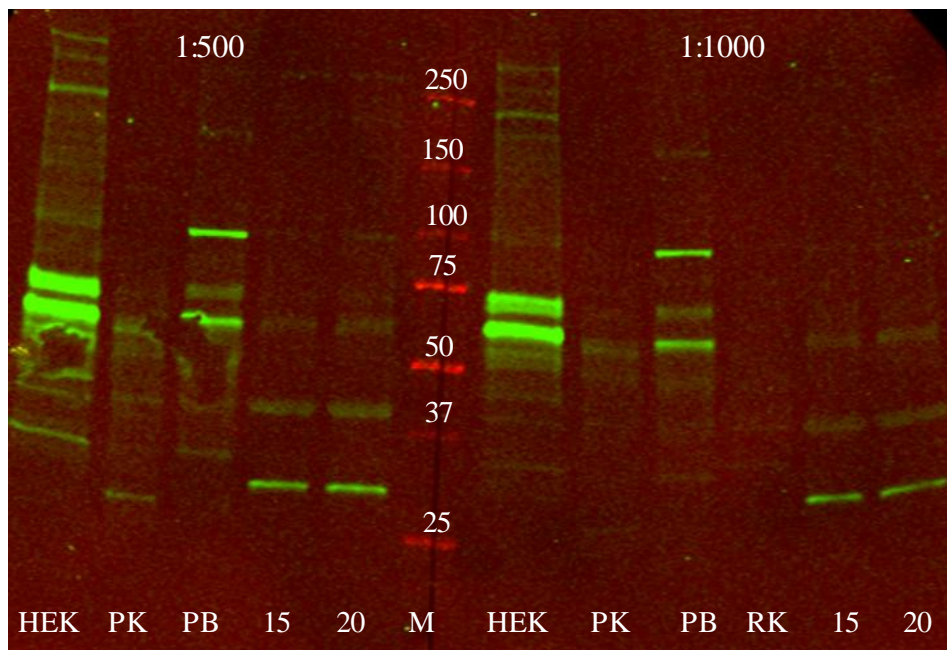


**Figure 38** Western blot analysis of Nox4 protein blocked with 5% milk, incubated with Nox4 antibody **(ab109225)** (1:500 or 1:1000)(~63 kDa) using 15 μg HEK cells, pig kidney (PK), pig brain (PB) and rat kidney (RK) lysates as positive controls and 15-20 μg PCA from male pig.



**Figure 39** Western blot analysis of Nox4 protein blocked with 5% milk, incubated with Nox4 antibody (1:1000)(~63 kDa) using 15 μg pig brain (PB) lysate as positive control and 20 μg PCAs from five male ($M_A$- $M_E$) and five female ($F_A$- $F_E$) pigs. β-actin (1:100,000) (42 kDa) was used as a loading control (red band). β-actin band in $F_H$ sample was not clearly detected, therefore Western blotting for the same samples were repeated.

**Figure 40** Western blot analysis of Nox4 protein blocked with 5% milk, incubated with Nox4 antibody (1:1000)(~63 kDa) using 15μg pig brain (PB) lysate as positive control and 20 μg PCAs from five male ($M_A$- $M_E$) and five female ($F_A$- $F_E$) pigs. β-actin (1:100,000) (42 kDa) was used as a loading control (red band).
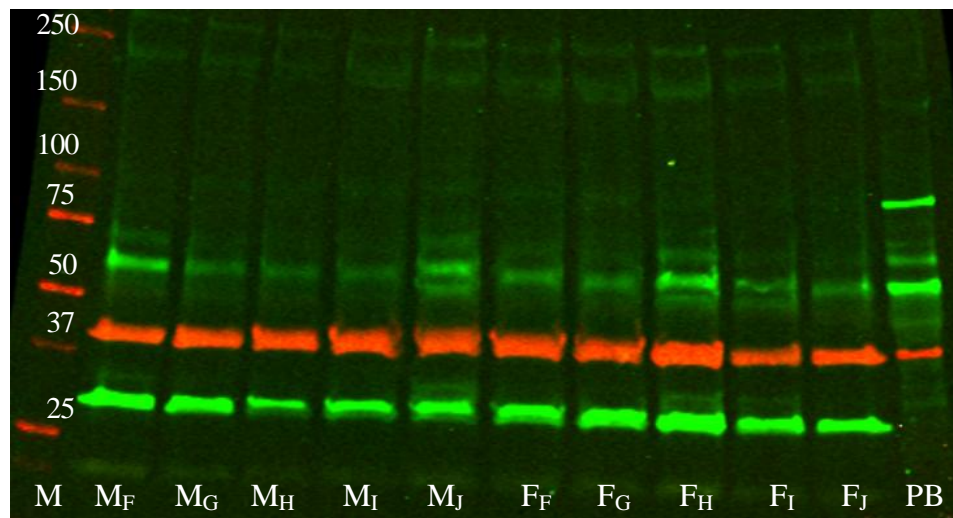


**Figure 41** Western blot analysis of Nox4 protein blocked with 5% milk, incubated with Nox4 antibody (1:1000)(~63 kDa) using 15μg pig brain (PB) lysate as positive control and 20 μg PCAs from five male ($M_F$- $M_J$) and five female ($F_F$- $F_J$) pigs. β-actin (1:100,000) (42 kDa) was used as a loading control (red band)

## D. Method development for Western Blot in Chapter 6

**1. TRPC3 (ACC-016) (Alomone Labs, Jurusalem, Israel)**



**Figure 42** Western blot analysis of TRPC3 protein blocked with 5% milk, incubated with TRPC3 antibody (1:200)(~100 kDa) using 2.5-5 μg rat heart lysate as positive control and 5-20 μg PCA from female pig (F1).
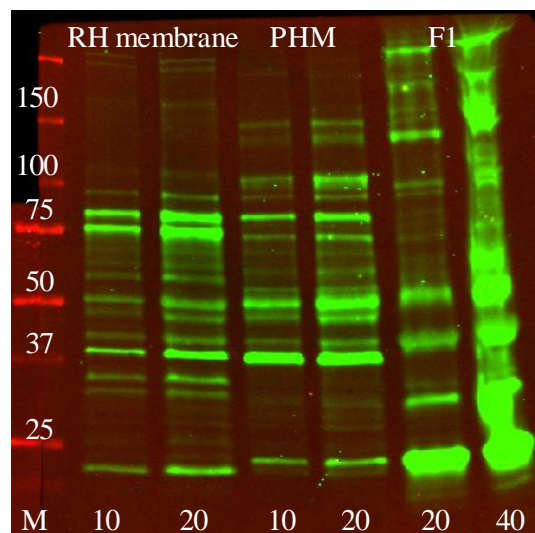


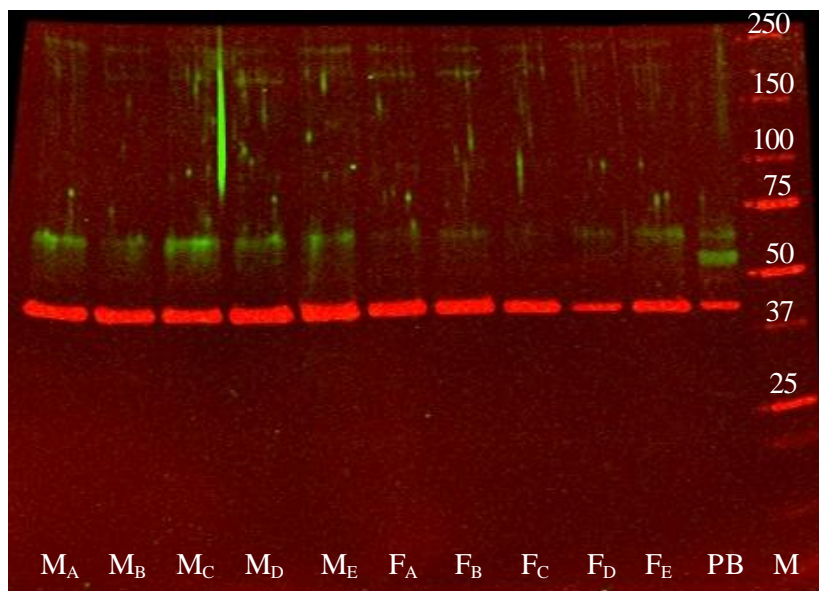**Figure 43** Western blot analysis of TRPC3 protein blocked with 5% milk, incubated with TRPC3 antibody (1:200)(~100 kDa) using 10-20 μg rat heart membrane and pig heart membrane (PHM) lysates as positive controls and 20-40 μg PCAs from female pigs. Multiple bands were detected in all samples, but in an attempt to compare the TRPC3 protein expression level between males and females, subsequent experiments focused on the top half of the blot as the molecular weight of TRPC3 is ~100 kDa.
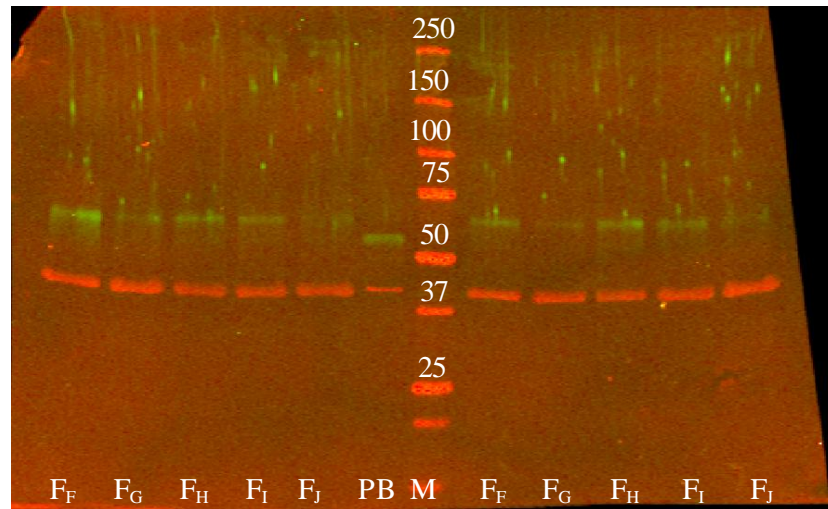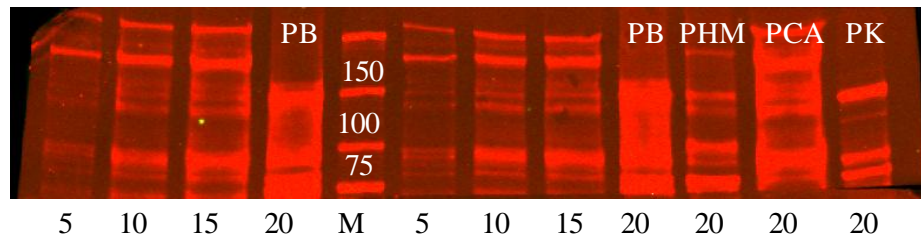
**Figure 44** Western blot analysis of TRPC3 protein blocked with 5% milk, incubated with TRPC3 antibody (1:200)(~100 kDa) using 20 µg pig brain (PB), pig heart membrane (PHM) and pig kidney (PK) lysates as positive controls and 5-20 µg PCA from female pig.
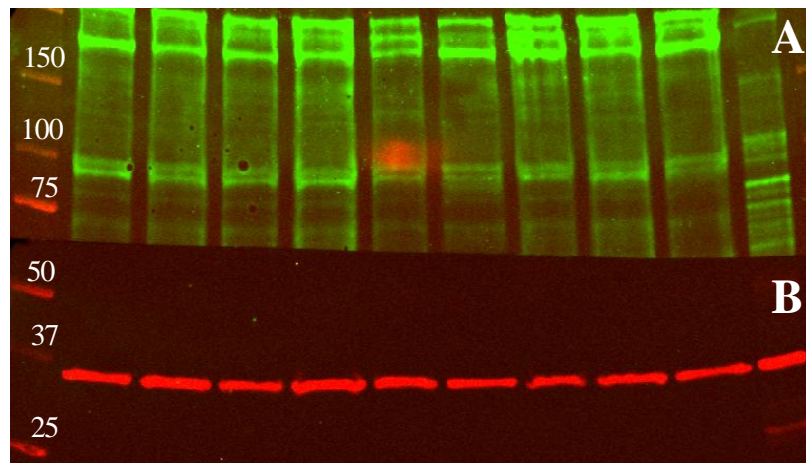


**Figure 45** Western blot analysis of TRPC3 protein blocked with 5% milk, incubated with TRPC3 antibody (1:200)(~100 kDa) (A) using 10 µg PCAs from male and female pigs with GAPDH (36 kDa) as the loading control (red band) (B). A double band appear slightly below 100 kDa but density of the band cannot be determined as they were too close together. With 84% sequence identities between TRPC3 and TRPC6 proteins, it is possible that the antibody is picking up TRPC3 (97.2 kDa) and TRPC6 (103 kDa) protein bands.
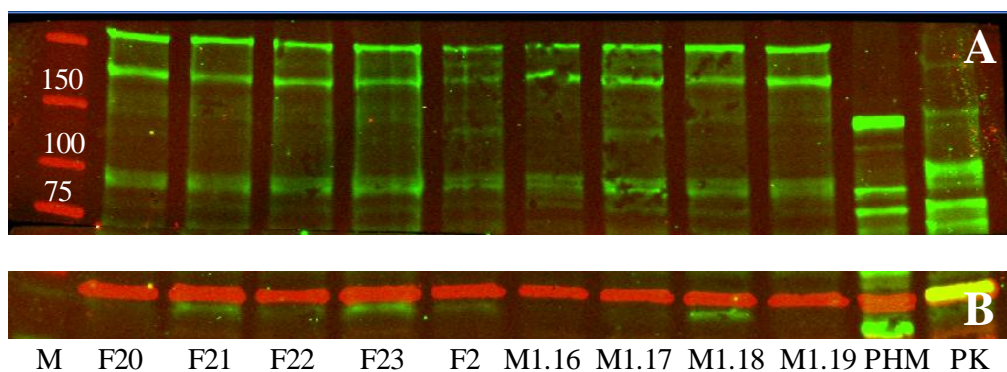
**Figure 46** Western blot analysis of TRPC3 protein blocked with 5% milk, incubated with TRPC3 antibody (1:200)(~100 kDa) (A) using 20 μg pig heart membrane (PHM) and pig kidney (PK) lysates as positive controls and 10 μg PCAs from male and female pigs with GAPDH as the loading control (B). Density of TRPC3 expression level cannot be determined due to the close proximity of the double band at ~100 kDa.

## 2. TRPC3 (ab70603) (Abcam®, Cambridge, UK)
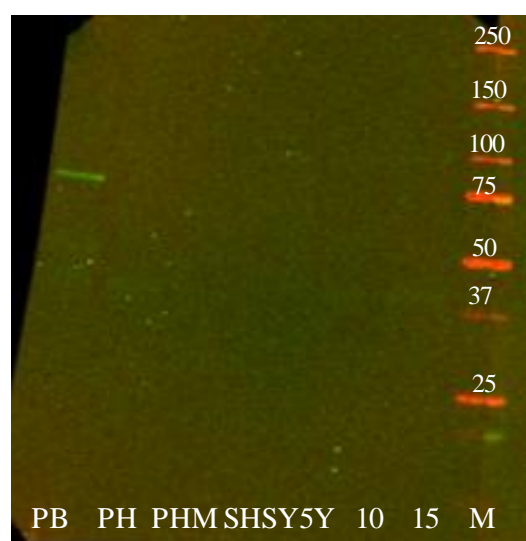


**Figure 47** Western blot analysis of TRPC3 protein blocked with 5% milk, incubated with TRPC3 antibody (ab70603 Lot 960430) (1:1000)(~100 kDa) using 15 μg pig brain (PB), pig heart (PH), pig heart membrane (PHM) and 10 μg SHSY-5Y cell lysates as positive controls and 10 and 20 μg PCA from male pig ($M_F$). Only a single band (~75 kDa) was detected in pig brain samples.
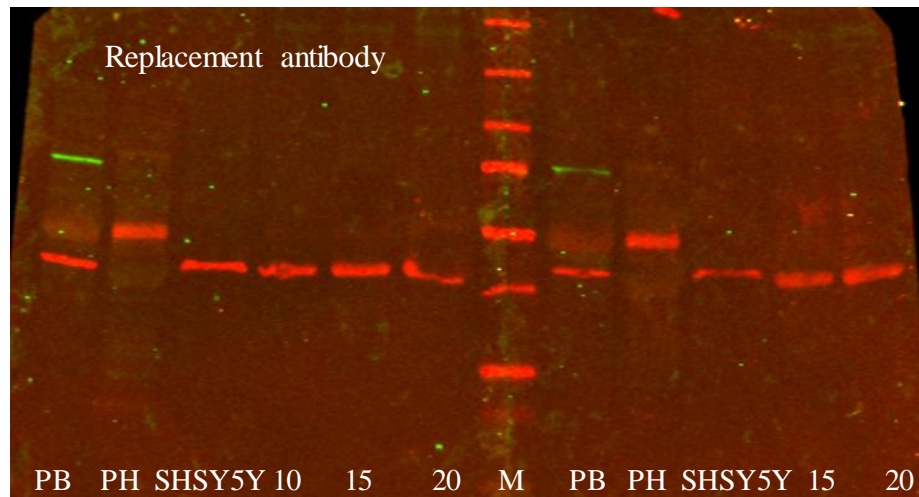
**Figure 48** Western blot analysis of TRPC3 protein blocked with 5% milk, incubated with TRPC3 antibody (both ab70603 Lot 960430) (1:1000)(~100 kDa) using 15 μg pig brain (PB), pig heart (PH) and 10 μg SHSY-5Y cell lysates as positive controls and 10, 15, 20 μg PCA from male pig ($M_C$). Only a single band (~75 kDa) was detected in pig brain samples. Replacement antibody was requested as the first batch was delivered over the weekend (could have been stored at room temperature).
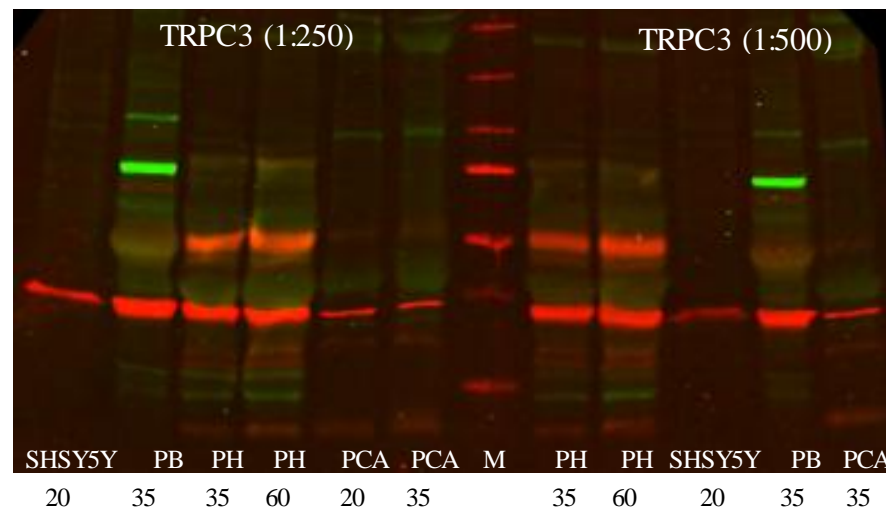


**Figure 49** Western blot analysis of TRPC3 protein blocked with 5% milk, incubated with TRPC3 antibody (ab70603 Lot 960430) (1:250 and 1:500 dilutions)(~100 kDa) using 35 μg pig brain (PB), 35 and 60 μg pig heart (PH) and 20 μg SHSY-5Y cell lysates as positive controls and 20 and 35 μg PCA from male pig ($M_G$). GAPDH (1:40 000) was used as loading control. Multiple bands were detected in pig tissue samples.

## 3. TRPV4 (ab94868) (Abcam®, Cambridge, UK)
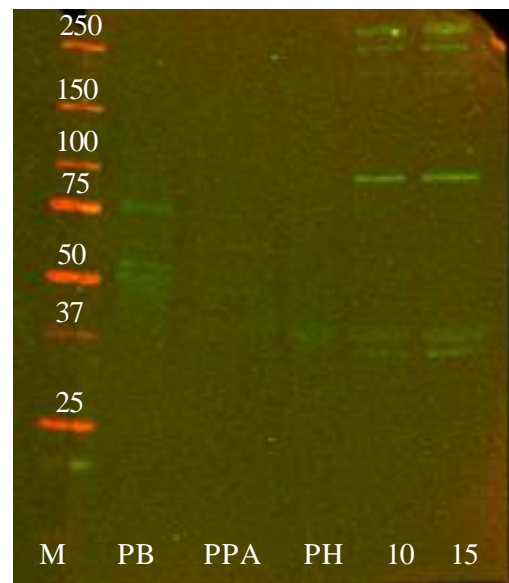

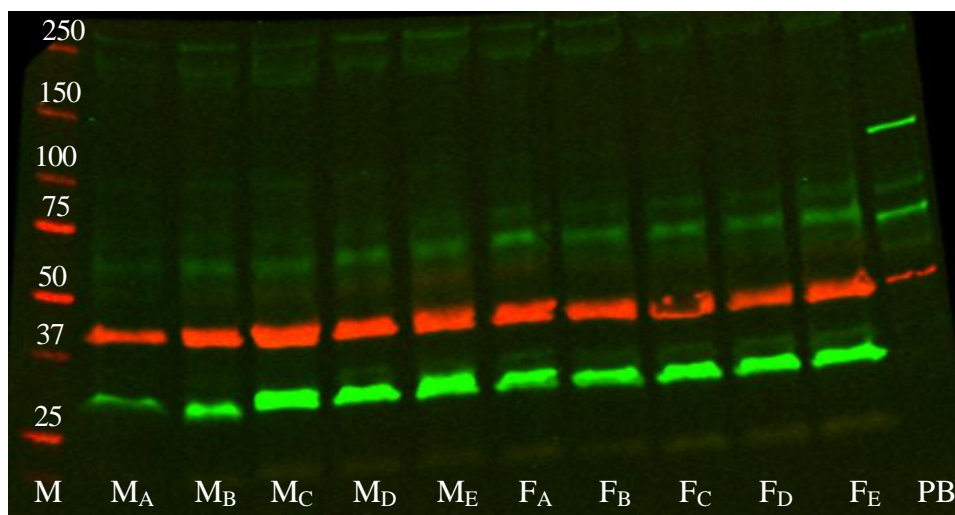
**Figure 50** Western blot analysis of TRPV4 protein blocked with 5% milk, incubated with TRPV4antibody (1:1000)(~100 kDa) using 15 μg pig brain (PB), pig pancreas artery (PPA) and pig heart (PH) lysates as positive controls and 10 and 15 μg PCA from female pig ($F_D$).
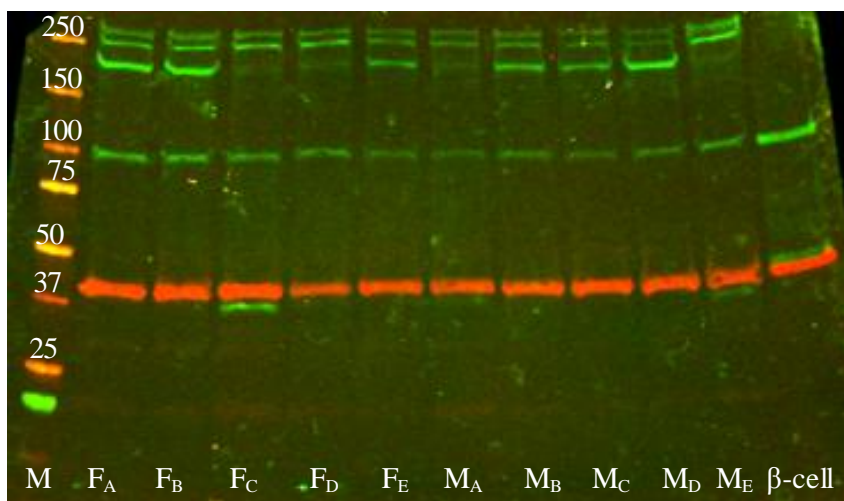


**Figure 51** Western blot analysis of TRPV4 protein blocked with 5% milk, incubated with TRPV4antibody (1:1000)(~100 kDa) using 15 μg human β-cell lysates as positive control and 15 μg PCA from female and male pigs. β-actin (1:100,000) (42 kDa) was used as a loading control (red band).
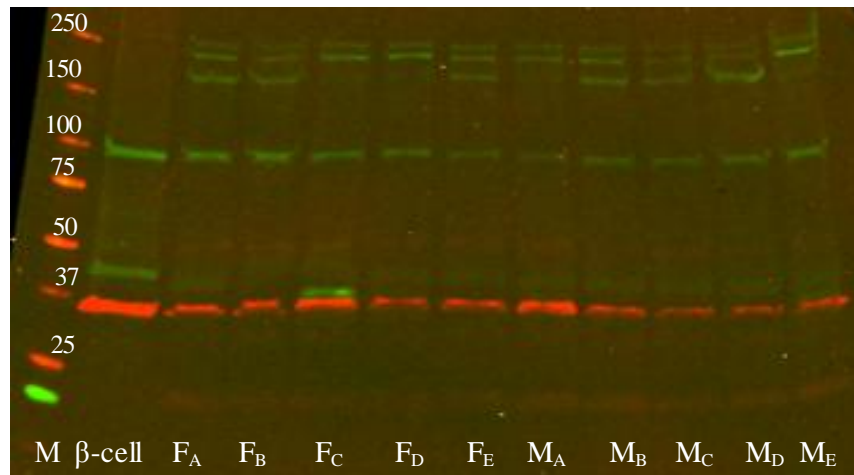
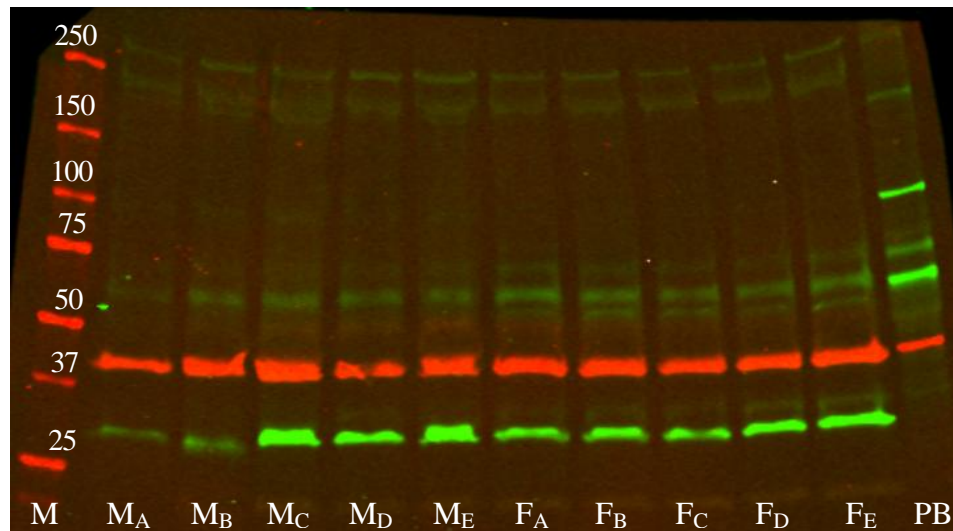**Figure 52** Western blot analysis of TRPV4 protein blocked with 5% milk, incubated with TRPV4 antibody (1:1000)(~100 kDa) using 15 μg human β-cell lysates as positive control and 15 μg PCA from female and male pigs. GAPDH (1:40,000) (36 kDa) was used as a loading control (red band).
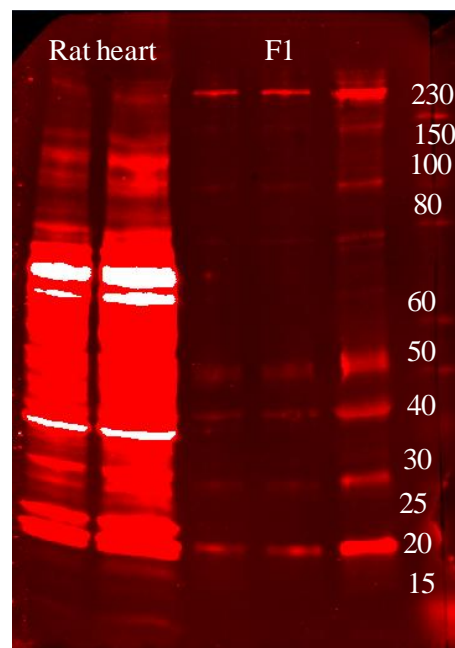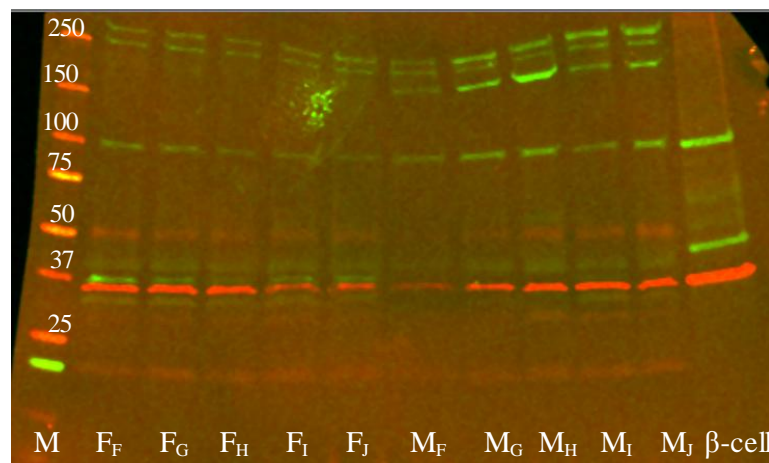


**Figure 53** Western blot analysis of TRPV4 protein blocked with 5% milk, incubated with TRPV4 antibody (1:1000)(~100 kDa) using 15 μg human β-cell lysates as positive control and 15 μg PCA from female and male pigs. GAPDH (1:40,000) (36 kDa) was used as a loading control (red band).

# References

Aizman O, Uhlen P, Lal M, Brismar H, Aperia A (2001). Ouabain, a steroid hormone that signals with slow calcium oscillations. *Proc Natl Acad Sci U S A* **98**(23)**:** 13420-13424.

Al-Shaer MH, Choueiri NE, Correia ML, Sinkey CA, Barenz TA, Haynes WG (2006). Effects of aging and atherosclerosis on endothelial and vascular smooth muscle function in humans. *Int J Cardiol* **109**(2)**:** 201-206.

Anabuki J, Hori M, Ozaki H, Kato I, Karaki H (1990). Mechanisms of pinacidil-induced vasodilatation. *Eur J Pharmacol* **190**(3)**:** 373-379.

Angulo J, Cuevas P, Fernandez A, Gabancho S, Allona A, Martin-Morales A*, et al.* (2003). Diabetes impairs endothelium-dependent relaxation of human penile vascular tissues mediated by NO and EDHF. *Biochem Biophys Res Commun* **312**(4)**:** 1202-1208.

Armstead WM (1999). Superoxide generation links protein kinase C activation to impaired ATP-sensitive K+ channel function after brain injury. *Stroke* **30**(1)**:** 153-159.

Arntz HR, Willich SN, Schreiber C, Bruggemann T, Stern R, Schultheiss HP (2000). Diurnal, weekly and seasonal variation of sudden death. Population-based analysis of 24,061 consecutive cases. *Eur Heart J* **21**(4)**:** 315-320.

Bagher P, Beleznai T, Kansui Y, Mitchell R, Garland CJ, Dora KA (2012). Low intravascular pressure activates endothelial cell TRPV4 channels, local Ca2+ events, and IKCa channels, reducing arteriolar tone. *Proc Natl Acad Sci U S A* **109**(44)**:** 18174-18179.

Bai D, del Corsso C, Srinivas M, Spray DC (2006). Block of specific gap junction channel subtypes by 2-aminoethoxydiphenyl borate (2-APB). *J Pharmacol Exp Ther* **319**(3)**:** 1452-1458.

Balzer M, Lintschinger B, Groschner K (1999). Evidence for a role of Trp proteins in the oxidative stress-induced membrane conductances of porcine aortic endothelial cells. *Cardiovasc Res* **42**(2)**:** 543-549.

Barber DA, Miller VM (1997). Gender differences in endothelium-dependent relaxations do not involve NO in porcine coronary arteries. *The American journal of physiology* **273**(5 Pt 2)**:** H2325-2332.

Bari MR, Akbar S, Eweida M, Kuhn FJ, Gustafsson AJ, Luckhoff A, *et al.* (2009). H2O2-induced Ca2+ influx and its inhibition by N-(p-amylcinnamoyl) anthranilic acid in the beta-cells: involvement of TRPM2 channels. *J Cell Mol Med* **13**(9B)**:** 3260-3267.

Barlow RS, White RE (1998). Hydrogen peroxide relaxes porcine coronary arteries by stimulating BKCa channel activity. *The American journal of physiology* **275**(4 Pt 2)**:** H1283-1289.

Barry WH, Hasin Y, Smith TW (1985). Sodium pump inhibition, enhanced calcium influx via sodium-calcium exchange, and positive inotropic response in cultured heart cells. *Circ Res* **56**(2)**:** 231-241.

Barton M, Beny JL, d'Uscio LV, Wyss T, Noll G, Luscher TF (1998). Endothelium-independent relaxation and hyperpolarization to C-type natriuretic peptide in porcine coronary arteries. *J Cardiovasc Pharmacol* **31**(3)**:** 377-383.

Bell DR, Rensberger HJ, Koritnik DR, Koshy A (1995). Estrogen pretreatment directly potentiates endothelium-dependent vasorelaxation of porcine coronary arteries. *The American journal of physiology* **268**(1 Pt 2)**:** H377-383.

Beny JL, Schaad O (2000). An evaluation of potassium ions as endothelium-derived hyperpolarizing factor in porcine coronary arteries. *Br J Pharmacol* **131**(5)**:** 965-973.

Beny JL, von der Weid PY (1991). Hydrogen peroxide: an endogenous smooth muscle cell hyperpolarizing factor. *Biochem Biophys Res Commun* **176**(1)**:** 378-384.

Beswick RA, Dorrance AM, Leite R, Webb RC (2001). NADH/NADPH oxidase and enhanced superoxide production in the mineralocorticoid hypertensive rat. *Hypertension* **38**(5)**:** 1107-1111.

Bolton TB, Lang RJ, Takewaki T (1984). Mechanisms of action of noradrenaline and carbachol on smooth muscle of guinea-pig anterior mesenteric artery. *J Physiol* **351:** 549-572.

Borras C, Sastre J, Garcia-Sala D, Lloret A, Pallardo FV, Vina J (2003). Mitochondria from females exhibit higher antioxidant gene expression and lower oxidative damage than males. *Free Radic Biol Med* **34**(5)**:** 546-552.

Bradford MM (1976). A rapid and sensitive method for the quantitation of microgram quantities of protein utilizing the principle of protein-dye binding. *Anal Biochem* **72:** 248-254.

Brahler S, Kaistha A, Schmidt VJ, Wolfle SE, Busch C, Kaistha BP, *et al.* (2009). Genetic deficit of SK3 and IK1 channels disrupts the endothelium-derived hyperpolarizing factor vasodilator pathway and causes hypertension. *Circulation* **119**(17)**:** 2323-2332.

Brandes RP, Mugge A (1997). Gender differences in the generation of superoxide anions in the rat aorta. *Life Sci* **60**(6)**:** 391-396.

Brondum E, Kold-Petersen H, Simonsen U, Aalkjaer C (2010). NS309 restores EDHF-type relaxation in mesenteric small arteries from type 2 diabetic ZDF rats. *Br J Pharmacol* **159**(1)**:** 154-165.

Brunner F, Wolkart G (2001). Relaxant effect of C-type natriuretic peptide involves endothelium and nitric oxide-cGMP system in rat coronary microvasculature. *Cardiovasc Res* **51**(3)**:** 577-584.

Bryja J, Koneân A (2003). Fast sex identification in wild mammals using PCR amplification of the Sry gene. *Folia Zoologica* **52**(3)**:** 269-274.

Bubolz AH, Mendoza SA, Zheng X, Zinkevich NS, Li R, Gutterman DD, *et al.* (2012). Activation of endothelial TRPV4 channels mediates flow-induced dilation in human coronary arterioles: role of Ca2+ entry and mitochondrial ROS signaling. *Am J Physiol Heart Circ Physiol* **302**(3)**:** H634-642.

Burgoyne JR, Oka S, Ale-Agha N, Eaton P (2013). Hydrogen peroxide sensing and signaling by protein kinases in the cardiovascular system. *Antioxid Redox Signal* **18**(9)**:** 1042-1052.

Burke TM, Wolin MS (1987). Hydrogen peroxide elicits pulmonary arterial relaxation and guanylate cyclase activation. *The American journal of physiology* **252**(4 Pt 2)**:** H721-732.

Busse R, Edwards G, Feletou M, Fleming I, Vanhoutte PM, Weston AH (2002). EDHF: bringing the concepts together. *Trends Pharmacol Sci* **23**(8)**:** 374-380.

Campbell WB, Gebremedhin D, Pratt PF, Harder DR (1996). Identification of epoxyeicosatrienoic acids as endothelium-derived hyperpolarizing factors. *Circ Res* **78**(3)**:** 415-423.

Chadha PS, Haddock RE, Howitt L, Morris MJ, Murphy TV, Grayson TH, *et al.* (2010). Obesity up-regulates intermediate conductance calcium-activated potassium channels and myoendothelial gap junctions to maintain endothelial vasodilator function. *J Pharmacol Exp Ther* **335**(2)**:** 284-293.

Chadha PS, Liu L, Rikard-Bell M, Senadheera S, Howitt L, Bertrand RL*, et al.* (2011). Endothelium-dependent vasodilation in human mesenteric artery is primarily mediated by myoendothelial gap junctions intermediate conductance calcium-activated K+ channel and nitric oxide. *J Pharmacol Exp Ther* **336**(3)**:** 701-708.

Chauhan SD, Nilsson H, Ahluwalia A, Hobbs AJ (2003). Release of C-type natriuretic peptide accounts for the biological activity of endothelium-derived hyperpolarizing factor. *Proc Natl Acad Sci U S A* **100**(3)**:** 1426-1431.

Chaytor AT, Edwards DH, Bakker LM, Griffith TM (2003). Distinct hyperpolarizing and relaxant roles for gap junctions and endothelium-derived H2O2 in NO-independent relaxations of rabbit arteries. *Proc Natl Acad Sci U S A* **100**(25)**:** 15212-15217.

Chaytor AT, Evans WH, Griffith TM (1998). Central role of heterocellular gap junctional communication in endothelium-dependent relaxations of rabbit arteries. *J Physiol* **508 ( Pt 2):** 561-573.

Chen F, Haigh S, Barman S, Fulton DJ (2012). From form to function: the role of Nox4 in the cardiovascular system. *Front Physiol* **3:** 412.

Chen J, Crossland RF, Noorani MM, Marrelli SP (2009). Inhibition of TRPC1/TRPC3 by PKG contributes to NO-mediated vasorelaxation. *Am J Physiol Heart Circ Physiol* **297**(1)**:** H417-424.

Chen T, Zhu J, Zhang C, Huo K, Fei Z, Jiang XF (2013). Protective effects of SKF-96365, a non-specific inhibitor of SOCE, against MPP+-induced cytotoxicity in PC12 cells: potential role of Homer1. *PLoS One* **8**(1)**:** e55601.

Coleman DA, Khalil RA (2002). Physiologic increases in extracellular sodium salt enhance coronary vasoconstriction and Ca2+ entry. *J Cardiovasc Pharmacol* **40**(1)**:** 58-66.

Coleman HA, Tare M, Parkington HC (2001). K+ currents underlying the action of endothelium-derived hyperpolarizing factor in guinea-pig, rat and human blood vessels. *J Physiol* **531**(Pt 2)**:** 359-373.

Cox MW, Fu W, Chai H, Paladugu R, Lin PH, Lumsden AB*, et al.* (2005). Effects of progesterone and estrogen on endothelial dysfunction in porcine coronary arteries. *J Surg Res* **124**(1)**:** 104-111.

Csanyi G, Lepran I, Flesch T, Telegdy G, Szabo G, Mezei Z (2007). Lack of endothelium-derived hyperpolarizing factor (EDHF) up-regulation in endothelial dysfunction in aorta in diabetic rats. *Pharmacol Rep* **59**(4)**:** 447-455.

Dalsgaard T, Kroigaard C, Bek T, Simonsen U (2009). Role of calcium-activated potassium channels with small conductance in bradykinin-induced vasodilation of porcine retinal arterioles. *Invest Ophthalmol Vis Sci* **50**(8)**:** 3819-3825.

de Wit C, Griffith TM (2010). Connexins and gap junctions in the EDHF phenomenon and conducted vasomotor responses. *Pflugers Arch* **459**(6)**:** 897-914.

Dehne N, Lautermann J, Petrat F, Rauen U, de Groot H (2001). Cisplatin ototoxicity: involvement of iron and enhanced formation of superoxide anion radicals. *Toxicol Appl Pharmacol* **174**(1)**:** 27-34.

Dikalov SI, Dikalova AE, Bikineyeva AT, Schmidt HH, Harrison DG, Griendling KK (2008). Distinct roles of Nox1 and Nox4 in basal and angiotensin II-stimulated superoxide and hydrogen peroxide production. *Free Radic Biol Med* **45**(9)**:** 1340-1351.

Ding H, Kubes P, Triggle C (2000). Potassium- and acetylcholine-induced vasorelaxation in mice lacking endothelial nitric oxide synthase. *Br J Pharmacol* **129**(6)**:** 1194-1200.

Dora KA, Gallagher NT, McNeish A, Garland CJ (2008). Modulation of endothelial cell KCa3.1 channels during endothelium-derived hyperpolarizing factor signaling in mesenteric resistance arteries. *Circ Res* **102**(10)**:** 1247-1255.

Dou D, Zheng X, Liu J, Xu X, Ye L, Gao Y (2012). Hydrogen peroxide enhances vasodilatation by increasing dimerization of cGMP-dependent protein kinase type Ialpha. *Circ J* **76**(7)**:** 1792-1798.

Drechsler C, Pilz S, Obermayer-Pietsch B, Verduijn M, Tomaschitz A, Krane V*, et al.* (2010). Vitamin D deficiency is associated with sudden cardiac death, combined cardiovascular events, and mortality in haemodialysis patients. *Eur Heart J* **31**(18)**:** 2253-2261.

Droge W (2002). Free radicals in the physiological control of cell function. *Physiol Rev* **82**(1)**:** 47-95.

Durand MJ, Gutterman DD (2013). Diversity in mechanisms of endothelium-dependent vasodilation in health and disease. *Microcirculation* **20**(3)**:** 239-247.

Dusting GJ, Moncada S, Vane JR (1977). Prostacyclin (PGX) is the endogenous metabolite responsible for relaxation of coronary arteries induced by arachindonic acid. *Prostaglandins* **13**(1)**:** 3-15.

Earley S, Brayden JE (2010). Transient receptor potential channels and vascular function. *Clin Sci (Lond)* **119**(1)**:** 19-36.

Earley S, Pauyo T, Drapp R, Tavares MJ, Liedtke W, Brayden JE (2009). TRPV4-dependent dilation of peripheral resistance arteries influences arterial pressure. *Am J Physiol Heart Circ Physiol* **297**(3)**:** H1096-1102.

Eckman DM, Hopkins N, McBride C, Keef KD (1998). Endothelium-dependent relaxation and hyperpolarization in guinea-pig coronary artery: role of epoxyeicosatrienoic acid. *Br J Pharmacol* **124**(1)**:** 181-189.

Edwards DH, Li Y, Griffith TM (2008). Hydrogen peroxide potentiates the EDHF phenomenon by promoting endothelial $Ca^{2+}$ mobilization. *Arterioscler Thromb Vasc Biol* **28**(10)**:** 1774-1781.

Edwards G, Dora KA, Gardener MJ, Garland CJ, Weston AH (1998). K+ is an endothelium-derived hyperpolarizing factor in rat arteries. *Nature* **396**(6708)**:** 269-272.

Edwards G, Feletou M, Weston AH (2010). Endothelium-derived hyperpolarising factors and associated pathways: a synopsis. *Pflugers Arch* **459**(6)**:** 863-879.

Edwards G, Gardener MJ, Feletou M, Brady G, Vanhoutte PM, Weston AH (1999). Further investigation of endothelium-derived hyperpolarizing factor (EDHF) in rat hepatic artery: studies using 1-EBIO and ouabain. *Br J Pharmacol* **128**(5)**:** 1064-1070.

Edwards G, Thollon C, Gardener MJ, Feletou M, Vilaine J, Vanhoutte PM, *et al.* (2000). Role of gap junctions and EETs in endothelium-dependent hyperpolarization of porcine coronary artery. *Br J Pharmacol* **129**(6)**:** 1145-1154.

Edwards G, Weston AH (2004). Potassium and potassium clouds in endothelium-dependent hyperpolarizations. *Pharmacol Res* **49**(6)**:** 535-541.

Ellis A, Pannirselvam M, Anderson TJ, Triggle CR (2003). Catalase has negligible inhibitory effects on endothelium-dependent relaxations in mouse isolated aorta and small mesenteric artery. *Br J Pharmacol* **140**(7)**:** 1193-1200.

Elmoselhi A, Butcher A, Samson SE, Grover AK (1994). Coronary artery contractility, Na(+)-pump and oxygen radicals. *Gen Physiol Biophys* **13**(3)**:** 247-256.

Faillace LS, Biggs C, Hunter MG (1994). Factors affecting the age at onset of puberty, ovulation rate and time of ovulation in Chinese Meishan gilts. *J Reprod Fertil* **100**(2)**:** 353-357.

Faraci FM, Didion SP (2004). Vascular protection: superoxide dismutase isoforms in the vessel wall. *Arterioscler Thromb Vasc Biol* **24**(8)**:** 1367-1373.

Feletou M, Vanhoutte PM (2009). EDHF: an update. *Clin Sci (Lond)* **117**(4)**:** 139-155.

Feletou M, Vanhoutte PM (2013). Endothelium-dependent hyperpolarization: no longer an f-word! *J Cardiovasc Pharmacol* **61**(2)**:** 91-92.

Feletou M, Vanhoutte PM (2006). Endothelium-derived hyperpolarizing factor: where are we now? *Arterioscler Thromb Vasc Biol* **26**(6)**:** 1215-1225.

Fitzgerald SM, Kemp-Harper BK, Parkington HC, Head GA, Evans RG (2007). Endothelial dysfunction and arterial pressure regulation during early diabetes in mice: roles for nitric oxide and endothelium-derived hyperpolarizing factor. *Am J Physiol Regul Integr Comp Physiol* **293**(2)**:** R707-713.

Fitzgerald SM, Kemp-Harper BK, Tare M, Parkington HC (2005). Role of endothelium-derived hyperpolarizing factor in endothelial dysfunction during diabetes. *Clin Exp Pharmacol Physiol* **32**(5-6)**:** 482-487.

Fleming I, Michaelis UR, Bredenkotter D, Fisslthaler B, Dehghani F, Brandes RP*, et al.* (2001). Endothelium-derived hyperpolarizing factor synthase (Cytochrome P450 2C9) is a functionally significant source of reactive oxygen species in coronary arteries. *Circ Res* **88**(1)**:** 44-51.

Fukao M, Hattori Y, Kanno M, Sakuma I, Kitabatake A (1997). Alterations in endothelium-dependent hyperpolarization and relaxation in mesenteric arteries from streptozotocin-induced diabetic rats. *Br J Pharmacol* **121**(7)**:** 1383-1391.

Furchgott RF, Zawadzki JV (1980). The obligatory role of endothelial cells in the relaxation of arterial smooth muscle by acetylcholine. *Nature* **288**(5789)**:** 373-376.

Gallo LC, Davel AP, Xavier FE, Rossoni LV (2010). Time-dependent increases in ouabain-sensitive Na+, K+ -ATPase activity in aortas from diabetic rats: The role of prostanoids and protein kinase C. *Life Sci* **87**(9-10)**:** 302-308.

Gao YJ, Zhang Y, Hirota S, Janssen LJ, Lee RM (2004). Vascular relaxation response to hydrogen peroxide is impaired in hypertension. *Br J Pharmacol* **142**(1)**:** 143-149.

Garland CJ, Dora KA (2008). Evidence against C-type natriuretic peptide as an arterial 'EDHF'. *Br J Pharmacol* **153**(1)**:** 4-5.

Garry A, Edwards DH, Fallis IF, Jenkins RL, Griffith TM (2009). Ascorbic acid and tetrahydrobiopterin potentiate the EDHF phenomenon by generating hydrogen peroxide. *Cardiovasc Res* **84**(2)**:** 218-226.

Ghanam K, Ea-Kim L, Javellaud J, Oudart N (2000). Involvement of potassium channels in the protective effect of 17beta-estradiol on hypercholesterolemic rabbit carotid artery. *Atherosclerosis* **152**(1)**:** 59-67.

Gianni D, Taulet N, Zhang H, DerMardirossian C, Kister J, Martinez L*, et al.* (2010). A novel and specific NADPH oxidase-1 (Nox1) small-molecule inhibitor blocks the formation of functional invadopodia in human colon cancer cells. *ACS Chem Biol* **5**(10)**:** 981-993.

Gilligan DM, Badar DM, Panza JA, Quyyumi AA, Cannon RO, 3rd (1994). Acute vascular effects of estrogen in postmenopausal women. *Circulation* **90**(2)**:** 786-791.

Gluais P, Edwards G, Weston AH, Falck JR, Vanhoutte PM, Feletou M (2005a). Role of SK(Ca) and IK(Ca) in endothelium-dependent hyperpolarizations of the guinea-pig isolated carotid artery. *Br J Pharmacol* **144**(4)**:** 477-485.

Gluais P, Edwards G, Weston AH, Vanhoutte PM, Feletou M (2005b). Hydrogen peroxide and endothelium-dependent hyperpolarization in the guinea-pig carotid artery. *Eur J Pharmacol* **513**(3)**:** 219-224.

Goto H, Hanada Y, Ohno T, Matsumura M (2004). Quantitative analysis of superoxide ion and hydrogen peroxide produced from molecular oxygen on photoirradiated TiO2 particles. *Journal of Catalysis* **225**(1)**:** 223-229.

Griffith TM (2004). Endothelium-dependent smooth muscle hyperpolarization: do gap junctions provide a unifying hypothesis? *Br J Pharmacol* **141**(6)**:** 881-903.

Gryglewski RJ, Palmer RM, Moncada S (1986). Superoxide anion is involved in the breakdown of endothelium-derived vascular relaxing factor. *Nature* **320**(6061)**:** 454-456.

Guzik B, Sagan A, Ludew D, Mrowiecki W, Chwala M, Bujak-Gizycka B*, et al.* (2013). Mechanisms of oxidative stress in human aortic aneurysms--association with clinical risk factors for atherosclerosis and disease severity. *Int J Cardiol* **168**(3)**:** 2389-2396.

Guzik TJ, Channon KM (2005). Measurement of vascular reactive oxygen species production by chemiluminescence. *Methods Mol Med* **108:** 73-89.

Hagenston AM, Rudnick ND, Boone CE, Yeckel MF (2009). 2-Aminoethoxydiphenyl-borate (2-APB) increases excitability in pyramidal neurons. *Cell Calcium* **45**(3)**:** 310-317.

Hammond S, Mathewson AM, Baker PN, Mayhew TM, Dunn WR (2011). Gap junctions and hydrogen peroxide are involved in endothelium-derived hyperpolarising responses to bradykinin in omental arteries and veins isolated from pregnant women. *Eur J Pharmacol* **668**(1-2)**:** 225-232.

Han X, Zhang R, Anderson L, Rahimian R (2014). Sexual dimorphism in rat aortic endothelial function of streptozotocin-induced diabetes: possible involvement of superoxide and nitric oxide production. *Eur J Pharmacol* **723:** 442-450.

Harris D, Martin PE, Evans WH, Kendall DA, Griffith TM, Randall MD (2000). Role of gap junctions in endothelium-derived hyperpolarizing factor responses and mechanisms of K(+)-relaxation. *Eur J Pharmacol* **402**(1-2)**:** 119-128.

Harris D, McCulloch AI, Kendall DA, Randall MD (2002). Characterization of vasorelaxant responses to anandamide in the rat mesenteric arterial bed. *J Physiol* **539**(Pt 3)**:** 893-902.

Hayabuchi Y, Nakaya Y, Matsuoka S, Kuroda Y (1998). Hydrogen peroxide-induced vascular relaxation in porcine coronary arteries is mediated by Ca2+-activated K+ channels. *Heart Vessels* **13**(1)**:** 9-17.

Hecquet CM, Ahmmed GU, Vogel SM, Malik AB (2008). Role of TRPM2 channel in mediating H2O2-induced Ca2+ entry and endothelial hyperpermeability. *Circ Res* **102**(3)**:** 347-355.

Hedegaard ER, Stankevicius E, Simonsen U, Frobert O (2011). Non-endothelial endothelin counteracts hypoxic vasodilation in porcine large coronary arteries. *BMC Physiol* **11**(1)**:** 8.

Heinzel B, John M, Klatt P, Bohme E, Mayer B (1992). Ca2+/calmodulin-dependent formation of hydrogen peroxide by brain nitric oxide synthase. *Biochem J* **281 ( Pt 3)**: 627-630.

Henrique-Silva F, Cervini M, Rios WM, Lusa AL, Lopes A, Goncalves D*, et al.* (2007). Rapid identification of capybara (Hydrochaeris hydrochaeris) using allele-specific PCR. *Braz J Biol* **67**(1)**:** 189-190.

Hill CE, Rummery N, Hickey H, Sandow SL (2002). Heterogeneity in the distribution of vascular gap junctions and connexins: implications for function. *Clin Exp Pharmacol Physiol* **29**(7)**:** 620-625.

Hinata M, Matsuoka I, Iwamoto T, Watanabe Y, Kimura J (2007). Mechanism of Na+/Ca2+ exchanger activation by hydrogen peroxide in guinea-pig ventricular myocytes. *J Pharmacol Sci* **103**(3)**:** 283-292.

Hobbs A, Foster P, Prescott C, Scotland R, Ahluwalia A (2004). Natriuretic peptide receptor-C regulates coronary blood flow and prevents myocardial ischemia/reperfusion injury: novel cardioprotective role for endothelium-derived C-type natriuretic peptide. *Circulation* **110**(10)**:** 1231-1235.

Honing ML, Smits P, Morrison PJ, Burnett JC, Jr., Rabelink TJ (2001). C-type natriuretic peptide-induced vasodilation is dependent on hyperpolarization in human forearm resistance vessels. *Hypertension* **37**(4)**:** 1179-1183.

Huang JH, He GW, Xue HM, Yao XQ, Liu XC, Underwood MJ*, et al.* (2011). TRPC3 channel contributes to nitric oxide release: significance during normoxia and hypoxia-reoxygenation. *Cardiovasc Res* **91**(3)**:** 472-482.

Huang PL, Huang Z, Mashimo H, Bloch KD, Moskowitz MA, Bevan JA*, et al.* (1995). Hypertension in mice lacking the gene for endothelial nitric oxide synthase. *Nature* **377**(6546)**:** 239-242.

Hyslop PA, Zhang Z, Pearson DV, Phebus LA (1995). Measurement of striatal H2O2 by microdialysis following global forebrain ischemia and reperfusion in the rat: correlation with the cytotoxic potential of H2O2 in vitro. *Brain Res* **671**(2)**:** 181-186.

Ide T, Tsutsui H, Ohashi N, Hayashidani S, Suematsu N, Tsuchihashi M*, et al.* (2002). Greater oxidative stress in healthy young men compared with premenopausal women. *Arterioscler Thromb Vasc Biol* **22**(3)**:** 438-442.

Inagami T, Naruse M, Hoover R (1995). Endothelium as an endocrine organ. *Annu Rev Physiol* **57:** 171-189.

Ingbar DH, Wendt CH (1997). The sodium pump and oxidant stress: if only it were so simple. *J Lab Clin Med* **130**(2)**:** 119-122.

Jia J, Verma S, Nakayama S, Quillinan N, Grafe MR, Hurn PD*, et al.* (2011). Sex differences in neuroprotection provided by inhibition of TRPM2 channels following experimental stroke. *J Cereb Blood Flow Metab* **31**(11)**:** 2160-2168.

Judkins CP, Diep H, Broughton BR, Mast AE, Hooker EU, Miller AA*, et al.* (2010). Direct evidence of a role for Nox2 in superoxide production, reduced nitric oxide bioavailability, and early atherosclerotic plaque formation in ApoE-/- mice. *Am J Physiol Heart Circ Physiol* **298**(1)**:** H24-32.

Katz SD, Krum H (2001). Acetylcholine-mediated vasodilation in the forearm circulation of patients with heart failure: indirect evidence for the role of endothelium-derived hyperpolarizing factor. *Am J Cardiol* **87**(9)**:** 1089-1092.

Kennedy DJ, Vetteth S, Xie M, Periyasamy SM, Xie Z, Han C*, et al.* (2006). Ouabain decreases sarco(endo)plasmic reticulum calcium ATPase activity in rat hearts by a process involving protein oxidation. *Am J Physiol Heart Circ Physiol* **291**(6)**:** H3003-3011.

Kenny LC, Baker PN, Kendall DA, Randall MD, Dunn WR (2002a). Differential mechanisms of endothelium-dependent vasodilator responses in human myometrial small arteries in normal pregnancy and pre-eclampsia. *Clin Sci (Lond)* **103**(1)**:** 67-73.

Kenny LC, Baker PN, Kendall DA, Randall MD, Dunn WR (2002b). The role of gap junctions in mediating endothelium-dependent responses to bradykinin

in myometrial small arteries isolated from pregnant women. *Br J Pharmacol* **136**(8): 1085-1088.

Kerr PM, Tam R, Ondrusova K, Mittal R, Narang D, Tran CH*, et al.* (2012). Endothelial feedback and the myoendothelial projection. *Microcirculation* **19**(5): 416-422.

Kerr S, Brosnan MJ, McIntyre M, Reid JL, Dominiczak AF, Hamilton CA (1999). Superoxide anion production is increased in a model of genetic hypertension: role of the endothelium. *Hypertension* **33**(6): 1353-1358.

Kim MS, Akera T (1987). $O_2$ free radicals: cause of ischemia-reperfusion injury to cardiac $Na^+$-$K^+$-ATPase. *The American journal of physiology* **252**(2 Pt 2): H252-257.

Kim MY, Seol GH, Liang GH, Kim JA, Suh SH (2005). Na+-K+ pump activation inhibits endothelium-dependent relaxation by activating the forward mode of Na+/Ca2+ exchanger in mouse aorta. *Am J Physiol Heart Circ Physiol* **289**(5): H2020-2029.

Kim N, Vardi Y, Padma-Nathan H, Daley J, Goldstein I, Saenz de Tejada I (1993). Oxygen tension regulates the nitric oxide pathway. Physiological role in penile erection. *J Clin Invest* **91**(2): 437-442.

Kleinschnitz C, Grund H, Wingler K, Armitage ME, Jones E, Mittal M*, et al.* (2010). Post-stroke inhibition of induced NADPH oxidase type 4 prevents oxidative stress and neurodegeneration. *PLoS Biol* **8**(9).

Knock GA, Poston L (1996). Bradykinin-mediated relaxation of isolated maternal resistance arteries in normal pregnancy and preeclampsia. *Am J Obstet Gynecol* **175**(6): 1668-1674.

Kobayashi H, Yoshiyama M, Zakoji H, Takeda M, Araki I (2009). Sex differences in the expression profile of acid-sensing ion channels in the mouse urinary bladder: a possible involvement in irritative bladder symptoms. *BJU Int* **104**(11): 1746-1751.

Kraft R, Grimm C, Frenzel H, Harteneck C (2006). Inhibition of TRPM2 cation channels by N-(p-amylcinnamoyl)anthranilic acid. *Br J Pharmacol* **148**(3): 264-273.

Kraft R, Grimm C, Grosse K, Hoffmann A, Sauerbruch S, Kettenmann H*, et al.* (2004). Hydrogen peroxide and ADP-ribose induce TRPM2-mediated

calcium influx and cation currents in microglia. *Am J Physiol Cell Physiol* **286**(1)**:** C129-137.

Kroigaard C, Dalsgaard T, Nielsen G, Laursen BE, Pilegaard H, Kohler R*, et al.* (2012). Activation of endothelial and epithelial K(Ca) 2.3 calcium-activated potassium channels by NS309 relaxes human small pulmonary arteries and bronchioles. *Br J Pharmacol* **167**(1)**:** 37-47.

Kun A, Kiraly I, Pataricza J, Marton Z, Krassoi I, Varro A*, et al.* (2008). C-type natriuretic peptide hyperpolarizes and relaxes human penile resistance arteries. *J Sex Med* **5**(5)**:** 1114-1125.

Kwan HY, Shen B, Ma X, Kwok YC, Huang Y, Man YB*, et al.* (2009). TRPC1 associates with BK(Ca) channel to form a signal complex in vascular smooth muscle cells. *Circ Res* **104**(5)**:** 670-678.

Lacy F, Kailasam MT, O'Connor DT, Schmid-Schonbein GW, Parmer RJ (2000). Plasma hydrogen peroxide production in human essential hypertension: role of heredity, gender, and ethnicity. *Hypertension* **36**(5)**:** 878-884.

Lang NN, Luksha L, Newby DE, Kublickiene K (2007). Connexin 43 mediates endothelium-derived hyperpolarizing factor-induced vasodilatation in subcutaneous resistance arteries from healthy pregnant women. *Am J Physiol Heart Circ Physiol* **292**(2)**:** H1026-1032.

Larsen BT, Bubolz AH, Mendoza SA, Pritchard KA, Jr., Gutterman DD (2009). Bradykinin-induced dilation of human coronary arterioles requires NADPH oxidase-derived reactive oxygen species. *Arterioscler Thromb Vasc Biol* **29**(5)**:** 739-745.

Lassegue B, Clempus RE (2003). Vascular NAD(P)H oxidases: specific features, expression, and regulation. *Am J Physiol Regul Integr Comp Physiol* **285**(2)**:** R277-297.

Leo CH, Hart JL, Woodman OL (2011). Impairment of both nitric oxide-mediated and EDHF-type relaxation in small mesenteric arteries from rats with streptozotocin-induced diabetes. *Br J Pharmacol* **162**(2)**:** 365-377.

Lerner DJ, Kannel WB (1986). Patterns of coronary heart disease morbidity and mortality in the sexes: a 26-year follow-up of the Framingham population. *Am Heart J* **111**(2)**:** 383-390.

Leung HS, Leung FP, Yao X, Ko WH, Chen ZY, Vanhoutte PM, *et al.* (2006). Endothelial mediators of the acetylcholine-induced relaxation of the rat femoral artery. *Vascul Pharmacol* **44**(5)**:** 299-308.

Leuranguer V, Gluais P, Vanhoutte PM, Verbeuren TJ, Feletou M (2008a). Openers of calcium-activated potassium channels and endothelium-dependent hyperpolarizations in the guinea pig carotid artery. *Naunyn Schmiedebergs Arch Pharmacol* **377**(2)**:** 101-109.

Leuranguer V, Vanhoutte PM, Verbeuren T, Feletou M (2008b). C-type natriuretic peptide and endothelium-dependent hyperpolarization in the guinea-pig carotid artery. *Br J Pharmacol* **153**(1)**:** 57-65.

Li PL, Jin MW, Campbell WB (1998). Effect of selective inhibition of soluble guanylyl cyclase on the K(Ca) channel activity in coronary artery smooth muscle. *Hypertension* **31**(1 Pt 2)**:** 303-308.

Li Y, Jia YC, Cui K, Li N, Zheng ZY, Wang YZ, *et al.* (2005). Essential role of TRPC channels in the guidance of nerve growth cones by brain-derived neurotrophic factor. *Nature* **434**(7035)**:** 894-898.

Liu D, Scholze A, Zhu Z, Kreutz R, Wehland-von-Trebra M, Zidek W, *et al.* (2005). Increased transient receptor potential channel TRPC3 expression in spontaneously hypertensive rats. *Am J Hypertens* **18**(11)**:** 1503-1507.

Liu D, Yang D, He H, Chen X, Cao T, Feng X, *et al.* (2009). Increased transient receptor potential canonical type 3 channels in vasculature from hypertensive rats. *Hypertension* **53**(1)**:** 70-76.

Liu MY, Hattori Y, Sato A, Ichikawa R, Zhang XH, Sakuma I (2002). Ovariectomy attenuates hyperpolarization and relaxation mediated by endothelium-derived hyperpolarizing factor in female rat mesenteric artery: a concomitant decrease in connexin-43 expression. *J Cardiovasc Pharmacol* **40**(6)**:** 938-948.

Liu Y, Bubolz AH, Mendoza S, Zhang DX, Gutterman DD (2011). H2O2 is the transferrable factor mediating flow-induced dilation in human coronary arterioles. *Circ Res* **108**(5)**:** 566-573.

Longo N, Griffin LD, Elsas LJ (1991). A simple method for evaluation of Rb+ transport and Na(+)-K+ pump stoichiometry in adherent cells. *The American journal of physiology* **260**(6 Pt 1)**:** C1341-1346.

Loria AS, Brinson KN, Fox BM, Sullivan JC (2014). Sex-specific alterations in NOS regulation of vascular function in aorta and mesenteric arteries from spontaneously hypertensive rats compared to Wistar Kyoto rats. *Physiol Rep* **2**(8).

Lucchesi PA, Belmadani S, Matrougui K (2005). Hydrogen peroxide acts as both vasodilator and vasoconstrictor in the control of perfused mouse mesenteric resistance arteries. *J Hypertens* **23**(3)**:** 571-579.

Luksha L, Agewall S, Kublickiene K (2009). Endothelium-derived hyperpolarizing factor in vascular physiology and cardiovascular disease. *Atherosclerosis* **202**(2)**:** 330-344.

Ma X, Du J, Zhang P, Deng J, Liu J, Lam FF, *et al.* (2013). Functional role of TRPV4-KCa2.3 signaling in vascular endothelial cells in normal and streptozotocin-induced diabetic rats. *Hypertension* **62**(1)**:** 134-139.

MacKenzie A, Filippini S, Martin W (1999). Effects of superoxide dismutase mimetics on the activity of nitric oxide in rat aorta. *Br J Pharmacol* **127**(5)**:** 1159-1164.

Makino A, Platoshyn O, Suarez J, Yuan JX, Dillmann WH (2008). Downregulation of connexin40 is associated with coronary endothelial cell dysfunction in streptozotocin-induced diabetic mice. *Am J Physiol Cell Physiol* **295**(1)**:** C221-230.

Martinkova M, Kubickova B, Stiborova M (2012). Effects of cytochrome P450 inhibitors on peroxidase activity. *Neuro Endocrinol Lett* **33 Suppl 3:** 33-40.

Matoba T, Shimokawa H, Kubota H, Morikawa K, Fujiki T, Kunihiro I, *et al.* (2002). Hydrogen peroxide is an endothelium-derived hyperpolarizing factor in human mesenteric arteries. *Biochem Biophys Res Commun* **290**(3)**:** 909-913.

Matoba T, Shimokawa H, Morikawa K, Kubota H, Kunihiro I, Urakami-Harasawa L, *et al.* (2003). Electron spin resonance detection of hydrogen peroxide as an endothelium-derived hyperpolarizing factor in porcine coronary microvessels. *Arterioscler Thromb Vasc Biol* **23**(7)**:** 1224-1230.

Matoba T, Shimokawa H, Nakashima M, Hirakawa Y, Mukai Y, Hirano K, *et al.* (2000). Hydrogen peroxide is an endothelium-derived hyperpolarizing factor in mice. *J Clin Invest* **106**(12)**:** 1521-1530.

Mattingly MT, Brandt RR, Heublein DM, Wei CM, Nir A, Burnett JC, Jr. (1994). Presence of C-type natriuretic peptide in human kidney and urine. *Kidney Int* **46**(3)**:** 744-747.

McCulloch AI, Bottrill FE, Randall MD, Hiley CR (1997). Characterization and modulation of EDHF-mediated relaxations in the rat isolated superior mesenteric arterial bed. *Br J Pharmacol* **120**(8)**:** 1431-1438.

McCulloch AI, Randall MD (1998). Sex differences in the relative contributions of nitric oxide and EDHF to agonist-stimulated endothelium-dependent relaxations in the rat isolated mesenteric arterial bed. *Br J Pharmacol* **123**(8)**:** 1700-1706.

McNeish AJ, Dora KA, Garland CJ (2005). Possible role for K+ in endothelium-derived hyperpolarizing factor-linked dilatation in rat middle cerebral artery. *Stroke* **36**(7)**:** 1526-1532.

Miller AA, Drummond GR, Mast AE, Schmidt HH, Sobey CG (2007). Effect of gender on NADPH-oxidase activity, expression, and function in the cerebral circulation: role of estrogen. *Stroke* **38**(7)**:** 2142-2149.

Miura H, Bosnjak JJ, Ning G, Saito T, Miura M, Gutterman DD (2003). Role for hydrogen peroxide in flow-induced dilation of human coronary arterioles. *Circ Res* **92**(2)**:** e31-40.

Miura H, Gutterman DD (1998). Human coronary arteriolar dilation to arachidonic acid depends on cytochrome P-450 monooxygenase and Ca2+-activated K+ channels. *Circ Res* **83**(5)**:** 501-507.

Miura H, Wachtel RE, Liu Y, Loberiza FR, Jr., Saito T, Miura M*, et al.* (2001). Flow-induced dilation of human coronary arterioles: important role of Ca(2+)-activated K(+) channels. *Circulation* **103**(15)**:** 1992-1998.

Moncada S, Gryglewski R, Bunting S, Vane JR (1976). An enzyme isolated from arteries transforms prostaglandin endoperoxides to an unstable substance that inhibits platelet aggregation. *Nature* **263**(5579)**:** 663-665.

Montezano AC, Touyz RM (2012). Reactive oxygen species and endothelial function--role of nitric oxide synthase uncoupling and Nox family nicotinamide adenine dinucleotide phosphate oxidases. *Basic Clin Pharmacol Toxicol* **110**(1)**:** 87-94.

Morikawa K, Fujiki T, Matoba T, Kubota H, Hatanaka M, Takahashi S, *et al.* (2004). Important role of superoxide dismutase in EDHF-mediated responses of human mesenteric arteries. *J Cardiovasc Pharmacol* **44**(5)**:** 552-556.

Morimura K, Yamamura H, Ohya S, Imaizumi Y (2006). Voltage-dependent Ca2+-channel block by openers of intermediate and small conductance Ca2+-activated K+ channels in urinary bladder smooth muscle cells. *J Pharmacol Sci* **100**(3)**:** 237-241.

Moyes AJ, Khambata RS, Villar I, Bubb KJ, Baliga RS, Lumsden NG, *et al.* (2014). Endothelial C-type natriuretic peptide maintains vascular homeostasis. *J Clin Invest* **124**(9)**:** 4039-4051.

Muzaffar S, Shukla N, Massey Y, Angelini GD, Jeremy JY (2011). NADPH oxidase 1 mediates upregulation of thromboxane A2 synthase in human vascular smooth muscle cells: inhibition with iloprost. *Eur J Pharmacol* **658**(2-3)**:** 187-192.

Nagao T, Vanhoutte PM (1992). Hyperpolarization as a mechanism for endothelium-dependent relaxations in the porcine coronary artery. *J Physiol* **445:** 355-367.

Nichols M, Townsend N, Luengo-Fernandez R, Leal J, Gray A, Scarborough P, *et al.* (2012). *European Cardiovascular Disease Statistics 2012*. European Heart Network, Brussels: European Society of Cardiology, Sophia Antipolis.

Ohashi J, Sawada A, Nakajima S, Noda K, Takaki A, Shimokawa H (2012). Mechanisms for enhanced endothelium-derived hyperpolarizing factor-mediated responses in microvessels in mice. *Circ J* **76**(7)**:** 1768-1779.

Palmer RM, Ferrige AG, Moncada S (1987). Nitric oxide release accounts for the biological activity of endothelium-derived relaxing factor. *Nature* **327**(6122)**:** 524-526.

Paravicini TM, Touyz RM (2008). NADPH oxidases, reactive oxygen species, and hypertension: clinical implications and therapeutic possibilities. *Diabetes Care* **31 Suppl 2:** S170-180.

Pomp D, Good BA, Geisert RD, Corbin CJ, Conley AJ (1995). Sex identification in mammals with polymerase chain reaction and its use to examine sex effects on diameter of day-10 or -11 pig embryos. *J Anim Sci* **73**(5)**:** 1408-1415.

Poteser M, Graziani A, Rosker C, Eder P, Derler I, Kahr H, *et al.* (2006). TRPC3 and TRPC4 associate to form a redox-sensitive cation channel. Evidence for expression of native TRPC3-TRPC4 heteromeric channels in endothelial cells. *J Biol Chem* **281**(19)**:** 13588-13595.

Qamirani E, Ren Y, Kuo L, Hein TW (2005). C-reactive protein inhibits endothelium-dependent NO-mediated dilation in coronary arterioles by activating p38 kinase and NAD(P)H oxidase. *Arterioscler Thromb Vasc Biol* **25**(5)**:** 995-1001.

Quignard JF, Feletou M, Thollon C, Vilaine JP, Duhault J, Vanhoutte PM (1999). Potassium ions and endothelium-derived hyperpolarizing factor in guinea-pig carotid and porcine coronary arteries. *Br J Pharmacol* **127**(1)**:** 27-34.

Randall MD, Griffith TM (1991). Differential effects of L-arginine on the inhibition by NG-nitro-L-arginine methyl ester of basal and agonist-stimulated EDRF activity. *Br J Pharmacol* **104**(3)**:** 743-749.

Ray R, Murdoch CE, Wang M, Santos CX, Zhang M, Alom-Ruiz S, *et al.* (2011). Endothelial Nox4 NADPH oxidase enhances vasodilatation and reduces blood pressure in vivo. *Arterioscler Thromb Vasc Biol* **31**(6)**:** 1368-1376.

Rogers PA, Chilian WM, Bratz IN, Bryan RM, Jr., Dick GM (2007). H2O2 activates redox- and 4-aminopyridine-sensitive Kv channels in coronary vascular smooth muscle. *Am J Physiol Heart Circ Physiol* **292**(3)**:** H1404-1411.

Rogers PA, Dick GM, Knudson JD, Focardi M, Bratz IN, Swafford AN, Jr., *et al.* (2006). H2O2-induced redox-sensitive coronary vasodilation is mediated by 4-aminopyridine-sensitive K+ channels. *Am J Physiol Heart Circ Physiol* **291**(5)**:** H2473-2482.

Rosolowsky M, Campbell WB (1993). Role of PGI2 and epoxyeicosatrienoic acids in relaxation of bovine coronary arteries to arachidonic acid. *The American journal of physiology* **264**(2 Pt 2)**:** H327-335.

Sandow SL, Hill CE (2000). Incidence of myoendothelial gap junctions in the proximal and distal mesenteric arteries of the rat is suggestive of a role in endothelium-derived hyperpolarizing factor-mediated responses. *Circ Res* **86**(3)**:** 341-346.

Sandow SL, Neylon CB, Chen MX, Garland CJ (2006). Spatial separation of endothelial small- and intermediate-conductance calcium-activated potassium channels (K(Ca)) and connexins: possible relationship to vasodilator function? *J Anat* **209**(5)**:** 689-698.

Sandow SL, Tare M (2007). C-type natriuretic peptide: a new endothelium-derived hyperpolarizing factor? *Trends Pharmacol Sci* **28**(2)**:** 61-67.

Sandow SL, Tare M, Coleman HA, Hill CE, Parkington HC (2002). Involvement of myoendothelial gap junctions in the actions of endothelium-derived hyperpolarizing factor. *Circ Res* **90**(10)**:** 1108-1113.

Scarborough P, Bhatnagar P, Wickramasinghe K, Smolina K, Mitchell C, Rayner M (2010). *Coronary Heart Disease Statistics*. University of Oxford.

Schach C, Resch M, Schmid PM, Riegger GA, Endemann DH (2014). Type 2 diabetes: increased expression and contribution of IKCa channels to vasodilation in small mesenteric arteries of ZDF rats. *Am J Physiol Heart Circ Physiol* **307**(8)**:** H1093-1102.

Schroder K, Zhang M, Benkhoff S, Mieth A, Pliquett R, Kosowski J*, et al.* (2012). Nox4 is a protective reactive oxygen species generating vascular NADPH oxidase. *Circ Res* **110**(9)**:** 1217-1225.

Scotland RS, Madhani M, Chauhan S, Moncada S, Andresen J, Nilsson H*, et al.* (2005). Investigation of vascular responses in endothelial nitric oxide synthase/cyclooxygenase-1 double-knockout mice: key role for endothelium-derived hyperpolarizing factor in the regulation of blood pressure in vivo. *Circulation* **111**(6)**:** 796-803.

Senadheera S, Bertrand PP, Grayson TH, Leader L, Murphy TV, Sandow SL (2013). Pregnancy-induced remodelling and enhanced endothelium-derived hyperpolarization-type vasodilator activity in rat uterine radial artery: transient receptor potential vanilloid type 4 channels, caveolae and myoendothelial gap junctions. *J Anat* **223**(6)**:** 677-686.

Senadheera S, Kim Y, Grayson TH, Toemoe S, Kochukov MY, Abramowitz J*, et al.* (2012). Transient receptor potential canonical type 3 channels facilitate endothelium-derived hyperpolarization-mediated resistance artery vasodilator activity. *Cardiovasc Res* **95**(4)**:** 439-447.

Shesely EG, Maeda N, Kim HS, Desai KM, Krege JH, Laubach VE*, et al.* (1996). Elevated blood pressures in mice lacking endothelial nitric oxide synthase. *Proc Natl Acad Sci U S A* **93**(23)**:** 13176-13181.

Shi Y, Niculescu R, Wang D, Patel S, Davenpeck KL, Zalewski A (2001). Increased NAD(P)H oxidase and reactive oxygen species in coronary arteries after balloon injury. *Arterioscler Thromb Vasc Biol* **21**(5)**:** 739-745.

Shimokawa H (2010). Hydrogen peroxide as an endothelium-derived hyperpolarizing factor. *Pflugers Arch* **459**(6)**:** 915-922.

Shimokawa H, Morikawa K (2005). Hydrogen peroxide is an endothelium-derived hyperpolarizing factor in animals and humans. *J Mol Cell Cardiol* **39**(5)**:** 725-732.

Shimokawa H, Yasutake H, Fujii K, Owada MK, Nakaike R, Fukumoto Y*, et al.* (1996). The importance of the hyperpolarizing mechanism increases as the vessel size decreases in endothelium-dependent relaxations in rat mesenteric circulation. *J Cardiovasc Pharmacol* **28**(5)**:** 703-711.

Silverthorn D, Johnson B (2010) *Human Physiology An Integreated Approach* Fifth edn, Pearson Benjamin Cummings. pp538.

Sokoya EM, Burns AR, Marrelli SP, Chen J (2007). Myoendothelial gap junction frequency does not account for sex differences in EDHF responses in rat MCA. *Microvasc Res* **74**(1)**:** 39-44.

Stingo AJ, Clavell AL, Heublein DM, Wei CM, Pittelkow MR, Burnett JC, Jr. (1992). Presence of C-type natriuretic peptide in cultured human endothelial cells and plasma. *The American journal of physiology* **263**(4 Pt 2)**:** H1318-1321.

Streeter J, Thiel W, Brieger K, Miller FJ, Jr. (2013). Opportunity nox: the future of NADPH oxidases as therapeutic targets in cardiovascular disease. *Cardiovasc Ther* **31**(3)**:** 125-137.

Sukumaran SV, Singh TU, Parida S, Narasimha Reddy Ch E, Thangamalai R, Kandasamy K*, et al.* (2013). TRPV4 channel activation leads to endothelium-dependent relaxation mediated by nitric oxide and endothelium-derived hyperpolarizing factor in rat pulmonary artery. *Pharmacol Res* **78:** 18-27.

Tagawa H, Shimokawa H, Tagawa T, Kuroiwa-Matsumoto M, Hirooka Y, Takeshita A (1997). Short-term estrogen augments both nitric oxide-mediated and non-nitric oxide-mediated endothelium-dependent forearm vasodilation in postmenopausal women. *J Cardiovasc Pharmacol* **30**(4)**:** 481-488.

Tang EH, Vanhoutte PM (2008). Gap junction inhibitors reduce endothelium-dependent contractions in the aorta of spontaneously hypertensive rats. *J Pharmacol Exp Ther* **327**(1)**:** 148-153.

Tare M, Emmett SJ, Coleman HA, Skordilis C, Eyles DW, Morley R*, et al.* (2011). Vitamin D insufficiency is associated with impaired vascular endothelial and smooth muscle function and hypertension in young rats. *J Physiol* **589**(Pt 19)**:** 4777-4786.

Tarpey MM, Fridovich I (2001). Methods of detection of vascular reactive species: nitric oxide, superoxide, hydrogen peroxide, and peroxynitrite. *Circ Res* **89**(3)**:** 224-236.

Taylor SG, Weston AH (1988). Endothelium-derived hyperpolarizing factor: a new endogenous inhibitor from the vascular endothelium. *Trends Pharmacol Sci* **9**(8)**:** 272-274.

Teoh H, Man RY (2000). Enhanced relaxation of porcine coronary arteries after acute exposure to a physiological level of 17beta-estradiol involves non-genomic mechanisms and the cyclic AMP cascade. *Br J Pharmacol* **129**(8)**:** 1739-1747.

Thakali K, Davenport L, Fink GD, Watts SW (2006). Pleiotropic effects of hydrogen peroxide in arteries and veins from normotensive and hypertensive rats. *Hypertension* **47**(3)**:** 482-487.

Thengchaisri N, Kuo L (2003). Hydrogen peroxide induces endothelium-dependent and -independent coronary arteriolar dilation: role of cyclooxygenase and potassium channels. *Am J Physiol Heart Circ Physiol* **285**(6)**:** H2255-2263.

Thilo F, Loddenkemper C, Berg E, Zidek W, Tepel M (2009). Increased TRPC3 expression in vascular endothelium of patients with malignant hypertension. *Mod Pathol* **22**(3)**:** 426-430.

Togashi K, Inada H, Tominaga M (2008). Inhibition of the transient receptor potential cation channel TRPM2 by 2-aminoethoxydiphenyl borate (2-APB). *Br J Pharmacol* **153**(6)**:** 1324-1330.

Torondel B, Vila JM, Segarra G, Lluch P, Medina P, Martinez-Leon J*, et al.* (2004). Endothelium-dependent responses in human isolated thyroid arteries from donors. *J Endocrinol* **181**(3)**:** 379-384.

Touyz RM, Schiffrin EL (2001). Increased generation of superoxide by angiotensin II in smooth muscle cells from resistance arteries of hypertensive patients: role of phospholipase D-dependent NAD(P)H oxidase-sensitive pathways. *J Hypertens* **19**(7)**:** 1245-1254.

Uhiara CO, Alexander SP, Roberts RE (2009). Effect of inhibition of extracellular signal-regulated kinase on relaxations to beta-adrenoceptor agonists in porcine isolated blood vessels. *Br J Pharmacol* **158**(7)**:** 1713-171

van Kempen MJ, Jongsma HJ (1999). Distribution of connexin37, connexin40 and connexin43 in the aorta and coronary artery of several mammals. *Histochem Cell Biol* **112**(6)**:** 479-486.

Versari D, Daghini E, Virdis A, Ghiadoni L, Taddei S (2009). Endothelium-dependent contractions and endothelial dysfunction in human hypertension. *Br J Pharmacol* **157**(4)**:** 527-536.

Villar IC, Hobbs AJ, Ahluwalia A (2008). Sex differences in vascular function: implication of endothelium-derived hyperpolarizing factor. *J Endocrinol* **197**(3)**:** 447-462.

Villar IC, Panayiotou CM, Sheraz A, Madhani M, Scotland RS, Nobles M*, et al.* (2007). Definitive role for natriuretic peptide receptor-C in mediating the vasorelaxant activity of C-type natriuretic peptide and endothelium-derived hyperpolarising factor. *Cardiovasc Res* **74**(3)**:** 515-525.

Walia M, Sormaz L, Samson SE, Lee RM, Grover AK (2000). Effects of hydrogen peroxide on pig coronary artery endothelium. *Eur J Pharmacol* **400**(2-3)**:** 249-253.

Wei CM, Hu S, Miller VM, Burnett JC, Jr. (1994). Vascular actions of C-type natriuretic peptide in isolated porcine coronary arteries and coronary vascular smooth muscle cells. *Biochem Biophys Res Commun* **205**(1)**:** 765-771.

Weston AH, Feletou M, Vanhoutte PM, Falck JR, Campbell WB, Edwards G (2005). Bradykinin-induced, endothelium-dependent responses in porcine coronary arteries: involvement of potassium channel activation and epoxyeicosatrienoic acids. *Br J Pharmacol* **145**(6)**:** 775-784.

Wheal AJ, Alexander SP, Randall MD (2012). Hydrogen peroxide as a mediator of vasorelaxation evoked by N-oleoylethanolamine and anandamide in rat small mesenteric arteries. *Eur J Pharmacol* **674**(2-3)**:** 384-390.

White B The vascular effects of hydrogen sulphide. PhD, University of Nottingham, Nottingham, 2012.

White RM, Rivera CO, Davison CA (2000). Nitric oxide-dependent and -independent mechanisms account for gender differences in vasodilation to acetylcholine. *J Pharmacol Exp Ther* **292**(1)**:** 375-380.

Wilson AJ, Jabr RI, Clapp LH (2000). Calcium modulation of vascular smooth muscle ATP-sensitive K(+) channels: role of protein phosphatase-2B. *Circ Res* **87**(11)**:** 1019-1025.

Wind S, Beuerlein K, Armitage ME, Taye A, Kumar AH, Janowitz D*, et al.* (2010a). Oxidative stress and endothelial dysfunction in aortas of aged spontaneously hypertensive rats by NOX1/2 is reversed by NADPH oxidase inhibition. *Hypertension* **56**(3)**:** 490-497.

Wind S, Beuerlein K, Eucker T, Muller H, Scheurer P, Armitage ME*, et al.* (2010b). Comparative pharmacology of chemically distinct NADPH oxidase inhibitors. *Br J Pharmacol* **161**(4)**:** 885-898.

Wingler K, Altenhoefer SA, Kleikers PW, Radermacher KA, Kleinschnitz C, Schmidt HH (2012). VAS2870 is a pan-NADPH oxidase inhibitor. *Cell Mol Life Sci* **69**(18)**:** 3159-3160.

Wingler K, Hermans JJ, Schiffers P, Moens A, Paul M, Schmidt HH (2011). NOX1, 2, 4, 5: counting out oxidative stress. *Br J Pharmacol* **164**(3)**:** 866-883.

Wolin MS (2009). Reactive oxygen species and the control of vascular function. *Am J Physiol Heart Circ Physiol* **296**(3)**:** H539-549.

Xie W, Parker JL, Heaps CL (2012). Effect of exercise training on nitric oxide and superoxide/H(2)O(2) signaling pathways in collateral-dependent porcine coronary arterioles. *J Appl Physiol* **112**(9)**:** 1546-1555.

Yada T, Shimokawa H, Hiramatsu O, Kajita T, Shigeto F, Goto M*, et al.* (2003). Hydrogen peroxide, an endogenous endothelium-derived hyperpolarizing factor, plays an important role in coronary autoregulation in vivo. *Circulation* **107**(7)**:** 1040-1045.

Yang Q, Ge Z-D, Yang C-Q, Huang Y, He G-W (2003). Bioassay of endothelium-derived hyperpolarizing factor with abolishment of nitric oxide and the role of gap junctions in the porcine coronary circulation. *Drug Development Research* **58**(1)**:** 99-110.

Yang Q, Yim AP, He GW (2007). The significance of endothelium-derived hyperpolarizing factor in the human circulation. *Curr Vasc Pharmacol* **5**(1)**:** 85-92.

Yao X, Garland CJ (2005). Recent developments in vascular endothelial cell transient receptor potential channels. *Circ Res* **97**(9)**:** 853-863.

Young EJ, Hill MA, Wiehler WB, Triggle CR, Reid JJ (2008). Reduced EDHF responses and connexin activity in mesenteric arteries from the insulin-resistant obese Zucker rat. *Diabetologia* **51**(5)**:** 872-881.

Zhang DX, Borbouse L, Gebremedhin D, Mendoza SA, Zinkevich NS, Li R*, et al.* (2012a). H2O2-induced dilation in human coronary arterioles: role of protein kinase G dimerization and large-conductance Ca2+-activated K+ channel activation. *Circ Res* **110**(3)**:** 471-480.

Zhang R, Thor D, Han X, Anderson L, Rahimian R (2012b). Sex differences in mesenteric endothelial function of streptozotocin-induced diabetic rats: a shift in the relative importance of EDRFs. *Am J Physiol Heart Circ Physiol* **303**(10)**:** H1183-1198.

Zheng X, Nishijima Y, Zhang DX (2013a). Hydrogen peroxide modulates TRPV4-mediated Ca2+entry in human coronary artery endothelial cells. *Faseb Journal* **27**.

Zheng X, Zinkevich NS, Gebremedhin D, Gauthier KM, Nishijima Y, Fang J*, et al.* (2013b). Arachidonic acid-induced dilation in human coronary arterioles: convergence of signaling mechanisms on endothelial TRPV4-mediated Ca2+ entry. *J Am Heart Assoc* **2**(3)**:** e000080.

Zinkevich N, Wittenburg A, Gutterman D (2010). Role Of Cyclooxygenase In Flow-induced Dilation Of Human Coronary Arterioles Depends Upon Age. *Circulation* **122: A15764 (Abstract)**.